

3-9-2018

# Synthesis of Unnatural Sulfatides and Examination of their Role in Immunomodulation And Synthesis of Palmostatin M-derived Probes

KEVIN LUVAGA

*University of Connecticut - Storrs*, [irungu.luvaga@uconn.edu](mailto:irungu.luvaga@uconn.edu)

Follow this and additional works at: <https://opencommons.uconn.edu/dissertations>

---

## Recommended Citation

LUVAGA, KEVIN, "Synthesis of Unnatural Sulfatides and Examination of their Role in Immunomodulation And Synthesis of Palmostatin M-derived Probes" (2018). *Doctoral Dissertations*. 1700.  
<https://opencommons.uconn.edu/dissertations/1700>

# **Synthesis of Unnatural Sulfatides and Examination of their Role in Immunomodulation And Synthesis of Palmostatin M-derived Probes**

Kevin I. Luvaga, Ph. D.

University of Connecticut, 2018

The two main foci herein are the preparation of sulfatides that activate a subset of type II natural killer T (NKT) cells and the synthesis and exploitation of the reactivity of unusual strained heterocycles. Chapter 1 describes the synthesis of two unnatural sulfatides. The preparation of one of these, an  $\alpha$ -sulfatide, was motivated by the need to probe the effect of a potential  $\alpha$ -linked sulfatide impurity in a previously synthesized  $\beta$ -sulfatide which had been shown to stimulate higher than expected secretion of both IFN- $\gamma$  and IL-4. The synthesis of the  $\beta$ -sulfatide was motivated by the fact that a related plakoside derivative had shown strong interaction with CD1d, an antigen presenting protein for Natural Killer T (NKT) cells. The syntheses were achieved by taking into account three different aspects: the preparation of the ceramide acceptor (sphingoid base and acyl chain), the glycosylation reaction with a suitable galactosyl donor and a regioselective sulfation reaction. These sulfatides will provide our collaborators with tools to understand the role of sulfatide-reactive type II NKT cells. The long-range goal is to develop new derivatives for biomedical applications.

Chapter 2 focuses on new syntheses of 3,4-disubstituted  $\beta$ -lactones, such compounds are of importance in synthetic and medicinal chemistry. Herein, the utilization of  $\alpha$ -methylene- $\beta$ -lactones in transition metal-catalyzed transformations to access 3,4-disubstituted  $\beta$ -lactones is described. Two successful transformations include: a) olefin cross metathesis (CM) of  $\alpha$ -methylene- $\beta$ -lactones scaffolds coupled with stereoselective reduction and b) rhodium-catalyzed conjugate addition of aryl boronic acids to  $\alpha$ -methylene- $\beta$ -lactones. In particular, palmostatin M inspired  $\beta$ -lactones were prepared as tools to investigate the Ras palmitoylation/depalmitoylation cycle, which regulates the subcellular trafficking of

Kevin I. Luvaga – University of Connecticut, 2018

the N-Ras, H-Ras, and K-Ras4a isoforms, as a therapeutic target for selectively inhibiting the growth of malignancies with oncogenic N-Ras mutations. The long term goal of this project is to implement mechanistic strategies to selectively inhibit the growth of cancers with somatic Ras mutations.

**Synthesis of Unnatural Sulfatides and Examination of their Role in Immunomodulation And  
Synthesis of Palmostatin M-derived Probes**

Kevin Luvaga

B.Sc., The University of Nairobi, 2011

A Dissertation

Submitted in Partial Fulfillment of the

Requirement for the Degree of

Doctorate of Philosophy

at the

University of Connecticut

2018

Copyright © by

Kevin I. Luvaga

2018

## **Approval Page**

Doctor of Philosophy Dissertation

### **Synthesis of Unnatural Sulfatides and Examination of their Role in Immunomodulation And Synthesis of Palmostatin M-derived Probes**

Presented by

Kevin I. Luvaga

Major Advisor \_\_\_\_\_

Amy R. Howell, Ph. D.

Associate Advisor \_\_\_\_\_

Mark W. Peczu, Ph. D.

Associate Advisor \_\_\_\_\_

Alfredo Angeles-Boza, Ph. D.

University of Connecticut

2018

*To Amy*  
*and to my late father, James Luvaga*

## Acknowledgments

This PhD thesis is the zenith of a lifelong interest in chemistry and has turned into as much a labor of love as a scientific study. Numerous people over the years have helped me get here, so there are many people I need to thank.

First and foremost I would like to thank my advisor, Prof. Amy R. Howell for the guidance and support throughout the years. Supervision has been complicated over the five years of candidature, yet Amy has been a constant source of support and influence, even during that period when she was the head of the chemistry department. You cheerfully assisted in steering me through to the end with prompt feedback, practical working structures and useful conversations. Your enthusiasm, your encouragement, and your resolute dedication to research work have made me what I am today. You have set an example of excellence as a researcher, mentor, instructor, parent and role model.

Besides my advisor, I am also indebted to the rest of my thesis committee members. I thank Prof. Mark W Peczu for his insightful comments during my general exam and in this dissertation. Your discussion, ideas, and feedback have been absolutely invaluable. I greatly appreciate your support and encouragement in both the synthesis and the physical organic chemistry classes. My sincere thanks also go to Prof. Alfredo Angeles-Boza for accepting to be part of my advisory committee and for being a friend for the last five years. Your incisive comments and questions during my general exam inspired me to learn about crystal field theory and understand the relationship between ligand binding in metal complexes and the degeneracy of the d orbitals and between the geometry of a metal complex and the splitting of the d orbitals. I will never forget our time during pick-up soccer games, and I am hopeful that we will play together again. I would like to thank Dr. Fatma Selampinar for her mentorship when I taught general chemistry with her, and for agreeing to be part of my advisory committee. I also want to appreciate Prof. James Bobbit for his encouragement, support, and wisdom and for agreeing to be part of my advisory committee.



During my PhD studies, I had an exciting opportunity to work as a graduate research intern at Boehringer Ingelheim Pharmaceutical Company (BI). I would like to express my sincere gratitude to Dr. Maurice Marsini. Maurice is among very few people who are respectful and worth listening to. I am extremely thankful to have worked with him, and I appreciate the time he took out of his busy schedule to teach me the ground realities of the chemical world. I am extremely grateful for instilling a sense of confidence and responsibility in me by allowing me to work on challenging projects on my own. While at BI, I was also privileged to work with Dr. Jonathan Reeves. Jon was and still is one of the nicest and most helpful people I know. I thank Jon for his encouragement and support and for allowing me to work on his exciting projects during my stay at BI. As I move forward in my professional endeavours, I will take with me all that I learned under your guidance Jon. I thank the entire greatest scientists I was privileged to interact and collaborate with: Dr. Frederick Buono, Dr. Keith Fandrick, Jolaine Savoie, Dr. Daniel Rivalenti, Dr. Ivan Volchkov, Dr. Xudong Wei, Dr. Li Guisheng and Dr. Carl Busacca. I want to thank Guisheng for his help in the lab and for the insightful discussions about my future plans, Jolaine Savoie for teaching me FTIR spectroscopy with in-situ ReactIR and Ivan for help in the lab and for translating the Russian papers into English. Lastly, I want to thank Dr. Chris Senanayake for allowing me to work with his team and for his incredible support and encouragement during my stay at BI.

The people I met and worked with have made a huge contribution to my learning and ultimate success in the PhD process and for that, I will always be thankful. To the immediate former graduate students: Kaddy Camara, Song Li, Christian Malapit, Divya Chennamadhavuni, Donald R. Caldwell, Kendricks Lao and Nicole Sassu. I thank Kaddy Camara, my mentor, for introducing me to Howell lab, for teaching me most of the basic research lab techniques I know today and for motherly protection and encouragement during hard times. See you soon Kaddy. One of the initial companions in Howell lab was Christian A. Malapit whose friendship and intelligence was vital for a number of reasons. One of his excellent skills was to listen intently and have useful contributions to make when my ideas were unfocused, managing to find the point I was struggling to express. Christian taught me some of the

important organic techniques that I use today to run experiments efficiently and I thank him for that. I remember how he helped me acquire my first red nissan altima and I am looking forward for more funding from CAM foundation in the future (I was a little mad when he never went to my PhD defense because he had to go back and switch off his rotary evaporator in Sanford lab). I thank Divya for help in the lab and encouragement during tough times. Donald Caldwell was my labmate and a great friend in the last four years (he is still a great friend, who drove 7 hrs just to attend my PhD defense). I thank him for his help in the lab particularly in the setting up fire/smoke free Simmons-Smith cyclopropanation reactions. I and Don set a new world record of working in the lab every single day of 2017 academic year. Nicole was my protective sister in the lab and I will miss her so much. I wish her all the best in her future endeavor.

To the current members of the group (Chulangani Weerasooriya ‘Chula’, Katherine Cavanaugh, Pascal Louis Riel and Jason ‘The Boy’ An), thanks for the fun and support. It was real fun having Chula and Pascal as my roommates in the lab. I have witnessed Chula changing from an extremely shy girl to a confident lady, and I wish her all the best on her research. I thank Pascal for the friendship and for being such a good mentee. It was a real pleasure working with you and I wish you all the best (thank you for the sweet wine from Portugal). To The Boy, many thanks for help both inside and outside the lab and for the great company. Of all the people I have worked with in the Howell group, I will easily miss hanging out with you the most. I wish you all the best and hope all of your crazy ideas will work out well. To Katherine, it was a pleasure to work with you and I wish you all the best in everything.

I am extremely thankful to Dr. Stewart Richardson for advice, inspiration and help in the lab. Stewart has been so resourceful especially in terms of research. Thank you for teaching me glycosylation protocols and for helping in setting up my first Simmons-Smith cyclopropanation reaction using highly inflammable diethyl zinc (I was extremely scared initially). Thank you for helping in the editing of my dissertation, for the feedback and for useful insights. To my best undergraduate student Emi Kanyo, It was a privilege to have you as my mentee and as a friend. I have learnt a lot from you Emi and thanks for taking off from your job and drove for hours just to attend my PhD defense. I wish you all the best and I

will always miss you. I am also thankful to other undergraduate students who worked in the Howell group during my stay at UCONN namely, Armando, Jenasia, Nicholas, Samuel, Tania, Patrick, Lanna, Faith, Michael and Xiaoxiao. Best wishes and keep the enthusiasm alive. To our neighbouring research groups including Pz's and Jie's labs, many thanks for sharing ideas and exciting moments both inside and outside the department. I thank Aditya for the great friendship, for numerous help both on and off campus and for being a brother from another mother here in the United States. I thank Akram for the friendship and for the insightful discussion and comments on the  $\beta$ -lactone project in the second chapter of this dissertation. I wish you all the best.

The Department of Chemistry at UCONN has been my home for the last five years or so. I am thankful to all the members of the faculty for their intellectual contributions to my development as a scientist. I am indebted to Dr. Vitaliy Gurbatyuk and Dr. Nick Eddy for their assistance in many of my NMR spectroscopy experiment. I thank Dr. You-Jun Fu for running most of the HRMS experiments described in throughout this thesis, and for his help with GC-MS analysis. To Emilie, Ashley, and Charlene, thanks for your help and support throughout my grad school life.

Now life as a student isn't all milk and honey, and I'm very thankful to the sources that have supported me financially. I thank the chemistry department for the scholarship award and the Natiaonal Institute of Health for funding our projects.

I am indebted to all my friends who have supported me over the past few years. They are far too many to name but there are some people I would like to especially thank. I am very fortunate to have met Laura A. Achola. She has been an invaluable friend for the better part of my grad school life, and I am so grateful. Thank you for your support, encouragement and advice especially during those tough times when I was just about to give up and for your help both on and off campus. Simply, I haven't met anyone who believes in me as much as you do. It's been great witnessing you grow scientifically, and I wish you great things in your research. I have enjoyed many useful and entertaining discussions with Dietz, Kyle, Sisi, Kelly, Lei and Damaris. I am so thankful for the friendship. Thank you Damaris for your help both on and

off campus and for ~~going~~ not going to my PhD defense even when you knew about it two weeks in advance.

There are a number of people behind this piece of work who deserve to be both acknowledged and thanked here. I would like to thank my wife for her unremitting encouragement. Your support throughout this process has enhanced my ability to get through it all and succeed in the end. On a more personal note, I would like to thank my mum, Jane, for never letting me doubt myself and for reminding me there is a whole world outside of my PhD. I am eternally grateful to my siblings, Patriciah, Beverly, Mercy and Arnold and those family members more recently rediscovered. Thank you for encouraging me, supporting me and making me realise that I should never let being 10000 miles away from home hold me back from what I want to do. This PhD is a testament to your faith in me, and I hope I made you all proud.

It is easy to forget how much of an impact certain people will have in your life. We often tend to forget the ‘little things’ people do for us. These special thanks go to Mapili Millicent Mapili who went through hard times together, cheered me on, encouraged me and celebrated each accomplishment at the University of Nairobi (UoN) together. Thank you so much for being a great friend and for your help during our time at UoN. I will always miss you and I wish you all the best.

I would not have studied this PhD without the wise counsel of Prof. Jacob O. Midiwo, who played a significant role in steering me through my undergraduate career in the University of Nairobi and ensured that everything was taken care of before I started this journey. You believed in me and taught me to do the right things and always avoid trouble. Words cannot express my gratitude for everything you have done. Thank you so much Prof.

Lastly, I thank God for blessing me with gift of seeking knowledge and for making this journey complete.

## Table of Contents

<b>Chapter 1.....</b>	<b>1</b>
<b>Synthesis of Unnatural Sulfatides and Examination of their Role in Immunomodulation.....</b>	<b>1</b>
1.1 Introduction.....	2
1.1.1 Glycosphingolipids .....	2
1.1.2 Sulfatides.....	3
1.1.3 CD1 Proteins .....	4
1.1.4 Natural Killer T (NKT) Cells.....	5
1.1.5 NKT Cells Activation. ....	6
1.1.6 Sulfatides as Activators of a Subset of Type II NKT Cells .....	9
1.1.7 Type II NKT Cell Function in Mice and Humans .....	11
1.1.8 Purpose of Study .....	16
1.1.9 Synthetic Strategies.....	19
1.1.10 Summary .....	23
1.2 Results and Discussion .....	23
1.2.1 Research Objective .....	23
1.2.2 Synthesis of $\alpha$ -Sulfatide <b>12</b> .....	23
1.2.3 Synthesis of $\beta$ -sulfatide <b>17</b> .....	27
1.3 Experimental.....	33
1.3.1 General Information .....	33
1.3.2 Synthesis of $\alpha$ -sulfatide <b>12</b> .....	33
1.3.3 Synthesis of $\beta$ -sulfatide <b>17</b> .....	40
1.4 References.....	55
<b>Chapter 2.....</b>	<b>59</b>
<b>Synthesis of Palmostin M-derived Probes .....</b>	<b>59</b>
2.1 Introduction.....	60
2.1.1 $\beta$ -Lactones in Natural Products.....	60
2.1.2 General Reactivity of $\beta$ -Lactones .....	62
2.1.3 Acyl Protein Thioesterase (APT) inhibitors as Probes of Dynamic S-Palmitoylation.....	65

2.1.4 $\beta$ -Lactones as APT Inhibitors .....	67
2.1.5 Targeting Oncogenic N-Ras in Cancer .....	70
2.1.6 Purpose of Study .....	71
2.2 Approaches to $\beta$ -Lactone Inhibitors of Fatty Acid Synthase (FAS) .....	73
2.2.1 Ketene Dimerization/Hydrogenation Sequence .....	73
2.2.2 Tandem Mukaiyama Aldol Lactonization (TMAL) Approach .....	75
2.2.3 Olefin Cross-Metathesis (CM) of $\alpha$ -Methylene- $\beta$ -Lactones .....	76
2.2.4 Rhodium Catalyzed Conjugate Addition of Aryl Boronic Acids .....	85
2.3 Conclusion .....	96
2.4 Experimental .....	96
2.4.1 General Information .....	96
2.4.2 Preparation of 4-(8- <i>tert</i> -butyldimethylsilyloxyoctanyl)-3-methyleneoxetan-2-one ( <b>108</b> ) .....	97
2.4.3 Preparation of $\alpha$ -alkylidene- $\beta$ -lactone via olefin cross-metathesis .....	100
2.4.4 Diastereoselective Reductions .....	101
2.4.5 Cleavage of silyl protecting group .....	102
2.4.6 Appel bromination .....	105
2.4.7 Nucleophilic substitution of the bromide with dimethylamine .....	107
2.4.8 Rh-catalyzed conjugate additions of aryl boronic acids to $\alpha$ -methylene- $\beta$ -lactones <b>108</b> .....	109
2.4.9 Elaboration of $\beta$ -lactones <b>127</b> .....	120
2.5 References .....	128

## List of Figures

<b>Figure 1.</b> Basic structure for a glycosphingolipid: a) structural skeleton of glycolipids; b) types of sphingoid bases; c) glycosidic bonds .....	2
<b>Figure 2.</b> Examples of natural $\alpha$ -glycolipids .....	3
<b>Figure 3.</b> Structures of the glycolipid sulfatide and of the most abundant mammalian fatty acids	3
<b>Figure 4.</b> The mouse CD1d structure a) the ribbon diagram of mouse CD1d with each domain labeled, with $\beta$ strands in purple and $\alpha$ helices in red; b) top view of the ligand binding $\alpha 1$ and $\alpha 2$ domains <sup>11a</sup> .....	5
<b>Figure 5.</b> Structure of KRN7000 (3) and sulfatide (4) .....	6
<b>Figure 6.</b> Structural features of the mCD1d-glycolipids complex: a) side view of bound glycolipid OCH (yellow); <sup>18</sup> b) bound <i>cis</i> -tetracosenoyl sulfatide (C24:1). <sup>19</sup> .....	7
<b>Figure 7.</b> Stereo view of the hydrogen-bond network between CD1d and glycolipid; a) H-bond network between mCD1d and an $\alpha$ -Galcer ligand; <sup>18</sup> b) H-bond network between sulfatide and mCD1d <sup>19</sup> .....	8
<b>Figure 8.</b> Cytokine secretion from NKT cell activation.....	9
<b>Figure 9.</b> Overview of the docking orientations: a) type II NKT cell complex with the mCD1d-sulfatide; b) type I NKT cell complex with mCD1d-KRN7000; c) view looking down showing the orthogonal docking mode in the type II-sulfatide-CD1d complex; d) view looking down showing the parallel docking mode in the type I-KRN7000-CD1d complex. <sup>23</sup> .....	10
<b>Figure 10.</b> Type II NKT cells TCR interactions with sulfatides; a) XV19 TCR interaction with <i>cis</i> -tetracosenoyl sulfatide shown in magenta, van der Waal interaction shown in red dashes and H-bonds shown in black dash; <sup>23</sup> b) Hy19.3 TCR interaction with lyso-sulfatide (free amine, has no acyl chain attached) shown in yellow, H-bond and van der Waal interactions are shown in blue dashes. <sup>25</sup> .....	11
<b>Figure 11.</b> Examples of natural sulfatides.....	13

<b>Figure 12.</b> Previously synthesized sulfatides .....	17
<b>Figure 13.</b> KRN7000 analog and unnatural sulfatides targets .....	18
<b>Figure 14.</b> Plakoside A analog <b>16</b> of KRN7000 and its sulfatide analog target <b>17</b> .....	18
<b>Figure 15.</b> Anchimeric assistance to enhance $\beta$ -selectivity .....	20
<b>Figure 16.</b> A model of Flitsch's regioselective sulfation of deprotected galactoside .....	23
<b>Figure 17.</b> Synthetic strategy to $\alpha$ -sulfatide <b>12</b> .....	24
<b>Figure 18.</b> Synthetic strategy to $\beta$ -sulfatide <b>17</b> .....	28
<b>Figure 19.</b> $\beta$ -Lactone-containing natural products.....	61
<b>Figure 20.</b> Acylation of enzymes .....	62
<b>Figure 21.</b> Primary reactivity modes of $\beta$ -lactones .....	62
<b>Figure 22.</b> A dynamic <i>S</i> -palmitoylation .....	66
<b>Figure 23.</b> a) APT competitive enzyme inhibition by $\beta$ -lactones; b) structure of palmostatin B; c) structure of palmostatin M.....	67
<b>Figure 24.</b> Inhibitor development based on substrate similarity <sup>34</sup> .....	69
<b>Figure 25.</b> An alkynyl palmostatin M analogue ( <b>84</b> ) .....	70
<b>Figure 26.</b> Targeted palmostatin M derivatives .....	73
<b>Figure 27.</b> Retrosynthesis of palmostatin M-inspired $\beta$ -lactones.....	79
<b>Figure 28.</b> Retrosynthesis to $\alpha$ -methylene- $\beta$ -lactone <b>95</b> .....	79
<b>Figure 29.</b> Retrosynthesis to palmostatin M-inspired $\beta$ -lactones <b>85</b> and <b>86</b> .....	82
<b>Figure 30.</b> Scope for Rh-catalyzed conjugate addition of phenyl boronic acid to <b>108</b> <sup>62</sup> .....	94



## List of Schemes

<b>Scheme 1.</b> Glycosylation approaches .....	19
<b>Scheme 2.</b> Tanahashi's synthesis of sulfatide <b>22</b> .....	21
<b>Scheme 3.</b> Marinier's synthesis of sulfatide <b>23</b> .....	22
<b>Scheme 4.</b> Synthesis of azido-sphingosine acceptor <b>31</b> .....	25
<b>Scheme 5.</b> Synthesis of $\alpha$ -aminoglycoside <b>41</b> .....	26
<b>Scheme 6.</b> Synthesis of $\alpha$ -sulfatide <b>12</b> .....	27
<b>Scheme 7.</b> Synthesis of iodide <b>52</b> .....	29
<b>Scheme 8.</b> Synthesis of sphinganine <b>45</b> .....	30
<b>Scheme 9.</b> Synthesis of benzoyl-protected ceramide acceptor <b>46</b> .....	31
<b>Scheme 10.</b> Synthesis of sugar donor <b>47</b> .....	32
<b>Scheme 11.</b> Synthesis of $\beta$ -sulfatide <b>17</b> .....	32
<b>Scheme 12.</b> Lewis acid promoted rearrangements; a) dyotropic rearrangements; b) ring expansion via a transacylation/debenzylation sequence; c) rearrangement of $\beta$ -lactones with pendant silyl ethers .....	63
<b>Scheme 13.</b> Diastereoselective electrophilic reactions of $\beta$ -lactones enolates .....	64
<b>Scheme 14.</b> Nucleophilic ring-opening of $\beta$ -lactones .....	64
<b>Scheme 15.</b> Disubstituted $\beta$ -lactone synthesis via ketene dimerization/hydrogenation sequence .....	75
<b>Scheme 16.</b> Epimerization of <i>cis</i> - $\beta$ -lactones to the <i>trans</i> -isomers .....	75
<b>Scheme 17.</b> Tandem Mukaiyama Aldol lactonization (TMAL) approach .....	76
<b>Scheme 18.</b> $\beta$ -Lactones synthesis by cross-metathesis/reduction sequence .....	78
<b>Scheme 19.</b> An attempt to prepare $\alpha$ -methylene- $\beta$ -lactone <b>107</b> via a mercury-mediated cyclization.....	80
<b>Scheme 20.</b> Preparation of $\alpha$ -methylene- $\beta$ -lactone <b>108</b> .....	81

<b>Scheme 21.</b> An attempt to convert alcohol <b>114</b> to bromide <b>115</b> under Appel's condition.....	81
<b>Scheme 22.</b> CM reaction to access $\alpha$ -alkylidene- $\beta$ -lactone <b>116</b> .....	82
<b>Scheme 23.</b> Synthesis of palmostatin M derived $\beta$ -lactone <b>Z-85</b> .....	83
<b>Scheme 24.</b> Synthesis of palmostatin M derived $\beta$ -lactone <b>E-85</b> .....	83
<b>Scheme 25.</b> Diastereoselective reductions to give <i>cis</i> - and <i>trans</i> - $\beta$ -lactones <b>120</b> .....	84
<b>Scheme 26.</b> Synthesis of palmostatin M-derived $\beta$ -lactone <i>trans</i> - <b>86</b> .....	84
<b>Scheme 27.</b> Synthesis of palmostatin M-derived $\beta$ -lactone <i>cis</i> - <b>86</b> .....	84
<b>Scheme 28.</b> Rh-catalyzed conjugate addition.....	85
<b>Scheme 29.</b> The first rhodium-catalyzed conjugate addition reaction reported .....	86
<b>Scheme 30.</b> Examples of Rh-catalyzed conjugate addition of aryl boronic acids with endocyclic systems.....	87
<b>Scheme 31.</b> Rh-catalyzed conjugate addition to dihydropyridinone for the synthesis of (–)-paroxetine.....	87
<b>Scheme 32.</b> Rhodium-catalyzed conjugate addition of exocyclic lactams with aryl boronic acids .....	88
<b>Scheme 33.</b> Rh-catalyzed conjugate addition of benzylidene Meldrum's acid with organoboron reagents .....	88
<b>Scheme 34.</b> Hypothesis and initial studies on the Rh-catalyzed conjugate addition.....	90
<b>Scheme 35.</b> $\beta$ -Hydride elimination (versus hydrolysis) from the $\alpha$ -metallated intermediate <b>127</b> .....	91
<b>Scheme 36.</b> Cleavage of silyl group .....	95
<b>Scheme 37.</b> Appel's bromination and <i>N</i> -alkylation with dimethylamine.....	95

## List of Tables

<b>Table 1.</b> Synthesis of alkylidene $\beta$ -lactones <b>92</b> via cross-metathesis.....	77
<b>Table 2.</b> Optimization of Rh-catalyzed conjugate addition (CA) of phenylboronic acid to <b>124a</b> <sup>62</sup> .....	92

## List of Abbreviations

3-Quinuclidinol	1-Azabicyclo[2.2.2]octan-3-ol
ABPP	Activity-based protein profiling
AcOH	Acetic acid
APC	Antigen presenting cell
APT	Acyl protein thioesterase
Ar	Aryl
Bf <sub>3</sub> •OEt <sub>2</sub>	Boron trifluoro etherate
Bn	Benzyl
Boc	<i>t</i> -Butyloxycarbonyl
br	Broad
Bu <sub>2</sub> SnO	Dibutyltin oxide
<i>n</i> -Bu <sub>4</sub> NI/TBAI	Tetrabutylammonium iodide
Bz	Benzoyl
CA	Conjugate addition
Calcd	Calculated
CD1d	Cluster of differentiation
CDCl <sub>3</sub>	Deuterated chloroform
CH <sub>2</sub> Cl <sub>2</sub> /DCM	Dichloromethane
CHCl <sub>3</sub>	Chloroform

CH <sub>3</sub> C(OEt) <sub>3</sub>	Triethyl orthoformate
Cl <sub>3</sub> CCN	Trichloroacetonitrile
CM	Cross-metathesis
cod	1,4-cyclooctadiene
DABCO	1,4-Diazabicyclo[2.2.2]octane
DBU	1,8-Diazabicycloundec-7-ene
DCC	<i>N,N</i> -Dicyclohexylcarbodiimide
DCM	Dichloromethane
DMAP	4-Dimethylamino pyridine
DMF	<i>N,N</i> -Dimethylformamide
DMP	2,2-Dimethoxypropane
DMSO	Dimethyl sulfoxide
dr	Diastereomeric ratio
EAE	Experimental Autoimmune Encephalomyelitis
Equiv	Molar equivalent
ESI	Electrospray ionization
Et <sub>2</sub> O	Diethyl ether
EtOAc	Ethyl acetate
FAS	Fatty acid synthase
FTIR	Fourier Transform Infrared

$\alpha$ -GalCer	$\alpha$ -Galactosylceramide
GlcCer	Glucosylceramide
GVHD	Graft-versus-host disease
h	hour
HC	Heck coupling
Hg(O <sub>2</sub> CCF <sub>3</sub> ) <sub>2</sub>	Mercury(II) trifluoroacetate
HRMS	High resolution mass spectrometry
Hz	Hertz
IC <sub>50</sub>	Half maximal inhibitory concentration
IFN- $\gamma$	Interferon-gamma
IL-4	Interlukin-4
IR	Infrared
J	Coupling constant value
KOH	Potassium hydroxide
m/z	Mass to charge ratio
MBH	Morita-Baylis-Hillman
Me	Methyl
MeCN	Acetonitrile
MeOH	Methanol

MHC	Major Histocompatibility Complex
min	Minutes
nbd	Norbornadiene
NKT cells	Natural killer T cells
NMR	Nuclear Magnetic Resonance
NOD	Non-obese diabetic
Nosyl	Nitrobenzene sulfonyl
NR	No reaction
OAc	Acetate
PBL	Peripheral blood lymphocytes
PCy3	Tricyclohexyl phosphine
Ph	Phenyl
PPh3	Triphenyl phosphine
ppm	Parts per million
PTSA	<i>p</i> -Toluenesulfonic acid
PPTS	Pyridinium <i>p</i> -toluenesulfonate
PPTs	Protein palmitoyl thioesterases
py	Pyridine
rt	Room temperature
SAR	Structure activity relationship

SEGPPOS	5,5'-Bis(diphenylphosphino)-4,4'-bi-1,3-benzodioxole
SH	Serine hydrolase
T1D	Type 1 diabetes
TBAF	Tetrabutylammonium fluoride
TBDMS/TBS	<i>tert</i> -Butyldimethylsilyl
TBDPS	<i>tert</i> -Butyldiphenyl silyl
TCR	T-cell receptor
Tf	Trifluoromethanesulfonyl
Th	T helper
THF	Tetrahydrofuran
THL	Tetrahydrolipstatin
TLC	Thin layer chromatography
TMAL	Tandem Mukaiyama Aldol Lactonization
TMS	Trimethylsilyl
TMSI	Trimethylsilyl iodide
Tol	Toluene
UCSF	University of California, San Francisco
Wilkinson's catalyst, RhCl(PPh <sub>3</sub> ) <sub>3</sub>	Tris(triphenylphosphine)rhodium(I) chloride



## **Chapter 1**

### **Synthesis of Unnatural Sulfatides and Examination of their Role in Immunomodulation**

## 1.1 Introduction

### 1.1.1 Glycosphingolipids

Glycosphingolipids are an important class of lipids found in membranes of vertebrate cells. They play a major role in many biological processes, such as the formation of membrane microdomains and the interaction of pathogenic microbes or their secreted toxins with host cells.<sup>1</sup> The basic structure for a glycosphingolipid consists of glucose or galactose, attached directly to a ceramide molecule and resulting in, respectively, glucosylceramide (glucocerebroside; GlcCer) or galactosylceramide (galactocerebroside; GalCer) (Figure 1a). The ceramide is made up of a sphingoid base (phytosphingosine, sphingosine, or sphinganine) (Figure 1b) and fatty acyl chain connected through *N*-acylation. The sugar is connected to the ceramide via a glycosidic bond that can be either alpha or beta linked (Figure 1c). This combination structure results in an amphiphilic molecule with a hydrophilic carbohydrate region and a hydrophobic lipid region.

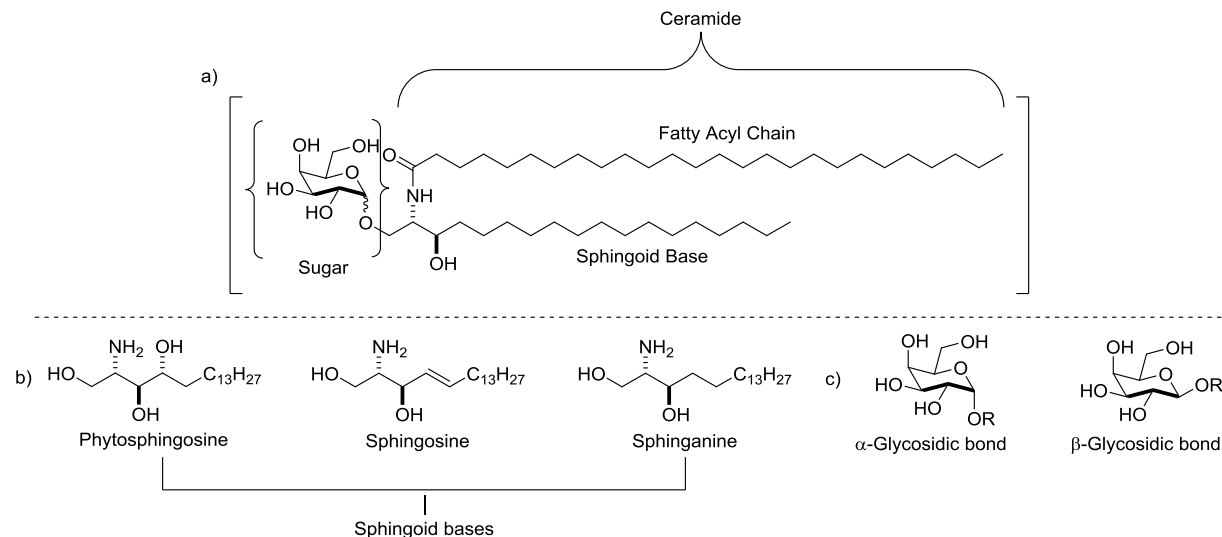


**Figure 1.** Basic structure for a glycosphingolipid: a) structural skeleton of glycolipids; b) types of sphingoid bases; c) glycosidic bonds

Most mammalian glycolipids are  $\beta$ -configured with the exception of C24:1- $\alpha$ -galactosylceramide (**1**), which was recently reported by Kain and co-workers (Figure 2).<sup>2</sup> Agelasphin-9b (**2**) is another example of a glycolipid isolated from a natural source with the galactose unit  $\alpha$ -linked to the ceramide portion.

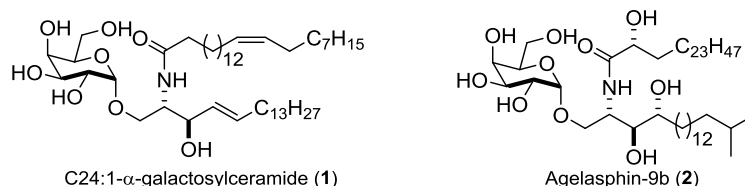


**Figure 2.** Examples of natural  $\alpha$ -glycolipids

### 1.1.2 Sulfatides

Sulfatides consist of sulfated galactosylceramides, in which the galactose is sulfated at position 3 and is linked via a  $\beta$ -glycosidic bond to the primary hydroxyl group of a *N*-acylated D-erythro-sphingosine base, typically with a C-18 backbone (Figure 3).<sup>3</sup>

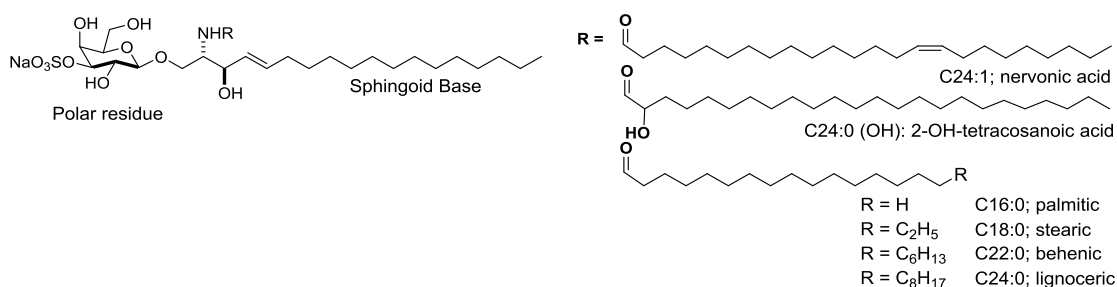


**Figure 3.** Structures of the glycolipid sulfatide and of the most abundant mammalian fatty acids

Sulfatides display structural variation in the composition of the fatty acid residue that trimethyl the amino group of sphingosine. The alkyl or alkenyl residues are different in lengths, and they can be also hydroxylated. The variation in structure represents a cell type-specific pattern, which at least in part can be explained by the different expression of the enzymes involved in sulfatide biosynthesis. The nervonic acid (C24:1)-containing sulfatide is the most abundant in myelin, while significantly elevated levels of stearic acid (C18:0)-containing sulfatide are found in the cortical grey matter.<sup>4</sup> Mammalian kidney sulfatides are instead particularly rich in C22:0 acid, which is found in quantities more than 10 times

higher than those in the brain. On the other hand, mass spectroscopic analyses of pancreatic sulfatides revealed a high proportion of short chain C-16 fatty acid and no hydroxylated form.<sup>5</sup>

Several glycolipids and phospholipids derived from mammalian, bacterial, protozoan and plant species have recently been identified as natural ligands (antigens) for NKT cells.<sup>6</sup> Natural killer T (NKT) cells have been shown by a number of studies to play a protective role against cancers, autoimmune diseases and infectious diseases.<sup>6</sup> The hydrophobic alkyl portions of these glycolipids binds directly to CD1 proteins and position the polar or hydrophilic head groups of bound lipids and glycolipids for highly specific interactions with T cell antigen receptors. The following introductory sections will include a background on the roles of CD1 molecules and NKT cells. NKT cells' activation mechanism and sulfatides as activators of type II NKT cells will also be highlighted. Lastly, synthetic strategies to access sulfatides are described.

### **1.1.3 CD1 Proteins**

CD1 proteins are specialized antigen-presenting molecules that directly bind a wide variety of lipids and present them for T cell recognition at the surface of antigen-presenting cells (APCs) such as dendritic cells, macrophages, and subsets of B cells. CD1 proteins are homologous to major histocompatibility complex (MHC) class I proteins. Unlike MHC which binds to an invariant partner, CD1 proteins bind and present a variety of lipids and glycolipids, both innate (e.g. phospholipids,<sup>7</sup> glycosphingolipids and sulfoglycolipids<sup>8a</sup>) and foreign (e.g. mycobacterial)<sup>9</sup> to NKT receptors. The human CD1 family is composed of five nonpolymorphic MHC class I-like glycoproteins (CD1a to CD1e). These proteins can be classified into two groups based mainly on the homology of nucleotide and amino acid sequences.<sup>10</sup> Group 1 consists of CD1a, CD1b, CD1c and CD1e, whereas human CD1d together with the only murine isoform, mouse CD1d, are members of group 2. Based on mouse(m) CD1d's crystal structure, its antigen binding groove is narrow, but deep, when compared with MHC class I and class II peptide-binding grooves.<sup>11</sup> In general, the secondary, tertiary, and quaternary structural units in mCD1d displays similarity to those of MHC class I and II molecules and related proteins (Figs. 4). The  $\alpha$  chain, which is closely

related to  $\beta 2$ -microglobulin ( $\beta 2M$ ), folds into the standard three domains ( $\alpha 1$ ,  $\alpha 2$ ,  $\alpha 3$ ). An eight-stranded antiparallel  $\beta$ -pleated sheet with two long antiparallel  $\alpha$ -helical structures that sit on the top of, and traverse the  $\beta$ -sheet platform forms a binding groove superdomain that constitutes the  $\alpha 1$  and  $\alpha 2$  domains (Figure 4). A c-type Ig folds is displayed by  $\alpha 3$  and  $\beta 2M$  domains.

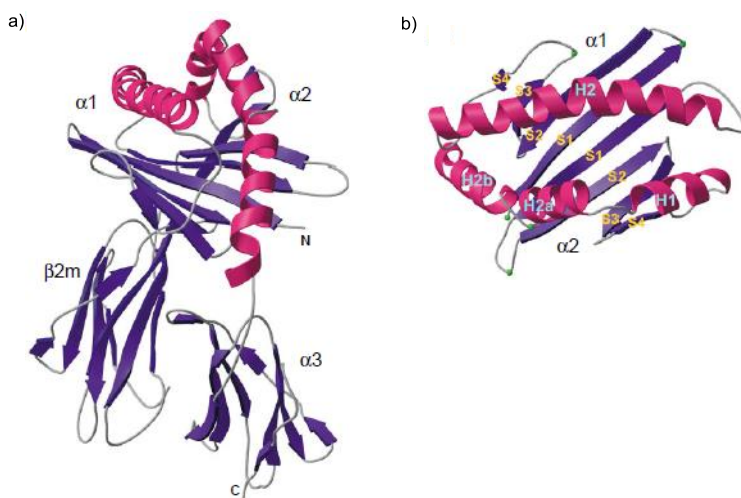


**Figure 4.** The mouse CD1d structure a) the ribbon diagram of mouse CD1d with each domain labeled, with  $\beta$  strands in purple and  $\alpha$  helices in red; b) top view of the ligand binding  $\alpha 1$  and  $\alpha 2$  domains<sup>11a</sup>

#### 1.1.4 Natural Killer T (NKT) Cells

Natural killer T (NKT) cells are innate-like T cells that express TCR- $\alpha\beta$  chains in addition to the typical NK cell markers and possess a crucial immunoregulatory role in inflammatory conditions, including autoimmune diseases, infectious diseases and cancer.<sup>12</sup> NKT cells perform a function of traversing between innate and adaptive immunities.<sup>13</sup> Both exogenous and endogenous lipid antigens can be recognized by NKT cells.<sup>14</sup> NKT cells are CD1d-restricted, which means they only recognize lipid antigens presented by CD1d proteins for their activation. The two main subsets of CD1d-restricted NKT cells include type I or invariant, NKT cells and type II or diverse NKT cells. Type I NKT cells are the most common in mice and comprise ~50% of murine intrahepatic lymphocytes.<sup>15</sup> Type I NKT cells express a conserved semi-invariant  $\alpha\beta$ TCR that is encoded predominantly by germ line V $\alpha$  gene (V $\alpha$ 24 in humans and V $\alpha$ 14 in mice) and J $\alpha$ 18 gene segments. Type I NKT cells comprise ~0.1–1% of the

circulating T cells in humans. CD4<sup>-</sup> and CD4<sup>+</sup> type I NKT cells predominantly secrete Th1- and Th2-type cytokines, respectively. Extensive research has been conducted on type I NKT cells utilizing a potent  $\alpha$ -galactosylceramide, KRN7000 (**3**) (Figure 5) and its analogs.<sup>16</sup>

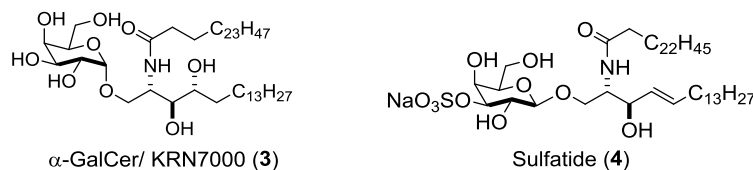


**Figure 5.** Structure of KRN7000 (**3**) and sulfatide (**4**)

Type II NKT cells are more abundant than type I NKT cells in humans, and as in mice, they express relatively diverse TCR- $\alpha$ - and TCR- $\beta$  chains. While many ligands that activate type I NKT cells have been described, few SAR studies have been conducted around ligands that activate type II NKT cells. Currently, the most widely studied antigen for type II NKT cells is sulfatide (**4**) (Figure 5).<sup>8</sup> Some biases in TCR chain usage have been described in type II NKT cells. A good example is in mice type II NKT cells, where they appear to be enriched for particular TCR  $\alpha$ -chain V segments (namely V $\alpha$ 3 and V $\alpha$ 8 for V $\beta$ 8).<sup>17</sup> Additionally, the TCRs of sulfatide-reactive type II NKT cells can have a more conserved CDR3 $\beta$  region than type I NKT TCRs.<sup>8b</sup> Interestingly, a recent study of human sulfatide-reactive type II NKT cells suggested that this population includes some V $\delta$ 1+  $\gamma\delta$  T cells. The diverse nature of type II NKT cells highlights the fact that a great deal needs to be learned about CD1d-restricted antigen specificity and recognition by type II NKT TCRs. The aim of this work is to design and synthesize unnatural sulfatides to provide our collaborators with tools to understand the role of the sulfatide-reactive type II NKT cells and ultimately to harness their activation for therapeutic purposes. In the following section, the mechanism of NKT cells activation is described.

### 1.1.5 NKT Cells Activation.

Two important consecutive cellular recognitions are necessary for a glycolipid to promote activation. First, the glycolipid is recognized by the CD1d protein to form a binary complex. Then, the binary

complex interacts with the NKT cell receptor (TCR) to form the active ternary complex. The crystallographic data of the mouse-CD1d/alpha-galactosylceramide analog OCH complex reported by Sullivan et al<sup>18</sup> and of sulfatide-mCD1d reported by Zajonc et al<sup>19</sup> have provided useful information that allowed the study of the stabilizing interactions between the ligand and its host (Figure 6).

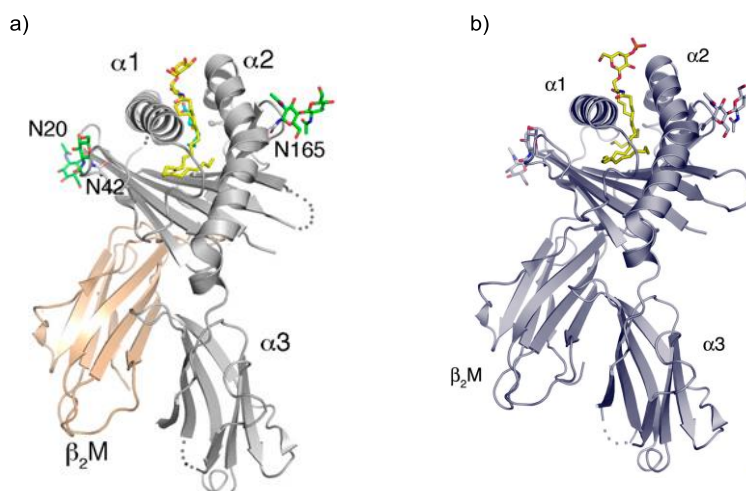


**Figure 6.** Structural features of the mCD1d-glycolipids complex: a) side view of bound glycolipid OCH (yellow);<sup>18</sup> b) bound *cis*-tetracosenoyl sulfatide (C24:1).<sup>19</sup>

Hydrogen-bonding between the glycolipid ligand and CD1d plays a crucial role in anchoring the ligand in a distinct orientation which allows each of the two alkyl chains to be inserted into its respective pocket (Figure 7). The 2' and 3' hydroxyl groups of the galactose head group are stabilized by Asp153 ( $\alpha$ 2-helix) of CD1d and the 3-, 4-hydroxyl groups of the phytosphingosine hydrogen bond to Asp80. Additionally, interaction of the  $\alpha$ 1-helix (Asp80) with the C3, C4-hydroxyl groups of the sphingosine backbone leads to a ligand orientation in which the sphingosine chain can only be accommodated in the F' pocket and not in the A' pocket. The A and C (or F) pockets are further stabilized with  $\beta$ -helix sheets via van der Waals interactions. The same hydrogen bonds seen in the CD1d-KRN7000 binary complex are also observed in CD1d-sulfatide (galactose moiety C2-OH-D153, C1-O'-T156, sphingoid base moiety C3-OH-D80 and the amide NH-T156) (Figure 7b). Furthermore, sulfatides form three extra H-bonds with CD1d (C6-OH-R79, sulfate group with Q154, and the carbonyl group of the amide with Met69). The

hydrogen bond between the sulfate group and the backbone nitrogen of Gln154 is H<sub>2</sub>O mediated (Figure 7b).

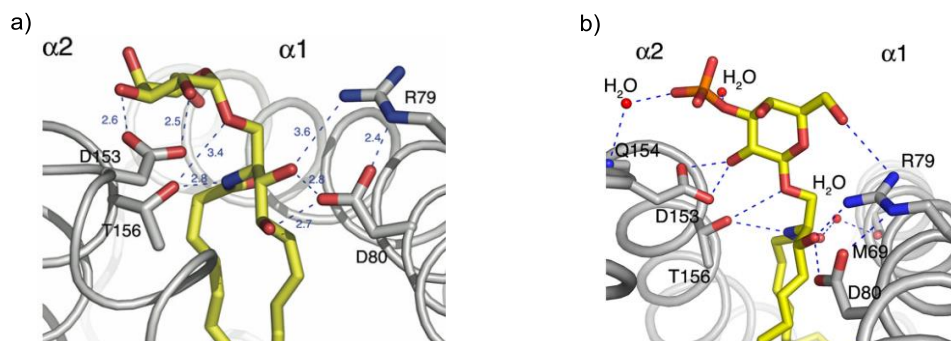


**Figure 7.** Stereo view of the hydrogen-bond network between CD1d and glycolipid; a) H-bond network between mCD1d and an  $\alpha$ -Galcer ligand;<sup>18</sup> b) H-bond network between sulfatide and mCD1d<sup>19</sup>

As shown in figure 6, galactose rings in the binary complex crystal structures are well ordered and extend above the surfaces of the lipid-binding grooves (pinned down between the  $\alpha$ -1 and  $\alpha$ -2 helices of CD1d). These exposed positions seem suitable for recognition by the NKT TCR leading to the formation of the ternary complex. Successful formation of the ternary complex activates NKT cells to release different cytokines, communication devices for immune responses (Figure 8). Depending on their biological activities, these cytokines can be classified as having T helper 1 (Th1) and T helper 2 (Th2) types of responses. Th1 cytokines include IFN- $\gamma$ , IL-2, IL-3 and TNF- $\beta$ ; they induce proinflammatory activities, a defense mechanism for the immune system to fight diseases, such as viral, bacterial, and parasitic infections. Th1 cytokines have also been shown to have antitumor activity.<sup>16</sup> Th2 cytokines include IL-4, IL-5, IL-10 and IL-13. They are responsible for autoimmuno-regulatory activities, which are relevant for the treatment of diabetes and other autoimmune conditions. The most studied glycolipids for NKT cell activation are KRN7000 for type I NKT cells and recently sulfatides for type II NKT cells. In the next section, sulfatides as activators of type II NKT cells is emphasized.



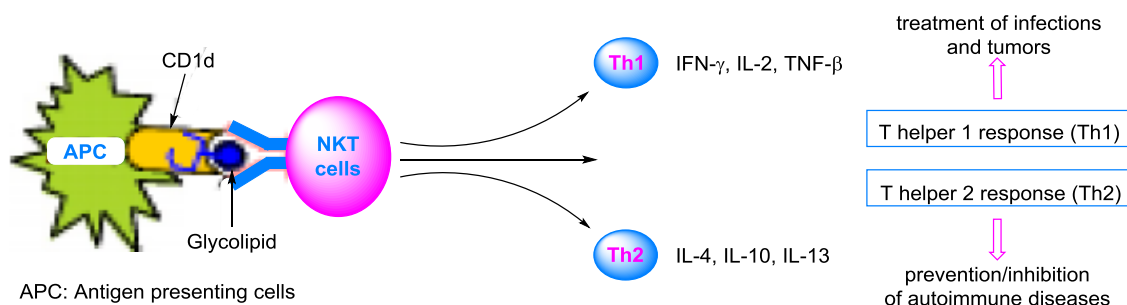


**Figure 8.** Cytokine secretion from NKT cell activation

### 1.1.6 Sulfatides as Activators of a Subset of Type II NKT Cells

Sulfatides make up to 4-6% of the myelin lipids and are also found in various other tissues, including membranes in the kidneys, the pancreas, and the gastrointestinal and respiratory tracts.<sup>20,21</sup> Sulfatides participate in intracellular signaling mechanisms and can be presented to the immune system by the CD1 family of antigen-presenting surface proteins to T cells to activate them for cytokine secretion.<sup>22</sup> The  $\beta$ -glycosidic linkage in sulfatides causes their sugar moieties to protrude from the  $\alpha$ -helices of CD1d. Under these condition, structural studies showed a diagonal docking mode arising from the interactions of sulfatides with the TCR's on the surface of some type II NKT cells found above the A pocket of CD1d.<sup>23</sup> In contrast, the  $\alpha$ -glycosidic bond in KRN7000 causes the sugar moiety to be buried more in the  $\alpha$ -helices of CD1d, favoring its presentation to type I NKT cells positioned above the F or C pocket of CD1d in a parallel docking mode (Figure 9).

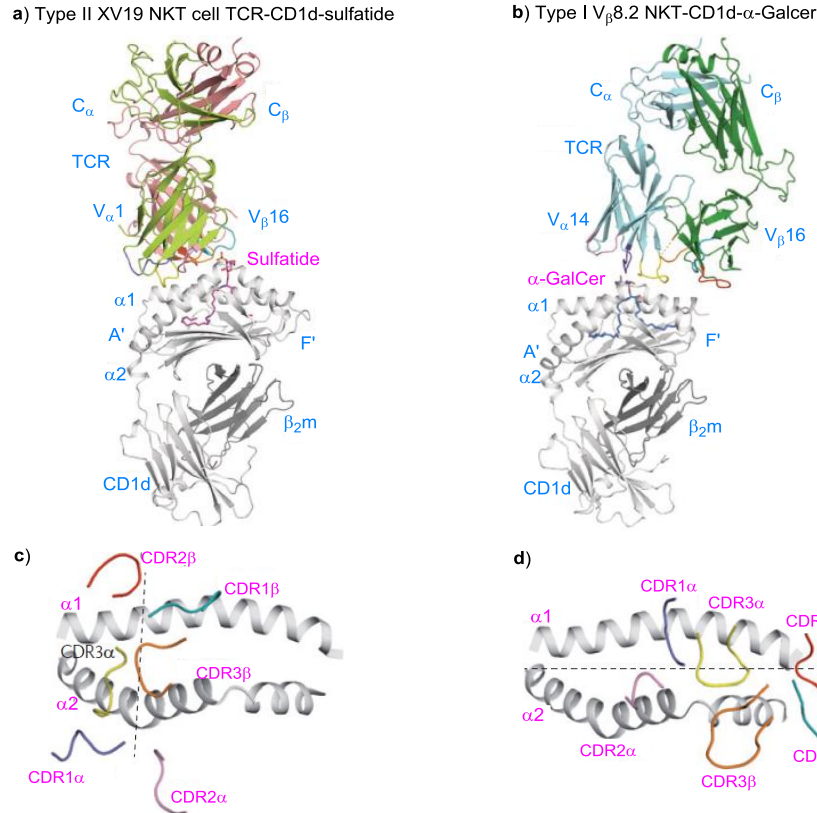


**Figure 9.** Overview of the docking orientations: a) type II NKT cell complex with the mCD1d-sulfatide; b) type I NKT cell complex with mCD1d-KRN7000; c) view looking down showing the orthogonal docking mode in the type II-sulfatide-CD1d complex; d) view looking down showing the parallel docking mode in the type I-KRN7000-CD1d complex.<sup>23</sup>

In spite of the antigen specificity of type II NKT cells being poorly understood, they are clearly distinct from that of type I NKT cells. Indeed, type II NKT cells are partly defined by their lack of reactivity to CD1d-KRN7000; instead, some of these cells recognize a range of sulfatides presented by CD1d.<sup>24</sup> The key factors in the understanding of type II NKT cell biology lies in elucidating how their TCRs recognize CD1d-restricted antigens. This has inspired crystal structure studies of CD1d-sulfatide-type II complexes to unravel how sulfatides interact with the NKT cells. The crystal structure of sulfatide reactive-TCRs of type II NKT cells was recently solved using *cis*-tetracosenoyl sulfatide-CD1d-XV19 TCR complex, in a study conducted by the group of Rossjohn.<sup>23</sup> They showed lack of H-bonding between the sulfate moiety and any amino acid residues of the TCRs (Figure 10). The only H-bonding interaction observed was between the C2-OH of the sugar and tryptophan residue W97β (unlike the KRN7000-type I NKT TCR

interaction, which showed a compacted H-bonding interaction of the sugar moiety and TCRs). The complexes were stabilized, in addition to the C2-OH-W97 $\beta$  H-bond, by van der Waal interactions of the TCRs amino acid residues and the ligands (Figure 10b). Similar results were obtained when the group of Zajonc solved the structure of sulfatide reactive-TCRs type II NkT cells using lyso-sulfatide (free amine, has no acyl chain)-CD1d-Hy19.3 TCR complex. From both studies, the lack of an intricate H-bonding network between the sulfate moieties of sulfatides suggested that other  $\beta$ -glycolipids can activate type II NKT cells. It also validated  $\beta$ -GalCer stimulation of XV19 (a sulfatide reactive type II NKT cell) TCR, although this happens to a lesser extent than with sulfatides.<sup>25</sup>

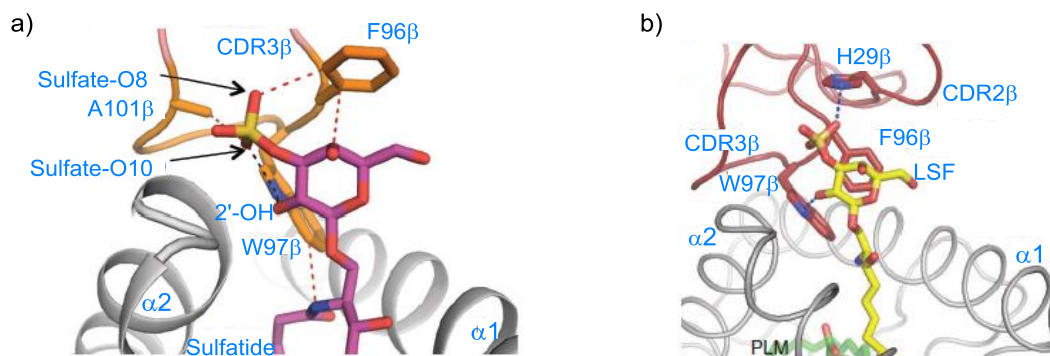


**Figure 10.** Type II NKT cells TCR interactions with sulfatides; a) XV19 TCR interaction with *cis*-tetracosenoyl sulfatide shown in magenta, van der Waal interaction shown in red dashes and H-bonds shown in black dash;<sup>23</sup> b) Hy19.3 TCR interaction with lyso-sulfatide (free amine, has no acyl chain attached) shown in yellow, H-bond and van der Waal interactions are shown in blue dashes.<sup>25</sup>

### 1.1.7 Type II NKT Cell Function in Mice and Humans

Natural killer T cells have potent immunoregulatory functions that determine the outcome of activation of the immune system, including autoimmunity and response to infections and tumors. Because of this, research has focused on activation of NKT cells as an approach to the treatment of a variety of diseases/conditions. Promising developments in the field suggests that NKT cell-directed therapy can be developed to enhance tumor immunity, prevent autoimmunity and improve vaccines. However in order to fully explore NKT cells for biological purposes it is imperative for the less characterized type II NKT cell activation and cytokine secretion mechanism to be understood. For example, type II NKT cells have been demonstrated to be the innate arm of immunoregulatory T cells; the majority of their function being

attributed so far to their role in inhibiting the proinflammatory functions of type I NKT cells, conventional T cells, and dendritic cells.<sup>26</sup> The discovery of sulfatide as one of the major antigens for CD1d-restricted type II NKT cells in mice has been instrumental in the characterization of these cells, including the TCR repertoire, the crystal structure of the CD1d/lipid/TCR complex, and their function, even though initial experiments conducted to identify active sulfatides were difficult. This is mainly due to sulfatide structural similarities which make the isolation of individual species challenging. Early analyses were performed with a mixture of sulfatides. Modifications in the ceramide moiety can influence the interactions the ligands have with CD1d and T cell receptors and, consequently, also the type of responses induced.

In a study carried out by Jahng et al.<sup>8a</sup> in their effort to find out ligands that can activate type II NKT cells, a first sulfatide-CD1d complex recognition by type II NKT cells was reported using Hy 19.3 (which is a subclone of XV19, a sulfatide reactive type II NKT cell). They treated Hy 19.3 with different CD1d-glycolipid complexes, including sulfatide mixtures, KRN7000 ( $\alpha$ -GalCer),  $\beta$ -GalCer ( $\beta$ -anomer of KRN7000) and mono-GM1 (with a negatively charged sialic acid instead of sulfate). From this study, they found out that only the sulfatide mixtures were able to stimulate the secretion of cytokines (IFN- $\gamma$  and IL-4). Later on, Kumar and co-workers demonstrated that the sulfatide active against Hy 19.3 was lyso-sulfatide **5** (Figure 11).<sup>27</sup> Sulfatides, **4**, **6** and **7**, which were part of the previously analyzed mixture, were found to be inactive. While working on development of the first CD1d-sulfatide binary complex (CD1d-sulfatide **7**), Wilson and co-workers tested **7** with other sulfatides (its saturated acyl chain version **4**, lyso-sulfatide **5** and short chain **6**) for cytokine proliferation, and **7** displayed the highest stimulation of <sup>3</sup>H-thymidine (a cell proliferation assay to test the potency of ligands in stimulating lymphocytes) secretion.<sup>19</sup>

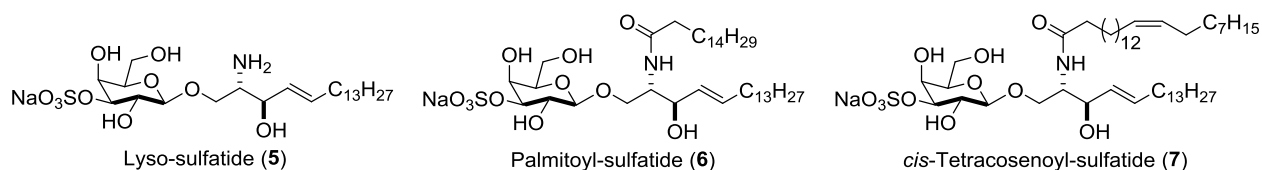


**Figure 11.** Examples of natural sulfatides

Despite the fact that many factors influence glycolipid stimulation of NKT cells, information thus far on sulfatide activation of type II NKT cells infer the stability of the antigen-NKT cell ternary complex to be the determining factor for individual sulfatide stimulatory results.<sup>28</sup> Highlighted below is an overview of different human and murine immune responses in which type II NKT cells have been shown to play a crucial role.

#### 1.1.7.1 Experimental Autoimmune Encephalomyelitis (EAE) and Multiple Sclerosis (MS)

Multiple sclerosis is a demyelinating autoimmune disease in which myelin-derived protein antigens are targets for autoimmune attack by conventional T cells. The CD1-restricted T cells from peripheral blood lymphocytes (PBL) were found to be activated by several glycolipid components of the myelin sheath, including sulfatide. An increase in the frequencies of reactive cells in PBL from patients with MS, suggested that the cells may be involved in the autoimmune reaction of this disease.<sup>29</sup> However, in these studies, it was not addressed whether the sulfatide reactivity of these T cells was restricted by CD1d or by other human CD1 isoforms that are all known to present sulfatide to T cells.

Subsequently, a study done by Kumar et al. demonstrated that sulfatide was a ligand for a murine type II NKT hybridoma.<sup>12a</sup> The infiltration of the CNS during the course of EAE (a murine model for MS) by sulfatide-specific type II NKT cells, but not type I NKT cells, suggested that sulfatide may act as a self-ligand, activating type II NKT cells during this disease. Moreover, sulfatide administration at the time of induction of EAE leads to decreased IFN- $\gamma$  and IL-4 production by pathogenic autoantigen-reactive T cells and almost completely prevented the disease in WT mice, but not in CD1d-deficient mice.

#### **1.1.7.2 Type 1 Diabetes**

Type 1 diabetes (T1D) results from the T cell-mediated destruction of pancreatic  $\beta$ -cells of the Langerhans' islets. Initial work on the non-obese diabetic (NOD) mouse model has established a protective role of type I NKT cells in T1D.<sup>30</sup> Utilizing 24 $\alpha\beta$  transgenic mice overexpressing a type II NKT cell TCR on the NOD genetic background, it has been shown that type II NKT cells also have a disease regulatory function in this model.<sup>31</sup> Mice overexpressing type II NKT cells were protected from disease, and T1D induced by diabetogenic NOD T cells in transfer models was inhibited by 24 $\alpha\beta$  type II NKT cells demonstrating a dominant protection. Sulfatide is associated with insulin in the  $\beta$ -cells of pancreatic islets of Langerhans, suggesting that sulfatide-specific type II NKT cells might be activated by pancreas-associated sulfatide during the destruction of this tissue. The fact that antibodies to sulfatide are found in patients with T1D but not in healthy individuals nor in patients with type 2 diabetes, suggests that sulfatide induces an immune response in this disease.<sup>32</sup> A recent work provides data supporting that sulfatide-reactive type II NKT cells can ameliorate T1D; sulfatide treatment of NOD mice reduced T1D incidence and islet-specific T cell responses, and further, cells positive for the CD1d-tetramer loaded with sulfatide were found in pancreas-draining lymph nodes in diabetic mice.<sup>33</sup>

#### **1.1.7.3 Ulcerative Colitis**

Ulcerative colitis is an inflammatory bowel disease characterized by superficial mucosal inflammation and tissue destruction in the colon associated with a TH2-skewed cytokine profile. A search for NKT cells in the inflamed tissue of patients with colitis revealed a high frequency of type II NKT cells, and not type I NKT cells.<sup>34</sup> The colitis-associated type II NKT cells produced high amounts of IL-13 upon activation and were cytotoxic for intestinal epithelial cells. Thus, both murine and human studies suggest a proinflammatory role for IL-13 producing NKT cells in colitis.

#### **1.1.7.4 Bone Marrow Transfer and Graft-Versus-Host Disease**

Bone marrow transplantation is an efficient therapy for some haematological malignancies; however, graft-versus-host disease (GVHD) is a serious complication that can follow this treatment. Bone marrow,

together with the liver, is the site where NKT cells are found in the highest proportion among T lymphocytes. Study of GVHD in mice aiming to elucidate immunoregulatory mechanisms demonstrated that type II NKT cells in the bone marrow graft could protect the recipient mice from GVHD. Protection was mediated by type II NKT cell-derived IFN- $\gamma$  that induced apoptosis in donor-derived T cells and IL-4 that skewed the immune response to a protective TH2 profile.<sup>35</sup> In human bone marrow, the type II NKT cells (which are more frequent than type I NKT cells) displayed a TH2-biased cytokine profile and suppressed mixed lymphocyte reactions in vitro.

#### **1.1.7.5 Obesity**

Type II NKT cells have been recently implied in diet-induced obesity, in a study conducted using mice lacking type I NKT cells only, or both type I and type II NKT cells (CD1d-deficient mice). Less body weight gain and development of hepatosteatosis was observed in high fat diet fed CD1d-deficient mice compared both to mice lacking type I NKT cells only and to wild-type mice. Further investigation suggested that type II NKT cells initiated liver and adipose tissue inflammation and aggravated the course of obesity leading to insulin resistance.<sup>36</sup>

#### **1.1.7.6 Hepatitis**

NKT cells are a target for hepatitis treatment, a disease condition characterized by the presence of inflammatory cells and tissues in the liver. Type I NKT cells have been shown to mediate concanavalin A (a lectin carbohydrate binding protein) induced experimental hepatitis. Kumar and co-workers have reported cytokines secreted by type II NKT cells upon sulfatide injection to prevent this type I induced liver damage.<sup>37</sup> The mode of this prevention is through the inactivation of pathogenic type I NKT cells.

#### **1.1.7.7 Other Infectious Diseases**

Recent studies have demonstrated that type II NKT cells have a unique role in infections with the parasite *Trypanosoma cruzi*<sup>38</sup> by promoting an excessive inflammation and mortality, accompanied by decreased pathogen-specific antibody production. Conversely, type I NKT cells prevented the detrimental effects of

type II NKT cells, reducing inflammation and improving mortality and antibody titres. In addition, during murine *Schistosoma mansoni* infection, type I and type II NKT cells had opposing roles whereby type II NKT cells skewed the immune response to the parasite towards decreased IFN- $\gamma$  production and increased TH2 cytokine secretion, while type I NKT cells restored the IFN- $\gamma$  response.

#### **1.1.7.8 Tumor Immunity**

Type I NKT cells have been screened for tumor immunity due to the fact that they can produce cytokines capable of preventing tumor metastasis in mice. In contrast, sulfatide-reactive type II NKT cells released cytokines enhance tumor metastasis by suppressing immunosurveillance (the method employed by the immune system to recognize transformed cells in order to inhibit their growth into neoplastic tissues).<sup>26</sup> Ambrosino *et al.* evaluated sulfatides' stimulatory activity in tumor metastasis using three mice genotypes, J $\alpha$ 18KO mice (only express type II NKT cells not type I NKT cells), WT mice (contain both type I and type II NKT cells) and CD1dKO mice (do not express either NKT cells). The J $\alpha$ 18KO mice showed augmented tumor metastasis while type I NKT cells prevented metastasis. The CD1dKO mice showed no response.

#### **1.1.8 Purpose of Study**

Sulfatides participate in intracellular signaling mechanisms and are presented to the immune system by the CD1 family of antigen-presenting surface proteins. Herein we focus on sulfatides that are presented by CD1d to a subset of Natural Killer T (NKT) cells. While many ligands that activate invariant NKT (*i*NKT) cells (or Type I NKT cells) have been described, few SAR studies have been conducted around sulfatides that activate a subset of Type II NKT cells. With the potential of exploring type II NKT cells for therapeutic purposes based on their vital role in immune responses, the Howell group has focused on the preparation of analogues of the natural glycolipid antigens, combining the structural features of sulfated  $\beta$ -GalCer (sulfatide **4**) and KRN7000 as shown in figure 12.



Working with our collaborators at the NIH, biological analysis on sulfatide **7**, which possesses a double bond in its acyl chain, showed it stimulated a higher secretion of both IFN- $\gamma$  and IL-4 than sulfatide **4**, which has no double bond in its acyl chain. This outcome suggested that the degree of unsaturation in the acyl chain could be important in determining the ability of lipids to stimulate type II NKT cells. This discovery sparked an interest in accessing targets containing double bonds in their acyl chain (Figure 12). In order to evaluate the effect of a higher degree of unsaturation in the acyl chain, sulfatide **10** with an extra double bond in its acyl chain was also synthesized. Furthermore, our group prepared analogs **8**, **9** and **11**, which are phytosphingosine analogs of compounds **4**, **7** and **10** respectively. These analogs (**8**, **9** and **11**) were of interest owing to the ability of phytosphingosine-containing  $\alpha$ -galactosylceramide to activate type I NKT cells (the natural sulfatides that have been reported to activate type II NKT cells have sphingosine bases). These analogs possessing a phytosphingosine are important in determining the role of the sphingosine-phytosphingosine difference in the specificity of these glycolipids for various subsets of NKT cells. One of my goals was to prepare  $\alpha$ -sulfatide **12** to probe the effect of a potential  $\alpha$ -linked sulfatide impurity that may be present in previously synthesized  $\beta$ -sulfatide **7**.

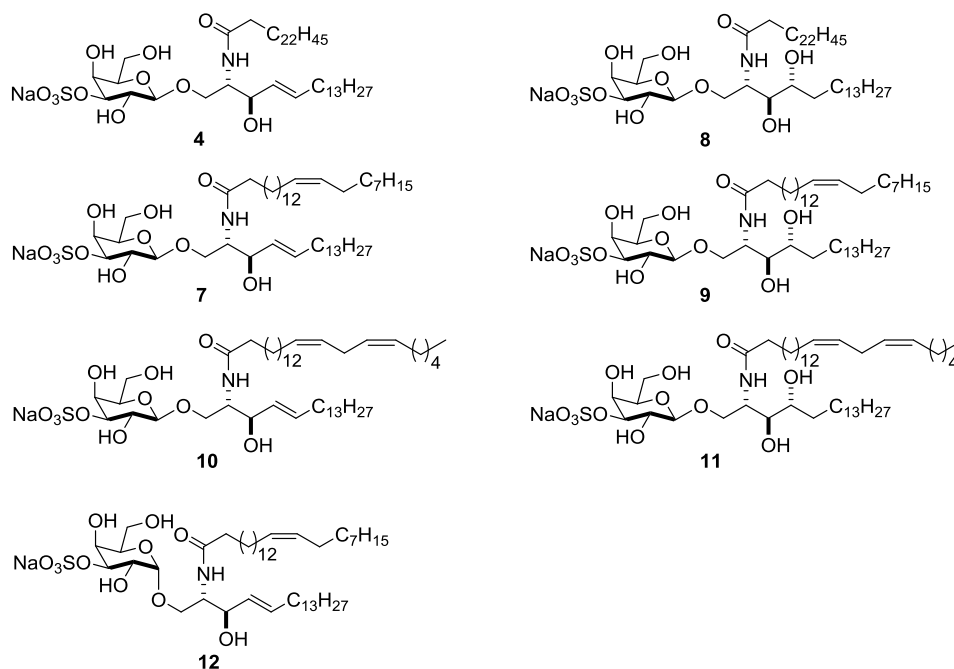


**Figure 12.** Previously synthesized sulfatides

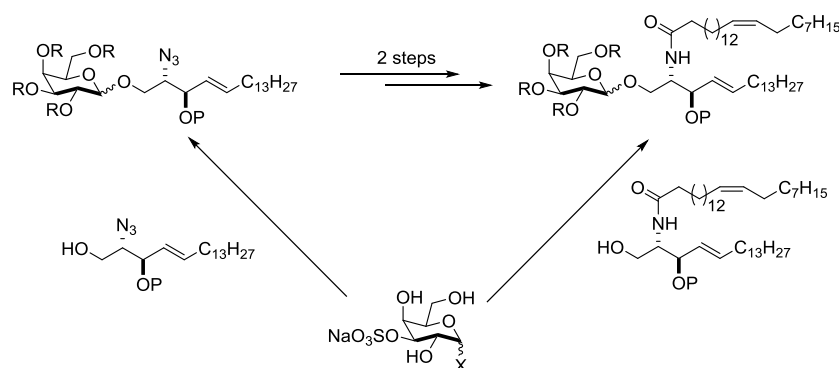


### 1.1.9 Synthetic Strategies

A careful analysis of sulfatide structures reveals that their synthesis requires three different aspects: the preparation of the ceramide acceptor (sphingoid base and acyl chain), the glycosylation reaction with a suitable galactosyl donor and a regioselective sulfation reaction. The construction of the lipid part and of the galactosylceramide (GalCer) scaffold are indeed the most challenging tasks during the preparation, as the sulfation reaction is now well established. Lately, much effort has been focused on the synthesis and glycosylation of sphingosine and ceramides as a consequence of the extensive studies on the activation of the immune system mediated by CD1 proteins.<sup>41</sup> The following sections will describe approaches utilized to accomplish the two key steps (glycosylation and sulfation reaction) in the preparation of sulfatides.

#### 1.1.9.1 The Glycosylation Reaction

The formation of the glycosidic bond between a carbohydrate and ceramide or sphingoid base is the key step in the synthesis of glycosphingolipids. A variety of glycosyl donors have been utilized, including glycosyl trichloroacetamides, fluorides, phosphates and sulfides.<sup>42</sup> Nevertheless, the glycosylation reaction is still one of the main challenges in the synthesis, because glycosylations of ceramides are generally plagued by low yields.<sup>43</sup> This problem has been attributed to the low nucleophilicity of ceramides. Among others, the use of azido-sphingosine instead of ceramides has been applied to circumvent this challenge (Scheme 1).<sup>44</sup>



**Scheme 1.** Glycosylation approaches

One of the most pertinent factors to consider in glycoconjugate synthesis is the control of stereochemical outcome in the glycosylation. The strategic choice relies mainly in the type of acceptor used in the glycosylation, either sphingoid base or ceramide, and in the selection of the proper galactosyl donor. The formation of the 1,2-*cis* glycosidic bond ( $\alpha$ -glycosidic bond) linkages can be achieved by working under thermodynamic conditions (anomeric effect), in appropriate solvents (ethereal solvent effect),<sup>45</sup> and by using non-participating protecting groups at the C-2 hydroxyl, typically benzyl groups. Solvent manipulations have been successful in favoring  $\alpha$ -anomers and have been extensively utilized in the synthesis of  $\alpha$ -glycosphingolipids (KRN7000 and analogs).

1,2-*trans* Glycosidic bonds ( $\beta$ -glycosidic bond) can be readily accessed by taking advantage of neighboring group assistance by ester protecting groups such as *O*-acetyl or *O*-benzoyl at C-2 of galactose. This principle is known as anchimeric assistance, also referred to as neighboring group participation, and is a common strategy utilized in carbohydrate chemistry to give  $\beta$ -selectivity. During the glycosylation processes, the neighboring acyl group of the donor assists in the departure of an activated leaving group and subsequently leads to the formation of a more stable dioxolenium ion. Consequently, the glycosyl acceptor can only attack from the backside to form  $\beta$ -glycoside (Figure 15).

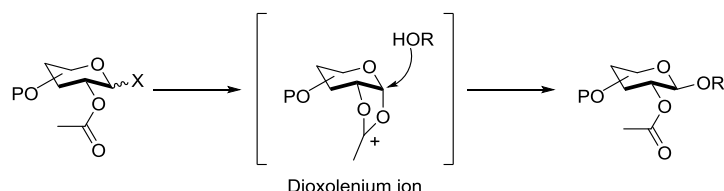


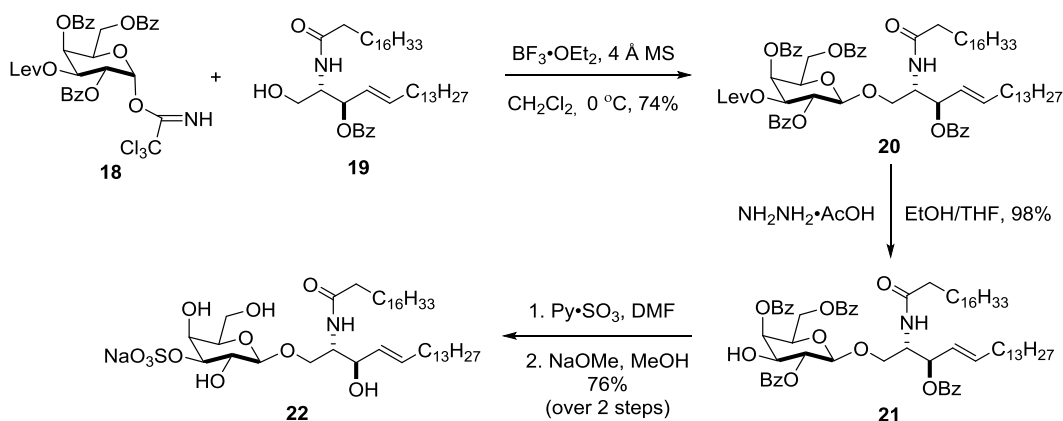
**Figure 15.** Anchimeric assistance to enhance  $\beta$ -selectivity

### 1.1.9.2 The Sulfation Reaction

The presence of the sulfate group at the C3-OH position of the galactose unit is the characterizing element which differentiates sulfatides from other glycolipids. Therefore, regioselective installation of the sulfate group at the C3-OH position of the galactose unit is a critical step in sulfatide synthesis. Due to the fact

that the sulfate moiety is acid sensitive, its installation always takes place in the late stages of the synthesis.

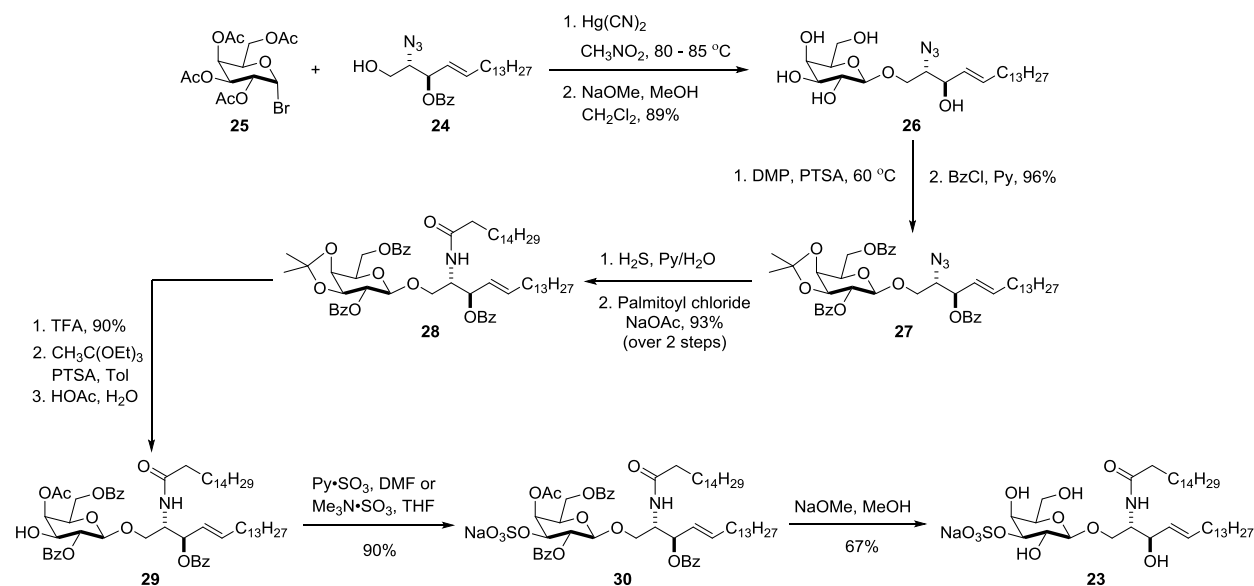
Traditional methods for regioselective installation of a sulfate moiety relied on protecting group manipulation strategies. Tanahashi and co-workers demonstrated the synthesis of various sulfatides as selectin ligands/inhibitors via glycosylation utilizing a ceramide as a glycosyl acceptor, followed by protecting group manipulation to insert the sulfate group at the C3-OH position (Scheme 2).<sup>46</sup> Their synthetic work involved coupling of trichloroacetimidate donor **18** (prepared using at least three orthogonal protecting groups) with ceramide acceptor **19** to give **20**. Selective removal of the levulinoyl (Lev) protecting group gave **21**. Sulfation of the C3-OH with sulfur trioxide pyridine (Py•SO<sub>3</sub>) complex, followed by cleavage of the benzoyl groups, gave the desired sulfatide **22**.



**Scheme 2.** Tanahashi's synthesis of sulfatide **22**

A similar strategy was employed by Marinier *et al.* in the synthesis of sulfatide **23** utilizing azidosphingosine (**24**) as the glycosyl acceptor (Scheme 3).<sup>47</sup> Helferich glycosylation conditions were used to couple the bromo galactose donor **25** with acceptor **24** to give the  $\beta$ -glycoside. Global cleavage of the acetyl and benzoyl protecting groups gave azido-glycolipid **26**. Protection of the C3- and C4-*cis* hydroxyl groups using 2,2-dimethoxypropane, followed by benzoyl protection of the remaining hydroxyl groups, gave glycolipid **27**. Azide reduction, followed by *N*-acylation, provided **28**. Cleavage of the 2,2-dimethoxypropane group, followed by acetate protection of the C4-OH via an orthoester, gave the free

C3-OH product **29**. This compound underwent sulfation with either trimethylamine sulfur trioxide ( $\text{Me}_3\text{N}\cdot\text{SO}_3$ ) complex or sulfur trioxide pyridine ( $\text{Py}\cdot\text{SO}_3$ ) complex to give **30**. Removal of all protecting groups provided the desired product **23**.



**Scheme 3.** Marinier's synthesis of sulfatide **23**

Arguably, the most straightforward and well-established selective sulfation protocol utilizes the treatment of deprotected galactoside with dibutyltin oxide and the reactive sulfation reagent, sulfur trioxide-trimethylamine complex ( $\text{Me}_3\text{N}\cdot\text{SO}_3$ ). This strategy was first pioneered by Flitsch and co-workers,<sup>48</sup> and it allows for the presence of other common functional groups in the system. The methodology relies on the almost exclusive formation of the five membered cyclic dibutylstannylene acetal with the C-3 and C-4 *cis* hydroxyl groups after the addition of dibutyltin oxide to the deprotected galactoside (Figure 16). Under these conditions, the nucleophilicity of the equatorial 3-OH group is enhanced towards acylation, alkylation and even silylation. Therefore, the introduction of dibutylstannylene acetal to the reactive sulfation reagent ( $\text{Me}_3\text{N}\cdot\text{SO}_3$ ) gives almost exclusively the 3-*O*-sulfated derivative with no sulfation at the ceramide allylic hydroxyl group. This sulfation protocol is now the most widely used in the synthesis of sulfatides and is applied here in both syntheses.

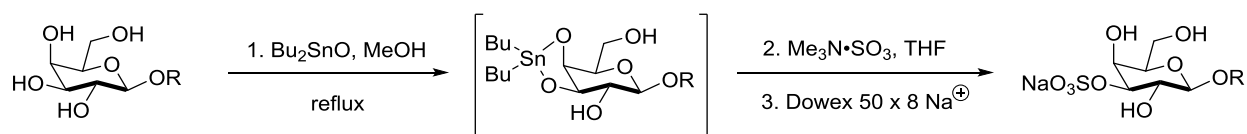


**Figure 16.** A model of Flitsch's regioselective sulfation of deprotected galactoside

### 1.1.10 Summary

Sulfatides are among the most ubiquitous endogenous acidic glycolipids found in mammalian membranes. They exist in various isoforms with different physicochemical properties. The immunostimulatory activity of sulfatides has sparked interest in their isolation from human cells and in the evaluation of their role in type II NKT cell activation as testified by an increasing number of literature reports. This work focuses on the syntheses of two unnatural sulfatides differing in the sphingoid base to provide our collaborators at NIH with tools to better understand the role of these sulfatide-reactive type II NKT cells and, ultimately, to harness their activation for therapeutic applications.

## 1.2 Results and Discussion

### 1.2.1 Research Objective

The specific aim of this work was to synthesize two unnatural sulfatides: 1)  $\alpha$ -sulfatide **12**, motivated by the need to probe the effect of potential  $\alpha$ -linked sulfatide impurity present in the previously synthesized  $\beta$ -sulfatide **7** and 2)  $\beta$ -sulfatide **17** motivated by a highly stimulatory related  $\alpha$ -linked plakoside A derivative (**16**) that showed strong interaction with CD1d.

### 1.2.2 Synthesis of $\alpha$ -Sulfatide **12**

The plan to access  $\alpha$ -linked sulfatide **12** was to utilize azido-sphingosine **31** and 2,3,4,6-tetra-*O*-tetramethylsilyl- $\alpha$ ,D-galactopyranosyl iodide (**32**) as the key building blocks in the synthesis. Both **31** and **32** could be obtained from commercially available *D-ribo*-phytosphingosine **33** and D-galactose respectively. Condensation of **31** with **32** followed by cleavage of the protecting groups should give glycoside **34**. Reduction of the azide followed by *N*-acylation with activated *cis*-15-tetracosenoic fatty

acid **35** will provide galactosylceramide **36**. The key step will be achieved by selective sulfation of the desired hydroxyl group on the sugar residue of galactosylceramide **36** using the stannylene methodology described in section 1.1.8.2 to give 3'-sulfated  $\alpha$ -galactosyl ceramide **12** (Figure 17).

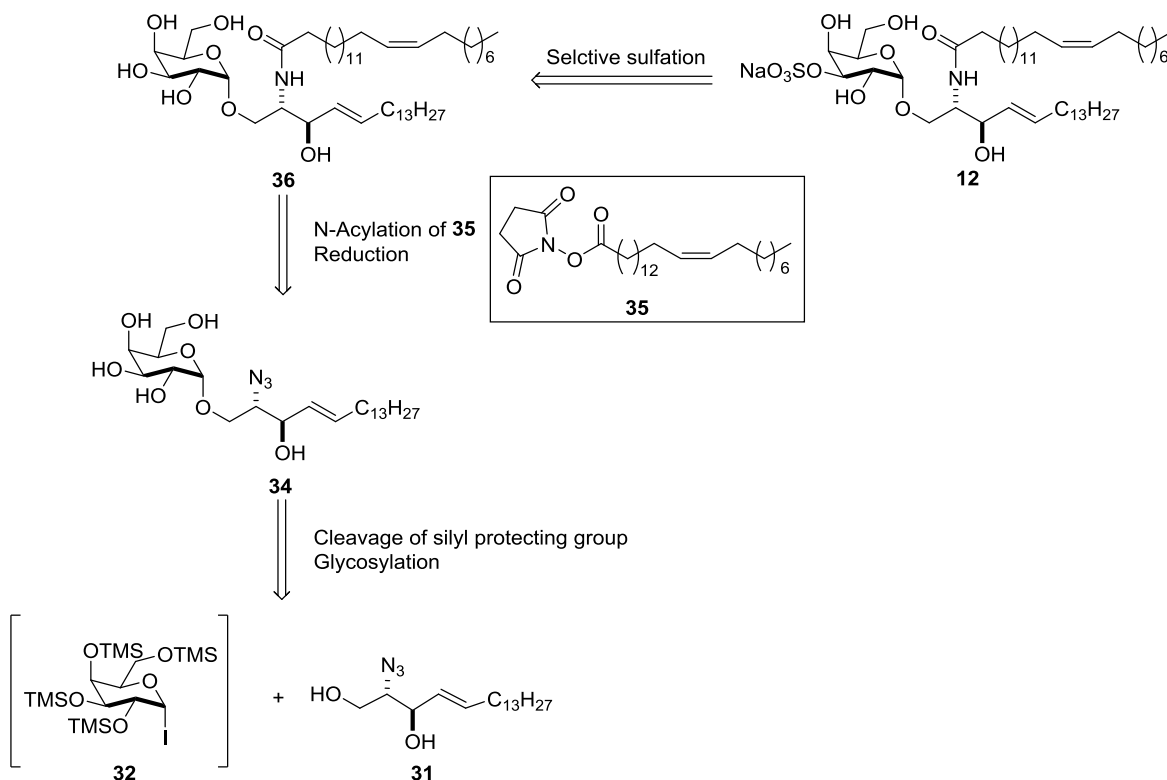


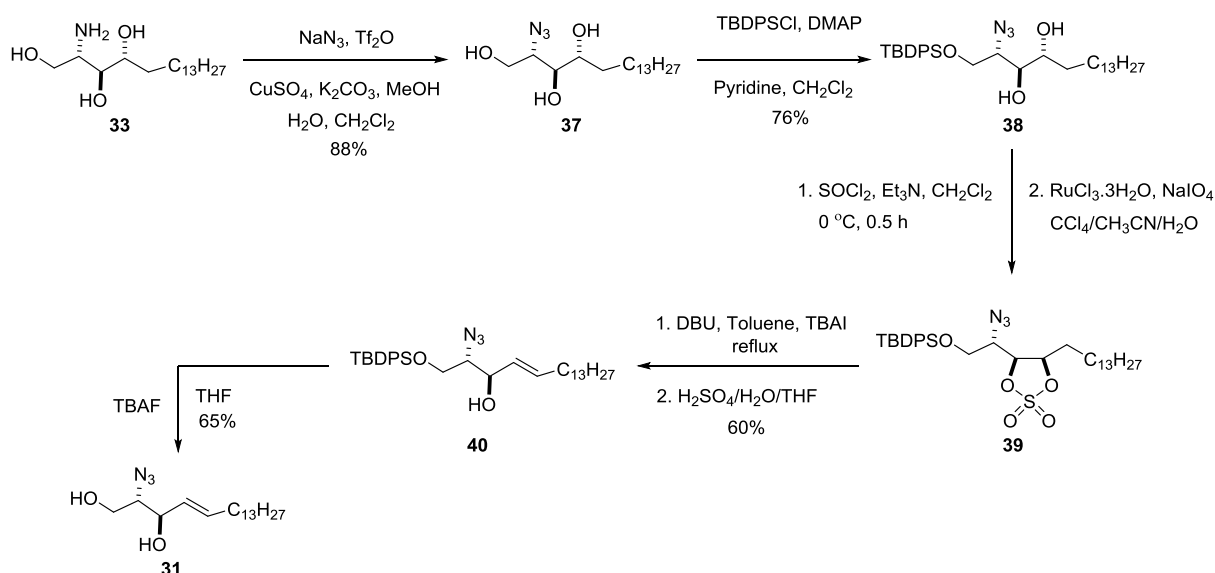
**Figure 17.** Synthetic strategy to  $\alpha$ -sulfatide **12**

### 1.2.2.1 Synthesis of Azidosphingosine **31**

Azidosphingosine **31** was synthesized from *D*-ribo-phytosphingosine (**33**) following a procedure reported by Kim *et al.*<sup>49</sup> The synthesis commenced with the protection of the amine functional group and the primary hydroxyl group of *D*-ribo-phytosphingosine (**33**). The amine was protected by converting it to the corresponding azide **37** following a methodology developed by Wong *et al.*<sup>50</sup> The amine-azide interconversion proceeded via a diazo transfer reaction of the amine with  $\text{TiF}_3\text{N}$ , generated *in situ* from  $\text{NaN}_3$  and  $\text{TiF}_2\text{O}$ . The primary alcohol was protected selectively as its silyl ether using *tert*-butyldiphenylsilyl chloride (TBDPSCl) to give diol **38**. The free diols in **38** were activated with thionyl chloride to give the cyclic sulfite, which was oxidized with a catalytic amount of ruthenium (III) chloride



hydrate ( $\text{RuCl}_2 \cdot 3\text{H}_2\text{O}$ ) to give cyclic sulfate **39**. Opening of **39** with tetrabutylammonium iodide ( $\text{Bu}_4\text{NI}$ ), followed by 1,8-Diazabicyclo[5.4.0]undec-7-ene (DBU) promoted elimination, gave a sulfated olefin. Subsequent hydrolysis with aqueous  $\text{H}_2\text{SO}_4$  gave desired allylic alcohol **40** with complete *E*-selectivity. The cleavage of the silyl group with *tetra*-*n*-butylammonium fluoride (TBAF) furnished the desired azido-sphingosine acceptor **31** in 65% isolated yield.<sup>49</sup>

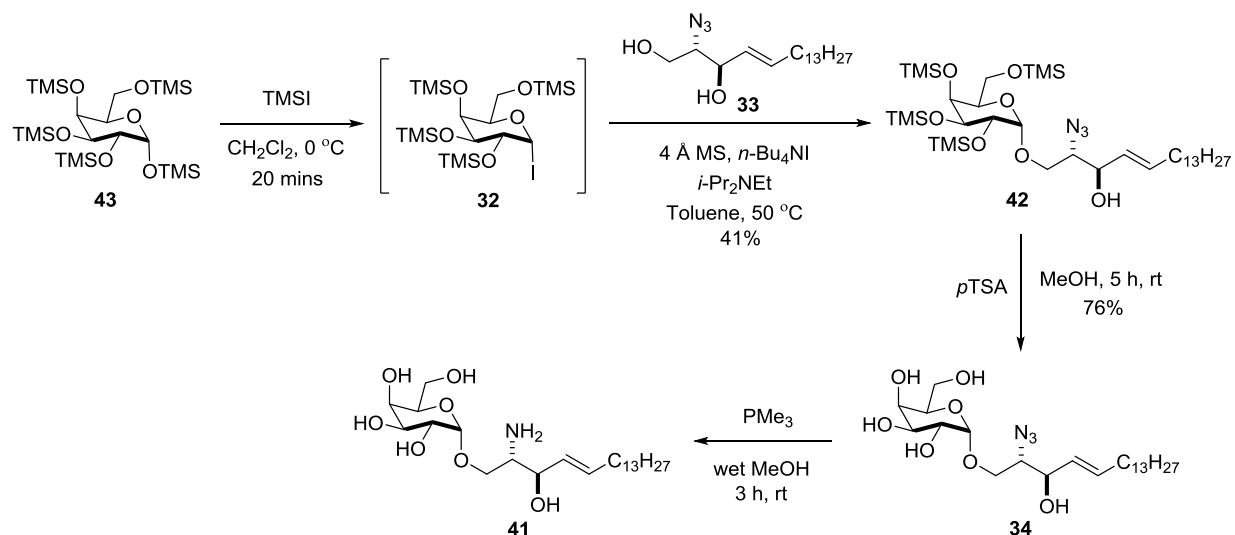


**Scheme 4.** Synthesis of azido-sphingosine acceptor **31**

#### 1.2.2.2 Synthesis of $\alpha$ -Glycoside **41**

Due to the fact that the formation of the glycosidic bond between a carbohydrate and ceramide or sphingoid base is the key step in the synthesis of glycosphingolipids, the choice of both glycosyl donor and acceptor plays a crucial role in determining the stereochemical outcomes. With the aim to achieve  $\alpha$ -selectivity, the glycosylation protocol developed by Gervay-Hague, which potentially provides straightforward access to  $\alpha$ -glycosides in high yields and with complete  $\alpha$ -selectivity was explored.<sup>51</sup> According to this procedure, transient TMS-protected glycosyl iodide **32** is reacted with fully functionalized and unprotected azido-sphingosine **31**. TBAI was utilized to enhance in situ anomerization of  $\alpha$ -glycosyl iodide **32** to the corresponding  $\beta$ -iodide, which is more reactive and which subsequently undergoes  $\text{S}_\text{N}2$ -like displacement, affording  $\alpha$ -glycosides almost quantitatively. This technology allows

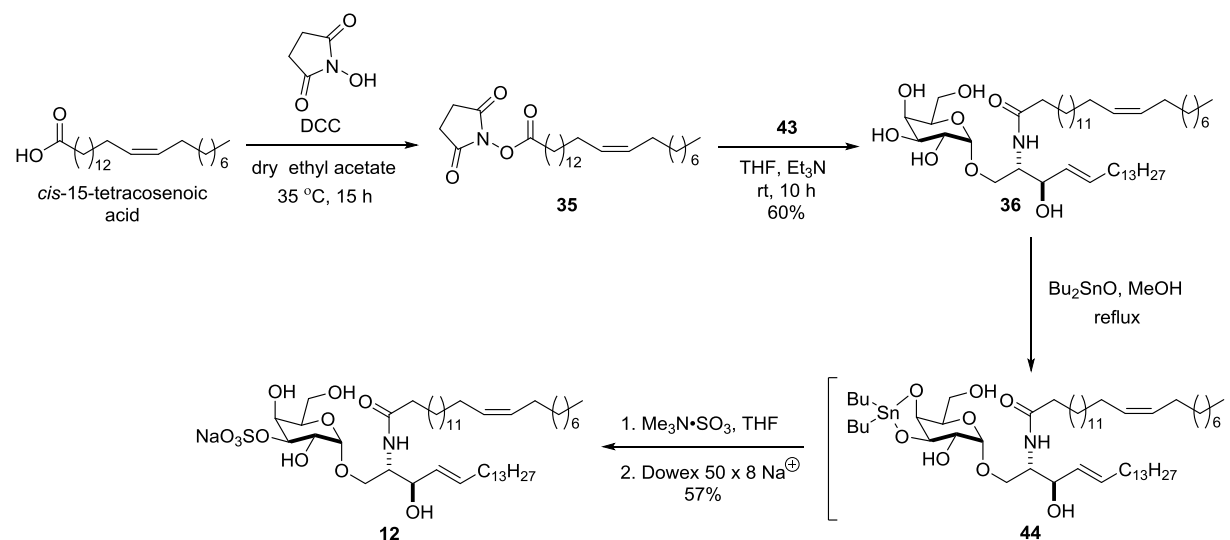
for the presence of other functional groups such as esters, amides and alkenes. Furthermore, the trimethylsilyl protecting group is readily removed upon exposure to *p*-toluenesulfonic acid (PTSA). We applied this protocol to azido-sphingosine acceptor **31**, conducting glycosylation as shown (Scheme 5). Cleavage of the silyl protecting groups of **42** gave free glycolipid **34** which was then subjected to trimethylphosphine (Pme<sub>3</sub>) azide reduction to give free amino-glycolipid **41**. This was utilized in the subsequent *N*-acylation step without purification.



**Scheme 5.** Synthesis of  $\alpha$ -glycoside **41**

### 1.2.2.3 *N*-Acylation and Selective Sulfation

*N*-Acylation of **41** with activated *cis*-15-tetracosenoic acid (**35**) gave intermediate **36**, which was then subjected to Flitsch's protocol for regioselective sulfation of the C3-OH of the galactose unit.<sup>48</sup> Glycolipid **36** was refluxed with Bu<sub>2</sub>SnO in MeOH to give cyclic dibutylstannylene acetal **44**. Treatment of **44** with Me<sub>3</sub>N•SO<sub>3</sub> complex provided desired  $\alpha$ -sulfatide **12** (Scheme 6).



**Scheme 6.** Synthesis of  $\alpha$ -sulfatide **12**

### 1.2.3 Synthesis of $\beta$ -sulfatide **17**

Our synthetic plan for the preparation of  $\beta$ -sulfatide **17** was to carry out an *N*-acylation between sphinganine **45** and activated fatty acid **35**, followed by protecting group manipulation to form ceramide acceptor **46**. Sphingoid base **45** could be obtained in eleven total steps from commercially available 1,7-heptanediol **49**. The glycosylation reaction between galactose unit **47** (obtained in 4 steps from commercially available D-galactose) with ceramide acceptor **46**, followed by global cleavage of all protecting groups should provide  $\beta$ -glycoside **48**. A final selective sulfation of the 3-OH of galactose unit would give the desired  $\beta$ -sulfatide **17** (Figure 18).

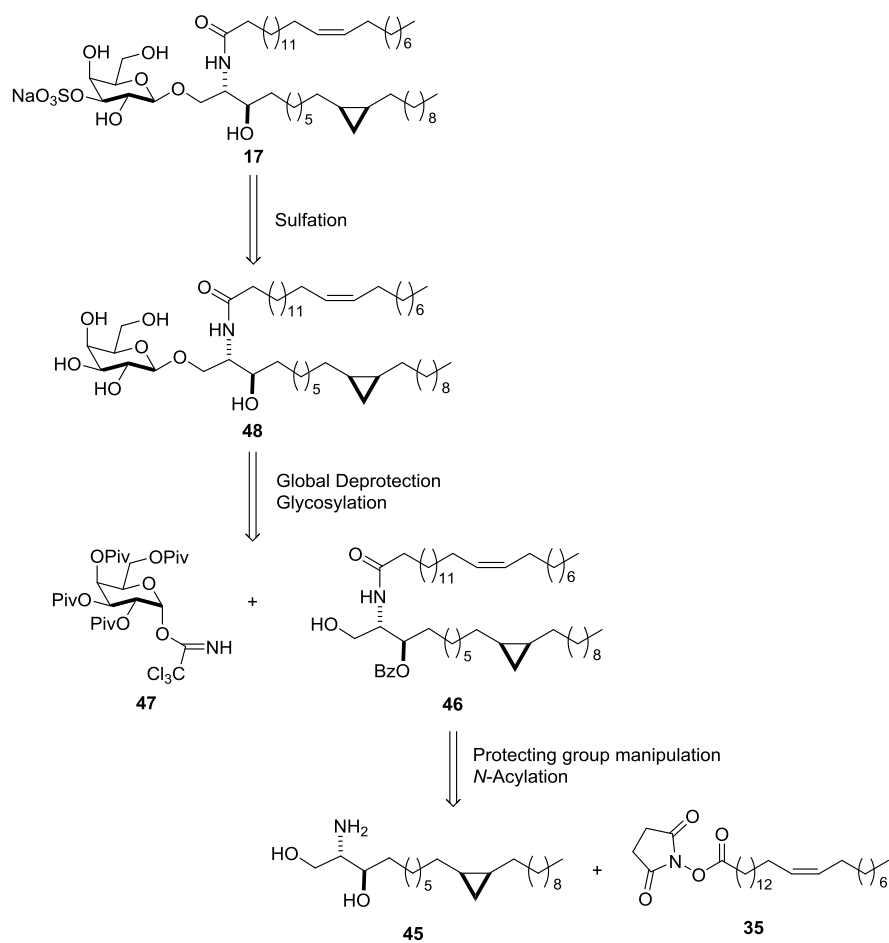
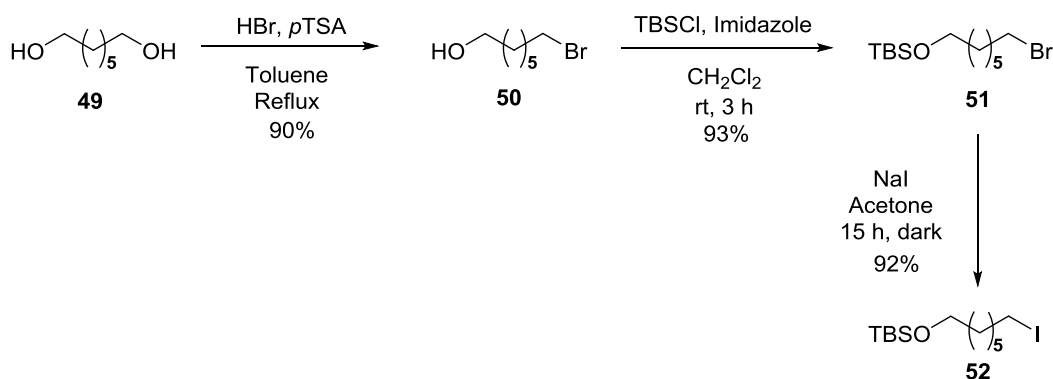


**Figure 18.** Synthetic strategy to  $\beta$ -sulfatide **17**

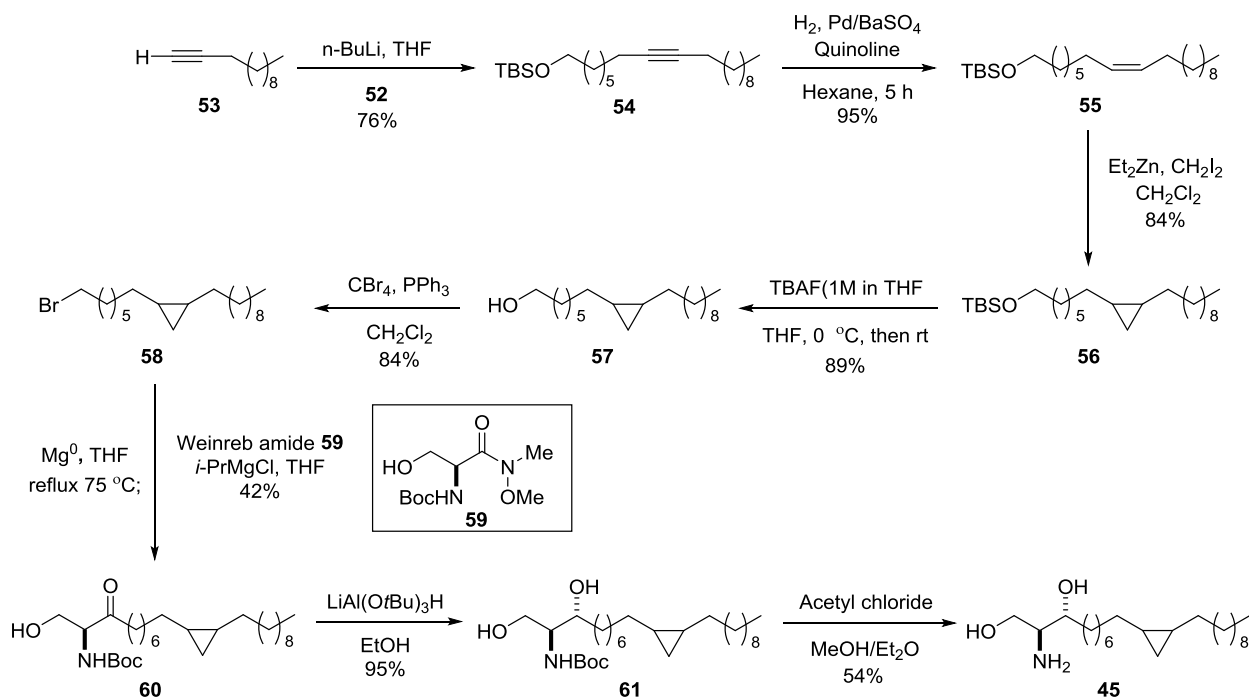
### 1.2.3.1 Synthesis of Sphinganine **45**

The synthesis of sphinganine **45** commenced with monobromination of commercially available 1,7-heptanediol (**49**) to give bromo-alcohol **50**. Protection of the primary alcohol as its silyl ether gave compound **51**. The substitution of the bromide to Finkelstein reaction conditions gave iodide **52** (Scheme 7)



**Scheme 7.** Synthesis of iodide **52**

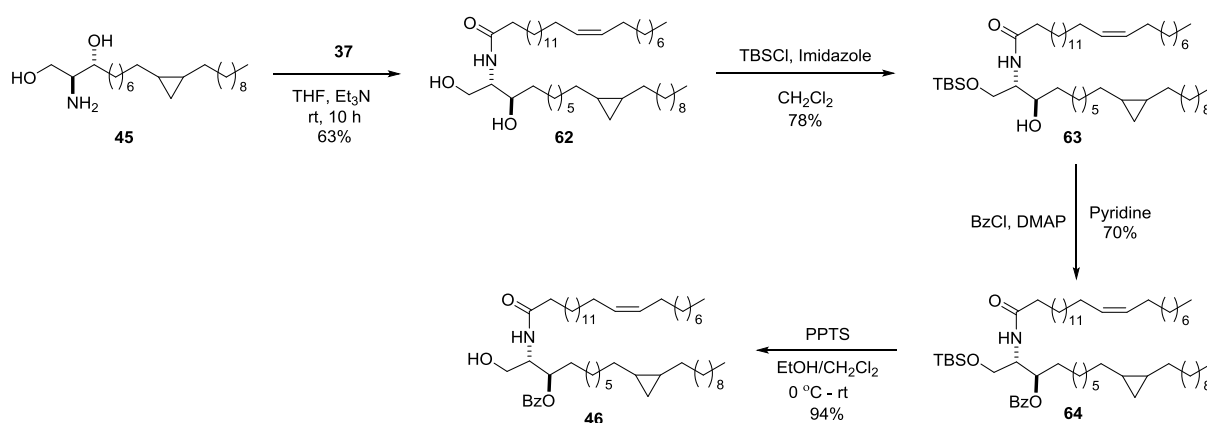
Starting with commercially available 1-dodecyne (**53**), the synthesized iodide **52** was subjected to an iodide-alkyne coupling reaction mediated by *n*-butyllithium to give alkyne **54**. Hydrogenation under palladium on carbon catalysis poisoned with traces of lead and quinolone (Lindlar's catalyst)<sup>52</sup> gave the *Z*-isomer of alkene **55**. Alkene **55** was then subjected to Simmons-Smith cyclopropanation reaction<sup>53</sup> conditions using highly inflammable diethyl zinc and diiodomethane in dichloromethane, yielding cyclopropane **56**. Cleavage of the silyl group using TBAF gave alcohol **57** which was then converted to bromide **58** utilizing Appel's bromination reaction conditions.<sup>54</sup> The bromide was then used in a Grignard reaction whereby it was reacted with magnesium metal in THF under reflux to form an alkyl magnesium bromide.<sup>55</sup> The resultant Grignard product was immediately reacted with serine derived Weinreb amide **59** to give carbamate protected aminoketone **60**. As demonstrated by Hoffman *et al.*, diastereoselective reduction of aminoketone **60** using lithium *tri-tert*butoxyaluminum hydride gave the *anti*-carbamate protected amino alcohol **61**.<sup>55</sup> Cleavage of the *t*-butyl carbamate using *in-situ* generated HCl from acetyl chloride in a mixture of ethanol and ethyl ether gave sphinganine **45** in 54% isolated yield (Scheme 8).



**Scheme 8.** Synthesis of sphinganine **45**

### 1.2.3.2 Synthesis of Ceramide Acceptor **46**

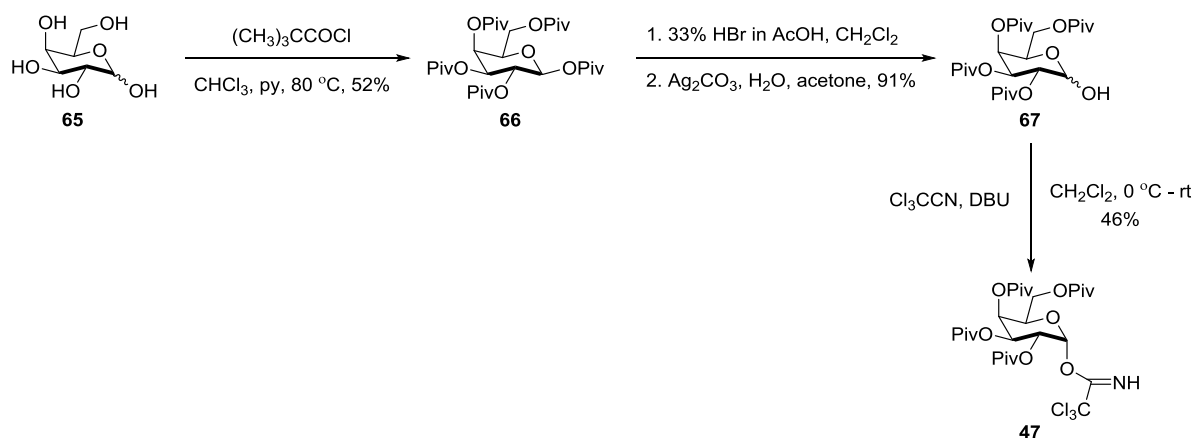
Having synthesized sphinganine **45**, we directed our effort towards the preparation of the appropriate ceramide acceptor **46** in readiness for the glycosylation reaction. In this synthesis, the choice of hydroxyl protecting groups is of great significance in order to avoid their cleavage and/or migration. The sphinganine (**45**) was first subjected to *N*-acylation with activated *cis*-15-tetracosenoic fatty acid **35** to obtain ceramide **62**. The primary alcohol in **62** was then protected using a silyl group while the secondary alcohol was protected using a benzoyl protecting group to yield compound **64**. An attempt to cleave the silyl group selectively, using *tert*-butyl ammonium fluoride (TBAF) or using *in-situ* generated HCl from acetyl chloride in MeOH/H<sub>2</sub>O, resulted in the migration of the benzoyl protecting group from the secondary alcohol to the primary alcohol. To circumvent the benzoyl migration, we decided to employ pyridinium *p*-toluenesulfonate (PPTS), a weakly acidic catalyst. To our delight, the reaction gave the desired ceramide **46** with no migration of the benzoyl group (Scheme 9).



**Scheme 9.** Synthesis of benzoyl-protected ceramide acceptor **46**

### 1.2.3.3 Synthesis of Pivaloyl-protected Trichloroacetimidate Sugar **47**

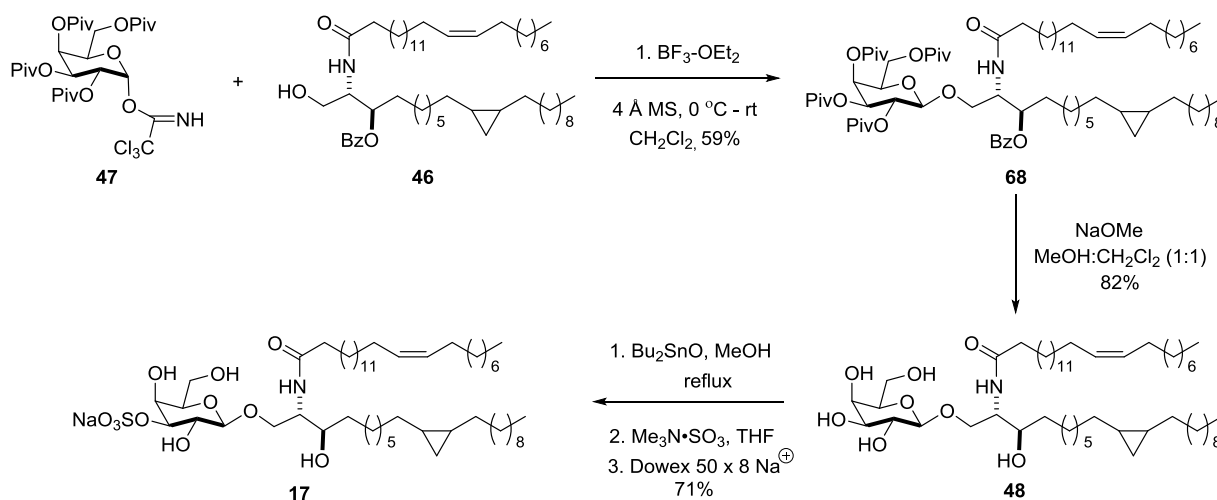
Pivaloyl-protected trichloroacetimidate sugar **47** was chosen as the sugar donor because of the successes reported in the literature in obtaining  $\beta$ -selectivity and the ease of activating the trichloroacetimidate group under mildly acidic conditions.<sup>56</sup> Its synthesis, which was carried out by Dr. Stewart K. Richardson (a senior member of the Howell group), involved an initial global protection of D-galactose **65** to give **66** (Scheme 10).<sup>57</sup> Cleavage of the anomeric pivaloyl group can be achieved via a two-step hydrolysis, as employed by Menger and Mbadugha in the cleavage of an anomeric benzoyl-protected sugar, to give lactol **67**.<sup>58</sup> Pentapivaloyl galactose **66** was first treated with HBr (33% in AcOH) to give a bromo sugar, which was then reacted with Ag<sub>2</sub>CO<sub>3</sub> in aqueous acetone to give lactol **67**. Activation of lactol **67** using trichloroacetonitrile and DBU gave trichloroacetimidate sugar donor **47** (Scheme 10).



**Scheme 10.** Synthesis of sugar donor **47**

#### 1.2.3.4 Glycosylation and Selective Sulfation

Sugar donor **47** and acceptor **46** were coupled in the presence of  $\text{BF}_3 \cdot \text{OEt}_2$  as an activator to give glycolipid **68** along with traces of its  $\alpha$ -isomer. The  $\alpha$ -isomer was readily separated via column chromatography providing  $\beta$ -product **68**. Global cleavage of all protecting groups of **68** gave the free glycoside **48**, which was then subjected to Flitsch's protocol for regioselective sulfation of the C3-OH of the galactose unit to give the desired  $\beta$ -sulfatide **17** (scheme 11).



**Scheme 11.** Synthesis of  $\beta$ -sulfatide **17**

In summary we have completed the synthesis of two sulfatides (**12** and **17**).  $\alpha$ -Sulfatide **12** was prepared in 14 steps from commercially available phytosphingosine and  $\beta$ -sulfatide **17** was prepared in 18 steps



from commercially available 1,7-heptanediol (**49**). These compounds have been sent to our collaborators at the National Cancer Institute for investigation of the role of sulfatide-reactive type II NKT cells for therapeutic applications.

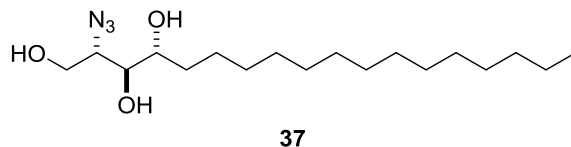
### 1.3 Experimental

#### 1.3.1 General Information

All moisture sensitive reactions were run in a flame-dried flask under N<sub>2</sub>. Tetrahydrofuran (THF) was dried using a J. C. Meyer Solvent Dispensing System (SDS) and dispensed under N<sub>2</sub>. All other solvents were dried over CaH<sub>2</sub> or 4 Å molecular sieves. Deuterated chloroform (CDCl<sub>3</sub>), was dried over 4 Å molecular sieves. All starting materials and reagents were purchased from commercial sources and used as received. All <sup>1</sup>H NMR experiments were recorded on a 400 MHz spectrometer. All <sup>13</sup>C NMR experiments were recorded at 100 MHz. Chemical shifts (δ) are given in ppm, and coupling constants (*J*) are given in Hz. The 7.26 resonance of residual CHCl<sub>3</sub> for proton spectra and the 77.23 ppm resonance of CDCl<sub>3</sub> for carbon spectra were used as internal references. High resolution mass spectroscopy (HRMS) was performed on a TOF instrument with ESI in positive ionization mode.

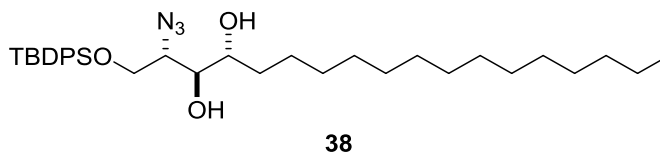
Unless otherwise stated, reaction progress was monitored by thin layer chromatography (TLC) performed on glass plates coated with silica gel UV254. Visualization was achieved by ultraviolet light (254 nm), 0.5% KmnO<sub>4</sub> in 0.1 M aqueous NaOH solution and/or 5% phosphomolybdic acid in ethanol. Column chromatography was performed using silica gel, 40 microns flash silica.

#### 1.3.2 Synthesis of α-sulfatide **12**



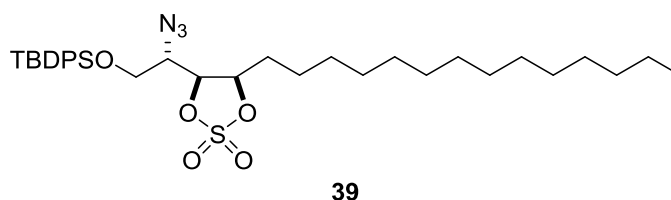
**(2*S*,3*S*,4*R*)-2-Azido-octadecan-1,3,4-triol (37).** TfN<sub>3</sub> was freshly prepared prior to the reaction as follows: DCM (82 mL) was added to a stirred solution of NaN<sub>3</sub> (19.7 g, 301 mmol) in H<sub>2</sub>O (50 mL) at 0

°C, then Tf<sub>2</sub>O (10.0 mL, 60.2 mmol) was added dropwise over 15 min with vigorous stirring of the mixture. The flask was left open and the mixture stirred at 0 °C for 2 h. The reaction was stopped by careful addition of saturated NaHCO<sub>3</sub> (150 mL), while stirring until gas evolution ceased. The organic layer was separated, and the aqueous layer was extracted with DCM (2 x 100 mL). The combined organic layers were used in the subsequent step. K<sub>2</sub>CO<sub>3</sub> (6.2 g, 45.0 mmol) and CuSO<sub>4</sub> (75 mg, 0.30 mmol) in H<sub>2</sub>O (100 mL) and a solution of triflyl azide in DCM (~60 mmol, 300 mL) were added to a stirred suspension of *D-ribo*-phytosphingosine (**33**) (9.6 g, 30.1 mmol) in MeOH (300 mL). Stirring was continued for 18 h. The reaction was stopped by addition of H<sub>2</sub>O (400 mL). The organic phase was separated, and the aqueous layer was extracted with EtOAc (3 x 200 mL). The combined organic extracts were dried (MgSO<sub>4</sub>) and then concentrated, after which a white solid was collected. Purification by flash column chromatography on silica gel (EtOAc/hexane 9:1) provided **37** as white crystals (10.1 g, 97%):<sup>49</sup> <sup>1</sup>H NMR (400 MHz, CDCl<sub>3</sub>/CD<sub>3</sub>OD 3:1) δ 3.78 (dd, *J* = 11.8, 4.3 Hz, 1H), 3.64 (dd, *J* = 11.7, 5.9 Hz, 1H), 3.51–3.44 (m, 2H), 3.39 (ddd, *J* = 5.4, 5.4, 5.4 Hz, 1H), 1.50–1.34 (m, 2H), 1.32–1.05 (m, 24H), 0.72 (t, *J* = 6.6 Hz, 3H); <sup>13</sup>C NMR (100 MHz, CDCl<sub>3</sub>/CD<sub>3</sub>OD 3:1) δ 74.4, 72.0, 63.8, 61.4, 32.1, 31.8, 29.6, 29.3, 25.7, 22.6, 13.9.

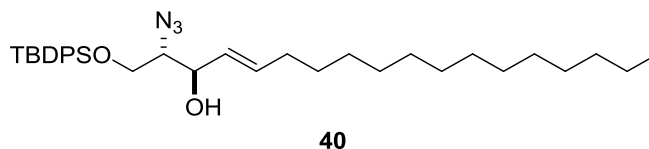


**(2*S*,3*S*,4*R*)-2-Azido-1-(*tert*-butyldiphenylsilyloxy)octadecan-3,4-diol (**38**).** Dimethylaminopyridine (DMAP) (0.084 g, 0.69 mmol) was added to a mixture of (2*S*,3*S*,4*R*)-2-azido-octadecan-1,3,4-triol (**37**) (4.72 g, 13.7 mmol) and chlorodiphenyl-*t*-butylsilane (4.53 g, 16.5 mmol) in pyridine (15 mL) and DCM (70 mL) at 0 °C. The reaction was stirred for 24 h, diluted with EtOAc (50 mL) and washed with brine (100 mL). The aqueous layer was extracted with EtOAc (2 x 70 mL). The combined organic extracts were dried (Na<sub>2</sub>SO<sub>4</sub>) and concentrated. Purification by flash column chromatography on silica gel (hexanes/EtOAc 17:3) provided **38** as a pale yellow oil (7.90 g, 98%):<sup>49</sup> <sup>1</sup>H NMR (400 MHz, CDCl<sub>3</sub>) δ

7.74–7.68 (m, 4H), 7.49–7.38 (m, 6H) 4.05 (dd,  $J = 11.0, 4.1$  Hz, 1H), 3.93 (dd,  $J = 11.0, 5.8$  Hz, 1H), 3.72–3.66 (m, 2H), 3.61–3.55 (m, 1H), 1.61–1.38 (m, 3H), 1.37–1.24 (m, 23H), 1.10 (s, 9H), 0.90 (t,  $J = 6.6$  Hz, 3H);  $^{13}\text{C}$  NMR (100 MHz,  $\text{CDCl}_3$ )  $\delta$  135.8, 135.8, 132.8, 132.7, 130.2, 128.1, 74.3, 72.6, 64.4, 63.7, 32.1, 32.0, 29.9, 29.9, 29.8, 29.8, 29.6, 27.0, 25.9, 22.9, 19.3, 14.3.

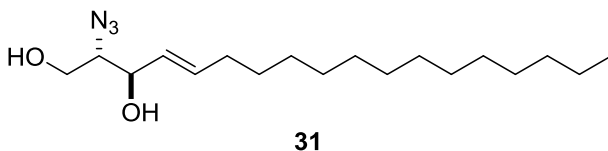


**(2*S*,4*S*,5*R*)-[2-Azido-2-(2,2-dioxo-5-tetradecyl-2 $\lambda^6$ -[1,3,2]dioxathiolan-4-yl)ethoxy]-*tert*-butyldiphenylsilane (39).**  $\text{Et}_3\text{N}$  (6.29 mL, 45.3 mmol) and thionyl chloride (2.20 mL, 30.2 mmol) were added to a solution of (2*S*,3*S*,4*R*)-2-azido-1-(*tert*-butyldiphenylsilyloxy)octadecan-3,4-diol (**38**) (8.81 g, 15.1 mmol) in DCM (80 mL) at 0 °C. After 30 min, the reaction mixture was poured into brine (70 mL) and extracted with EtOAc (3 x 70 mL). The organic extracts were dried ( $\text{Na}_2\text{SO}_4$ ) and concentrated. The crude cyclic sulfite was dried in vacuo for 3 h and then dissolved in a mixture of  $\text{CCl}_4/\text{CH}_3\text{CN}/\text{H}_2\text{O}$  (102 mL, 1:1:1) while stirring.  $\text{RuCl}_3 \cdot 3\text{H}_2\text{O}$  (0.47 g, 2.27 mmol) and  $\text{NaIO}_4$  (9.69 g, 45.3 mmol) were added to the resulting solution. After this reaction mixture was stirred at rt for 2 h, it was diluted with EtOAc (100 mL) and washed with saturated aqueous  $\text{NaHSO}_3$  (150 mL). The organic layer was dried ( $\text{Na}_2\text{SO}_4$ ) and concentrated to give **39** as a colorless oil (12.4 g) which was utilized in the subsequent step without further purification.

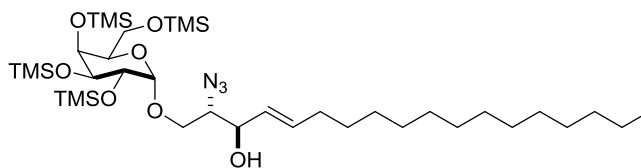


**(2*S*,3*R*,4*E*)-2-Azido-1-(*tert*-butyldiphenylsilyloxy)octadec-4-en-3-ol (40).**  $\text{Bu}_4\text{NI}$  (9.3 g, 28.8 mmol) and DBU (4.3 mL, 28.8 mmol) were added to a solution of (2*S*,4*S*,5*R*)-[2-azido-2-(2,2-dioxo-5-tetradecyl-2 $\lambda^6$ -[1,3,2]dioxathiolan-4-yl)ethoxy]-*tert*-butyldiphenylsilane (**39**) (12.4 g, 19.2 mmol) in toluene (100 mL).

The reaction mixture was heated at reflux for 2 h. The reaction was allowed to cool to rt, and a mixture of conc. H<sub>2</sub>SO<sub>4</sub>/H<sub>2</sub>O/THF (56 mL, 3.4:4.6:48.0) was added while stirring. The mixture was stirred for 1 h at rt and then diluted with EtOAc (100 mL). It was washed with saturated aqueous NaHCO<sub>3</sub> (150 mL) and brine (150 mL). The organic layer was dried (Na<sub>2</sub>SO<sub>4</sub>) and concentrated. Purification by flash column chromatography on silica gel (hexane/EtOAc 97:3) provided **40** as a colorless oil (5.37 g, 63%):<sup>49</sup> <sup>1</sup>H NMR (400 MHz, CDCl<sub>3</sub>) δ 7.73–7.66 (m, 4H), 7.48–7.38 (m, 6H) 5.75 (ddd, *J* = 15.4, 6.6, 6.6 Hz, 1H), 5.45 (dd, *J* = 15.4, 7.2 Hz, 1H), 4.23 (ddd, *J* = 5.2, 5.2, 5.2 Hz, 1H), 3.83 (dd, *J* = 10.8, 6.3 Hz, 1H), 3.79 (dd, *J* = 10.6, 4.6 Hz, 1H), 3.52 (ddd, *J* = 5.0, 5.0, 5.0 Hz, 1H), 2.12 (d, *J* = 5.0 Hz, 1H), 2.06–1.98 (m, 2H), 1.37–1.24 (m, 22H), 1.09 (s, 9H), 0.90 (t, *J* = 6.6 Hz, 3H); <sup>13</sup>C NMR (100 MHz, CDCl<sub>3</sub>) δ 135.8, 135.6, 133.0, 130.1, 128.1, 128.0, 73.0, 67.1, 64.3, 32.5, 32.1, 29.9, 29.8, 29.7, 29.6, 29.4, 29.2, 26.9, 22.9, 19.3, 14.3.



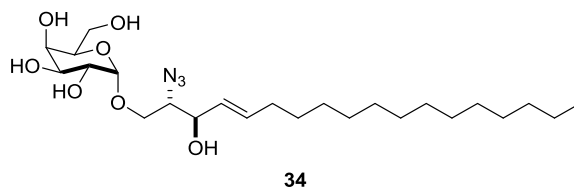
**(2*S*,3*R*,4*E*)-2-Azido-octadec-4-ene-1,3-diol (31).** TBAF (19.1 mL, 19.1 mmol, 1M in THF) was added to a solution of (2*S*,3*R*,4*E*)-2-azido-1-(*tert*-butyldiphenylsilyloxy)octadec-4-en-3-ol (**40**) (5.37 g, 9.53 mmol) in THF (47 mL) at rt. The reaction mixture was stirred for 2 h, diluted with H<sub>2</sub>O (50 mL) and extracted with EtOAc (3 x 70 mL). The combined organic layers were washed with brine (150 mL), dried (Na<sub>2</sub>SO<sub>4</sub>) and concentrated. Purification by flash column chromatography on silica gel (hexane/EtOAc 7:3) provided **31** as a colorless oil (1.88 g, 60%):<sup>49</sup> <sup>1</sup>H NMR (400 MHz, CDCl<sub>3</sub>) δ 5.81 (ddd, *J* = 15.4, 6.7, 6.7 Hz, 1H), 5.52 (dd, *J* = 15.4, 7.3 Hz, 1H), 4.23 (t, *J* = 6.4 Hz, 1H), 3.78 (dd, *J* = 11.8, 4.8 Hz, 1H), 3.75 (dd, *J* = 11.8, 5.6 Hz, 1H), 3.47 (ddd, *J* = 5.4, 5.4, 5.4 Hz, 1H), 2.54 (br s, 2H), 2.11–2.00 (m, 2H), 1.42–1.23 (m, 22H), 0.90 (t, *J* = 6.6 Hz, 3H); <sup>13</sup>C NMR (100 MHz, CDCl<sub>3</sub>): δ 136.2, 128.2, 73.9, 66.9, 62.7, 32.5, 32.1, 29.9, 29.8, 29.7, 29.5, 29.4, 29.1, 22.9, 14.3.



42

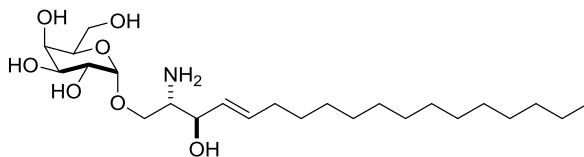
**(2*S*,3*R*,4*E*)-2-Azido-1-(2,3,4,6-*tetra-O*-trimethylsilyl- $\alpha$ -D-galactopyranosyloxy)octadec-4-ene-3-ol**

**(42).** TMSI (500  $\mu$ L, 3.69 mmol) was added to a solution of per-*O*-silylated sugar (**43**) (2.00 g, 3.69 mmol) in DCM (20 mL) at 0 °C. The reaction mixture was stirred under N<sub>2</sub> for 15 min. Approximately three quarter of the solvent was removed under reduced pressure, and the glycosyl iodide intermediate (**32**) obtained was dissolved in toluene (10 mL) and kept under N<sub>2</sub>. In a separate flask, a mixture of activated 4 Å molecular sieves (1.0 g), *n*-Bu<sub>4</sub>NI (3.00 g, 8.1 mmol), *i*-Pr<sub>2</sub>Net (1.00 mL, 5.9 mmol), and (2*S*,3*R*,4*E*)-2-azidooctadec-4-ene-1,3-diol (**31**) (0.90 g, 2.8 mmol) in toluene (25 mL) was prepared and stirred under N<sub>2</sub> at 50 °C for 30 min. The solution of glycosyl iodide in toluene was then added dropwise over 20 min to this mixture, and the resulting mixture was stirred overnight. After removal of the solvent under reduced pressure, DCM (50 mL) and H<sub>2</sub>O (50 mL) were added, and the phases were separated. The aqueous layer was extracted with DCM (3 x 40 mL). The combined organic extracts were dried (Na<sub>2</sub>SO<sub>4</sub>) and concentrated. Purification by flash column chromatography on silica gel (hexane/EtOAc 19:1) provided **42** (single  $\alpha$ -anomer) as a colorless oil (1.38 g, 64%): IR (neat) 3427 (br), 2924, 2854, 2098, 1249, 1144, 1103, 1033 cm<sup>-1</sup>; <sup>1</sup>H NMR (400 MHz, CDCl<sub>3</sub>)  $\delta$  5.80 (ddd, *J* = 15.4, 6.8, 6.8 Hz, 1H), 5.47 (dd, *J* = 15.4, 6.4 Hz, 1H), 4.70 (d, *J* = 3.4 Hz, 1H), 4.46–4.41 (m, 1H), 4.11 (dd, *J* = 10.4, 2.4 Hz, 1H), 3.93 (dd, *J* = 9.5, 3.4 Hz, 1H), 3.93–3.89 (m, 1H), 3.85 (dd, *J* = 9.5, 2.6 Hz, 1H), 3.83–3.76 (m, 2H), 3.69–3.55 (m, 2H), 3.43 (d, *J* = 8.8 Hz, 1H), 3.09–3.04 (m, 1H), 2.10–2.01 (m, 2H), 1.43–1.34 (m, 2H), 1.33–1.23 (m, 20H), 0.88 (t, *J* = 6.6 Hz, 3H), 0.16 (s, 9H), 0.14 (s, 9H), 0.14 (s, 9H), 0.13 (s, 9H); <sup>13</sup>C NMR (100 MHz, CDCl<sub>3</sub>)  $\delta$  134.0, 129.3, 101.1, 74.9, 72.4, 70.6, 69.6, 69.3, 63.1, 61.5, 32.5, 32.1, 29.9, 29.8, 29.7, 29.5, 29.4, 29.2, 22.9, 14.3, 0.8, 0.5, 0.4, –0.3; HRMS (ESI) calcd for C<sub>36</sub>H<sub>78</sub>N<sub>3</sub>O<sub>7</sub>Si<sub>4</sub> (M + H)<sup>+</sup> *m/z* 776.4917, found 776.4923.



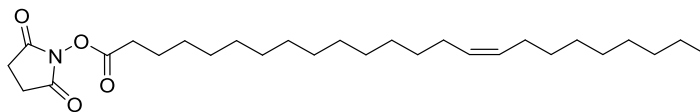
34

**(2*S*,3*R*,4*E*)-2-Azido-1-( $\alpha$ -D-galactopyranosyloxy)octadec-4-ene-3-ol (34).** PTSA (20.0 mg, 0.12 mmol) was added to the solution of (2*S*,3*R*,4*E*)-2-azido-1-(2,3,4,6-*tetra-O*-trimethylsilyl- $\alpha$ -D-galactopyranosyloxy)octadec-4-ene-3-ol (**42**) (0.89 g, 1.14 mmol) in MeOH (15 mL), and the mixture was stirred for 5 h at rt. Aqueous NaHCO<sub>3</sub> (100 mg, 1.19 mmol) was added and the mixture was filtered. The filtrate was then concentrated in vacuo. Purification by flash column chromatography on silica gel (DCM/MeOH 9.4:0.6) provided **34** as a white foam (638 mg, 70%): IR (neat) 3348 (br), 2923, 2853, 1667, 1520, 1464, 1111 cm<sup>-1</sup>; <sup>1</sup>H NMR (400 MHz, CDCl<sub>3</sub>/CH<sub>3</sub>OD 3:1)  $\delta$  5.79 (ddd,  $J$  = 15.4, 6.7, 6.7 Hz, 1H), 5.50 (dd,  $J$  = 15.4, 7.3 Hz, 1H), 4.88 (d,  $J$  = 3.4 Hz, 1H), 4.17 (dd,  $J$  = 6.9, 6.9 Hz, 1H), 4.02–3.92 (m, 2H), 3.90–3.84 (m, 1H), 3.84–3.72 (m, 4H), 3.66 (dd,  $J$  = 10.6, 5.9 Hz, 1H), 3.44–3.37 (m, 1H), 2.10–2.02 (m, 2H), 1.44–1.34 (m, 2H), 1.33–1.22 (m, 20H), 0.87 (t,  $J$  = 6.4 Hz, 3H); <sup>13</sup>C NMR (100 MHz, CDCl<sub>3</sub>/CH<sub>3</sub>OD 3:1)  $\delta$  134.9, 128.3, 99.6, 71.6, 70.6, 70.0, 69.8, 68.8, 67.9, 65.2, 61.8, 32.2, 31.8, 29.5, 29.3, 29.2, 29.1, 28.9, 22.5, 13.8; HRMS (ESI) calcd for C<sub>24</sub>H<sub>46</sub>N<sub>3</sub>O<sub>7</sub> (M + H)<sup>+</sup>  $m/z$  488.3336, found 488.3582.



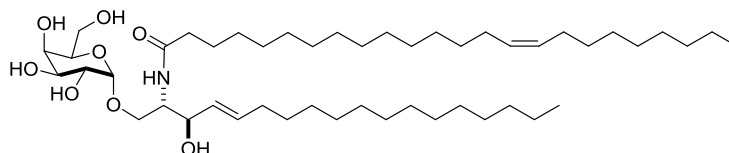
41

**(2*S*,3*R*,4*E*)-2-Amino-1-( $\alpha$ -D-galactopyranosyloxy)octadec-4-ene-3-ol (41).** Pme<sub>3</sub> (38.0  $\mu$ L, 0.36 mmol) was added to a solution of (2*S*,3*R*,4*E*)-2-azido-1-( $\alpha$ -D-galactopyranosyloxy)octadec-4-ene-3-ol (**34**) (50 mg, 0.10 mmol) in wet MeOH (2.9 mL) at rt, and the resulting solution was stirred for 2 h. Solvent was removed under reduced pressure to give a white residue which was then subjected to high vacuum to remove the Me<sub>3</sub>PO byproduct. Amine **41** was used in the next step without further purification.



**35**

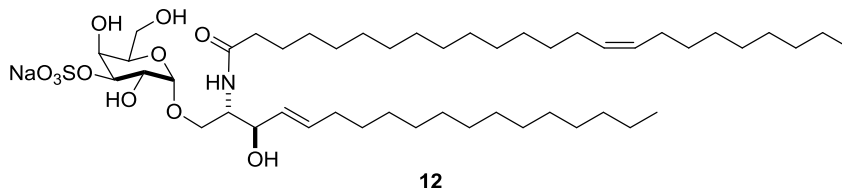
**Succinimidyl (Z)-tetracos-15-enoate (33).** *N,N*-Dicyclohexylcarbodiimide (0.31 g, 1.50 mmol) was added to a mixture of 15-tetracosenoic acid (**43**) (0.50 g, 1.36 mmol) and *N*-hydroxysuccinimide (0.17 g, 1.50 mmol) in EtOAc (50 mL) at 0 °C and stirred at this temperature for 2 h, followed by stirring at 35 °C for 15 h. The mixture was allowed to cool to rt, filtered through celite and the celite was then washed with EtOAc (30 mL). The filtrate was concentrated to give **35** as a white solid which was utilized in the next step without further purification.



**36**

**(2S,3R,4E)-1-(α-D-Galactopyranosyloxy)-2-(N-15Z-tetracosenoylamino)octadec-4-ene-3-ol (36).**

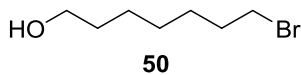
(2S,3R,4E)-2-Amino-1-(α-D-galactopyranosyloxy)octadec-4-ene-3-ol (**41**) (32 mg, 0.10 mmol) and Et<sub>3</sub>N (81 μL, 0.58 mmol) were added to a solution of succinimidyl (Z)-tetracos-15-enoate (**35**) (100 mg, 0.215 mmol) in THF (3 mL) and the solution was stirred at rt for 15 h. The mixture was then concentrated. Purification by flash column chromatography on silica gel (DCM/MeOH 9.5:0.5) provided **36** as a white foam (50 mg, 60%): IR (neat) 3397 (br), 2917, 2850, 1708, 1642, 1071, 1029 cm<sup>-1</sup>; <sup>1</sup>H NMR (400 MHz, CDCl<sub>3</sub>/CH<sub>3</sub>OD 3:1) δ 5.72 (ddd, *J* = 15.4, 6.7, 6.7 Hz, 1H), 5.44 (dd, *J* = 15.4, 6.9 Hz, 1H), 5.38–5.28 (m, 2H), 4.87 (d, *J* = 2.3 Hz, 1H), 4.07 (dd, *J* = 6.7, 6.7 Hz, 1H), 4.01–3.90 (m, 2H), 3.83–3.67 (m, 7H), 2.18 (t, *J* = 7.5 Hz, 2H), 2.07–1.97 (m, 6H), 1.64–1.53 (m, 2H), 1.39–1.22 (m, 54H), 0.87 (t, *J* = 6.4 Hz, 6H); <sup>13</sup>C NMR (100 MHz, CDCl<sub>3</sub>/CH<sub>3</sub>OD 3:1) δ 174.6, 133.8, 129.5, 129.1, 99.7 (C-1, anomeric carbon), 71.8, 70.5, 70.0, 69.5, 68.8, 67.2, 61.4, 53.6, 53.5, 36.2, 32.1, 31.6, 29.4, 29.3, 29.2, 29.1, 29.0, 29.0, 26.8, 25.7, 22.3, 13.5; HRMS (ESI) calcd for C<sub>48</sub>H<sub>91</sub>NNaO<sub>8</sub> (M + Na)<sup>+</sup> *m/z* 832.6642, found 832.6596.



**12**

**(2*S*,3*R*,4*E*)-1-(3-*O*-Sodiumsulfonyl- $\alpha$ -*D*-galactopyranosyloxy)-2-(*N*-15*Z*-tetracosenoylamino)octadec-4-ene-3-ol (12).** (2*S*,3*R*,4*E*)-1-( $\alpha$ -*D*-Galactopyranosyloxy)-2-(*N*-15*Z*-tetracosenoylamino)octadec-4-ene-3-ol (**36**) (0.023 g, 0.029 mmol) and Bu<sub>2</sub>SnO (0.011 g, 0.044 mmol) were stirred in MeOH (1.5 mL) at reflux under argon for 2h. The solvent was evaporated under reduced pressure, and the dibutylstannylene complex (**44**) was treated with Me<sub>3</sub>N•SO<sub>3</sub> (0.010 g, 0.070 mmol) in THF (2 mL) and stirred for 2 h. The solvent was removed under reduced pressure. The residue was dissolved in CHCl<sub>3</sub>/MeOH (2 mL, 1:1), loaded onto a cation-exchange resin column (Dowex 50 x 8 Na<sup>+</sup> form, 0.5 x 6 cm), eluted with CHCl<sub>3</sub>/MeOH (1:1) and concentrated. Purification by flash column chromatography on silica gel (CHCl<sub>3</sub>/MeOH 9:1) provided **12** as a white foam (70%, 0.030 g): IR (neat) 3407 (br), 2923, 2852, 1638, 1465, 1214, 1012 cm<sup>-1</sup>; <sup>1</sup>H NMR (500 MHz, CDCl<sub>3</sub>/CH<sub>3</sub>OD 3:1)  $\delta$  5.73 (ddd, *J* = 14.4, 6.6, 6.6 Hz, 1H), 5.43 (dd, *J* = 15.3, 7.0 Hz, 1H), 5.37–5.29 (m, 2H), 4.91 (d, *J* = 3.9 Hz, 1H), 4.45 (dd, *J* = 10.2, 3.1 Hz, 1H), 4.33–4.32 (m, 1H), 4.10 (dd, *J* = 7.1, 7.1 Hz, 1H), 4.01–3.94 (m, 2H), 3.85–3.69 (m, 5H), 2.18 (dd, *J* = 7.7 Hz, 2H), 2.05–1.96 (m, 6H), 1.63–1.53 (m, 2H), 1.38–1.22 (m, 54H), 0.86 (t, *J* = 5.3 Hz, 6H); <sup>13</sup>C NMR (125 MHz, CDCl<sub>3</sub>):  $\delta$  174.9, 134.3, 129.8, 128.9, 99.5, 77.9, 72.0, 70.4, 68.3, 67.6, 66.7, 61.7, 53.5, 36.3, 32.3, 31.8, 31.8, 29.7, 29.6, 29.6, 29.5, 29.5, 29.4, 29.3, 29.3, 29.2, 29.2, 27.1, 25.9, 22.6, 13.9; HRMS (ESI) calcd for C<sub>48</sub>H<sub>90</sub>NNaO<sub>11</sub>S (M – Na)<sup>–</sup> *m/z* 888.6240, found 888.6238.

### 1.3.3 Synthesis of $\beta$ -sulfatide 17

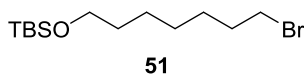


**50**

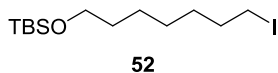
**7-Bromoheptan-1-ol (50).** A mixture of 1,7-heptanediol (**49**) (20.0 g, 151 mmol) and 48% HBr (aq.) (18.8 mL, 166 mmol) in toluene (360 mL) was refluxed for 15 h. The mixture was allowed to cool to rt and



then H<sub>2</sub>O (150 mL) and EtOAc (150 mL) were added. The organic layer was separated, and the aqueous layer was extracted with EtOAc (2 x 100 mL). The combined organic extracts were washed with brine, dried (MgSO<sub>4</sub>) and concentrated. Purification by flash column chromatography on silica gel (hexanes/EtOAc 7:3) provided **50** as a colorless oil (25.7 g, 87%): IR (neat) 3324 (br), 2929, 2855, 1460, 1430, 1250, 1053 cm<sup>-1</sup>; <sup>1</sup>H NMR (400 MHz, CDCl<sub>3</sub>) δ 3.60 (t, *J* = 6.6 Hz, 2H), 3.38 (t, *J* = 6.8 Hz, 2H), 1.83 (br s, 1H), 1.83 (quin, *J* = 14.1, 6.9 Hz, 2H), 1.54 (quin, *J* = 13.6, 6.6 Hz, 2H), 1.46–1.37 (m, 2H), 1.37–1.26 (m, 4H); <sup>13</sup>C NMR (100 MHz, CDCl<sub>3</sub>) δ 62.9, 34.1, 32.8, 32.7, 28.7, 28.2, 25.7; HRMS (ESI) calcd for C<sub>7</sub>H<sub>16</sub>BrO (M + H)<sup>+</sup> *m/z* 195.0385, found 195.0374.

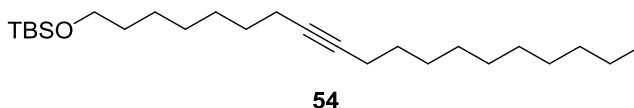


**7-Bromo-1-(tert-butyldimethylsilyloxy)heptane (51).** Imidazole (10.8 g, 158 mmol) was added over 20 min to a mixture of 7-bromoheptan-1-ol (**50**) (25.7 g, 132 mmol) and chlorodimethyl-*t*-butylsilane (23.8 g, 158 mmol) in DCM (660 mL) at 0 °C. After 10 min, the reaction mixture was allowed to warm to rt and then stirred for 4 h. H<sub>2</sub>O (200 mL) was added, the organic layer separated, and the aqueous layer was extracted with DCM (3 x 150 mL). The combined organic extracts were washed with brine (300 mL), dried (MgSO<sub>4</sub>) and concentrated. Purification by flash column chromatography on silica gel (hexanes/EtOAc 49:1) provided **51** as a pale yellow oil (40.0 g, 96%): IR (neat) 2929, 2856, 1471, 1462, 1253, 1096 cm<sup>-1</sup>; <sup>1</sup>H NMR (400 MHz, CDCl<sub>3</sub>) δ 3.59 (t, *J* = 6.5 Hz, 2H), 3.40 (t, *J* = 6.9 Hz, 2H), 1.85 (quin, *J* = 14.1, 7.0 Hz, 2H), 1.55–1.47 (m, 2H), 1.46–1.38 (m, 2H), 1.37–1.28 (m, 4H), 0.89 (s, 9H), 0.04 (s, 6H); <sup>13</sup>C NMR (100 MHz, CDCl<sub>3</sub>) δ 63.4, 34.1, 33.0, 32.9, 28.8, 28.4, 26.2, 25.9, 18.6, –5.1; HRMS (ESI) calcd for C<sub>13</sub>H<sub>30</sub>BrOSi (M + H)<sup>+</sup> *m/z* 309.1249, found 309.1259.

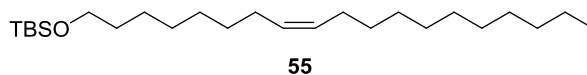


**1-(tert-Butyldimethylsilyloxy)-7-iodoheptane (52).** 7-Bromo-1-(tert-butyldimethylsilyloxy)heptane (**51**) (39.0 g, 126 mmol) was dissolved in dry acetone (428 mL) containing NaI (56.6 g, 378 mmol). The

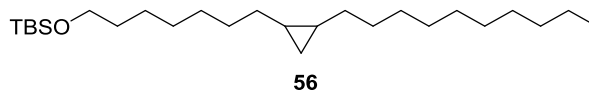
mixture was stirred in the dark for 24 h. The crystallized salts were filtered and washed with petroleum ether twice. Solvents were evaporated, and Et<sub>2</sub>O (150 mL) was added to the crude residue. This organic phase was then washed with H<sub>2</sub>O (100 mL), and brine (100 mL), dried (MgSO<sub>4</sub>), and concentrated. Purification by flash column chromatography on silica gel (hexanes) provided **52** as a pale yellow liquid (40.0 g, 89%): IR (neat) 2928, 2855, 1470, 1462, 1251, 1097 cm<sup>-1</sup>; <sup>1</sup>H NMR (400 MHz, CDCl<sub>3</sub>) δ 3.59 (t, *J* = 6.5 Hz, 2H), 3.18 (t, *J* = 7.0 Hz, 2H), 1.82 (quin, *J* = 14.2, 7.0 Hz, 2H), 1.55–1.45 (m, 2H), 1.44–1.28 (m, 6H), 0.89 (s, 9H), 0.04 (s, 6H); <sup>13</sup>C NMR (100 MHz, CDCl<sub>3</sub>) δ 63.3, 33.7, 32.9, 30.7, 28.5, 26.2, 25.8, 18.7, 7.3, –5.1; HRMS (ESI) calcd for C<sub>13</sub>H<sub>30</sub>IOSi (M + H)<sup>+</sup> *m/z* 357.1111, found 357.1127.



**1-(tert-Butyldimethylsilyloxy)-nonadec-8-yne (54).** n-Butyllithium (2.20 g, 35.1 mmol) was added to a solution of 1-dodecyne (**53**) (3.90 g, 23.3 mmol) in THF (15 mL) at 0 °C under N<sub>2</sub> over a period of 30 min. The reaction was stirred at 0 °C for 20 min. 1-(tert-Butyldimethylsilyloxy)-7-iodoheptane (**52**) (10.0 g, 28.1 mmol) in HMPA (14.8 mL) was added, and the reaction mixture was allowed to warm to rt and was stirred for 20 h. The reaction was stopped by the addition of concentrated aqueous NH<sub>4</sub>Cl (70 mL) and then Et<sub>2</sub>O (50 mL). The organic layer was separated and the aqueous layer was extracted with Et<sub>2</sub>O (3 x 80 mL). The combined organic extracts were washed with brine (150 mL), dried (MgSO<sub>4</sub>) and concentrated. Purification by flash column chromatography on silica gel (hexanes/EtOAc 99.75:0.25) provided **54** as a colorless oil (5.40 g, 59%): IR (neat) 2925, 2854, 1462, 1252, 1098 cm<sup>-1</sup>; <sup>1</sup>H NMR (400 MHz, CDCl<sub>3</sub>) δ 3.60 (t, *J* = 6.6 Hz, 2H), 2.18–2.10 (m, 4H), 1.56–1.42 (m, 6H), 1.42–1.24 (m, 20H), 0.89 (s, 9H), 0.88 (t, *J* = 7.0 Hz, 3H), 0.05 (s, 6H); <sup>13</sup>C NMR (100 MHz, CDCl<sub>3</sub>) δ 80.5, 80.4, 63.5, 33.1, 32.1, 29.9, 29.8, 29.8, 29.7, 29.6, 29.4, 29.4, 29.2, 29.1, 26.3, 26.2, 26.0, 22.9, 19.0, 18.6, 14.3, –5.1; HRMS (ESI) calcd for C<sub>25</sub>H<sub>51</sub>Osi (M + H)<sup>+</sup> *m/z* 395.3709, found 395.3710.



**(Z)-1-(*tert*-Butyldimethylsilyloxy)-nonadec-8-ene (55).** A solution of 1-(*tert*-butyldimethylsilyloxy)nonadec-8-yne (**54**) (6.00 g, 15.1 mmol) in hexanes (170 mL) was hydrogenated by stirring in an atmosphere of hydrogen in the presence of 10 percent palladium on barium sulfate (0.98 g, 0.92 mmol) and quinolone (2.4 mL). After 12 h of stirring, the mixture was filtered through a pad of celite, the celite washed with hexanes (50 mL) and the filtrate concentrated. Purification by flash column chromatography on silica gel (hexanes/EtOAc 99.5:0.5) provided **55** as a colorless oil (3.9 g, 65%): IR (neat) 2923, 2853, 1462, 1253, 1098  $\text{cm}^{-1}$ ;  $^1\text{H}$  NMR (400 MHz,  $\text{CDCl}_3$ )  $\delta$  5.41–5.30 (m, 2H), 3.61 (t,  $J$  = 6.6 Hz, 2H), 2.07–1.96 (m, 4H), 1.56–1.47 (m, 2H), 1.38–1.25 (m, 24H), 0.91 (s, 9H), 0.89 (t,  $J$  = 7.0 Hz, 3H), 0.05 (s, 6H);  $^{13}\text{C}$  NMR (100 MHz,  $\text{CDCl}_3$ )  $\delta$  130.2, 130.1, 63.5, 33.2, 32.2, 30.0, 30.0, 29.9, 29.8, 29.6, 29.6, 29.6, 27.5, 26.2, 26.1, 23.0, 18.6, 14.4, –5.0; HRMS (ESI) calcd for  $\text{C}_{25}\text{H}_{53}\text{Osi}$  ( $\text{M} + \text{H}$ ) $^+$   $m/z$  397.3866, found 397.3868.

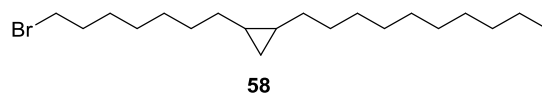


**(8*S*\*,9*R*\*)-1-(*tert*-Butyldimethylsilyloxy)-8,9-methylenenonadecane (56).** Diethylzinc (3.1 mL, 30.6 mmol) was added dropwise to a stirred solution of 2,4,6-trichlorophenol (6.0 g, 30.6 mmol) in DCM (140 mL) at –40 °C. The reaction mixture was stirred at this temperature for 15 min. Diodomethane (8.2 g, 30.6 mmol) was then added and the reaction mixture stirred for another 15 min. 1-(*tert*-Butyldimethylsilyloxy)-nonadec-8-ene (**55**) was added and the reaction mixture was allowed to warm to rt. After 15 h of stirring, the reaction was stopped by dropwise addition of petroleum ether (100 mL) and 10% HCl solution (100 mL). The mixture was extracted with DCM (3 x 150 mL), then the combined organic extracts were washed with saturated aqueous  $\text{NaHCO}_3$  (250 mL), saturated aqueous  $\text{Na}_2\text{SO}_3$  (200 mL), brine (250 mL), dried ( $\text{MgSO}_4$ ) and concentrated. Purification by flash column chromatography on silica gel (hexanes) provided **56** as a colorless oil (3.4 g, 54%): IR (neat) 2923, 2853, 1462, 1253, 1097

cm<sup>-1</sup>; <sup>1</sup>H NMR (400 MHz, CDCl<sub>3</sub>) δ 3.61 (t, *J* = 6.6 Hz, 2H), 1.56–1.48 (m, 2H), 1.44–1.25 (m, 26H), 1.19–1.10 (m, 2H), 0.90 (s, 9H), 0.89 (t, *J* = 7.0 Hz, 3H), 0.67–0.61 (m, 2H), 0.60–0.51 (m, 1H), 0.05 (s, 6H), –0.33 (ddd, *J* = 5.1, 5.1, 5.1 Hz, 1H); <sup>13</sup>C NMR (100 MHz, CDCl<sub>3</sub>) δ 63.6, 33.2, 32.2, 30.5, 30.4, 30.0, 30.0, 29.9, 29.8, 29.6, 29.0, 29.0, 26.2, 26.1, 23.0, 18.6, 16.0, 14.4, 11.2, –5.0; HRMS (ESI) calcd for C<sub>26</sub>H<sub>55</sub>Osi (M + H)<sup>+</sup> *m/z* 411.4022, found 411.5027.

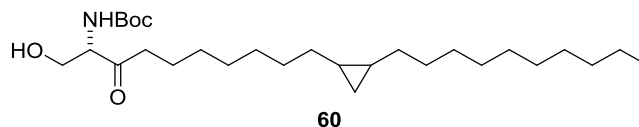


**(8*S*\*,9*R*\*)-8,9-methylenenonadecan-1-ol (57).** A solution of (8*S*\*,9*R*\*)-1-(*tert*-Butyldimethylsilyloxy)-8,9-methylenenonadecane (**56**) (7.3 g, 17.7 mmol) in DCM (102 mL) was treated with TBAF (36 mL, 1M soln in THF) at 0 °C. After 15 min, the reaction mixture was allowed to warm to rt. After 5 h, the solution was concentrated and then DCM (70 mL) was added. The resulting mixture was washed with H<sub>2</sub>O (80 mL) and brine (70 mL), dried (MgSO<sub>4</sub>), filtered and concentrated. Purification by flash column chromatography on silica gel (hexanes/EtOAc 9:1) provided **57** as a colorless oil (3.5 g, 65%): IR (neat) 3310 (br), 2921, 2852, 1464, 1054, 1020 cm<sup>-1</sup>; <sup>1</sup>H NMR (400 MHz, CDCl<sub>3</sub>) δ 3.63 (t, *J* = 6.6 Hz, 2H), 1.61–1.52 (m, 2H), 1.41–1.22 (m, 26H), 1.17–1.08 (m, 2H), 0.87 (t, *J* = 6.6 Hz, 3H), 0.68–0.60 (m, 2H), 0.59–0.52 (m, 1H), –0.34 (ddd, *J* = 5.1, 5.1, 5.1 Hz, 1H); <sup>13</sup>C NMR (100 MHz, CDCl<sub>3</sub>) δ 63.3, 33.0, 32.1, 30.4, 30.4, 30.0, 29.9, 29.8, 29.7, 29.6, 28.9, 28.9, 26.0, 22.9, 16.0, 14.3, 11.1; HRMS (ESI) calcd for C<sub>20</sub>H<sub>41</sub>O (M + H)<sup>+</sup> *m/z* 297.3157, found 297.3139.



**(8*S*\*,9*R*\*)-1-Bromo-8,9-methylenenonadecane (58).** Tetrabromomethane (5.84 g, 17.6 mmol) and triphenylphosphine (9.23 g, 35.1 mmol) were added to a solution of (8*S*\*,9*R*\*)-8,9-methylenenonadecan-1-ol (**57**) (3.5 g, 11.7 mmol) in DCM (216 mL) at 0 °C. After 1 h, the reaction mixture was diluted with petroleum ether (150 mL) and then concentrated. Purification by flash column chromatography on silica

gel (hexanes) provided **58** as a colorless oil (2.9 g, 69%): IR (neat) 2921, 2852, 1462, 1020  $\text{cm}^{-1}$ ;  $^1\text{H}$  NMR (400 MHz,  $\text{CDCl}_3$ )  $\delta$  3.41 (t,  $J$  = 6.9 Hz, 2H), 1.90–1.81 (m, 2H), 1.48–1.23 (m, 26H), 1.18–1.09 (m, 2H), 0.88 (t,  $J$  = 6.6 Hz, 3H), 0.69–0.61 (m, 2H), 0.60–0.53 (m, 1H), –0.33 (ddd,  $J$  = 5.1, 5.1, 5.1 Hz, 1H);  $^{13}\text{C}$  NMR (100 MHz,  $\text{CDCl}_3$ )  $\delta$  34.2, 33.1, 32.2, 30.4, 30.3, 30.0, 29.9, 29.7, 29.6, 29.1, 29.0, 28.9, 28.4, 22.9, 16.0, 16.0, 14.3, 11.2; HRMS (ESI) calcd for  $\text{C}_{20}\text{H}_{40}\text{Br}$  ( $\text{M} + \text{H}$ ) $^+$   $m/z$  359.2313, found 359.2342.



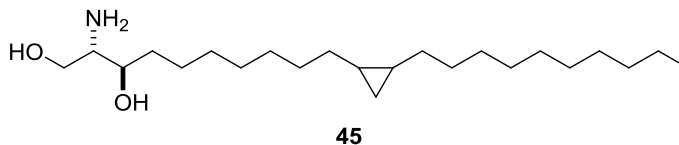
**(2*S*,11*S*\*,12*R*\*)-2-(*N*-tert-Butyloxycarbonylamino)-1-hydroxy-11,12-methylenedocosan-3-one (60).**

(8*S*\*,9*R*\*)-1-Bromo-8,9-methylenenonadecane (**58**) (0.94 g, 2.62 mmol), polished magnesium turnings (82 mg, 3.4 mmols) and THF (7.0 mL) were charged into a flame-dried and  $\text{N}_2$ -flushed round-bottom flask equipped with a stir-bar and a septum. The mixture was then placed in a pre-heated oil bath at 80  $^\circ\text{C}$  and stirred under reflux. As refluxing started, 2 crystals of iodine were quickly added and the reaction refluxed for 1 h. This was then left to cool to rt. Weinreb amide (**59**) (0.47 g, 1.90 mmol) and THF (10 mL) were charged into a separate flame-dried and  $\text{N}_2$ -flushed 50 ml round-bottom flask equipped with a stir-bar and a septum. The solution was then cooled to –15  $^\circ\text{C}$ . Isopropylmagnesium chloride was added dropwise using a syringe, and the solution was stirred for 15 min. The prepared Grignard reagent was then transferred via cannula into this solution. The mixture was allowed to warm to rt and was stirred for 20 h. The reaction was stopped by first cooling it to –15  $^\circ\text{C}$ , followed by the dropwise addition of conc. aqueous  $\text{NH}_4\text{Cl}$  (20 mL). The biphasic mixture was allowed to warm to rt and was diluted with EtOAc (50 mL). The organic phase was separated and the aqueous layer extracted with EtOAc (3 x 50 mL). The combined organic extracts were washed with  $\text{H}_2\text{O}$  (100 mL) and brine (100 mL), dried ( $\text{MgSO}_4$ ) and then concentrated. Purification by flash column chromatography on silica gel (hexanes/EtOAc 17:3) provided **60** as a colorless oil (0.40 g, 45%): IR (neat) 3409 (br), 2921, 2852, 1708, 1496, 1456, 1366, 1165  $\text{cm}^{-1}$ ;  $^1\text{H}$  NMR (400 MHz,  $\text{CDCl}_3$ )  $\delta$  5.63 (br s, 1H), 4.33 (br s, 1H) 3.98–3.86 (m, 2H), 2.65–2.47 (m, 2H),

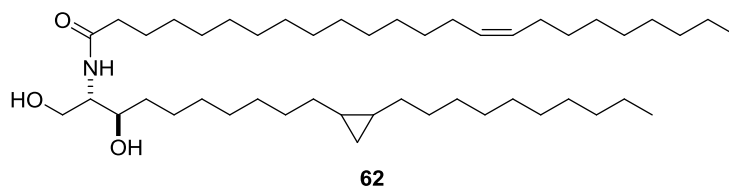
1.75–1.05 (m, 39H), 0.87 (t,  $J = 6.6$  Hz, 3H), 0.68–0.59 (m, 2H), 0.59–0.52 (m, 1H), –0.34 (ddd,  $J = 5.0$ , 5.0, 5.0 Hz, 1H);  $^{13}\text{C}$  NMR (100 MHz,  $\text{CDCl}_3$ )  $\delta$  208.1, 156.2, 80.5, 63.5, 61.8, 40.2, 32.1, 30.4, 30.3, 29.9, 29.9, 29.9, 29.6, 29.6, 29.4, 28.9, 28.9, 28.5, 23.7, 22.9, 16.0, 15.9, 14.3, 11.1; HRMS (ESI) calcd for  $\text{C}_{28}\text{H}_{54}\text{NO}_4$  ( $\text{M} + \text{H}$ ) $^+$   $m/z$  468.4053, found 468.4067.



**(2S,3R,11S\*,12R\*)-2-(N-tert-Butyloxycarbonylamino)-11,12-methylenedocosan-1,3-diol (61).** A solution of lithium tri-*tert*-butoxyaluminumhydride (2.08 g, 8.2 mmol) in EtOH (17 mL) was stirred at –78 °C in a dry and  $\text{N}_2$ -flushed flask equipped with a septum. (2S,11S\*,12R\*)-2-(N-*tert*-Butyloxycarbonylamino)-1-hydroxy-11,12-methylenedocosan-3-one (**60**) (0.64 g, 1.4 mmol) in EtOH (17 mL) was then added dropwise and the solution stirred at –78 °C for 7 h. The reaction was stopped by the addition of 10% aqueous citric acid (25 mL); then DCM (25 mL) was added. The mixture was then allowed to warm to rt and was stirred for 3 h. The organic phase was separated, and the aqueous layer was extracted with DCM (3 x 80 mL). The combined organic extracts were washed with brine (100 mL), dried ( $\text{Na}_2\text{SO}_4$ ) and concentrated. Purification by flash column chromatography on silica gel (hexanes/EtOAc 4:1) provided **61** as a colorless oil (0.60 g, 94%): IR (neat) 3409 (br), 2921, 2852, 1169  $\text{cm}^{-1}$ ;  $^1\text{H}$  NMR (400 MHz,  $\text{CDCl}_3$ )  $\delta$  5.41 (d,  $J = 7.3$  Hz, 1H), 4.03–3.93 (m, 1H) 3.83–3.69 (m, 2H), 3.58–3.47 (m, 1H), 2.90–2.60 (m, 2H), 1.70–1.05 (m, 41H), 0.87 (t,  $J = 6.5$  Hz, 3H), 0.68–0.60 (m, 2H), 0.59–0.52 (m, 1H), –0.34 (ddd,  $J = 5.0$ , 5.0, 5.0 Hz, 1H);  $^{13}\text{C}$  NMR (100 MHz,  $\text{CDCl}_3$ )  $\delta$  156.3, 79.9, 74.6, 62.9, 55.0, 34.7, 32.1, 30.4, 30.4, 29.9, 29.9, 29.9, 29.8, 29.6, 28.9, 28.9, 28.6, 26.2, 22.9, 16.0, 16.0, 14.3, 11.1; HRMS (ESI) calcd for  $\text{C}_{28}\text{H}_{56}\text{NO}_4$  ( $\text{M} + \text{H}$ ) $^+$   $m/z$  470.4209, found 470.4215.

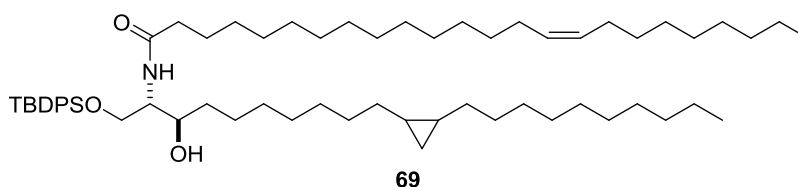


**(2S,3R,11S\*,12R\*)-2-Amino-11,12-methylenedocosan-1,3-diol (45).** Acetyl chloride (4.0 mL, 57 mmol) was added dropwise to a flask containing stirring MeOH (34 mL) at 0 °C. This solution was then treated with (2S,3R,11S\*,12R\*)-2-(*N*-*tert*-butoxycarbonylamino)-11,12-methylenedocosan-1,3-diol (**61**) (0.60 g, 1.3 mmol) solution in Et<sub>2</sub>O (34 mL). The resulting mixture was allowed to warm to rt and was stirred for 15 h. The reaction mixture was cooled to 0 °C and conc. aqueous NH<sub>4</sub>Cl (50 mL) was added while stirring. After 15 min, DCM (60 mL) was added and the organic phase separated. The aqueous layer was extracted with DCM (3 x 40 mL). The combined organic extracts were washed with brine (100 mL), dried (Na<sub>2</sub>SO<sub>4</sub>) and concentrated. Purification by flash column chromatography on silica gel (CH<sub>3</sub>Cl/MeOH/NH<sub>4</sub>OH 135:25:4) provided **45** as white foam (0.33 g, 70%): IR (neat) 3349 (br), 2920, 2851, 1464, 1019 cm<sup>-1</sup>; <sup>1</sup>H NMR (400 MHz, CDCl<sub>3</sub>) δ 3.78–3.65 (m, 2H), 3.64–3.54 (m, 1H) 2.95–2.70 (m, 1H), 2.27 (br s, 4H), 1.53–1.442 (m, 2H), 1.42–1.22 (m, 28H), 1.19–1.08 (m, 2H) 0.88 (t, *J* = 6.5 Hz, 3H), 0.69–0.60 (m, 2H), 0.59–0.52 (m, 1H), –0.34 (ddd, *J* = 5.0, 5.0, 5.0 Hz, 1H); <sup>13</sup>C NMR (100 MHz, CDCl<sub>3</sub>) δ 74.8, 63.7, 55.9, 34.6, 34.0, 32.1, 30.4, 29.9, 29.8, 29.6, 28.9, 26.3, 22.9, 19.0, 16.0, 16.0, 14.3, 11.1; HRMS (ESI) calcd for C<sub>23</sub>H<sub>48</sub>NO<sub>2</sub> (M + H)<sup>+</sup> *m/z* 370.3685, found 370.3709.



**(2S,3R,11S\*,12R\*)-2-(N-15Z-Tetracosenoylamino)-11,12-methylenedocosan-1,3-diol (62).** A solution of succinimidyl (Z)-tetracos-15-enoate (**35**) (0.25 g, 0.54 mmol) in THF (8 mL) was treated with (2S,3R,)-2-amino-11,12-methylenedocosan-1,3-diol (**45**) (0.12 g, 0.26 mmol) and Et<sub>3</sub>N (0.2 mL). The reaction was stirred at rt for 20 h. EtOAc (10 mL) was added to the mixture and then concentrated. Purification by

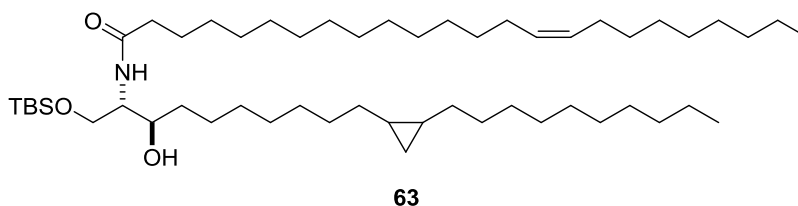
flash column chromatography on silica gel (DCM/MeOH 49:1) provided **62** as a white foam (0.24 g, 75%): IR (neat) 3294 (br), 2919, 2851, 1642, 1547, 1461, 1072  $\text{cm}^{-1}$ ;  $^1\text{H}$  NMR (400 MHz,  $\text{CDCl}_3$ )  $\delta$  6.39 (d,  $J = 7.8$  Hz, 1H), 5.39–5.29 (m, 2H), 3.99 (dd,  $J = 11.3, 3.3$  Hz, 1H), 3.82 (ddd,  $J = 7.0, 7.0, 3.4$  Hz, 1H), 3.79–3.70 (m, 2H), 2.96 (br s, 1H), 2.83 (br s, 1H), 2.22 (t,  $J = 7.5$  Hz, 2H), 2.07–1.95 (m, 4H), 1.68–1.58 (m, 2H), 1.57–1.48 (m, 2H), 1.40–0.08 (m, 62H), 0.88 (t,  $J = 6.6$  Hz, 6H), 0.68–0.60 (m, 2H), 0.59–0.52 (m, 1H),  $-0.34$  (ddd,  $J = 5.0, 5.0, 5.0$  Hz, 1H);  $^{13}\text{C}$  NMR (100 MHz,  $\text{CDCl}_3$ )  $\delta$  173.9, 130.1, 74.4, 62.7, 54.0, 37.1, 34.7, 32.1, 30.4, 30.0, 30.0, 29.9, 29.8, 29.7, 29.6, 29.5, 28.9, 27.4, 26.2, 26.0, 22.9, 16.0, 16.0, 14.3, 11.2; HRMS (ESI) calcd for  $\text{C}_{47}\text{H}_{92}\text{NO}_3$  ( $\text{M} + \text{H}$ ) $^+$   $m/z$  718.7077, found 718.7093.



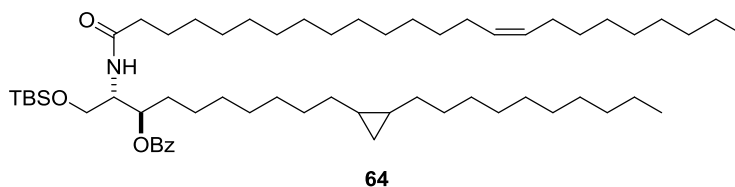
**(2*S*,3*R*,11*S*\*,12*R*\*)-1-(*tert*-Butyldiphenylsilyloxy)-2-(*N*-15*Z*-tetracosenoylamino)-11,12-methylenedocosan-3-ol (**69**).** Imidazole (0.068 g, 1.0 mmol) was added over 5 min to a solution of (2*S*,3*R*,11*S*\*,12*R*\*)-2-(*N*-15*Z*-tetracosenoylamino)-11,12-methylenedocosan-1,3-diol (**62**) (0.24 g, 0.33 mmol) and chlorodiphenyl-*t*-butylsilane (0.10 g, 0.365 mmol) in DMF (1 mL) at rt. A catalytic amount of DMAP was added, and the mixture was stirred for 15 h.  $\text{H}_2\text{O}$  (15 mL) was added, and the solution was extracted with DCM (3 x 20 mL). The combined organic extracts were washed with brine (50 mL), dried ( $\text{Na}_2\text{SO}_4$ ) and concentrated. Purification by flash column chromatography on silica gel (hexanes/EtOAc 17:3) provided **69** as colorless oil (0.11 g, 36%): IR (neat) 3307 (br), 2922, 2852, 1639, 1427, 1361, 1110  $\text{cm}^{-1}$ ;  $^1\text{H}$  NMR (400 MHz,  $\text{CDCl}_3$ )  $\delta$  7.68–7.59 (m, 4H), 7.48–7.35 (m, 6H), 6.23 (d,  $J = 7.8$  Hz, 1H), 5.40–5.30 (m, 2H), 3.99 (dd,  $J = 10.6, 3.4$  Hz, 1H), 3.94–3.86 (m, 1H), 3.84 (dd,  $J = 10.6, 2.8$  Hz, 1H), 3.70–3.58 (m, 1H), 3.19 (d,  $J = 8.6$  Hz, 1H), 2.15 (t,  $J = 7.4$  Hz, 2H), 2.06–1.98 (m, 4H), 1.66–1.57 (m, 2H), 1.55–1.45 (m, 2H), 1.42–1.23 (m, 62H), 1.08 (s, 9H), 0.89 (t,  $J = 6.5$  Hz, 6H), 0.70–0.61 (m, 2H), 0.60–0.53 (m, 1H),  $-0.32$  (ddd,  $J = 5.0, 5.0, 5.0$  Hz, 1H);  $^{13}\text{C}$  NMR (100 MHz,  $\text{CDCl}_3$ )  $\delta$  173.2, 135.7,



135.7, 132.6, 130.3, 130.3, 130.1, 128.1, 74.0, 64.3, 53.6, 37.0, 34.7, 32.1, 30.4, 30.0, 29.9, 29.9, 29.8, 29.8, 29.7, 29.6, 29.6, 29.5, 28.9, 27.4, 27.1, 26.2, 26.0, 22.9, 19.3, 16.0, 14.3, 11.1; HRMS (ESI) calcd for C<sub>63</sub>H<sub>110</sub>NO<sub>3</sub>Si (M + H)<sup>+</sup> *m/z* 956.8255, found 956.8220.

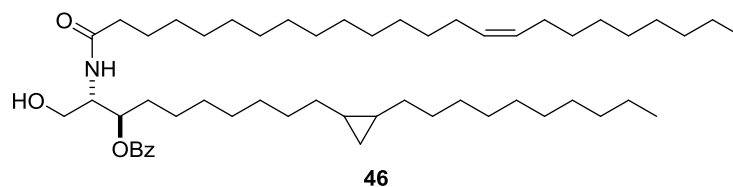


**(2*S*,3*R*,11*S*<sup>\*</sup>,12*R*<sup>\*</sup>)-1-(*tert*-Butyldimethylsilyloxy)-2-(*N*-15*Z*-tetracosenoylamino)-11,12-methylene-docosan-3-ol (63).** Imidazole (49 mg, 0.72 mmol) was added over 5 min to a solution of (2*S*,3*R*,11*S*<sup>\*</sup>,12*R*<sup>\*</sup>)-2-(*N*-15*Z*-tetracosenoylamino)-11,12-methylenedocosan-1,3-diol (**62**) (0.17 g, 0.24 mmol) and chlorodimethyl-*t*-butylsilane (0.043 g, 0.29 mmol) in DCM (6 mL) at 0 °C. After 10 min, the reaction mixture was allowed to warm to rt and then stirred for 12 h. H<sub>2</sub>O (10 mL) was added, the organic layer was separated, and the aqueous layer was extracted with DCM (3 x 20 mL). The combined organic extracts were washed with brine (40 mL), dried (MgSO<sub>4</sub>) and concentrated. Purification by flash column chromatography on silica gel (hexanes/EtOAc 9:1) provided **63** as a colorless oil (156 mg, 78%): IR (neat) 2921, 2852, 1642, 1463, 1252, 1086 cm<sup>-1</sup>; <sup>1</sup>H NMR (400 MHz, CDCl<sub>3</sub>) δ 6.30 (d, *J* = 7.7 Hz, 1H), 5.39–5.28 (m, 2H), 3.97 (dd, *J* = 10.2, 2.3 Hz, 1H), 3.88–3.78 (m, 2H), 3.65–3.55 (m, 1H), 3.22 (d, *J* = 9.5 Hz, 1H), 2.20 (t, *J* = 7.4 Hz, 2H), 2.05–1.95 (m, 4H) 1.68–1.46 (m, 4H), 1.41–1.21 (m, 62H), 0.89 (s, 9H), 0.87 (t, *J* = 7.0 Hz, 6H), 0.68–0.59 (m, 2H), 0.58–0.51 (m, 1H), 0.07 (s, 3H), 0.06 (s, 3H), –0.34 (ddd, *J* = 5.0, 5.0, 5.0 Hz, 1H); <sup>13</sup>C NMR (100 MHz, CDCl<sub>3</sub>) δ 173.2, 130.1, 74.5, 63.7, 52.8, 37.1, 35.1, 32.1, 30.4, 30.0, 30.0, 29.9, 29.8, 29.7, 29.7, 29.6, 29.5, 28.9, 27.4, 26.2, 26.0, 22.9, 18.3, 16.0, 16.0, 14.3, 11.1, –5.4; HRMS (ESI) calcd for C<sub>53</sub>H<sub>106</sub>NO<sub>3</sub>Si (M + H)<sup>+</sup> *m/z* 832.7897, found 832.7957.



**(2*S*,3*R*,11*S*\*,12*R*\*)-3-Benzoyloxy-1-(*tert*-butyldimethylsilyloxy)-2-(*N*-15*Z*-tetracosenoylamino)-**

**11,12-methylenedocosane (64).** Benzoyl chloride (0.091 mL, 0.75 mmol) was added dropwise over 5 min to a mixture of (2*S*,3*R*,11*S*\*,12*R*\*)-1-(*tert*-butyldimethylsilyloxy)-2-(*N*-15*Z*-tetracosenoylamino)-11,12-methylenedocosan-3-ol (**63**) (156 mg, 0.187 mmol) and a catalytic amount of DMAP in pyridine (3.7 mL) at 0 °C. The reaction mixture was allowed to warm to rt and stirred for 20 h. H<sub>2</sub>O (10 mL) was added, the organic layer separated, and the aqueous layer was extracted with DCM (3 x 15 mL). The combined organic extracts were washed with brine (40 mL), dried (Na<sub>2</sub>SO<sub>4</sub>) and concentrated. Purification by flash column chromatography on silica gel (hexanes/EtOAc 97.5:2.5) provided **64** as a brown oil (83 mg, 46%): IR (neat) 2922, 2852, 1720, 1644, 1267, 1174 cm<sup>-1</sup>; <sup>1</sup>H NMR (400 MHz, CDCl<sub>3</sub>) δ 8.06–8.01 (m, 2H), 7.56–7.53 (m, 1H), 7.48–7.41 (m, 2H), 5.97 (d, *J* = 9.2 Hz, 1H), 5.40–5.30 (m, 2H), 5.24–5.17 (m, 1H), 4.36–4.28 (m, 1H), 3.78 (dd, *J* = 10.3, 2.9 Hz, 1H), 3.63 (dd, *J* = 10.2, 4.2 Hz, 1H), 2.20 (t, *J* = 7.4 Hz, 2H), 2.06–1.95 (m, 4H), 1.82–1.70 (m, 2H), 1.69–1.58 (m, 2H), 1.45–1.04 (m, 62H), 0.87 (t, *J* = 6.4 Hz, 6H), 0.86 (s, 9H), 0.67–0.57 (m, 2H), 0.57–0.50 (m, 1H), –0.02 (s, 3H), –0.03 (s, 3H), –0.36 (ddd, *J* = 5.0, 5.0, 5.0 Hz, 1H); <sup>13</sup>C NMR (100 MHz, CDCl<sub>3</sub>) δ 172.8, 166.3, 133.2, 130.5, 130.1, 129.9, 128.6, 74.4, 61.9, 52.3, 37.3, 32.1, 31.9, 30.4, 30.4, 30.0, 30.0, 29.9, 29.8, 29.7, 29.6, 29.6, 29.5, 29.5, 28.9, 28.9, 27.4, 26.0, 25.6, 22.9, 18.4, 16.0, 16.0, 14.3, 11.1, –5.4, –5.5; HRMS (ESI) calcd for C<sub>60</sub>H<sub>110</sub>NO<sub>4</sub>Si (M + H)<sup>+</sup> *m/z* 936.8193 found 936.8100.



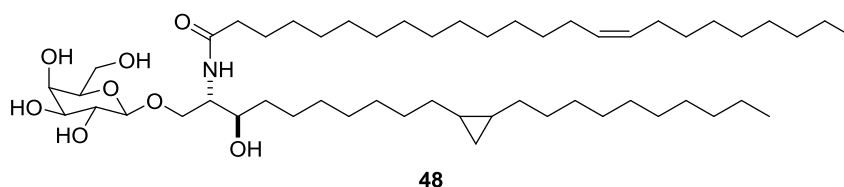
**(2*S*,3*R*,11*S*\*,12*R*\*)-3-Benzoyloxy-2-(*N*-15*Z*-tetracosenoylamino)-11,12-methylenedocosan-1-ol (46).**

Pyridinium *p*-toluenesulfonate (PPTS) (7 mg, 0.03 mmol) was added to a mixture of (2*S*,3*R*,11*S*\*,12*R*\*)-3-benzoyloxy-1-(*tert*-butyldimethylsilyloxy)-2-(*N*-15*Z*-tetracosenoylamino)-11,12-methylenedocosane (**64**) (0.083 g, 0.089 mmol) and EtOH/DCM (3 mL, 1:1). The resulting mixture was then placed in a preheated oil bath (55 °C) for 3 h under reflux. The reaction was allowed to cool to rt, Et<sub>3</sub>N (0.5 mL) was added, and then the solution was concentrated. Purification by flash column chromatography on silica gel (hexanes/EtOAc 4:1) provided **46** as a colorless oil (70 mg, 96%): IR (neat) 3287 br, 2922, 2852, 1721, 1649, 1463, 1271 cm<sup>-1</sup>; <sup>1</sup>H NMR (400 MHz, CDCl<sub>3</sub>) δ 8.08–8.02 (m, 2H), 7.63–7.57 (m, 1H), 7.50–7.43 (m, 2H), 6.32 (d, *J* = 8.7 Hz, 1H), 5.40–5.29 (m, 2H), 5.09 (ddd, *J* = 8.8, 8.8, 3.4 Hz, 1H), 4.23–4.15 (m, 1H), 3.71–3.57 (m, 2H), 3.18 (br s, 1H), 2.22 (t, *J* = 7.5 Hz, 2H), 2.06–1.95 (m, 4H), 1.89–1.70 (m, 2H), 1.69–1.59 (m, 2H), 1.40–1.05 (m, 62H), 0.88 (t, *J* = 6.3 Hz, 6H), 0.67–0.57 (m, 2H), 0.53 (ddd, *J* = 7.6, 7.6, 3.7 Hz, 1H), –0.36 (ddd, *J* = 5.0, 5.0, 5.0 Hz, 1H); <sup>13</sup>C NMR (100 MHz, CDCl<sub>3</sub>) δ 173.7, 168.0, 133.8, 130.1, 130.1, 129.5, 128.8, 74.6, 62.1, 53.6, 37.1, 32.1, 31.8, 30.4, 30.3, 30.0, 29.9, 29.9, 29.8, 29.7, 29.6, 29.5, 28.9, 28.9, 27.4, 25.9, 25.9, 22.9, 16.0, 15.9, 14.3, 11.1; HRMS (ESI) calcd for C<sub>54</sub>H<sub>96</sub>NO<sub>4</sub> (*M* + *H*)<sup>+</sup> *m/z* 822.7328, found 822.7322.



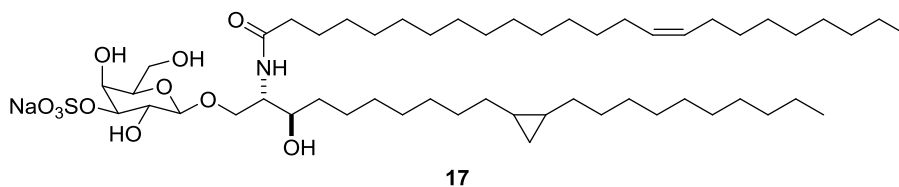
**(2*S*,3*R*,11*S*\*,12*R*\*)-2-(*N*-15*Z*-Tetracosenoylamino)-1-(2,3,4,6-tetra-*O*-pivaloyl-β-*D*-galactopyranosyloxy)-11,12-methylenedocosane (68).** (2,3,4,6-Tetra-*O*-pivaloyl-α-*D*-galactopyranosyl)-1-trichloroacetimidate (**47**) (85 mg, 0.13 mmol) and (2*S*,3*R*,11*S*\*,12*R*\*)-3-benzoyloxy-2-(*N*-15*Z*-tetracosenoylamino)-

11,12-methylenedocosan-1-ol (**46**) (0.070 g, 0.086 mmol) were added to dry DCM (1 mL), and the mixture stirred in the presence of 4Å MS (100 mg) at 0 °C for 10 min. BF<sub>3</sub>•OEt<sub>2</sub> (3.2 μL, 0.021 mmol) in dry DCM (2 mL) was added dropwise over 10 min. The reaction mixture was then allowed to warm to rt and stirred for 12 h. The reaction mixture was diluted with petroleum ether (6 mL) and then filtered. The filtrate was treated with saturated aqueous NaHCO<sub>3</sub> (15 mL). The organic layer was separated and the aqueous phase was extracted with DCM (3 x 15 mL). The combined organic extracts were dried (NaSO<sub>4</sub>), filtered and concentrated. Purification by flash column chromatography on silica gel (hexanes/EtOAc 9:1) provided **68** as a colorless oil (67 mg, 43%): IR (neat) 2923, 2853, 1740, 1276, 1144 cm<sup>-1</sup>; <sup>1</sup>H NMR (400 MHz, CDCl<sub>3</sub>) δ 8.05–7.99 (m, 2H), 7.58–7.53 (m, 1H), 7.48–7.41 (m, 2H), 5.92 (d, *J* = 8.9 Hz, 1H), 5.40–5.29 (m, 3H), 5.26–5.18 (m, 1H), 5.18–5.12 (m, 1H), 5.07 (dd, *J* = 10.4, 3.2 Hz, 1H), 4.52–4.40 (m, 2H), 4.00 (dd, *J* = 10.0, 4.0 Hz, 1H), 3.91–3.80 (m, 3H), 3.64 (dd, *J* = 9.9, 3.9 Hz, 1H), 2.15 (t, *J* = 7.6 Hz, 2H), 2.05–1.95 (m, 4H), 1.80–1.52 (m, 4H), 1.44–1.00 (m, 98H), 0.87 (t, *J* = 6.4 Hz, 6H), 0.66–0.56 (m, 2H), 0.53 (ddd, *J* = 7.7, 7.7, 3.8 Hz, 1H), –0.36 (ddd, *J* = 5.0, 5.0, 5.0 Hz, 1H); <sup>13</sup>C NMR (100 MHz, CDCl<sub>3</sub>) δ 177.9, 177.5, 177.0, 177.0, 173.0, 166.0, 133.2, 130.4, 130.1, 129.9, 128.7, 101.1, 74.2, 71.2, 71.0, 69.1, 67.6, 66.7, 61.0, 50.8, 39.3, 39.0, 39.0, 38.9, 37.1, 32.1, 31.7, 30.4, 30.4, 30.0, 30.0, 29.9, 29.8, 29.7, 29.6, 29.6, 29.5, 28.9, 27.4, 27.4, 27.3, 27.3, 25.9, 25.5, 22.9, 16.0, 15.9, 14.3, 11.1; HRMS (ESI) calcd for C<sub>80</sub>H<sub>137</sub>NNaO<sub>13</sub> (M + Na)<sup>+</sup> *m/z* 1342.9977, found 1342.9890.



**(2S,3R,11S\*,12R\*)-1-(β-D-Galactopyranosyloxy)-2-(N-15Z-tetracosenoylamino)-11,12-methylenedocosan-3-ol (48).** NaOMe (0.012 g, 0.224 mmol) was added to a solution of (2S,3R,11S\*,12R\*)-2-(N-15Z-tetracosenoylamino)-1-(2,3,4,6-tetra-*O*-pivaloyl-β-D-galactopyranosyl-oxy)-11,12-methylenedocosane (**68**) (0.049 g, 0.037 mmol) in a solution of DCM/MeOH (0.6 mL, 1:1). The solution was stirred at rt for 1

h and then neutralized to pH 2 with dowex ( $\text{H}^+$  resin). The mixture was filtered through a pad of celite, and the celite was washed with a 1:1 mixture of  $\text{CHCl}_3$  and MeOH (15 mL) and then concentrated. Purification by flash column chromatography on silica gel (DCM/MeOH 23:2) provided **48** as a white foam (27 mg, 82%): IR (neat) 3332 (br), 2922, 2852, 1649, 1458, 1021  $\text{cm}^{-1}$ ;  $^1\text{H}$  NMR (400 MHz,  $\text{CDCl}_3/\text{CD}_3\text{OD}$  3:1)  $\delta$  7.54 (d,  $J = 9.1$  Hz, 1H), 5.35–5.25 (m, 2H), 4.20–4.14 (m, 2H), 3.95–3.87 (m, 1H), 3.86–3.81 (m, 1H), 3.77 (dd,  $J = 11.6, 6.7$  Hz, 1H), 3.70 (dd,  $J = 11.6, 5.0$  Hz, 1H), 3.61–3.43 (m, 5H), 2.17 (t,  $J = 7.3$  Hz, 2H), 2.04–1.92 (m, 4H), 1.65–1.45 (m, 4H), 1.42–1.05 (m, 62H), 0.85 (t,  $J = 6.3$  Hz, 6H), 0.66–0.57 (m, 2H), 0.56–0.49 (m, 1H),  $-0.37$  (ddd,  $J = 4.8, 4.8, 4.8$  Hz, 1H);  $^{13}\text{C}$  NMR (100 MHz,  $\text{CDCl}_3/\text{CD}_3\text{OD}$  3:1)  $\delta$  174.5, 129.6, 103.5, 74.9, 73.2, 71.2, 70.6, 68.8, 68.7, 61.2, 53.2, 36.2, 33.5, 31.7, 30.0, 30.0, 29.5, 29.3, 29.3, 29.2, 29.1, 29.1, 29.0, 28.9, 28.5, 26.9, 25.8, 25.7, 22.4, 15.5, 13.6, 10.6; HRMS (ESI) calcd for  $\text{C}_{53}\text{H}_{101}\text{NNaO}_8$  ( $\text{M} + \text{Na}$ ) $^+ m/z$  902.7414, found 902.7250.



**(2*S*,3*R*,11*S*\*,12*R*\*)-1-(3-*O*-Sodiumsulfonyl- $\beta$ -D-galactopyranosyloxy)-2-(*N*-15*Z*-tetracosenoylamino)-11,12-methylenedocosan-3-ol (17).** (2*S*,3*R*,11*S*\*,12*R*\*)-1-( $\beta$ -D-Galactopyranosyloxy)-2-(*N*-15*Z*-tetracosenoylamino)-11,12-methylenedocosan-3-ol (**48**) (0.024 g, 0.029 mmol) and  $\text{Bu}_2\text{SnO}$  (0.011 g, 0.045 mmol) were stirred in MeOH (1.5 mL) at reflux under  $\text{N}_2$  for 2h. The solvent was evaporated under reduced pressure, and the dibutylstannylene complex was treated with  $\text{Me}_3\text{N}\cdot\text{SO}_3$  (0.009 g, 0.062 mmol) in THF (2 mL) with stirring for 2 h. The solvent was removed under reduced pressure, and the residue was then dissolved in  $\text{CHCl}_3/\text{MeOH}$  (2 mL, 1:1), loaded onto a cation-exchange resin column (Dowex 50 x 8  $\text{Na}^+$  form, 0.5 x 6 cm), eluted with  $\text{CHCl}_3/\text{MeOH}$  (1:1) and concentrated. Purification by flash column chromatography on silica gel ( $\text{CH}_2\text{Cl}_2/\text{MeOH}$  9:1) provided  $\beta$ -sulfatide **17** as a white foam (19 mg, 71%): IR (neat) 3379 (br), 2923, 2853, 2495 (br), 2246, 2137, 2072, 1627, 1463, 1221, 1120  $\text{cm}^{-1}$ ;  $^1\text{H}$  NMR (400

MHz, CDCl<sub>3</sub>/CD<sub>3</sub>OD 3:1)  $\delta$  7.55 (d,  $J$  = 9.1 Hz, 1H), 5.35–5.24 (m, 2H), 4.29 (d,  $J$  = 7.7 Hz, 1H), 4.26–4.20 (m, 2H), 3.95–3.85 (m, 1H), 3.81–3.66 (m, 4H), 3.60–3.50 (m, 3H), 2.17 (t,  $J$  = 7.4 Hz, 2H), 2.04–1.90 (m, 4H), 1.64–1.44 (m, 4H), 1.39–1.05 (m, 62H), 0.84 (t,  $J$  = 6.5 Hz, 6H), 0.65–0.56 (m, 2H), 0.52 (ddd,  $J$  = 7.6, 7.6, 3.8 Hz, 1H), –0.38 (ddd,  $J$  = 5.0, 5.0, 5.0 Hz, 1H); <sup>13</sup>C NMR (100 MHz, CDCl<sub>3</sub>/CD<sub>3</sub>OD 3:1)  $\delta$  174.8, 129.8, 103.2, 79.9, 74.4, 70.8, 69.3, 69.1, 67.5, 61.4, 54.7, 53.3, 36.4, 33.7, 31.8, 30.1, 30.1, 29.6, 29.6, 29.5, 29.4, 29.3, 29.2, 28.6, 27.1, 25.9, 25.8, 22.5, 15.6, 13.8, 10.7; HRMS (ESI) calcd for C<sub>53</sub>H<sub>100</sub>NnaO<sub>11</sub>S (M + Na)<sup>+</sup> m/z 958.7019, found 958.6970.

## 1.4 References

1. Degroote, S.; Wolthoorn, J.; van Meer, G. *Semin. Cell Dev. Biol.* **2004**, *15*, 375.
2. Kain, L.; Webb, B.; Anderson, B. L.; Deng, S.; Holt, M.; Costanzo, A.; Zhao, M.; Self, K.; Teyton, A.; Everett, C.; Kronenberg, M.; Zajonc, D. M.; Bendelac, A.; Savage, P. B.; Teyton, L. *Immunity* **2014**, *41*, 543.
3. Ishizuka, I. *Prog. Lipid Res.* **1997**, *36*, 245.
4. Isaac, G.; Pernber, Z.; Gieselmann, V.; Hansson, E.; Bergquist, J.; Månsson, J. E. *FEBS J.* **2006**, *273*, 1782.
5. Fredman, P.; Månsson, J. E.; Rynmark, B. M.; Josefsen, K.; Ekblond, A.; Halldner, L.; Osterbye, T.; Horn, T.; Bushard, K. *Glycobiology* **2000**, *10*, 39.
6. Tsuji, M. *Cell Mol. Life Sci.* **2006**, *63*, 1889.
7. Giabbai, B.; Sidobre, S.; Cripsin, M. D. M.; Sanchez-Ruiz, Y.; Bachi, A.; Kronenberg, M.; Wilson, I. A.; Degano, M. *J. Immunol.* **2005**, *175*, 977.
8. a) Jahng, A.; Maricic, I.; Aguilera, C.; Cardell, S.; Halder, R. C.; Kumar, V. *J. Exp. Med.* **2004**, *199*, 947; b) Arrenberg, P.; Halder, R. C.; Dai, Y.; Maricic, I.; Kumar, V. *Proc. Natl. Acad. Sci. USA* **2010**, *107*, 10984.
9. Wu, D.; Xin, G.-W.; Poles, M. A.; Horowitz, A.; Kinjo, Y.; Sullivan, B.; Bodmer-Narkevitch, V.; Plettenburg, O.; Kronenberg, M.; Tsuji, M.; Ho, D. D.; Wong, C.-H. *Proc. Natl. Acad. Sci. USA* **2005**, *102*, 1351.
10. Calabi, F.; Jarvis, J. M.; Martin, L.; Milstein, C. *Eur. J. Immunol.* **1989**, *19*, 285.
11. Zeng, Z.-H.; Castaño, A. R.; Segelke, B. W.; Stura, E. A.; Peterson, P. A.; Wilson, I. A. *Science* **1997**, *277*, 339.
12. (a) Arrenberg, P.; Halder, R. C.; Kumar, V. *J. Cell Physiol.* **2009**, *218*, 246; (b) Kumar, V.; Delovitch, T. L. *Immunology* **2014**, *142*, 321; (c) Rhost, S.; Sedimbi, S.; Kadri, N.; Cardell, S. L. *J. Immunol.* **2012**, *76*, 246.
13. Taniguchi, M.; Seino, K.; Nakayama, T. *Nat. Immunol.* **2003**, *4*, 1164.

14. (a) Bendelac, A.; Savage, P. B.; Teyton, L. *Annu. Rev. Immunol.* **2007**, *25*, 297; (b) Godfrey, D. I.; Stankovic, S.; Baxter, A. G. *Nat. Immunol.* **2010**, *11*, 197; (c) Brigl, M.; Brenner, M. B. *Annu. Rev. Immunol.* **2004**, *22*, 817.
15. Benlagha, K.; Weiss, A.; Beavis, A.; Teyton, L.; Bendelac, A. *J. Exp. Med.* **2000**, *191*, 1895.
16. Terabe, M.; Berzofsky, J. A. *Trends Immunol.* **2005**, *175*, 977.
17. Park, S.-H.; Weiss, A.; Benlagha, K.; Kyin, T.; Teyton, L.; Bendelac, A. *J. Exp. Med.* **2001**, *193*, 893.
18. Sullivan, B. A.; Nagaraja, N. A.; Wingender, G.; Wang, J.; Scott, I.; Tsuji, M.; Franck, R. W. Porcelli, S. A.; Zajonc, D. M.; Kronenberg, M. *J. Immunol.* **2010**, *184*, 141.
19. Zajonc, D. M.; Maricic, I.; Wu, D.; Halder, R. C.; Roy, K.; Wong, C.-H.; Kumar, V.; Wilson, I. *J. Exp. Med.* **2005**, *202*, 1517.
20. Blix, G. *Hoppe-Seyler's Zeitschrift Fur Physiologische* **1933**, *219*, 82.
21. Lingwood, C. A.; Hay, G.; Schachter, H. *Can. J. Biochem.* **1981**, *59*, 556.
22. Shamshiev, A.; Gober, H.-J.; Donda, A.; Mazorra, Z.; Mori, L.; De Libero, G. *J. Exp. Med.* **2002**, *195*, 1013.
23. Patel, O.; Pellicci, D. G.; Gras, S.; Sandoval-Romero, M. L.; Uldrich, A. P.; Mallevaey, T.; Clarke, A. J.; Le Nours, J.; Theodossis, A.; Cardell, S. L.; Gapin, L.; Godfrey, D. I.; Rossjohn, J. *Nat. Immunol.* **2012**, *13*, 857.
24. Godfrey, D. I.; MacDonald, H. R.; Kronenberg, M.; Smyth, M. J.; Van Kaer, L. *Nat. Rev. Immunol.* **2004**, *4*, 231.
25. Girardi, E.; Maricic, I.; Wang, J.; Mac, T.-T.; Iyer, P.; Kumar, V.; Zajonc, D. M. *Nat. Immunol.* **2012**, *13*, 851.
26. Ambrosino, E.; Terabe, M.; Halder, R. C.; Peng, J.; Takaku, S.; Miyake, S.; Yamamura, T.; Kumar, V.; Berzofsky, J. A. *J. Immunol.* **2007**, *179*, 5126.
27. Roy, K. C.; Maricic, I.; Khurana, A.; Smith, T. R. F.; Halder, R. C.; Kumar, V. *J. Immunol.* **2008**, *180*, 2942.



28. Duarte, N.; Stenström, M.; Campino, S.; Bergman, M.-L.; Lundholm, M.; Holmberg, D.; Cardell, S. L. *J. Immunol.* **2004**, *173*, 3112.
29. Shamshiev, A.; Donda, A.; Carena, I.; Mori, L.; Kappos, L.; De Libero, G. *Eur. J. Immunol.* **1999**, *29*, 1667.
30. Lehuen, A.; Diana, J.; Zacccone, P.; Cooke, A. *Nat. Rev. Immunol.* **2010**, *10*, 501.
31. Skold, M.; Faizunnessa, N. N.; Wang, C. R.; Cardell, S. *J. Immunol.* **2000**, *165*, 168.
32. Andersson, K.; Buschard, K.; Fredman, P.; Kaas, A.; Lidström, A.-M.; Madsbad, S.; Mortensen, H.; Mansson, J.-E. *Autoimmunity* **2002**, *35*, 463.
33. Subramanian, L.; Blumenfeld, H.; Tohn, R.; Ly, D.; Aguilera, C.; Maricic, I.; Mansson, J.-E.; Buschard, K.; Kumar, V.; Delovitch, T. L. *PloS One* **2012**, *7*, e37771.
34. Fuss, I. J.; Heller, F.; Boirivant, M.; Leon, F.; Yoshida, M.; Fichtner-Feigl, S.; Yang, Z.; Exley, M.; Kitani, A.; Blumberg, R. S.; Mannon, P.; Strober, W. *J. Clin. Invest.* **2004**, *113*, 1490.
35. Pillai, A. B.; George, T. I.; Dutt, S.; Teo, P.; Strober, S. *J. Immunol.* **2007**, *178*, 6242.
36. Satoh, M.; Andoh, Y.; Clingan, C. S.; Ogura, H.; Fujii, S.; Eshima, K.; Nakayama, T.; Taniguchi, M.; Hirata, N.; Ishimori, N.; Tsutsui, H.; Onoé, K.; Iwabuchi, K. *PloS One* **2012**, *7*, e30568.
37. Halder, R. C.; Aguilera, C.; Maricic, I.; Kumar, V. *J. Clin. Invest.* **2007**, *117*, 2302.
38. Baron, J. L.; Gardiner, L.; Nishimura, S.; Shinkai, K.; Locksley, R.; Ganem, D. *Immunity* **2002**, *16*, 583.
39. Li, X.; Fujio, M.; Imamura, M.; Wu, D.; Vasan, S.; Wong, C.-H.; Ho, D. D.; Tsuji, M. *Proc. Natl. Acad. Sci. USA* **2010**, *107*, 13010.
40. Tzysnik, A. J.; Farber, E.; Girardi, E.; Birkholz, A.; Li, Y.; Chitale, S.; So, R.; Arora, P.; Khurana, A.; Porcelli, S. A.; Zajonc, D. M.; Kronenberg, M.; Howell, A. R. *Chem. Biol.* **2011**, *18*, 1620.
41. Banchet-Cadeddu, A.; Hénon, E.; Dauchez, M.; Renault, J.-H.; Monneaux, F.; Haudrechy, A. *Org. Biomol. Chem.* **2011**, *9*, 3080.
42. Juang, K.-H.; Schmidt, R. R. *CRC Press: Sheffield* **1999**, 208.

43. (a) Martin, T. J.; Schmidt, R. R. *Tetrahedron Lett.* **1992**, 33, 6123; (b) Schmidt, R. R.; Zimmermann, P. *Angew. Chem. Int. Ed.* **1986**, 27, 481.
44. Du, W.; Gervay-Hague, J. *Org. Lett.* **2005**, 7, 2063.
45. For a general review about *O*-glycosylation see: (a) Pellissier, H. *Tetrahedron* **2005**, 61, 2947; (b) Demchenko, A. V. *Synlett* **2003**, 1225.
46. Tanahashi, E.; Murase, K.; Shibuya, M.; Igarashi, Y.; Ishida, H.; Hasegawa, A.; Kiso, M. *J. Carbohydr. Chem.* **1997**, 16, 831.
47. Marinier, A.; Martel, A.; Banville, J.; Bachand, C.; Remillard, R.; Lapointe, P.; Turmel, B.; Menard, M.; Harte, J. W. E.; Wright, J. J.; Todderud, G.; Tramposch, K. M.; Bajorath, J.; Hollenbaugh, D.; Aruffo, A. *J. Med. Chem.* **1997**, 40, 3234.
48. Guilbert, B.; Davis, N. J.; Pearce, M.; Aplin, R. T.; Flitsch, S. L. *Tetrahedron: Asymmetry* **1994**, 5, 2163.
49. Kim, S.; Lee, S.; Lee, T.; Ko, H.; Kim, D. *J. Org. Chem.* **2006**, 71, 8661.
50. Alper, P. B.; Hung, S.-C.; Wong, C.-H. *Tetrahedron Lett.* **1996**, 37, 6029.
51. Schombs, M.; Park, F. E.; Du, W.; Kulkarni, S. S.; Gervay-Hague, J. *J. Org. Chem.* **2010**, 75, 4891.
52. Lindlar, H.; Dubuis, R. *Org. Synth.* **1966**, 46, 89.
53. (a) Simmons, H. E.; Smith, R. D. *J. Am. Chem. Soc.* **1958**, 80, 5323; (b) Simmons, H. E.; Smith, R. D. *J. Am. Chem. Soc.* **1959**, 81, 4256.
54. Appel, R. *Angew. Chem. Int. Ed.* **1975**, 14, 801.
55. (a) Hoffman, R. V.; Maslouh, N.; Cervantes-Lee, F. *J. Org. Chem.* **2002**, 67, 1045; (b) So, R. C.; Ndonye, R.; Izmirian, D. P.; Richardson, S. K. Howell, A. R. *J. Org. Chem.* **2004**, 69, 3233.
56. Schmidt, R. R.; Stumpp, M. *Liebigs Ann. Chem.* **1983**, 1249.
57. Kunz, H.; Harreus, A. *Liebigs Ann. Chem.* **1982**, 41.
58. Mbadugha, B. N. A.; Menger, F. M. *Org. Lett.* **2003**, 5, 4041.

## **Chapter 2**

### **Synthesis of Palmostatin M-derived Probes**

## 2.1 Introduction

One of the major foci of research in the Howell group is exploiting the reactivity of architecturally strained heterocycles such as  $\beta$ -lactones (oxetan-2-one). The interest in  $\beta$ -lactones arises from the fact that they are present in a number of biologically active natural products and pharmaceutical agents.<sup>1</sup> Additionally, their versatile reactive nature, coupled with the unusual structural features of this species, makes them useful synthetic intermediates for transformations to more advanced structures.<sup>2,3</sup>

Herein, we describe the utilization of  $\alpha$ -methylene- $\beta$ -lactones in transition metal-catalyzed transformations to access  $\beta$ -lactones that are of importance in synthetic and medicinal chemistry. Two successful transformations include: (a) olefin cross metathesis (CM) of  $\alpha$ -methylene- $\beta$ -lactones coupled with stereoselective reductions and (b) Rh-catalyzed conjugate addition of aryl boronic acids to  $\alpha$ -methylene- $\beta$ -lactones. This work targets the discovery of novel  $\beta$ -lactone inhibitors of NRas palmitoylation. The following introductory sections will include a general background on  $\beta$ -lactones as biologically active compounds and as intermediates in organic synthesis. We will particularly focus on reactivities of  $\beta$ -lactones and their biological relevance. Recent transformations involving  $\alpha$ -methylene- $\beta$ -lactones are emphasized in the later sections.

### 2.1.1 $\beta$ -Lactones in Natural Products

Over the last four decades a notable amount of natural product possessing oxetan-2-one ring with interesting biological activity have been recognized. For example, lipstatin (**70**) (isolated from *Streptomyces toxytricini*)<sup>4,5</sup> and its crystalline, non-natural derivative, tetrahydrolipstatin (THL) (**71**), are known to be potent and irreversible pancreatic lipase inhibitors.<sup>6,7,8</sup> Esterastin (**72**) (first isolated from *Streptomyces lavendulae* MD4-C1)<sup>9,10</sup> is an oxetan-2-one closely related to lipstatin. Esterastin acts as a pancreatic lipase inhibitor but is less efficient than lipstatin and hence has received less attention. Ebelactones A (**73**) and B (**74**) (both isolated from *Streptomyces aburaviensis* MG7-G1) were reported to display inhibition of N-formylmethionine aminopeptidases located on the cellular membrane of various

kinds of animals cells.<sup>11</sup> Antibiotic 1233A (**75**), which was first isolated from *Cephalosporium sp.*, has been shown to inhibit 3-hydroxy-3-methylglutaryl coenzyme A synthase (HMG-CoA synthase), a key regulatory enzyme in the cholesterol biosynthetic pathway.<sup>12,13,14</sup> Obafluorin (**76**), isolated from *Pseudomonas sp.* SC 11,637, is known to display weak antibacterial activity (Figure 19).<sup>15</sup>

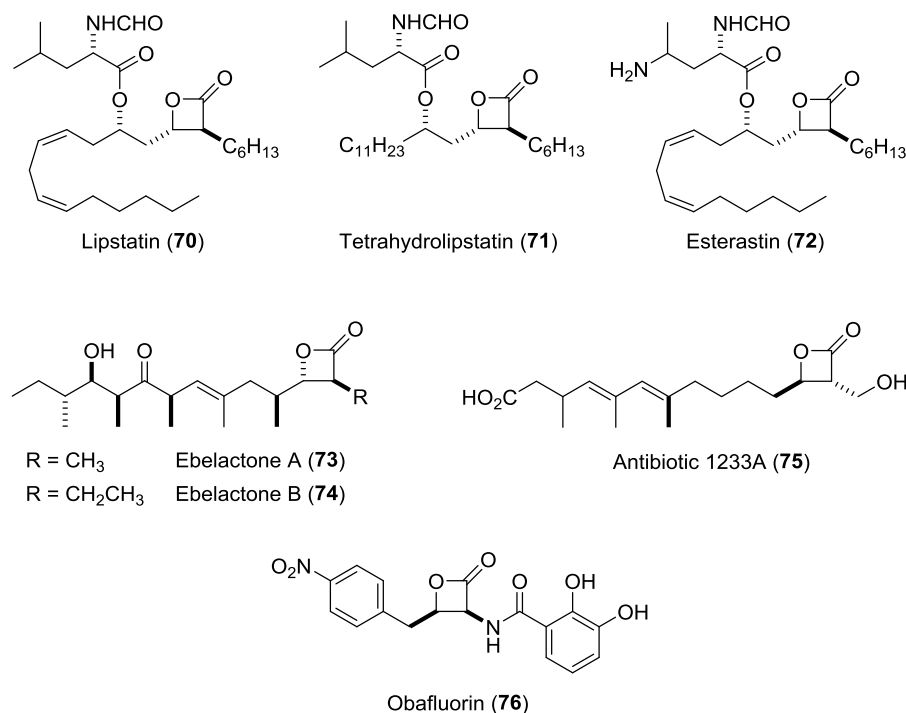


**Figure 19.**  $\beta$ -Lactone-containing natural products

The presence of the oxetan-2-one ring in these compounds is significant since often the ring is essential to the biological activity of the molecule. A good example is displayed by THL, an irreversible pancreatic lipase inhibitor. The purpose of pancreatic lipase is to cleave free fatty acids from their triglyceride precursors and facilitate their subsequent absorption by the organism. For these reasons, the inhibition of this enzyme should allow dietary fat to pass into the gut without being absorbed; hence making THL a promising candidate for obesity control. THL's mechanism of action involves an irreversible transesterification of the  $\beta$ -lactone ring by the hydroxyl group of serine 152 in pancreatic lipase, thereby inhibiting the enzyme (Figure 20).<sup>16,17</sup> Thus, the strain associated with  $\beta$ -lactone scaffold plays an important role in enhancing susceptibility to nucleophilic attack. This property results in easy irreversible

acylation of enzymes which prove therapeutically useful. The following section describes the general reactivity of  $\beta$ -lactones.

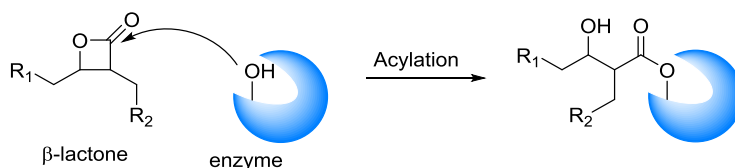


**Figure 20.** Acylation of enzymes

### 2.1.2 General Reactivity of $\beta$ -Lactones

The strained nature of  $\beta$ -lactones has presented opportunities for the invention of novel transformations. These include: (a) rearrangement leading to ring expansion (b) electrophilic reactions of  $\beta$ -lactone enolates and (c) nucleophilic ring opening to obtain 1,3-functionalized acyclic products (Figure 21).

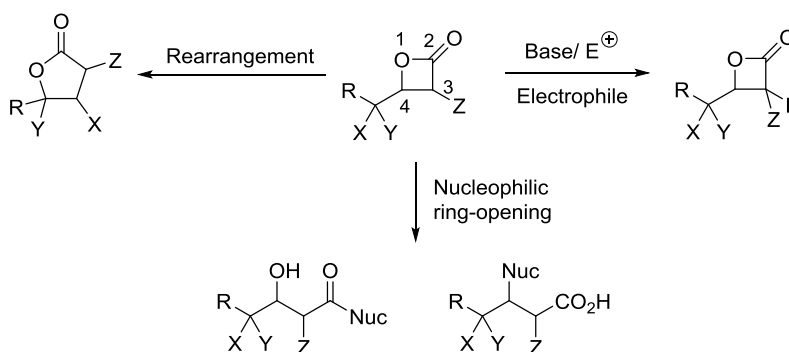
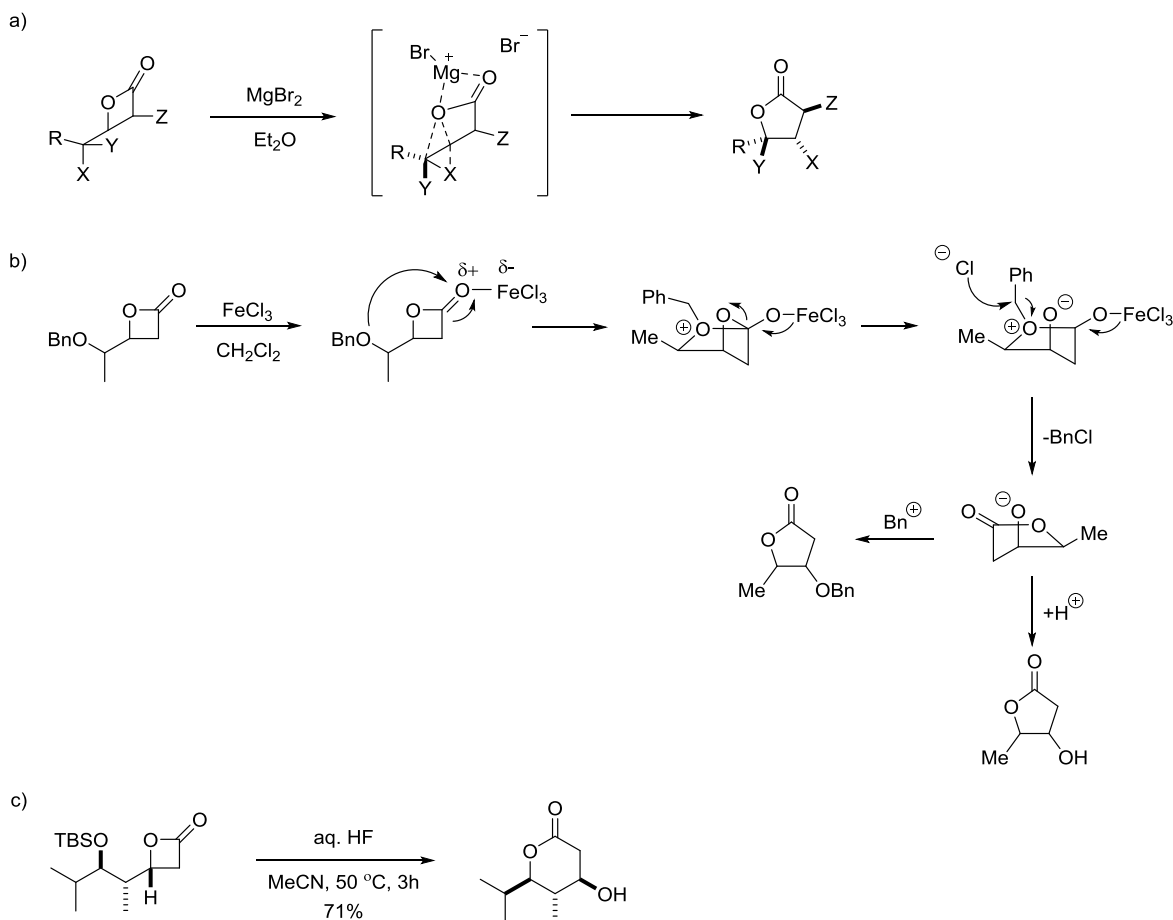


**Figure 21.** Primary reactivity modes of  $\beta$ -lactones

#### 2.1.2.1 Lewis Acid Promoted Rearrangement

Treatment of  $\beta$ -lactones with various Lewis acids can lead to dyotropic rearrangement (a transformation in which two  $\sigma$ -bonds simultaneously migrate intramolecularly).<sup>18</sup> This concerted process leads to ring expansion from four-membered lactones to five-membered lactones through the antiperiplanar transposition of the C–O bond and the neighboring C–Y bond (Scheme 12a). Lewis acids that promote this process include  $\text{MgBr}_2$ ,  $\text{MgCl}_2$ ,  $\text{TiCl}_4$ ,  $\text{Ti}(\text{OiPr})_4$ ,  $\text{BF}_3$ ,  $\text{FeBr}_3$ ,  $\text{AlBr}_3$ ,  $\text{SnCl}_4$ ,  $\text{ZnCl}_2$ , and  $\text{Cu}(\text{acac})_2$ .<sup>19</sup>  $\beta$ -Lactones bearing neighboring benzyl ethers can undergo ring expansion through a

transacylation/debenzylation sequence in the presence of  $\text{BF}_3$ ,  $\text{BCl}_3$ , or  $\text{FeCl}_3$  (Scheme 12b).<sup>20</sup> Recent studies have demonstrated the extension of rearrangement process to  $\beta$ -lactones with pendant silyl ethers (Scheme 12c).<sup>21</sup>  $\alpha,\beta$ -Unsaturated acids can also be accessed via dyotropic rearrangements.<sup>22</sup>

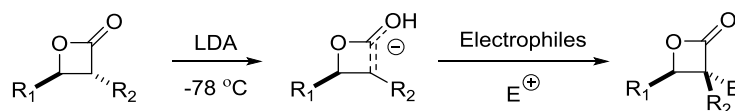


**Scheme 12.** Lewis acid promoted rearrangements; a) dyotropic rearrangements; b) ring expansion via a transacylation/debenzylation sequence; c) rearrangement of  $\beta$ -lactones with pendant silyl ethers

### 2.1.2.2 Reaction with Electrophiles

$\beta$ -Lactones can be deprotonated at low temperature ( $-78\text{ }^\circ\text{C}$ ) by lithium diisopropylamide (LDA) in THF.<sup>23</sup> The formed enolates were found to be stable at such a temperature and reacted with various electrophiles including alkyl, allyl and propargyl halides, aldehydes, dimethyl maleate and phenylisothiocyanate. The attack usually takes place opposite to the  $\beta$ -substituent for steric reasons, thus allowing control of asymmetric centers (diastereoselectivity) in a single operation (Scheme 13). Lithium

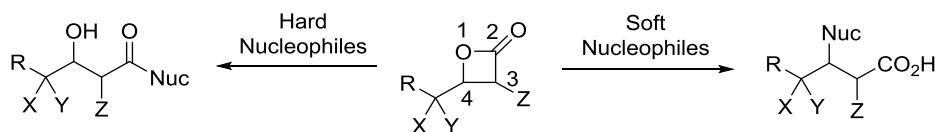
enolates of  $\alpha$ -substituted  $\beta$ -lactones were found to be stable and reacted with electrophiles smoothly. On the contrary, alkylation of  $\beta$ -lactone enolates without  $\alpha$ -substitution was difficult and often thwarted by side reactions such as self-acylation.<sup>24</sup> Recently, Parsons and Cowell had success in a total synthesis of (+/-)-tetrahydrolipstatin using low temperature, inverse addition, and an allyl iodide as electrophile.<sup>25</sup>



**Scheme 13.** Diastereoselective electrophilic reactions of  $\beta$ -lactones enolates

### 2.1.2.3 Reaction with Nucleophiles

Just as  $\beta$ -lactones can be prepared via oxygen-alkyl or oxygen-acyl bond formation, they also undergo, in the presence of nucleophiles, oxygen-alkyl or oxygen-acyl bond cleavage (Scheme 14).<sup>26</sup> Thus,  $\beta$ -lactones are ambident electrophiles, a property that renders them versatile intermediates for a variety of transformations. As a rule of thumb, hard nucleophiles such as alkoxides, alkyllithium reagents, and Grignard reagents react with  $\beta$ -lactones to cleave the acyl C–O bond (C2–O1), while alkyl C–O (C4–O1) cleavage occurs with soft nucleophiles, including organocuprates, azides, halides and thiolates.



**Scheme 14.** Nucleophilic ring-opening of  $\beta$ -lactones

From the perspective of biological activities, the strain associated with the  $\beta$ -lactone ring is responsible for its reactions in the biological systems i.e the enhanced susceptibility to nucleophilic attack. Like the better known azetidinone ( $\beta$ -lactam), this trait leads to easy, irreversible acylation of enzymes, which has proved to be therapeutically worthwhile. The following section will highlight the function of acyl protein thioesterase (APT) inhibitors as probes of dynamic S-palmitoylation and the role of  $\beta$ -lactones as inhibitors.



### 2.1.3 Acyl Protein Thioesterase (APT) inhibitors as Probes of Dynamic S-Palmitoylation

Protein palmitoylation refers to the formation of a thioester bond between a cysteine thiol side chain and a saturated 16-carbon fatty acid.<sup>27</sup> This hydrophobic modification is crucial in the functioning, trafficking, and localization of various proteins. From recent proteomics studies, hundreds of palmitoylated proteins<sup>28</sup> have been disclosed and shown to play an extensive role. Compared to the other lipid modifications that occur in the cell (prenylation and myristoylation), palmitoylation is readily reversible, which is accredited to the unstable thioester linkage. Therefore the rapid cycles of palmitoylation and depalmitoylation facilitate facile movement of proteins between the plasma membrane and the Golgi apparatus to regulate many cellular functions.

Protein palmitoyl thioesterases (PPTs) catalyze the de-palmitoylation and release of certain proteins from the plasma membrane, with the capacity of attenuating membrane coupled signaling pathways (Figure 22). The released proteins can then go through repalmitoylation by endomembrane-bound DHHC palmitoyl-transferases, sequentially imposing palmitoylation and resetting the cycle. Diverse proteins have been indicated as acyl protein thioesterase substrates in *in vitro* assays.<sup>29</sup> Ras proteins, which participate in an acylation/deacylation cycle, are an excellent example in this regard.<sup>30</sup>

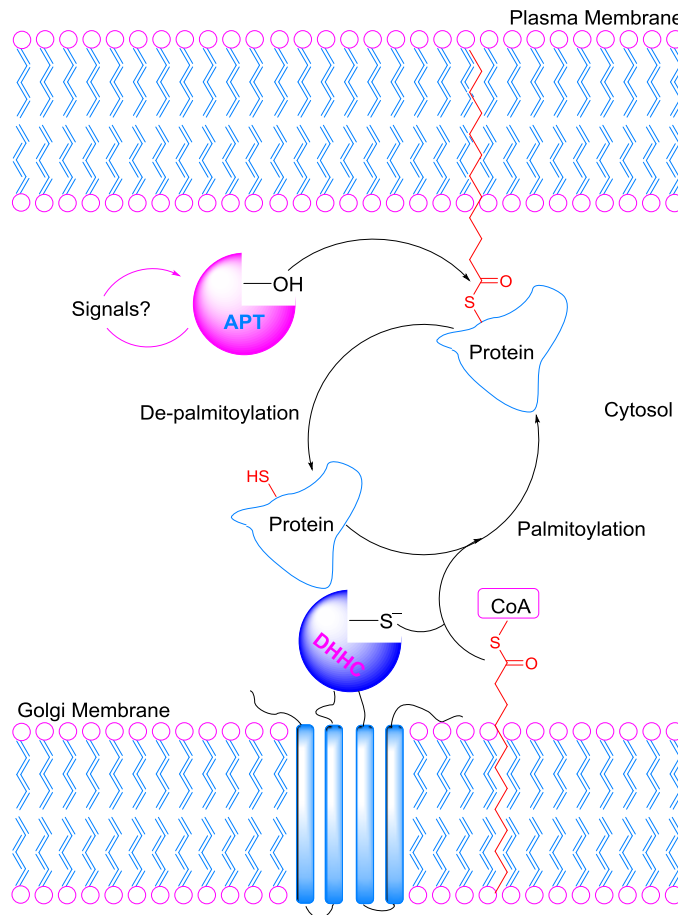


**Figure 22.** A dynamic S-palmitoylation

APTs belong to the metabolic serine hydrolase (SH) superfamily, characterized by the presence of an active site serine used for substrate hydrolysis that is implicated in amide, ester or thioester bond cleavage in peptides, proteins and lipids.<sup>31</sup> The identification of the cytosolic APT1 as the enzyme responsible for palmitate removal was first reported by Duncan and Gilman in 1998.<sup>29</sup> APT1 is a highly conserved  $\alpha/\beta$  hydrolase that contains both the S-H-D catalytic triad and a G-X-S-X-G motif and it is found mostly in cytosolic fractions in both *Sacharomyces cerevisiae* and mammalian cells. A second enzyme that plays a role in palmitate removal from proteins is APT2, also known as lysophospholipase II. Phylogenic analysis shows that invertebrates evolved only one APT enzyme, while vertebrates evolved two (APT1 and APT2). In spite of the fact that the palmitoylation site is not conserved in canine APT1 or invertebrate APTs, they (APT1 and APT2) have all been recognized as palmitoylated proteins.<sup>28d,32</sup>

The serine nucleophilic nature of APTs is crucial in enhancing the formation of a covalent acyl-intermediate with substrates, thereby creating the opportunity to develop covalent, mechanism-based inhibitors. The development of small molecule inhibitors of APTs has received much attention in recent years.<sup>27</sup> These include both competitive and non-competitive inhibitors, which have been useful tools in several studies supporting a functional role for APTs in enzymatic depalmitoylation. In the next section, we focus our attention on  $\beta$ -lactones as APT inhibitors.

### 2.1.4 $\beta$ -Lactones as APT Inhibitors

Previous work, focused on the synthesis and screening of a small library of  $\beta$ -lactones on the basis of active-site similarity between APT1 and gastric lipase (and the fact that  $\beta$ -lactones are known lipase acylating reagents), led to the discovery of palmostatin B (Figure 23b).<sup>33a,34</sup> Palmostatin B was found to be membrane-permeable and to display direct reactivities with APT1 and APT2 as both a substrate and an inhibitor in live cells.<sup>33a</sup>

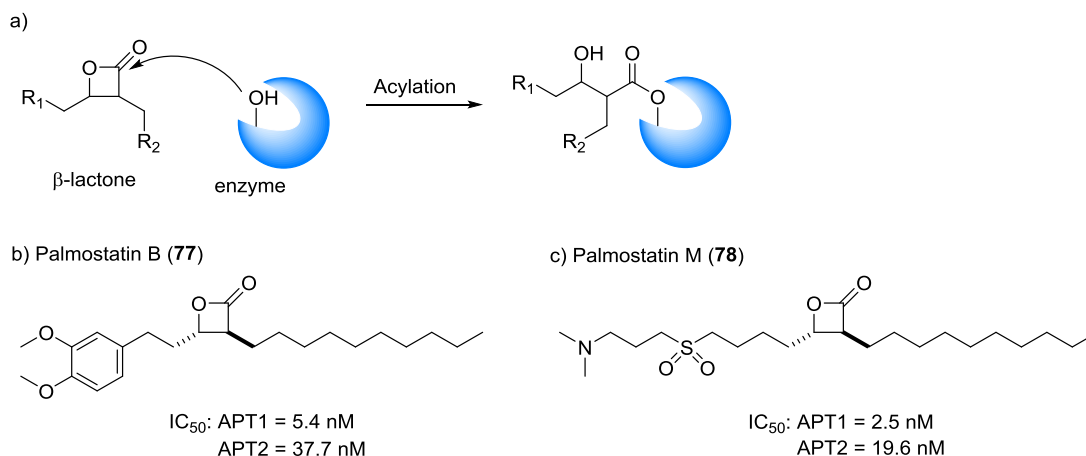


**Figure 23.** a) APT competitive enzyme inhibition by  $\beta$ -lactones; b) structure of palmostatin B; c) structure of palmostatin M

Experimental studies on the effect of APT inhibition have shown that palmostatin B (**77**) (with the half maximal inhibitory concentration,  $\text{IC}_{50}$ : APT1 = 5.4 nM, APT2 = 37.7 nM) impedes the growth of H-Ras or N-Ras transduced hematopoietic cells, but does not affect cells transduced with a non-palmitoylated

isoform of K-Ras.<sup>33b</sup> Such effects provide important pharmacological evidence of protein palmitoylation dynamics in live cells and clearly define a role for de-palmitoylation in Ras regulation.

The cytosolic enzyme (APT1) has a very broad substrate scope. APT1 not only performs the depalmitoylation of the C terminus of small GTPases, but also other G proteins, ghlerin, viral glycoproteins and lysophospholipids.<sup>34</sup> The unusual and exceptionally wide substrate tolerance of APT1 inspired Waldmann group<sup>34</sup> to employ the structural characteristics of different substrates as guiding arguments in designing a more potent family of inhibitors. From the fact that the activity of palmostatin B was found to rely on the stereochemistry of its electrophilic  $\beta$ -lactone core and the aliphatic substitution at its  $\alpha$  position, they surmised that selective recognition may be enhanced by the introduction of functionalities that enable hydrogen bonding and electrostatic interaction to the  $\beta$  position. Comparison of two known native APT1 substrates, lysophospholipid **79** and the H-Ras C terminus **80** led to the identification of a common recognition motif that consists of a negatively charged group at a distance five to six bonds (red) from the (thio-)ester functional group and a positively charged tail group ten to twelve bonds away (blue) (Figure 24a).

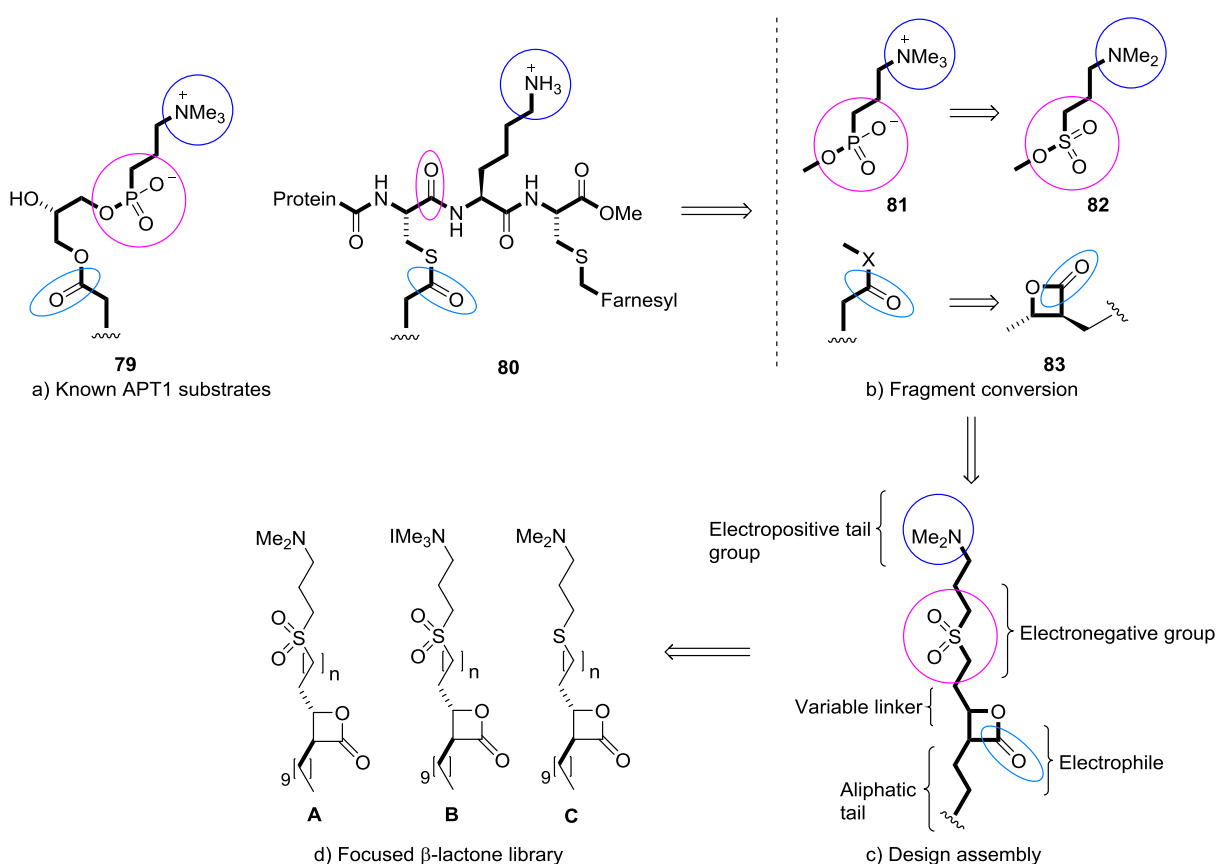


**Figure 24.** Inhibitor development based on substrate similarity<sup>34</sup>

They found that the phosphatidyl choline moiety **81** would provide the required electrostatic interactions but were worried that its zwitterionic nature might limit application in the cells. This moiety was then replaced by a sulfonyl-1,3-propylene-*N,N*-dimethylamino functionality **82** (Figure 24b). Fragment **82** was fused via a variable spacer to a *trans*- $\beta$ -lactone core **83**, which addressed the stereochemical preferences of APT1<sup>33a</sup> and served as a covalent modifier of the nucleophilic residue in the active site of the enzyme. In order to create affinity to the lipid-binding pocket of the enzyme, a lipophilic tail mimicking the palmitate moiety was introduced on the opposite side of the  $\beta$ -lactone core (Figure 24c). These criteria led to the design of a small focused library of three series of inhibitors, denoted A-C, which would define the structure-activity relationship (Figure 24d). This provided palmostin M which was found to be several times more active (with  $IC_{50}$  of 2.5 nM for APT1 and 19.6 nM for APT2) than palmstatin B ( $IC_{50}$  of 5.4

nM for APT1 and 37.7 nM for APT2). This represents an improved analog in comparison to palmostatin B (Figure 6b).<sup>34</sup>

Additionally, inspired by the fact that  $\beta$ -lactones form a semi-stable covalent complex with their targets, the Waldmann group developed an alkynyl palmostatin M analog to annotate potential cellular targets (Figure 25).<sup>35</sup> Lysates were labeled with an alkynyl probe (**84**), which was conjugated to a tri-functional rhodamine/biotin-azide by copper catalyzed click chemistry, enriched with streptavidin, and analyzed by in-gel fluorescence or mass spectrometry to identify candidate target proteins. These studies confirmed APT1 and APT2 as major palmostatin M targets, but also identified other serine hydrolases, including the lysosomal thioesterase PPT1 and retinoid-inducible serine carboxypeptidase (RISC). While these compounds are exceptionally potent, non-specific inhibition and poor drug-like properties limit the application of these probes for *in vivo* studies. The following section highlights the potential of  $\beta$ -lactones as targets for oncogenic N-Ras in cancer, which forms the basis of this study.

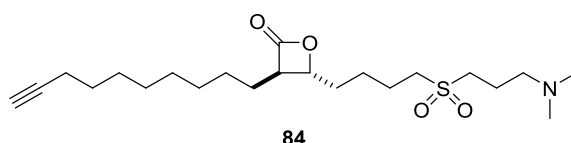


**Figure 25.** An alkynyl palmostatin M analogue (**84**)

### 2.1.5 Targeting Oncogenic N-Ras in Cancer

The kinetic trapping of the proteins at the Golgi by site-specific *S*-palmitoylation and *S*-depalmitoylation is the driving force that creates a precise steady-state localization of H-Ras and N-Ras, predominantly at the plasma membrane and the Golgi in the cytoplasm. This cyclic process, coupled with the directionality of the secretory pathway, is important for the maintenance of the dynamic spatial distribution of palmitoylated Ras-proteins.<sup>36</sup> In a study carried out by Waldmann group, they found that interference with the dynamic acylation cycle with small molecules at the level of depalmitoylation provided a means for randomizing Ras localization to all membranes, thereby affecting its signaling in the cell.<sup>33a</sup> A loss of the precise steady-state localization of still palmitoylated Ras proteins and a partial phenotype reversion of

MDCK-F3 cells were identified during long term palmostatin B inhibition of the cellular thioesterase activity. These studies revealed that the major contribution to the phenotype reversion is from the redistribution of palmitoylated oncogenic Ras, even though it is likely that other palmitoylated peripheral membrane proteins might also be affected in their spatial distribution. Furthermore, cell viability was not affected by thioesterase inhibition at the concentrations of palmostatin B used, showing that basal signaling necessary for cell survival remained active.

In another study, the Shannon group showed that the palmitoylation/depalmitoylation cycle of posttranslational processing is a potential therapeutic target for selectively inhibiting the growth of hematologic cancers with somatic N-Ras mutations.<sup>33b</sup> The investigation was carried out by constructing murine stem cell virus vectors and assaying the growth of myeloid progenitors. The outcome of this work proved that mutations within the N-Ras hypervariable region influenced N-Ras-mislocalization and attenuated aberrant progenitor growth. Similar findings were obtained when the transduced hematopoietic cells and bone marrow from N-Ras and K-Ras mutant mice were subjected to the acyl protein thioesterase inhibitor palmostatin B. Remarkably, the inhibition mediated by palmostatin B was selective for N-Ras mutant cells. Because interference with Ras signaling is regarded as a feasible strategy towards realization of new anticancer drugs,<sup>37,38</sup> palmostatins may be a valuable starting point for the development of modulators of pathological signaling by palmitoylated Ras proteins and hence validating this study. The following section will highlight the purpose of the study.

#### **2.1.6 Purpose of Study**

Ras proto-oncogenes are mutated in ~30% of human cancers resulting in an abnormal protein that drives malignant growth. To date, there are no mechanism-based treatments for reversing the biochemical output of oncogenic Ras proteins, and this has presented an exceedingly difficult target for rational drug discovery. Previous studies proved that APT1 and APT2 catalyze N-Ras depalmitoylation and that first generation chemical inhibitors designed to inhibit these enzymes (palmostatin B and palmostatin M) selectively reduced the growth of primary hematopoietic progenitors and leukemia cells expressing

oncogenic N-RasG12D.<sup>33b</sup> In a collaborative work with the Cravatt (Scripps Research Institute) and Shannon groups (UCSF), we are looking at generating preliminary data and novel reagents, which we will use to pursue the goals of: (1) identifying additional biochemical targets of the palmostatins; (2) developing new chemical inhibitors with improved potency and selectivity for palmostatin targets; (3) using these inhibitors combined with genetic methods to discern the relevant enzyme(s) that regulate N-Ras depalmitoylation in cancer cells, and, (4) utilizing human cancer cell lines and a new strains of mice to interrogate the palmitoylation/depalmitoylation cycle as a therapeutic target in early stage and advanced N-Ras-mutant cancers. With our expertise in synthetic chemistry, the objective of the Howell group is to synthesize the palmostatin M inspired  $\beta$ -lactones to provide our collaborators with tools to investigate the Ras palmitoylation/depalmitoylation cycle, which regulates the subcellular trafficking of the N-Ras, H-Ras, and K-Ras4a isoforms, as a therapeutic target for selectively inhibiting the growth of malignancies with oncogenic N-Ras mutations. In particular, we envisioned that palmostatin M derivative targets (Figure 26) with either sulfone or amine functional group in the C4 chain would answer whether both the sulfone and the amine functionalities in palmostatin M are vital for inhibitory activities. More, based on Howell group chemistry, there is the possibility of modifications in the C3 chain because  $\alpha$ -methylene- $\beta$ -lactones can undergo an olefin cross-metathesis (CM) with terminal alkenes. Herein, our initial targets are palmostatin M analogs containing a C4 chain with no sulfone moiety (targets **85** and **86**). The chain at C3 was fixed with 10 carbon atoms for initial analogs. The long term goal of this project is to implement mechanistic strategies to selectively inhibit the growth of cancers with somatic Ras mutations. The next section highlights various methodologies utilized to access 3,4-disubstituted  $\beta$ -lactones.



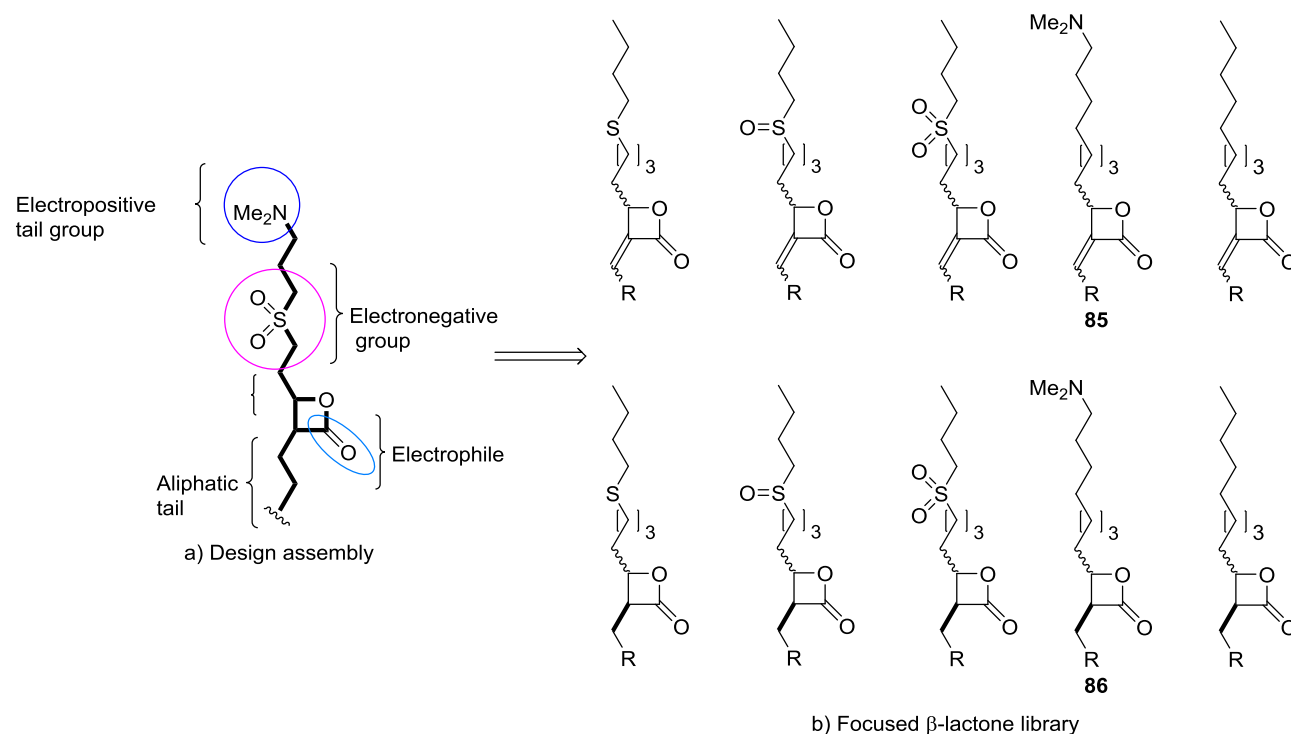


**Figure 26.** Targeted palmostatin M derivatives

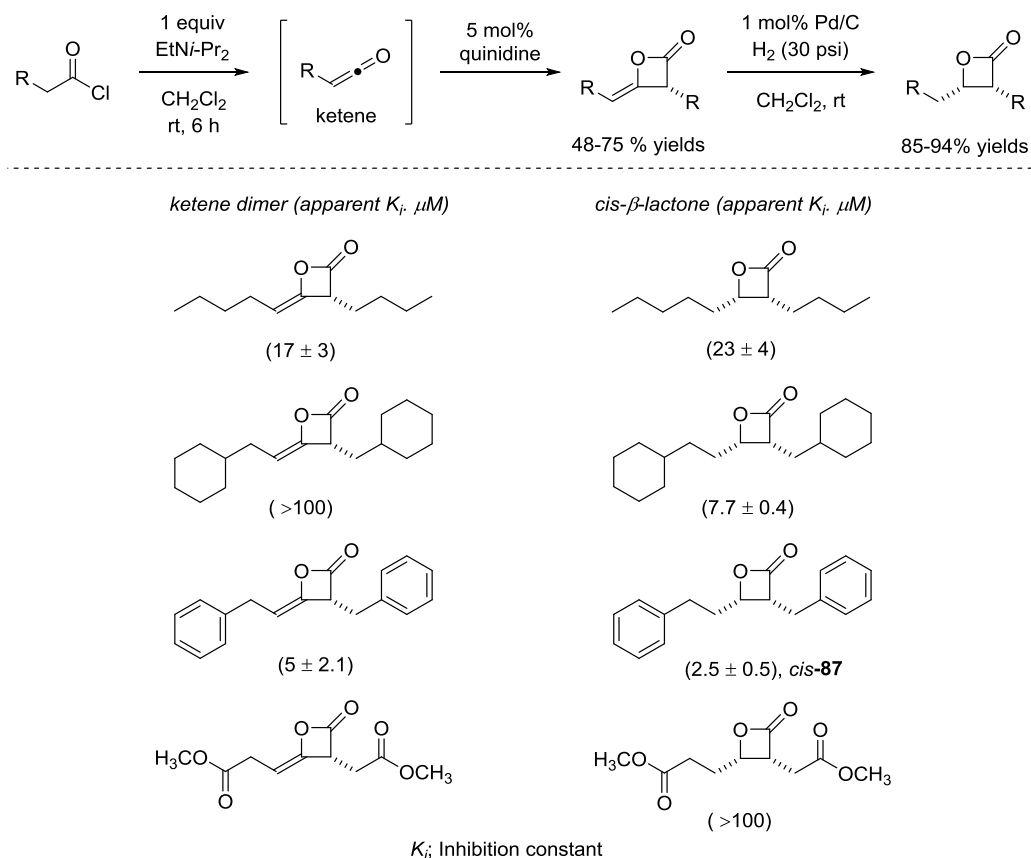
## 2.2 Approaches to $\beta$ -Lactone Inhibitors of Fatty Acid Synthase (FAS)

Due to the fact that  $\beta$ -lactone moiety is present in many biologically active natural products, much attention has been focused on the development of practical routes to various disubstituted  $\beta$ -lactones. The Howell group and others have reported methods to easily access various disubstituted  $\beta$ -lactones as small molecule inhibitors of FAS or other serine/threonine proteases.

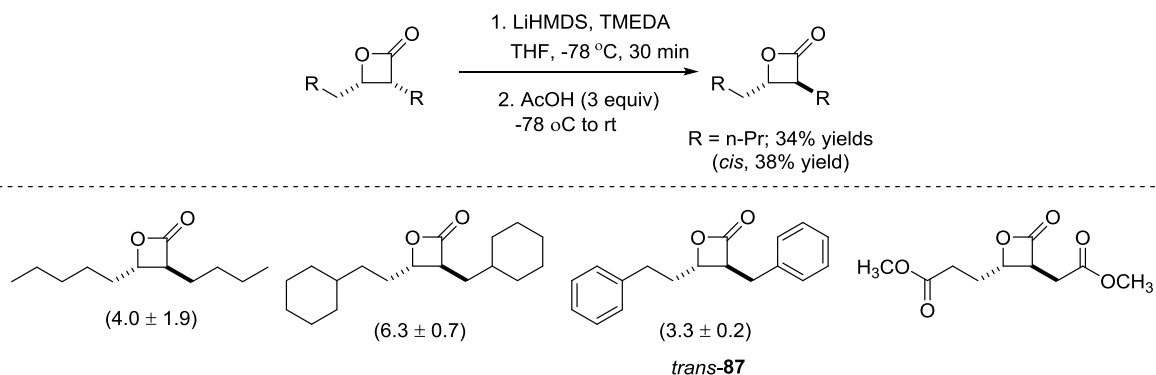
### 2.2.1 Ketene Dimerization/Hydrogenation Sequence

The Romo research group<sup>39</sup> has made a significant effort in the development of asymmetric reaction sequences that provide disubstituted  $\beta$ -lactone libraries. Their described methodology is based on a two-step process involving Calter's<sup>2b,40</sup> organocatalytic, asymmetric ketene dimerization, starting from acid chlorides, followed by a facial-selective hydrogenation leading to *cis*-substituted- $\beta$ -lactones (Scheme 15). This route is attractive in that the ketene dimer intermediates were found to be stable to flash chromatography, enabling opportunities for subsequent transformations of these optically active, reactive

intermediates. A number of acyl chlorides were subjected to quinidine catalyzed ketene dimerization and gave isolable  $\alpha$ -alkylidene- $\beta$ -lactones in good enantioselectivities. Hydrogenation of the ketene dimers under Pd catalysis provided *cis*- $\beta$ -lactones with excellent diastereoselectivities. Subsequent base mediated  $\alpha$ -epimerization allowed access to *trans*- $\beta$ -lactones (Scheme 16). The two major downsides of this protocol are: 1) the epimerization step is low yielding and 2) the approach is only applicable for synthesizing substrates with identical substituents (R groups). Nevertheless, this two-step process provided a practical and scalable process to prepare simple, pseudosymmetric dialkyl  $\beta$ -lactones from readily available acid chlorides in good overall yields and high enantioselectivities. Several ketene dimers and  $\beta$ -lactones obtained from this protocol showed antagonistic activity in competition with a fluorogenic substrate toward a recombinant form of the thioesterase domain FAS.  $\beta$ -Lactone **87** (both *cis* and *trans*, Schemes 15 and 16) displayed significant FAS inhibitory activities, only 10-fold lower than that of orlistat. The promising FAS inhibitory activity displayed by simple, disubstituted  $\beta$ -lactones opens opportunities specifically in developing other methods than can provide access to a more diverse range of  $\beta$ -lactones.



**Scheme 15.** Disubstituted  $\beta$ -lactone synthesis via ketene dimerization/hydrogenation sequence

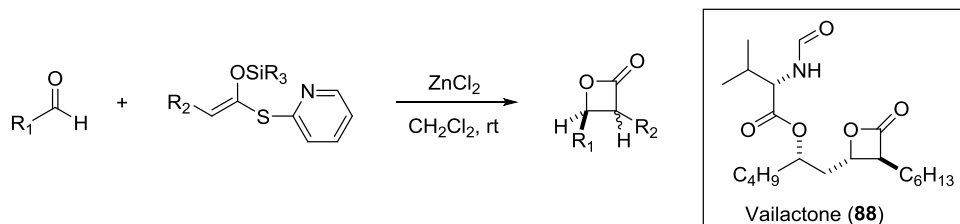


**Scheme 16.** Epimerization of cis- $\beta$ -lactones to the trans-isomers

## 2.2.2 Tandem Mukaiyama Aldol Lactonization (TMAL) Approach

In order to avoid depletion of the material in the epimerization step in the ketene dimerization/hydrogenation sequence, Smith *et al.*<sup>41</sup> developed a tandem Mukaiyama Aldol lactonization (TMAL) to give access to trans- $\beta$ -lactones with high enantiomeric purities (Scheme 17). The reaction

employs readily available thiopyridyl ketene and aldehydes providing direct access to 3,4-disubstituted- $\beta$ -lactones. This approach was best suited for diversification studies. It was utilized in the synthesis of orlistat together with some of its derivatives. It was also applied in the synthesis of valollactone (**88**), which has a higher inhibitory activity toward the thioesterase domain of FAS than orlistat, possibly due to its better solubility.



**Scheme 17.** Tandem Mukaiyama Aldol lactonization (TMAL) approach

### 2.2.3 Olefin Cross-Metathesis (CM) of $\alpha$ -Methylene- $\beta$ -Lactones

In exploring the reactivities of strained heterocycles with exocyclic unsaturation, the Howell group found that  $\alpha$ -methylene- $\beta$ -lactones such as **89** participated in cross-metathesis (CM) reactions with Type I alkenes.<sup>42</sup> The reactions proceeded in high yields and with excellent *Z*-selectivities in the presence of either Grubb's 2<sup>nd</sup> or Grubb's-Hoveyda 2<sup>nd</sup> generation catalysts (Cat. **90** and **92** respectively) (Table 1). The predominant *Z*-stereochemistries of the products were unexpected, because CM reactions of  $\alpha,\beta$ -unsaturated carbonyl compounds, including 1,1-disubstituted enones, with simple alkenes usually proceed with high *E*-selectivity.<sup>43</sup> The high *Z*-selectivity observed was attributed to steric effects from the group at C-4 position. A bulky substituent at C-4 position was anticipated to both direct reaction with the ruthenium alkylidene to the opposite lactone face and to direct the terminal alkenyl substituent toward the carbonyl moiety. The steric argument was confirmed by a drop in the selectivity when a less bulky group at C-4 was utilized.

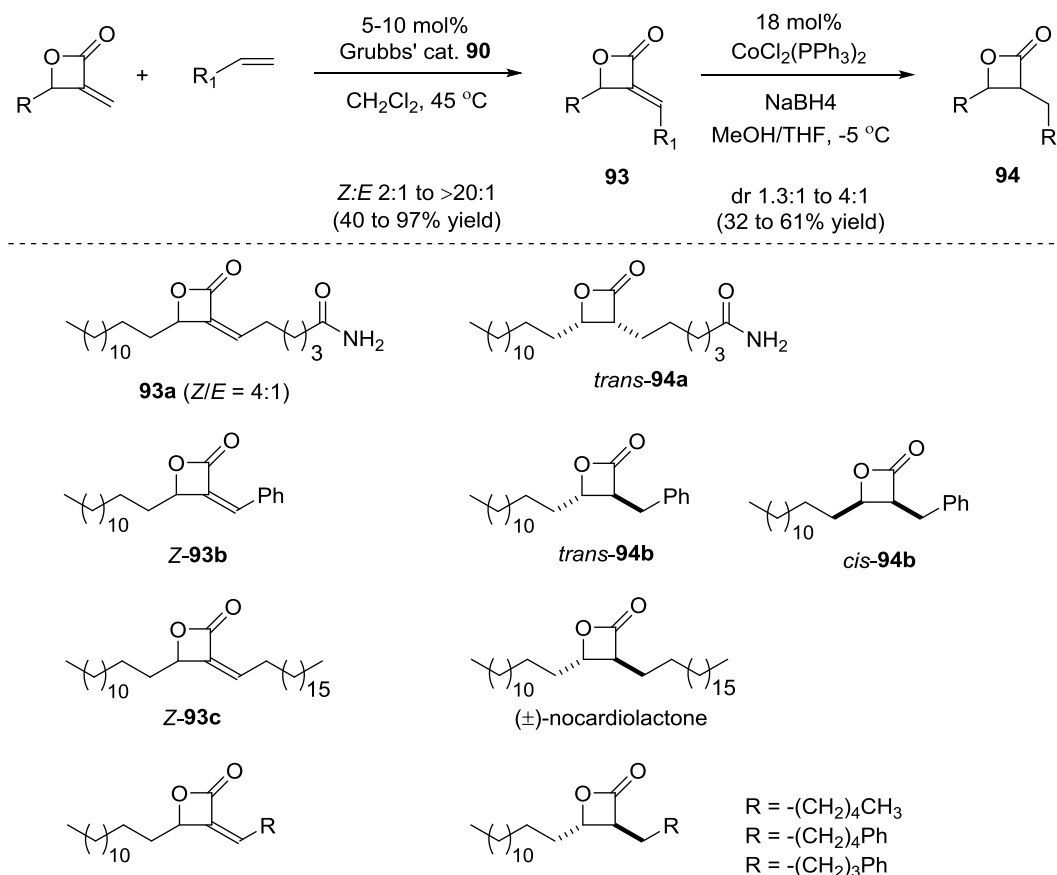
entry	R	Yield (%)	Z:E
a	(CH <sub>2</sub> ) <sub>2</sub> OAc	84	> 20:1
b	(CH <sub>2</sub> ) <sub>3</sub> OAc	90	> 20:1
c	(CH <sub>2</sub> ) <sub>4</sub> OAc	85	14:1
d	(CH <sub>2</sub> ) <sub>8</sub> OAc	84	> 20:1
e	Ph	55 <sup>b</sup>	> 20:1
f	(CH <sub>2</sub> ) <sub>2</sub> CH <sub>3</sub>	94	11:1
g	(CH <sub>2</sub> ) <sub>2</sub> Br	93	> 20:1
h	CH <sub>2</sub> Cl	80	12:1
i	(CH <sub>2</sub> ) <sub>2</sub> OTBDMS	88	9:1
j	CH <sub>2</sub> OR <sup>a</sup>	NR	

Catalyst **90** was used for entries **a-g** and **i**; catalyst **91** was used for entry **h**. <sup>a</sup>Reaction did not work with allylic alcohols, whether protected or not (R = Bn, Ac, TBDMS, or TBDPS). All yields are isolated yields for the combined Z/E-diastereomers. <sup>b</sup>Isolated yield for Z-diastereomer only.

**Table 1.** Synthesis of alkylidene  $\beta$ -lactones **92** via cross-metathesis

The CM reaction between  $\alpha$ -methylene- $\beta$ -lactones and terminal alkenes presents an attractive approach to a focused libraries of 3,4-disubstituted  $\beta$ -lactones **93**. This is due to fact that  $\alpha$ -alkylidene- $\beta$ -lactones **93** themselves can be used as probes. In addition to being used as probes,  $\alpha$ -alkylidene- $\beta$ -lactones can be converted selectively to *trans*- or *cis*- $\beta$ -lactones **94** via diastereoselective reductions. *cis*- $\beta$ -Lactones can be accessed by hydrogenation reactions under palladium on carbon catalysis, while their *trans* counterparts can be obtained via 1,4-reduction using NaBH<sub>4</sub> under cobalt catalysis (Scheme 18).<sup>42b</sup> In a combination of competitive gel- and MS-based ABPP experiments, individual  $\alpha$ -alkylidene- $\beta$ -lactones and their reduced  $\beta$ -lactone counterparts were found to display a broad reactivity profiles against a diverse array of serine hydrolases, including disease-relevant and uncharacterized enzymes that lack selective inhibitors.<sup>44</sup> Inspired by these biological outcomes and the ability of  $\alpha$ -methylene- $\beta$ -lactones to

undergo CM, we envisioned the synthesis of palmostatin M derived  $\beta$ -lactone motifs that target RAS depalmitoylation.



**Scheme 18.**  $\beta$ -Lactones synthesis by cross-metathesis/reduction sequence

### 2.2.3.1 Results and Discussions

#### 2.2.3.1.1 Initial Approach

$\beta$ -Lactones are an important class of heterocyclic compounds found in several synthetic and natural products of biological relevance.<sup>1</sup> Aside from the prevalence of  $\beta$ -lactones in natural products, they are considered privileged intermediates in organic synthesis as they offer a broad range of reactivities.<sup>2,3</sup> The Howell group has recently utilized a particular class of  $\beta$ -lactones,  $\alpha$ -methylene- $\beta$ -lactones, in a ruthenium catalyzed cross-metathesis reaction (see section 2.2.3). Inspired by the efficiency with which  $\alpha$ -methylene- $\beta$ -lactone undergo CM reaction coupled with diastereoselective reductions, we envisioned a

synthetic strategy to access palmostatin M analogs **85** and **86** (see section 2.1.4), wherein a CM reaction between  $\alpha$ -methylene- $\beta$ -lactone **95** and terminal alkenes **96** would generate a library of derivatives with different R-groups on the C3 chain ( $\alpha$ -alkylidene- $\beta$ -lactone **85**).<sup>42</sup>  $\alpha$ -Alkylidene- $\beta$ -lactone would then be subjected to diastereoselective reductions to access  $\beta$ -lactones **86** (Figure 27).<sup>42</sup>

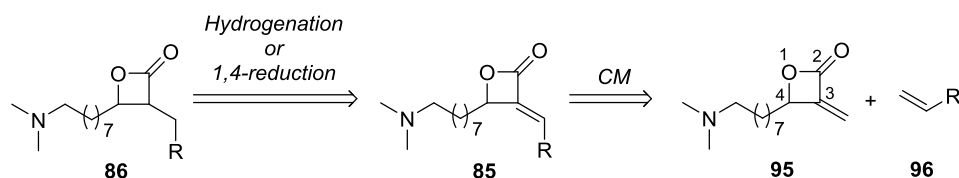


**Figure 27.** Retrosynthesis of palmostatin M-inspired  $\beta$ -lactones

$\alpha$ -Methylene- $\beta$ -lactone would in turn be prepared from lactonization of  $\alpha$ -methylene- $\beta$ -hydroxy acid **97**.<sup>45,46</sup>  $\beta$ -Hydroxy acid would be accessed from a one-pot, 2-step reaction sequence involving Morita-Baylis-Hillman (MBH) reaction of aldehyde **98** and methyl acrylate (**99**), followed by hydrolysis.<sup>45</sup> A more direct sequence to prepare  $\alpha$ -methylene- $\beta$ -lactones **95** would involve MBH reaction between aldehyde **98** and *t*-butyl thioacrylate (**100**), followed by mercury-mediated cyclization of MBH adduct **101** (Figure 28).<sup>45</sup>

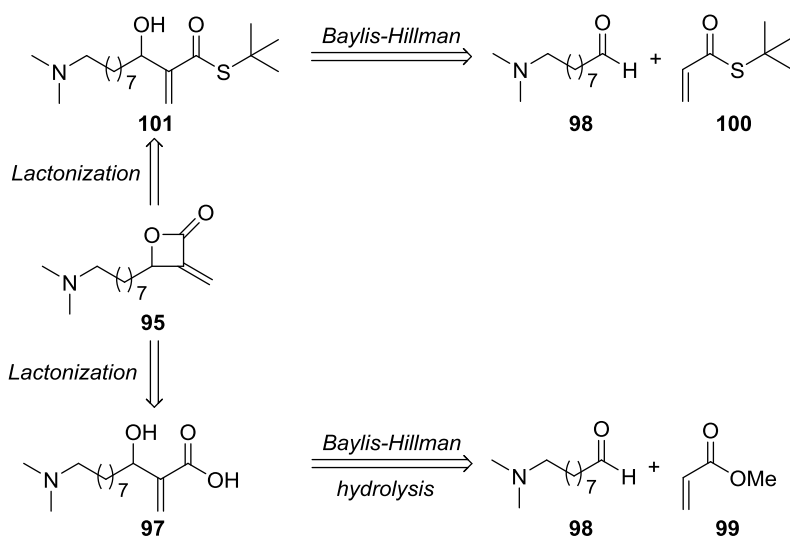
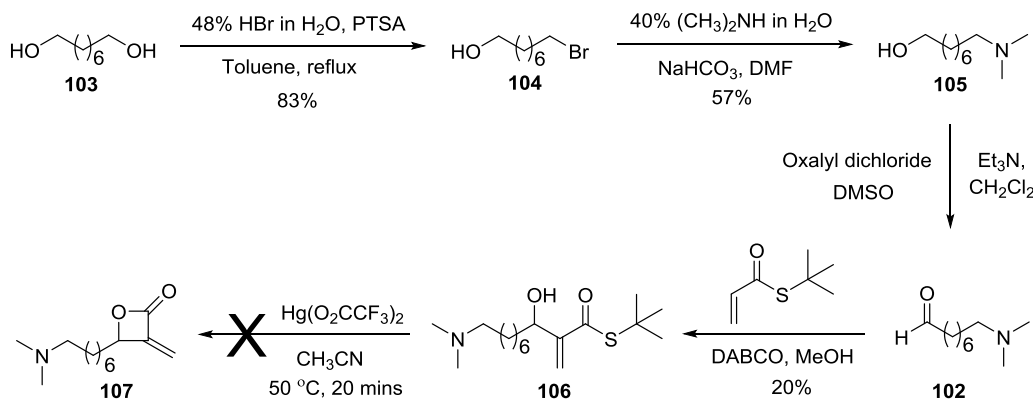


**Figure 28.** Retrosynthesis to  $\alpha$ -methylene- $\beta$ -lactone **95**

We began our investigation into this CM-inspired strategy with the synthesis of amino aldehyde **102**, starting with 1,8-octanediol (**103**) which we had available (Scheme 19). Subjection of **103** to monobromination conditions with 48% aqueous hydrobromic acid in the presence of catalytic amount of p-toluenesulfonic acid (PTSA) afforded 8-bromooctan-1-ol (**104**) in 83% yield. Nucleophilic aliphatic substitution of the bromide **104** with dimethyl amine gave compound **105** in 57% yield. This was followed by a Swern oxidation which converted the alcohol to amino aldehyde **102**. The  $^1\text{H}$  NMR spectrum of the crude aldehyde product showed to be fairly clean, and therefore it was used in the subsequent MBH reaction without purification. MBH adduct **106** was obtained in two days by using 1,4-diazabicyclo[2.2.2]octane (DABCO) as the organocatalyst.<sup>45</sup> A mercury-mediated cyclization attempt on MBH adduct **106** failed to give the desired  $\alpha$ -methylene- $\beta$ -lactone **107**, in spite of the fact that the starting MBH adduct **106** was consumed, as shown by the  $^1\text{H}$  NMR spectroscopic data of the crude mixture (neither characteristic peaks of the starting material nor corresponding lactone product was observed).

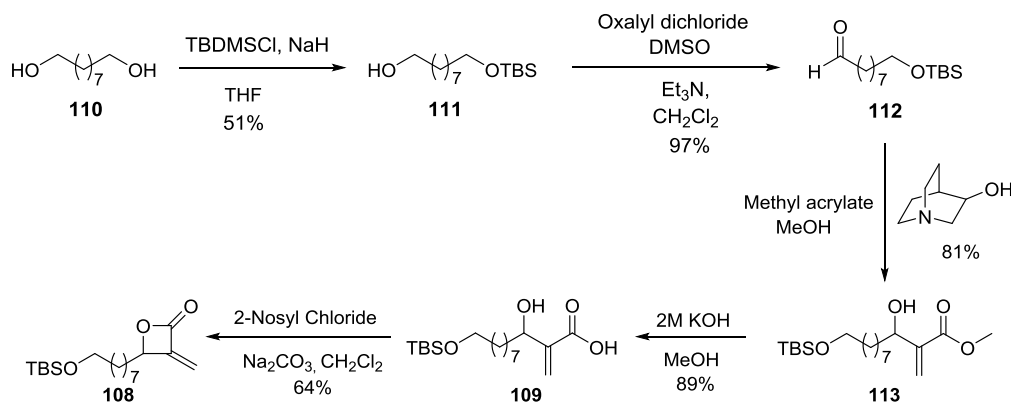


**Scheme 19.** An attempt to prepare  $\alpha$ -methylene- $\beta$ -lactone **107** via a mercury-mediated cyclization

To circumvent the problems encountered in our initial approach, we sought a sequence for installation of the amine functional group after the lactonization step. We decided on a route involving lactonization of a silyl-protected MBH adduct followed by elaboration of  $\alpha$ -methylene- $\beta$ -lactone. In this approach,  $\alpha$ -methylene- $\beta$ -lactone **108** was readily prepared from lactonization of  $\alpha$ -methylene- $\beta$ -hydroxy acid **109**.

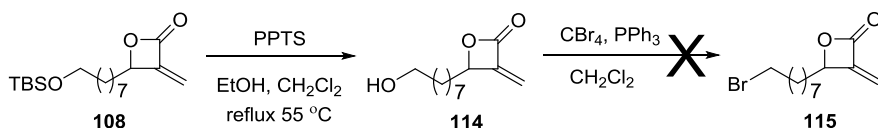


The synthesis was initiated from 1,9-nonandiol (**110**), which was first converted into monoprotected alcohol **111** in 51 % yield.<sup>47</sup> This was followed by a Swern oxidation, leading to the aldehyde **112** in 97% yield.<sup>47</sup> MBH adduct **113** was obtained in 81% yield in two days by using 3-quinuclidinol as the organocatalyst. Hydrolysis of the MBH adduct **113** gave  $\beta$ -hydroxy acid **109** in 89% yield. A nosyl chloride mediated lactonization<sup>45</sup> provided desired  $\alpha$ -methylene- $\beta$ -lactones **108** in percentage yield ranging from 38-64% (Scheme 20).



**Scheme 20.** Preparation of  $\alpha$ -methylene- $\beta$ -lactone **108**

Having accessed  $\alpha$ -methylene- $\beta$ -lactone **108**, we focused our attention on subsequent steps in the synthesis. Cleavage of the silyl group using *tetra*-*n*-butylammonium fluoride (TBAF) gave no desired product, even though the starting material was consumed based on  $^1\text{H}$  NMR of the reaction mixture. We then sought to use pyridinium *p*-toluenesulfonate (PPTS), a weakly acidic catalyst, which gave the desired product **114** albeit, in low yield. An attempt to convert alcohol **114** to bromide under Appel's condition<sup>48</sup> failed, as we did not observe the desired product **115** based on  $^1\text{H}$  NMR of the reaction mixture (Scheme 21). This was attributed to the conjugate addition of the nucleophilic bromide to the terminal alkene moiety.



**Scheme 21.** An attempt to convert alcohol **114** to bromide **115** under Appel's condition

Having encountered difficulties in the conversion of alcohol **114** to bromide **115**, we decided to carry out bromination at a later stage of the synthesis, after CM reaction since CM would convert the terminal alkene into an internal alkene which is normally less prone to conjugate addition. Cleavage of the silyl groups from  $\alpha$ -alkylidene- $\beta$ -lactone, followed by bromination should yield the bromide. A final nucleophilic substitution of the bromide with dimethyl amine should provide the desired target **85** (Figure 29a). The reduced  $\beta$ -lactone target **86** would be obtained via reduction, removal of silyl group, bromination and nucleophilic substitution of the bromide with dimethyl amine (Figure 29b). In the next section, olefin cross metathesis of  $\alpha$ -methylene- $\beta$ -lactone **108**, stereoselective reductions and incorporation of the amine functional group are described.

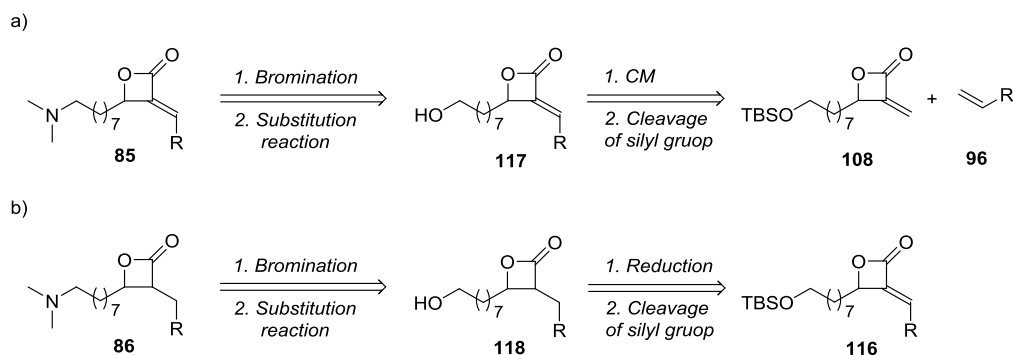
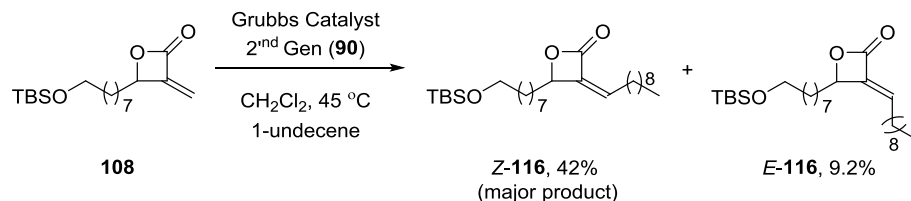


**Figure 29.** Retrosynthesis to palmostatin M-inspired  $\beta$ -lactones **85** and **86**

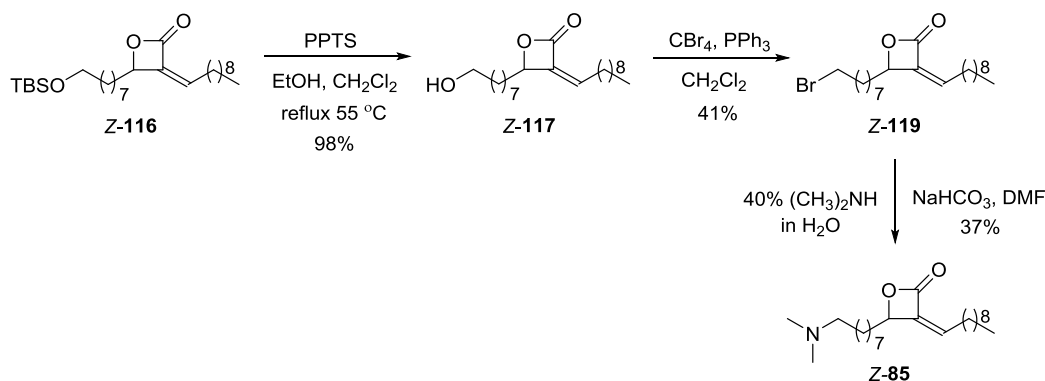
#### 2.2.3.1.2 CM of $\alpha$ -Methylene- $\beta$ -Lactone **108** Followed by Diastereoselective Reductions

After accessing the desired  $\alpha$ -methylene- $\beta$ -lactone **108**, CM reaction to obtain  $\alpha$ -alkylidene- $\beta$ -lactone was explored. Subjection of **108** to ruthenium catalyzed CM mediated by Grubbs 2<sup>nd</sup> generation catalyst (**90**) afforded  $\alpha$ -alkylidene- $\beta$ -lactone **116** with Z-selectivity (Scheme 22).

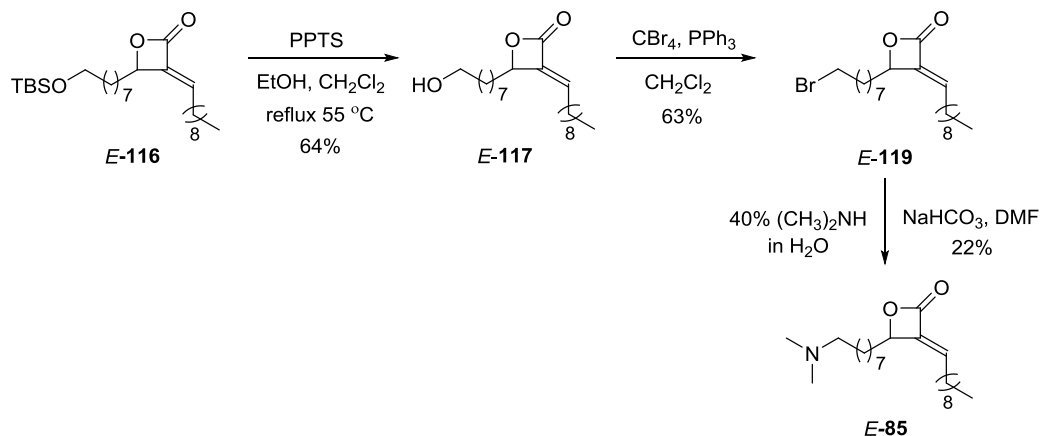


**Scheme 22.** CM reaction to access  $\alpha$ -alkylidene- $\beta$ -lactone **116**

Having prepared the  $\alpha$ -alkylidene- $\beta$ -lactones **116**, we next sought to finish the synthesis of palmostatin M-inspired  $\beta$ -lactones **85** and **86**. Starting with *Z*-**116**, cleavage of the silyl protecting group utilizing PPTS provided alcohol **117** in 91% yield. Appel bromination<sup>48</sup> using tetrabromomethane in the presence of triphenylphosphine gave bromide **119** in 67% yield. It is worth noting that we never observed any conjugate addition product during bromination reaction as opposed to when bromination was carried out on  $\alpha$ -methylene- $\beta$ -lactone **114** utilizing similar conditions. A subsequent *N*-alkylation with dimethylamine gave *Z*-isomer of the desired target **85** in 37% yield (Scheme 23). Similar transformations were applied to access the *E*-isomer in 22% isolated yield (Scheme 24).



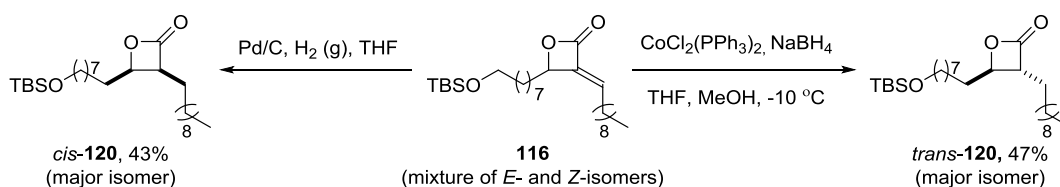
**Scheme 23.** Synthesis of palmostatin M derived  $\beta$ -lactone *Z*-**85**



**Scheme 24.** Synthesis of palmostatin M derived  $\beta$ -lactone *E*-**85**

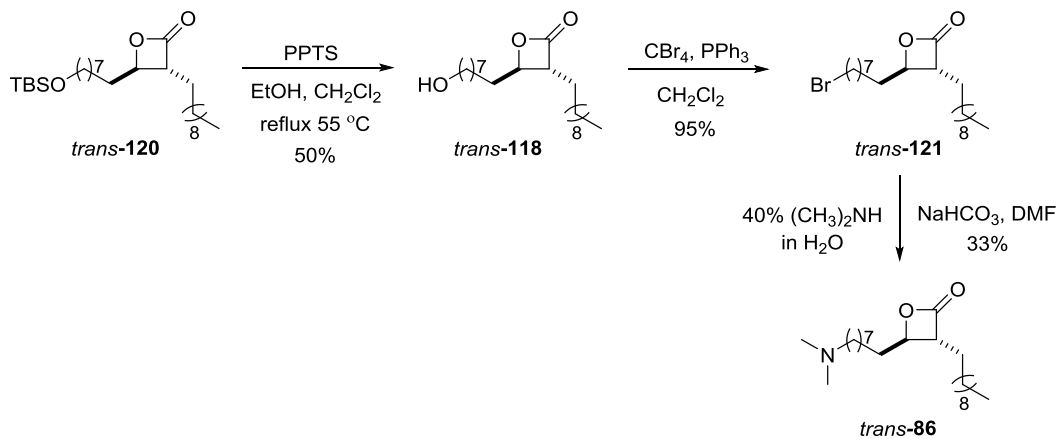
The reduced  $\beta$ -lactone motifs were obtained by hydrogenation to give the *cis*-lactone or by 1,4- reduction using sodium borohydride to obtain the *trans* product with modest selectivity (Scheme 25).<sup>42b</sup>

Hydrogenation and 1,4-reduction

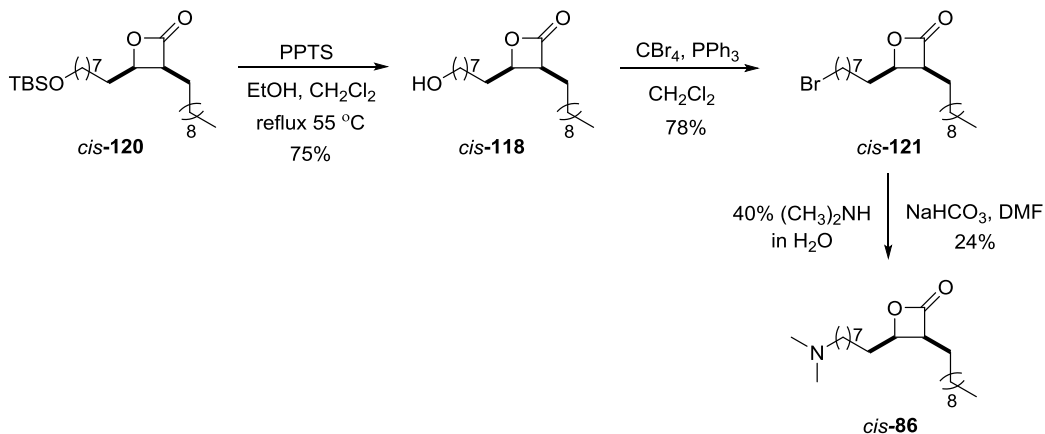


**Scheme 25.** Diastereoselective reductions to give *cis*- and *trans*- $\beta$ -lactones **120**

Elaboration of lactones **120** gave access to the *cis*- and *trans*-isomers of palmostatin M-inspired  $\beta$ -lactone **86**. This was done by incorporation of dimethylamino functionality via cleavage of silyl group, Appel bromination, and subsequent nucleophilic substitution of the bromide with dimethylamine (Schemes 26 and 27).



**Scheme 26.** Synthesis of palmostatin M-derived  $\beta$ -lactone *trans*-**86**

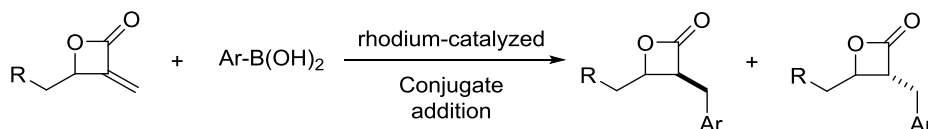


**Scheme 27.** Synthesis of palmostatin M-derived  $\beta$ -lactone *cis*-**86**

In summary, we have showcased the versatile reactive nature of  $\alpha$ -methylene- $\beta$ -lactone and their applications as useful synthetic intermediates for transformations to more advanced structures. CM reactions of  $\alpha$ -methylene- $\beta$ -lactones, followed by subsequent diastereoselective reductions, provided the four palmostatin M analogs (targets **85** and **86**). Elaboration of these disubstituted  $\beta$ -lactones furnished palmostatin M derivatives. The following section describe the development of a one-step preparation of 3,4-disubstituted  $\beta$ -lactones from  $\alpha$ -methylene- $\beta$ -lactones through Rh-catalyzed conjugate addition of arylboronic acids to  $\alpha$ -methylene- $\beta$ -lactones.

#### 2.2.4 Rhodium Catalyzed Conjugate Addition of Aryl Boronic Acids

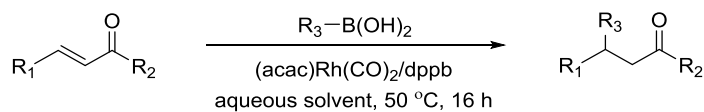
The previous section showcased how  $\alpha$ -methylene- $\beta$ -lactones could be used for the synthesis of structurally diverse 3,4-disubstituted  $\beta$ -lactones via CM and subsequent diastereoselective reductions. Despite the success of this methodology in assembling focused libraries of 3,4-disubstituted  $\beta$ -lactones, it suffers some drawbacks. First, the CM reaction typically requires high catalyst loading (5–10 mol %). Secondly, the 1,4-reduction to access the generally more biologically active trans  $\beta$ -lactones suffers from modest diastereoselectivities and yields. Taken together, the limitations make an alternative approach appealing. Here we report the development of an efficient process for Rh catalyzed conjugate addition, wherein readily available aryl boronic acids are combined with  $\alpha$ -methylene- $\beta$ -lactones to generate 3,4-disubstituted  $\beta$ -lactones (Scheme 29).



**Scheme 28.** Rh-catalyzed conjugate addition

The conjugate addition of organometallic reagents to enones is a powerful tool for appending organic residues to cyclic and acyclic substrates.<sup>49,50</sup> Substrates used in this reaction are usually  $\alpha,\beta$ -unsaturated ketones, aldehydes, esters, amides, sulfoxides, or nitro compounds. Often referred to as 1,4-addition,

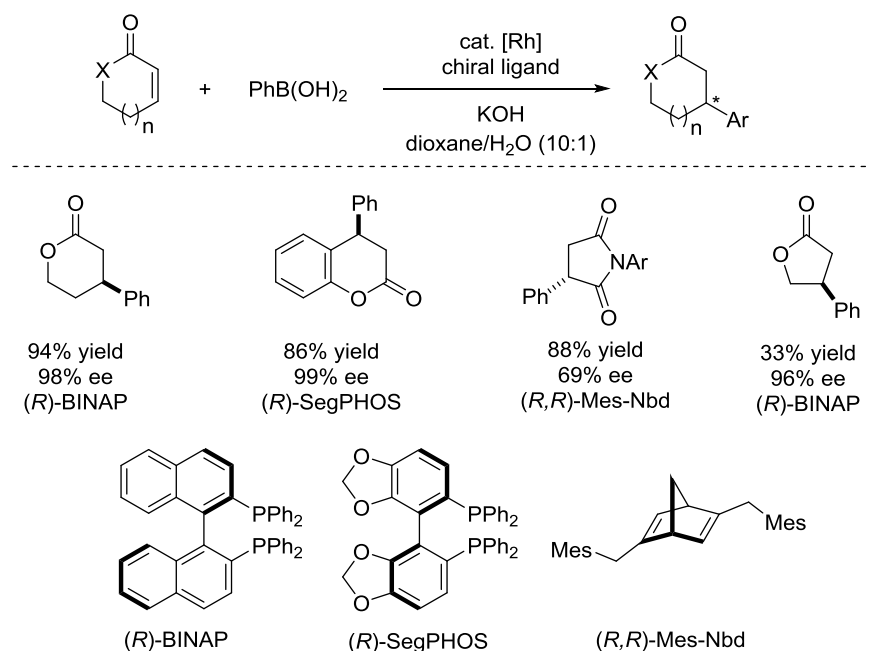
these reactions use a variety of organometallic reagents, the most common of which are organolithiums, and cuprates. Reactions involving organometallic reagents are generally run under anhydrous, oxygen-free conditions, leading to difficulty in handling and manipulation of reactions, as well as problems with broad functional group tolerance. Miyaura and co-workers<sup>49</sup> reported the first rhodium-catalyzed conjugate addition reaction to an enone (methyl vinyl ketone) with phenyl boronic acid (Scheme 30). Unlike previous transition metal catalyzed conjugate additions, the reaction was done in the presence of water as co-solvent. After this discovery, the synthetic chemistry community witnessed many advances in the field of rhodium-catalyzed conjugate addition. Specifically, new rhodium complexes and organoboron reagents have been developed.<sup>50,51</sup> In addition, various substrates, including  $\alpha,\beta$  unsaturated esters, amides, lactones, lactams, nitriles, and aldehydes, have been utilized.<sup>50</sup>



R<sub>1</sub> = alkyl, aryl; R<sub>2</sub> = alkyl, aryl, H; R<sub>3</sub> = aryl, 1-alkenyl

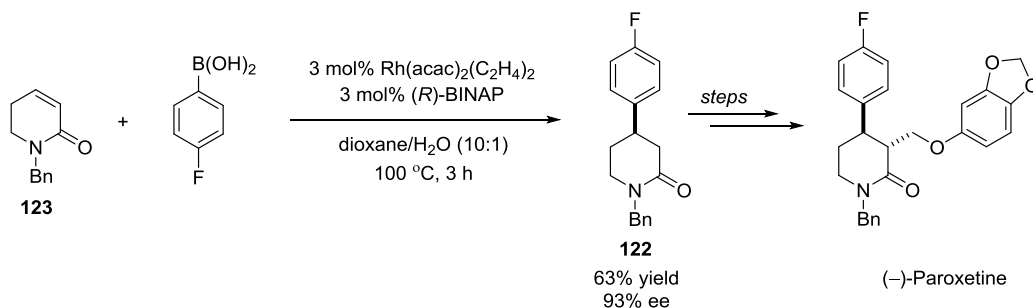
**Scheme 29.** The first rhodium-catalyzed conjugate addition reaction reported

The use of endocyclic  $\alpha,\beta$ -unsaturated lactones and lactams as candidates for the rhodium catalyzed conjugate addition transformation has recently been reported. Hayashi and co-workers showcased conjugate addition of aryl boronic acid to coumarins<sup>52</sup> and maleimides<sup>53</sup> proceeding under rhodium catalysis (Scheme 31). Most examples provided products in excellent yields, and in the presence of appropriate chiral ligands, high enantioselectivities were achieved. Application of similar reaction conditions (use of KOH, reaction temperature up to 100 °C) to  $\gamma$ -butyrolactone resulted in a low yield which was attributed to the potential instability of the 5-membered lactone under the conditions.



**Scheme 30.** Examples of Rh-catalyzed conjugate addition of aryl boronic acids with endocyclic systems

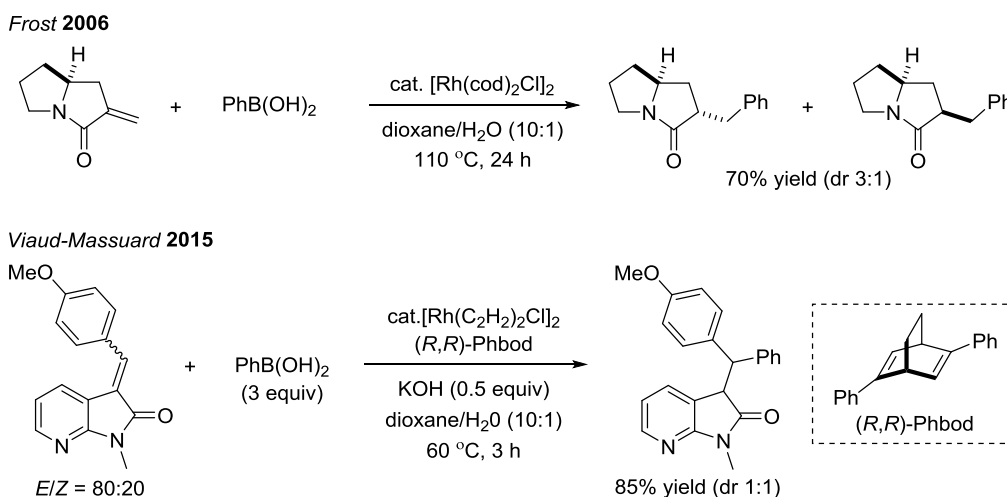
Dihydropyridinones were also utilized in Rh-catalyzed conjugate additions to access 4-arylpiperidinones.<sup>54</sup> The products of this transformation can be employed in further transformations. For example, 4-arylpiperidinone **122**, prepared from dihydropyridone **123**, was an intermediate in the synthesis of (–)-paroxetine,<sup>55</sup> a drug used for the treatment of Parkinson's disease (Scheme 32).



**Scheme 31.** Rh-catalyzed conjugate addition to dihydropyridinone for the synthesis of (–)-paroxetine

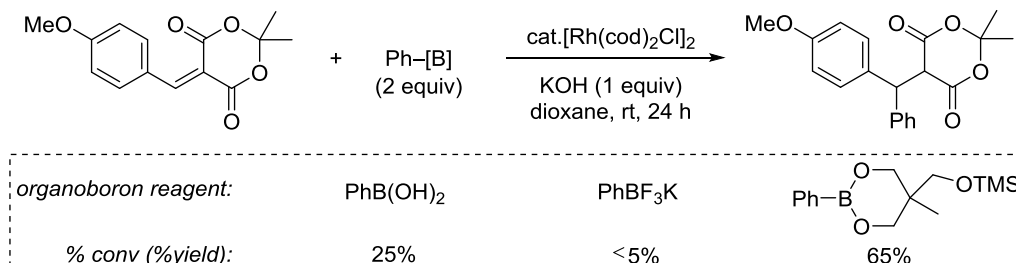
While the use of endocyclic  $\alpha,\beta$ -unsaturated lactones and lactams has enabled many rhodium-catalyzed conjugate additions with organoboron reagents, by contrast, the number of related transformations on exocyclic  $\alpha,\beta$ -unsaturated lactones and lactams is more limited, despite the emergence of some important

recent examples. Frost and co-workers<sup>56</sup> demonstrated a rhodium-catalyzed 1,4-additions with  $\alpha$ -methylene-pyrrolizidinones that provided products in good yields with modest selectivity towards the *trans*-adduct (Scheme 33). Very recently, Viaud-Massuard and co-workers<sup>57</sup> disclosed the conjugate addition of aryl boronic acids with  $\alpha$ -benzylidene-7-azaoxindoles.



**Scheme 32.** Rhodium-catalyzed conjugate addition of exocyclic lactams with aryl boronic acids

In similar work, Frost<sup>58</sup> showcased a Rh-catalyzed conjugate addition to benzylidene dilactones derived from Meldrum's acid (Scheme 34). This type of substrate usually faces the challenge of instability with nucleophiles, including water, requiring the need for anhydrous conditions.<sup>59</sup> Aryl boronic acids and potassium trifluoroborate salts were found ineffective, presumably due to their low solubility in organic solvents. However, novel TMS-protected aryl dioxaborinanes yielded desired products in moderate yields.



**Scheme 33.** Rh-catalyzed conjugate addition of benzylidene Meldrum's acid with organoboron reagents

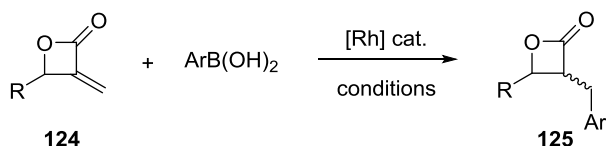


The successful realization of Rh-catalyzed conjugate addition reactions to exocyclic  $\alpha,\beta$ -unsaturated lactones and lactams led to our proposition that  $\alpha$ -methylene- $\beta$ -lactones could undergo similar transformations under rhodium catalysis to give 3,4-disubstituted  $\beta$ -lactones in a single step. At the onset, a number of factors were identified that could impede rhodium-catalyzed conjugate additions on  $\alpha$ -methylene- $\beta$ -lactones. First,  $\beta$ -lactones might not be compatible with the most commonly reported basic/aqueous conditions due to facile ring-opening of the starting material or products.<sup>60</sup> Secondly, control over selectivity in this kind of reaction could be problematic due to the fact that the reaction could lead to the formation of diastereomers. In the next sections, we summarize the development of a rhodium catalyzed conjugate addition reactions of  $\alpha$ -methylene- $\beta$ -lactones with aryl boronic acids. The optimization and scope of the reactions were investigated.

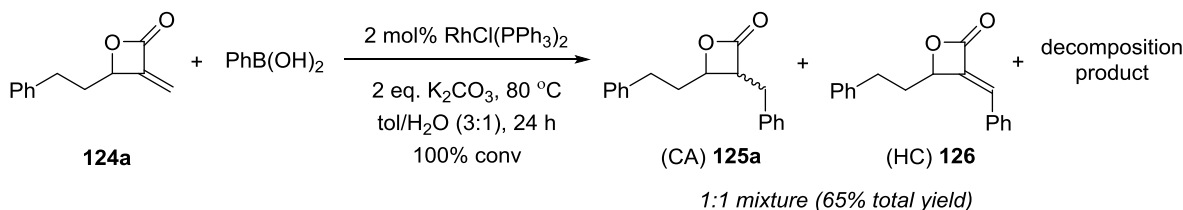
#### 2.2.4.1 Mechanistic Hypothesis and Initial Studies

Motivated by the biological activities displayed in disubstituted  $\beta$ -lactones and the previous report on the Rh-catalyzed conjugate additions on exocyclic  $\alpha,\beta$ -unsaturated lactones and lactams, we hypothesized that  $\alpha$ -methylene- $\beta$ -lactones such as **124** would undergo conjugate addition with organoboron reagents (Scheme 35). The initial studies, conducted by Dr. Christian A. Malapit (CAM), began with the investigation of the reaction of  $\alpha$ -methylene- $\beta$ -lactone **124a** with phenyl boronic acid in the presence of Wilkinson's catalyst.<sup>61</sup> Treatment of **124a** with phenyl boronic acid delivered a mixture of the desired conjugate addition product,  $\beta$ -lactone **125a**, together with the Heck-type product  $\alpha$ -alkylidene- $\beta$ -lactone **126** (Scheme 35). The Rh-catalyzed conjugate addition to give  $\beta$ -lactone **125a** constitutes a one-step process for disubstituted  $\beta$ -lactones from  $\alpha$ -methylene- $\beta$ -lactones, in contrast to the cross-metathesis/reduction sequence described in the previous section. Based on initial results, CAM carried out optimization in order to: (a) selectively obtain conjugate addition product, (b) prevent decomposition, and (c) improve the diastereoselectivity of the reaction.

Hypothesis:



Initial studies:



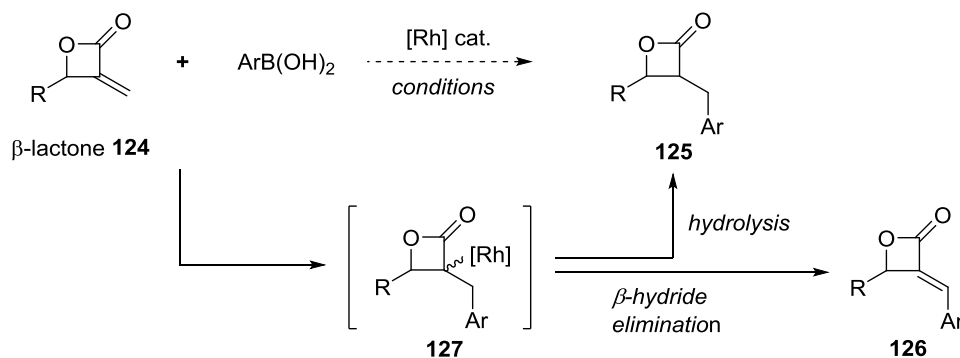
**Scheme 34.** Hypothesis and initial studies on the Rh-catalyzed conjugate addition

Herein we report a strategically distinct, one-step approach to access palmostatin inspired  $\beta$ -lactones from  $\alpha$ -methylene- $\beta$ -lactones. Optimization of reaction conditions to improve selectivity towards conjugate addition is summarized, as well as an exploration of the scope of the reaction.

## 2.2.4.2 Results and Discussions

### 2.2.4.2.1 Optimization of Reaction Conditions

The formation of Heck-type products in Rh-catalyzed reactions was previously observed when  $\alpha,\beta$ -unsaturated esters and amides were utilized.<sup>61</sup> This competitive pathway was proposed to occur via  $\beta$ -hydride elimination (versus protonolysis) from the  $\alpha$ -metallated intermediate **127** (Scheme 36). However, with  $\alpha,\beta$ -unsaturated esters and amides, prior studies had shown that conjugate addition products can be selectively obtained by using appropriate conditions.



**Scheme 35.**  $\beta$ -Hydride elimination (versus hydrolysis) from the  $\alpha$ -metallated intermediate **127**

In order to avoid decomposition and to improve selectivity towards conjugate addition, several parameters were varied including rhodium catalyst, temperature, solvent system, and base additives. Table 2 summarizes the results of the preliminary screening. Switching of the catalyst to  $[\text{Rh}(\text{cod})\text{Cl}]_2$  afforded complete conversion and a cleaner reaction, although still providing a mixture of conjugate addition and Heck products (2:1 ratio of **125a/126**) (entry 2). Using the  $[\text{Rh}(\text{cod})\text{Cl}]_2$ , multiple conditions were tested. In the absence of the base, very low conversion was observed (entry 3). The competition between Heck-type reaction and conjugate addition has been previously observed and mechanistically rationalized.<sup>61</sup> In some previous studies, it has been demonstrated that conjugate addition or Heck-type reaction can be selectively achieved by tuning the catalyst, solvent, reactant ratios, and/or additives. For our system, using a strong base, such as KOH, enhanced conjugate addition relative to Heck reaction (an increase from 2:1 to 3.5:1 ratio of **125a/126**) (entry 4). In an attempt to decrease the equivalents of KOH, a decrease in the conversion and selectivity was observed (entry 5). In addition, lowering of the temperature resulted in a decrease in the selectivity (entries 6 and 7). Using this information, it was reasoned that increasing the equivalents of KOH would improve selectivity towards CA product. Surprisingly, the use of 1 eq KOH resulted in 100% conversion and complete selectivity towards CA product (entry 8). The use of 2 equiv of KOH (entry 9) gave good selectivity but diminished isolated yield, possibly due to decomposition of the starting material or products. When other catalysts were screened with the optimized base, temperature, and solvent (entries 10 and 11),  $[\text{Rh}(\text{nbd})\text{Cl}]_2$  proved equally efficient to  $[\text{Rh}(\text{cod})\text{Cl}]_2$ . Subsequent studies

on the scope of the reaction employing  $[\text{Rh}(\text{cod})\text{Cl}]_2$  as the catalyst and KOH (1 equiv) as the base is summarized in the next section.

**124a** +  $\text{PhB}(\text{OH})_2$  (1.5 equiv)  $\xrightarrow[\text{conditions}]{[\text{Rh}] \text{ cat.}}$  Conj. add. product  $\beta$ -lactone **125a** + Heck product  $\beta$ -lactone **126**

entry	conditions	additives	conversion	<b>125a:126</b>
1	2 mol% $\text{RhCl}(\text{PPh}_3)_3$ , 80 °C, tol/ $\text{H}_2\text{O}$ (3:1)	2 eq $\text{K}_2\text{CO}_3$	100%	Product + decomposition
2	2 mol% $[\text{Rh}(\text{cod})\text{Cl}]_2$ , 60 °C dioxane/ $\text{H}_2\text{O}$ (10:1)	2 eq $\text{K}_2\text{CO}_3$	100%	2:1
3	5 mol% $[\text{Rh}(\text{cod})\text{Cl}]_2$ , 60 °C dioxane/ $\text{H}_2\text{O}$ (10:1)	none	5%	—
4	2 mol% $[\text{Rh}(\text{cod})\text{Cl}]_2$ , 60 °C dioxane/ $\text{H}_2\text{O}$ (10:1)	0.5 eq KOH	100%	3.5:1
5	2 mol% $[\text{Rh}(\text{cod})\text{Cl}]_2$ , 60 °C dioxane/ $\text{H}_2\text{O}$ (10:1)	0.1 eq KOH	95% (48 h)	2:1
6	2 mol% $[\text{Rh}(\text{cod})\text{Cl}]_2$ , 40 °C dioxane/ $\text{H}_2\text{O}$ (10:1)	0.1 eq KOH	71% (48 h)	1.5:1
7	2 mol% $[\text{Rh}(\text{cod})\text{Cl}]_2$ , rt dioxane/ $\text{H}_2\text{O}$ (10:1)	0.1 eq KOH	36% (48 h)	1:1
8	2 mol% $[\text{Rh}(\text{cod})\text{Cl}]_2$ , 60 °C dioxane/ $\text{H}_2\text{O}$ (10:1)	1.0 eq KOH	100% (1 h)	20:1 (92% yield)
9	2 mol% $[\text{Rh}(\text{cod})\text{Cl}]_2$ , 60 °C dioxane/ $\text{H}_2\text{O}$ (10:1)	2.0 eq KOH	100% (1 h)	20:1 (60% yield)
10	2 mol% $\text{RhCl}(\text{PPh}_3)_3$ , 60 °C dioxane/ $\text{H}_2\text{O}$ (10:1)	1.0 eq KOH	100% (24 h)	2:1
11	2 mol% $[\text{Rh}(\text{nbd})\text{Cl}]_2$ , 60 °C dioxane/ $\text{H}_2\text{O}$ (10:1)	1.0 eq KOH	100% (1 h)	20:1 (90% yield)

**Table 2.** Optimization of Rh-catalyzed conjugate addition (CA) of phenylboronic acid to **124a**<sup>62</sup>

#### 2.2.4.2.2 Scope of Rh-catalyzed Conjugate Addition

Using these optimized conditions, I then examined the scope of the reaction by using  $\alpha$ -methylene- $\beta$ -lactone **108** and organoboron reagents as coupling partners. As summarized in Figure 30, electron rich and electron-deficient aryl boronic acids are both suitable substrates, delivering 3,4-substituted  $\beta$ -lactones **127** in moderate to high yields (63%–87%). More importantly, diverse functional groups were tolerated,

including phenyl/benzyl ethers (**127d/127i**), aryl fluorides (**127f**), styrene (**127g**), phenyl amides (**127j**) and phenol (**127k**). Heterocyclic containing aryl boronic acid (**127h**) also underwent conjugate addition in good yield. In general, the lactone diastereomers were separable (see the experimental section). As previously mentioned, most monocyclic  $\beta$ -lactone natural products and close analogues that have been explored as drugs or probes are *trans* diastereomers.<sup>42b,44,60</sup> Nevertheless, *cis*- $\beta$ -lactones have been shown to be as potent as their *trans*-isomers in some cases.<sup>39,63</sup> Thus, at this stage, access to both diastereomers is advantageous from the standpoint of diversification.

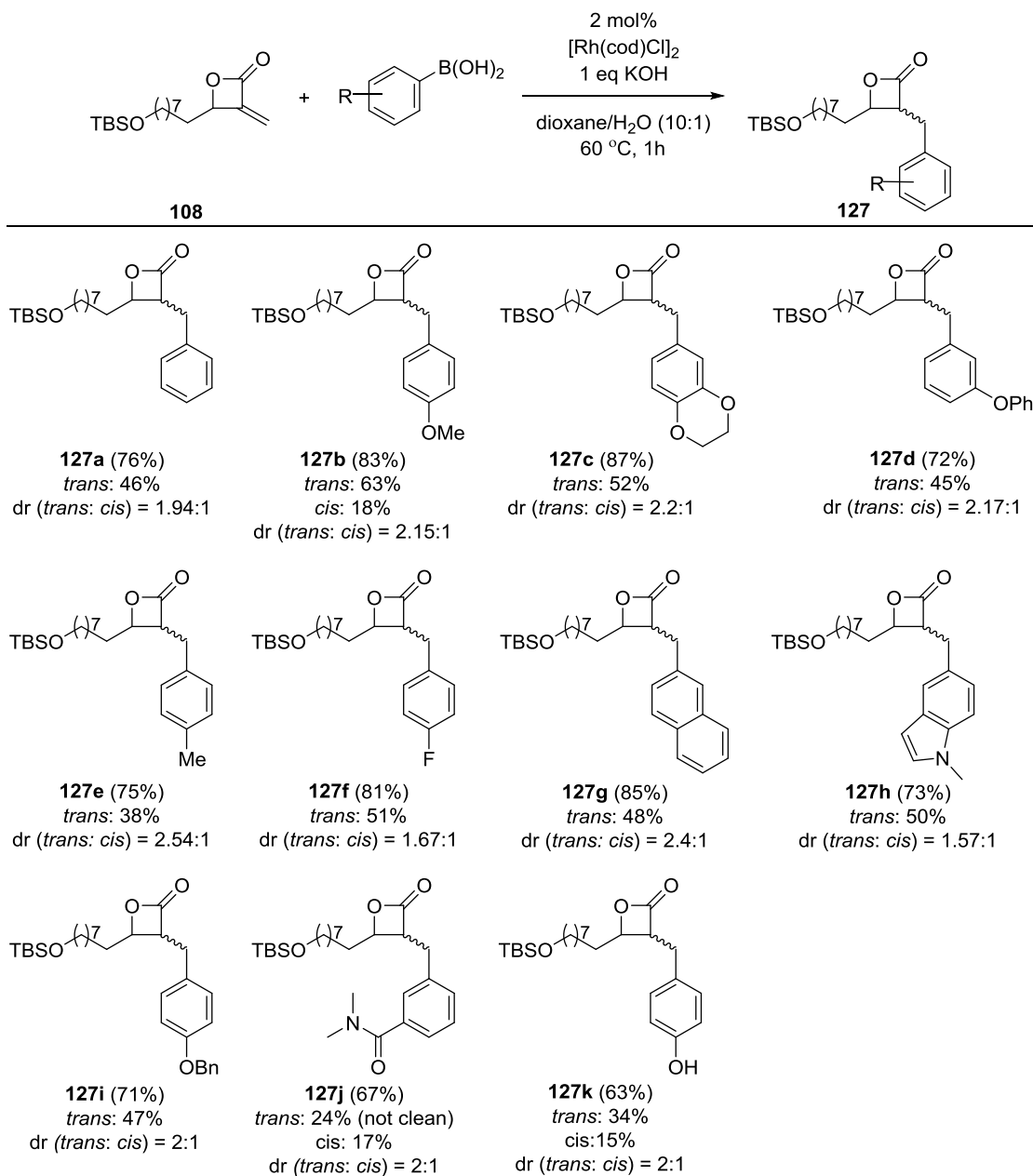
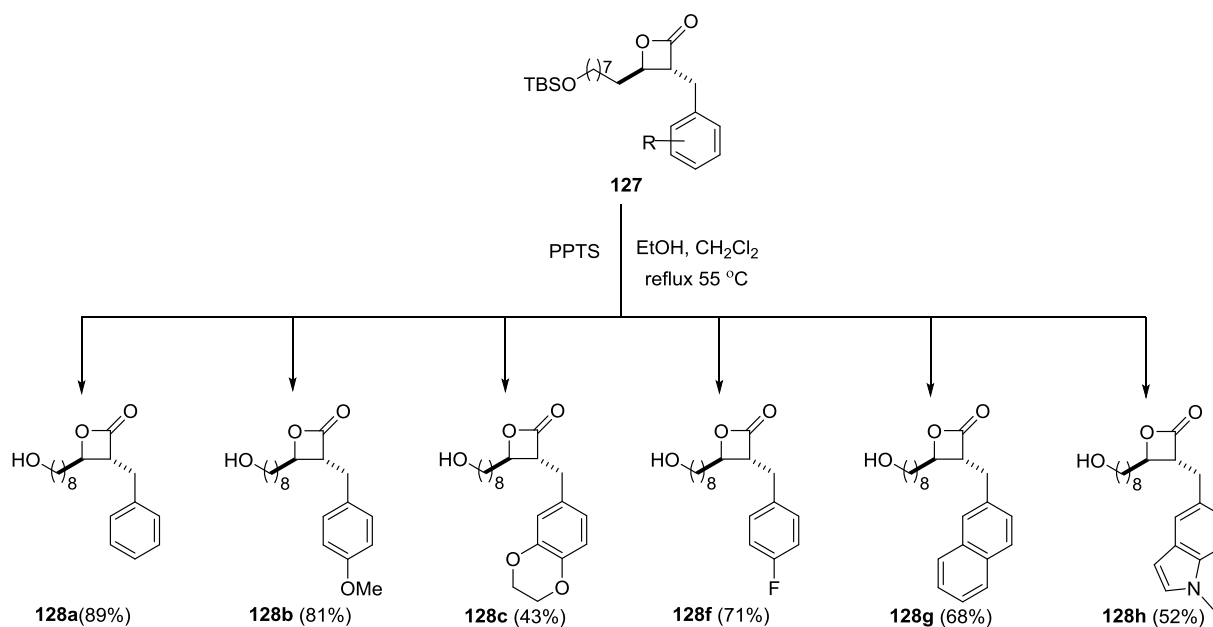


**Figure 30.** Scope for Rh-catalyzed conjugate addition of phenyl boronic acid to **108**<sup>62</sup>

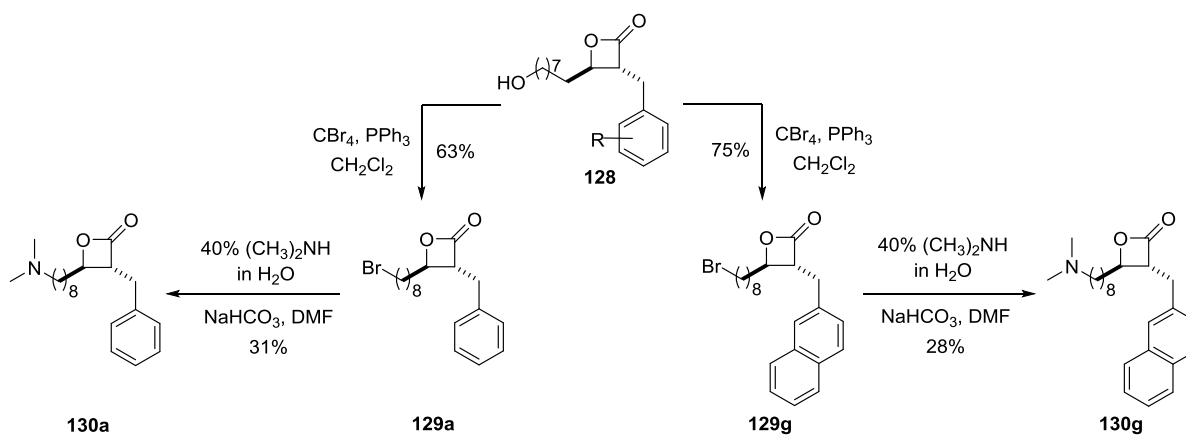
#### 2.2.4.2.3 Elaboration to Palmostatin M-Derivatives

The promising biological activities exhibited by  $\beta$ -lactones, in particular, disubstituted  $\beta$ -lactones, as inhibitors of serine hydrolases exposes the need to prepare diverse analogs of these compounds. The rhodium catalyzed conjugate addition of aryl boronic acids into  $\alpha$ -methylene- $\beta$ -lactones provided a one-step access to diverse disubstituted  $\beta$ -lactones as described in the previous section. We then sought to

explore the installation of the amine functional group at C4 chain of some of these disubstituted  $\beta$ -lactones for the construction and elaboration of palmostatin M derivatives. The functionalization at C4 chain could be rapidly achieved via short synthetic sequences involving the cleavage of the silyl group, Appel bromination, and subsequent N-alkylation with dimethylamine (Schemes 37 and 38).



**Scheme 36.** Cleavage of silyl group



**Scheme 37.** Appel bromination and N-alkylation with dimethylamine

In summary, the rhodium catalyzed conjugate addition of aryl boronic acids to  $\alpha$ -methylene- $\beta$ -lactones provided a one-step access to diverse disubstituted  $\beta$ -lactones. Through reaction optimization, selective

formation of the conjugate addition product over Heck-type coupling product was achieved. Owing to the compatibility of both electron-rich and electron deficient aryl boronic acids, this methodology provides a way to diversify advanced synthetic intermediates. Elaboration of some  $\beta$ -lactones by installation of the amine functional group at C4 chain terminal delivered palmostatin M derivatives.

## 2.3 Conclusion

$\alpha$ -Methylene- $\beta$ -lactones have been demonstrated to be important intermediates in synthetic and medicinal chemistry because of their versatile, reactive nature. This property makes them useful synthetic intermediates for transformations to more advanced structures. Two successful transformations include: a) olefin CM of  $\alpha$ -methylene- $\beta$ -lactones scaffolds coupled with diastereoselective reductions and b) rhodium-catalyzed conjugate addition of aryl boronic acids to  $\alpha$ -methylene- $\beta$ -lactones. This work targets the discovery of novel  $\beta$ -lactone inhibitors of N-Ras palmitoylation. The ultimate goal is to identify additional biochemical targets of the palmostatins and develop new chemical inhibitors with improved potency and selectivity for palmostatins targets.

## 2.4 Experimental

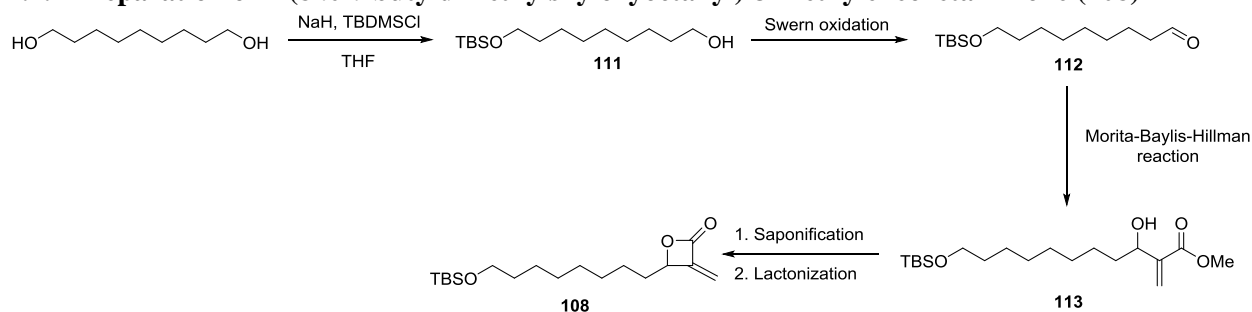
### 2.4.1 General Information

All moisture sensitive reactions were run in a flame-dried flask under  $N_2$ . THF was dried using a J. C. Meyer Solvent Dispensing System (SDS) and dispensed under  $N_2$ . All other solvents were dried over  $CaH_2$  or 4 Å molecular sieves. Deuterated chloroform ( $CDCl_3$ ), was dried over 4 Å molecular sieves. All starting materials and reagents were purchased from commercial sources and used as received. All  $^1H$  NMR experiments were recorded on a 400 MHz spectrometer. All  $^{13}C$  NMR experiments were recorded at 100 MHz. Chemical shifts ( $\delta$ ) are given in ppm, and coupling constants ( $J$ ) are given in Hz. The 7.26 resonance of residual  $CHCl_3$  for proton spectra and the 77.23 ppm resonance of  $CDCl_3$  for carbon spectra were used as internal references. High resolution mass spectroscopy (HRMS) was performed on a TOF instrument with ESI in positive ionization mode.



Unless otherwise stated, reaction progress was monitored by thin layer chromatography (TLC) performed on glass plates coated with silica gel UV254. Visualization was achieved by ultraviolet light (254 nm), 0.5%  $\text{KMnO}_4$  in 0.1 M aqueous NaOH solution and/or 5% phosphomolybdic acid in ethanol. Column chromatography was performed using silica gel, 40 microns flash silica.

#### 2.4.2 Preparation of 4-(8-*tert*-butyldimethylsilyloxyoctanyl)-3-methyleneoxetan-2-one (**108**)



**9-(*tert*-Butyldimethylsilyloxy)nonan-1-ol (**111**).** Sodium hydride (60% dispersion in mineral oil, 3.37 g, 140 mmol,) was suspended in dry THF (250 mL) under  $\text{N}_2$ , and 1,9-nonanediol (15.0 g, 93.6 mmol) was added at 0 °C in one portion. The mixture was stirred for 30 min; then TBSCl (16.9 g, 112 mmol) was added in one portion. The reaction mixture was then allowed to warm to ambient temperature, and stirring was continued for another 20 h. The reaction mixture was then cooled to 0 °C. Saturated aqueous  $\text{NaHCO}_3$  (300 mL) was added, and stirring was continued for 30 min. The organic layer was separated, and the aqueous layer was extracted with EtOAc (3 x 250 mL). The combined organic extracts were washed with brine (200 mL), dried ( $\text{MgSO}_4$ ) and concentrated. The crude product was purified by flash column chromatography on silica gel (hexanes/EtOAc 17:3) to give **111** as a colorless oil (15.4 g, 60%):<sup>47,62</sup>  $^1\text{H}$  NMR (400 MHz,  $\text{CDCl}_3$ )  $\delta$  3.63–3.55 (m, 4H), 1.74 (t,  $J$  = 4.8 Hz, 1H), 1.58–1.44 (m, 4H), 1.31 (br s, 10H), 0.87 (s, 9 H), 0.02 (s, 6H);  $^{13}\text{C}$  NMR (100 MHz,  $\text{CDCl}_3$ )  $\delta$  63.3, 62.9, 32.8, 32.7, 29.6, 29.4, 26.0, 25.8, 25.7, 18.4, –5.1.

**9-(*tert*-Butyldimethylsilyloxy)nonanal (**112**).** Dimethyl sulfoxide (9.55 mL, 134 mmol) in dry DCM (200 mL) was added dropwise over 30 min to a solution of oxalyl chloride (5.29 mL, 61.6 mmol) in dry DCM (120 mL) at –78 °C. Then, a solution of 9-(*tert*-butyldimethylsilyloxy)nonan-1-ol (**111**) (15.4 g,

56.0 mmol) in dry DCM (140 mL) was added over the same period of time, and the mixture was stirred for another 90 min. Triethylamine (28.5 mL, 205 mmol) was added dropwise, and the resulting slurry was stirred at  $-78^{\circ}\text{C}$  for 30 min then at ambient temperature for 1 h. The mixture was poured into  $\text{H}_2\text{O}$  (150 mL) and extracted with DCM (3 x 200 mL). The combined organic extracts were washed with  $\text{H}_2\text{O}$  (300 mL) and brine (200 mL), dried ( $\text{MgSO}_4$ ) and concentrated. The crude product was purified by flash column chromatography on silica gel (hexanes/EtOAc 25:1) to give **112** as a yellow oil (13.2 g, 86%):<sup>47,62</sup>  $^1\text{H}$  NMR (400 MHz,  $\text{CDCl}_3$ )  $\delta$  9.72 (t,  $J$  = 1.8 Hz, 1H), 3.56 (t,  $J$  = 6.6 Hz, 2H), 2.37 (dt,  $J$  = 7.4, 1.8 Hz, 2H), 1.61–1.55 (m, 2H), 1.55–1.46 (m, 2H) 1.27 (br s, 8H), 0.85 (s, 9H), 0.01 (s, 6H).  $^{13}\text{C}$  NMR (100 MHz,  $\text{CDCl}_3$ )  $\delta$  202.8, 63.3, 44.0, 33.0, 29.5, 29.4, 29.3, 26.1, 25.9, 22.2, 18.5,  $-5.1$ .

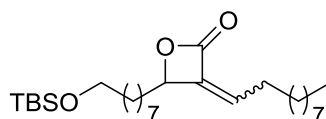
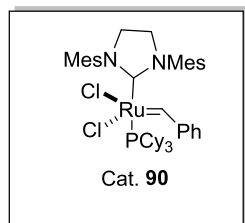
**Methyl 11-(tert-butyldimethylsilyloxy)-3-hydroxy-2-methyleneundecanoate (113).** 9-(tert-Butyldimethylsilyloxy)nonanal (**112**) (13.2 g, 48.3 mmol) and methyl acrylate (7.30 mL, 96.6 mmol) were combined. 3-Hydroxyquinuclidine (1.54 g, 12.1 mmol) was added, followed by MeOH (1.46 mL, 36.2 mmol). The resulting mixture was stirred for 3 d. MeOH and excess methyl acrylate were removed under reduced pressure. The resulting residue was diluted with saturated aqueous  $\text{NH}_4\text{Cl}$  solution (200 mL), and extracted with DCM (3 x 150 mL). The combined organic extracts were washed with brine (150 mL), dried ( $\text{MgSO}_4$ ) and concentrated. The crude product was purified by flash column chromatography on silica gel (hexanes/EtOAc 10:1) to give **113** as a colorless oil (12.7 g, 73%):<sup>62</sup> IR (neat) 3461 (br), 2927, 2855, 1719, 1438, 1283, 1094  $\text{cm}^{-1}$ ;  $^1\text{H}$  NMR (400 MHz,  $\text{CDCl}_3$ )  $\delta$  6.22 (s, 1H), 5.79 (s, 1H), 4.37–4.28 (m, 1H), 3.78 (s, 3H), 3.59 (t,  $J$  = 6.6 Hz, 2H), 2.49 (d,  $J$  = 6.9 Hz, 1 H), 1.69–1.59 (m, 2H), 1.51–1.46 (m, 3H), 1.29 (br s, 9H), 0.89 (s, 9H), 0.04 (s, 6H).  $^{13}\text{C}$  NMR (100 MHz,  $\text{CDCl}_3$ )  $\delta$  167.0, 143.0, 124.7, 71.3, 63.3, 51.8, 36.4, 32.9, 32.8, 29.6, 29.5, 26.0, 25.8, 18.4,  $-5.1$ ; HRMS (ESI) calcd for  $\text{C}_{19}\text{H}_{39}\text{O}_4\text{Si}$  ( $\text{M} + \text{H}$ )<sup>+</sup>  $m/z$  359.2618, found 359.2590.

**4-(8-tert-Butyldimethylsilyloxy)octanyl-3-methyleneoxetan-2-one (108).** Methyl 11-(tert-butyl-dimethylsilyloxy)-3-hydroxy-2-methyleneundecanoate (**113**) (12.7 g, 35.3 mmol) was dissolved in MeOH (64 mL). Aqueous KOH (2 M, 169 mL, 338 mmol) was added, and the reaction mixture was stirred

overnight at ambient temperature. Aqueous HCl (1M, 250 mL) and brine (250 mL) were added. The solution was then extracted with Et<sub>2</sub>O (3 x 100 mL). The combined organic extracts were washed with brine (200 mL), dried (MgSO<sub>4</sub>) and concentrated. The crude product, 11-(*tert*-butyldimethylsilyloxy)-3-hydroxy-2-methyleneundecanoic acid (**109**), was used directly in the next reaction:<sup>62</sup> <sup>1</sup>H NMR (400 MHz, CDCl<sub>3</sub>) δ 6.38 (m, 1H), 5.90 (m, 1H), 4.42 (m, 1H), 3.60 (t, *J* = 6.6 Hz, 2H), 1.68–1.59 (m, 2H), 1.50–1.48 (m, 3H), 1.27 (m, 9H), 0.89 (s, 9H), 0.05 (s, 6H); <sup>13</sup>C NMR (100 MHz, CDCl<sub>3</sub>) δ 170.7, 141.8, 127.3, 71.6, 63.4, 36.2, 32.8, 29.7, 29.5, 29.3, 26.0, 25.8, 18.4, –5.2. 11-(*tert*-Butyldimethylsilyloxy)-3-hydroxy-2-methyleneundecanoic acid (11.3 g, 32.7 mmol) was dissolved in dry DCM (270 mL). Dry Na<sub>2</sub>CO<sub>3</sub> (31.2 g, 295 mmol) was added, and the resulting suspension was stirred for 30 min. *o*-Nosyl chloride (10.9 g, 49.1 mmol) was added, and the resulting mixture was stirred for 3 d. The reaction was diluted with H<sub>2</sub>O (150 mL) and DCM (100 mL) while stirring for 20 min. The organic layer was separated, and the aqueous layer was extracted with DCM (3 x 100 mL). The combined organic extracts were washed with brine (150 mL), dried (Na<sub>2</sub>SO<sub>4</sub>) and concentrated. The crude product was purified by flash column chromatography on silica gel (hexanes/EtOAc 93:7) to give **108** as a brown oil (4.30 g, 38% over two steps):<sup>62</sup> IR (neat) 2927, 2855, 1822, 1251, 1081 cm<sup>-1</sup>; <sup>1</sup>H NMR (400 MHz, CDCl<sub>3</sub>) δ 5.90 (s, 1H), 5.41 (s, 1H), 4.95 (t, *J* = 6.4 Hz, 1H), 3.59 (t, *J* = 6.5 Hz, 2H), 1.84 (m, 2H), 1.50–1.43 (m, 4H), 1.30 (br s, 8H), 0.89 (s, 9H), 0.04 (s, 6H); <sup>13</sup>C NMR (100 MHz, CDCl<sub>3</sub>) δ 163.8, 146.7, 115.0, 79.8, 63.4, 33.5, 33.0, 29.6, 29.5, 29.4, 26.2, 26.0, 24.8, 18.6, –5.1; HRMS (ESI) calcd for C<sub>18</sub>H<sub>35</sub>O<sub>3</sub>Si (M + H)<sup>+</sup> *m/z* 327.2355, found 327.2350.

### 2.4.3 Preparation of $\alpha$ -alkylidene- $\beta$ -lactone via olefin cross-metathesis

#### Catalyst used in olefin cross-metathesis



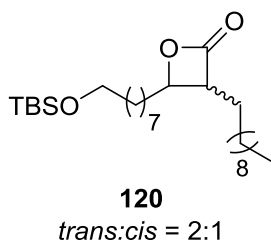
**116**  
Z/E = 2.2:1

**Z/E-4-(8-*tert*-Butyldimethylsilyloxy)octanyl-3-decanylideneoxetan-2-one (116).** Catalyst **90** (52 mg, 0.061 mmol) was added to a solution of 4-(8-*tert*-butyldimethylsilyloxy)octanyl-3-methyleneoxetan-2-one (**108**) (0.40 g, 1.2 mmol) and 1-undecene (0.28 g, 1.8 mmol) in dry DCM (70mL). The mixture was stirred overnight at 40 °C. The next day  $^1\text{H}$  NMR showed complete consumption of **108**. The reaction mixture was allowed to cool to rt and then concentrated to form a brown residue. The  $^1\text{H}$  NMR *Z:E* ratio of the crude reaction mixture was 2.2:1. Purification by flash column chromatography on silica gel (petroleum ether/EtOAc 49:1) provided **116** as a colorless oil (0.42 g, 76%). The isomers were separable by careful column chromatography using the same solvent system. **Z-116** (colorless oil) (0.23 g, 42%): IR (neat) 2925, 2854, 1808, 1251, 1095, 1073  $\text{cm}^{-1}$ ;  $^1\text{H}$  NMR (400 MHz,  $\text{CDCl}_3$ )  $\delta$  5.83 (t,  $J = 7.5$  Hz, 1H), 4.81 (t,  $J = 6.2$  Hz, 1H), 3.57 (t,  $J = 6.6$  Hz, 2H), 2.46 (app q,  $J = 7.4$  Hz, 2H), 1.77 (app q,  $J = 7.0$  Hz, 2H), 1.52–1.37 (m, 4H), 1.36–1.17 (m, 22H), 0.87 (s, 9H), 0.85 (t,  $J = 7.0$  Hz, 3H), 0.02 (s, 6H);  $^{13}\text{C}$  NMR (100 MHz,  $\text{CDCl}_3$ )  $\delta$  164.2, 137.7, 136.3, 78.7, 63.3, 33.9, 33.0, 32.0, 29.6, 29.5, 29.4, 29.4, 29.2, 29.0, 26.1, 25.9, 24.7, 22.8, 18.5, 14.2 –5.1; HRMS (ESI) calcd for  $\text{C}_{27}\text{H}_{53}\text{O}_3\text{Si}$  ( $\text{M} + \text{H}$ ) $^+$   $m/z$  453.3764 found 453.3776. **E-116** (colorless oil) (51 mg, 9.2%): IR 2926, 2854, 1815, 1463, 1251, 1095  $\text{cm}^{-1}$ ;  $^1\text{H}$  NMR (400 MHz,  $\text{CDCl}_3$ )  $\delta$  6.32 (ddd,  $J = 7.8, 7.8, 1.5$  Hz, 1H), 5.01–4.95 (m, 1H), 3.59 (t,  $J = 6.6$  Hz,

2H), 2.10 (app q,  $J = 14.9, 7.5$  Hz, 2H), 1.97–1.86 (m, 1H), 1.84–1.70 (m, 1H), 1.55–1.40 (m, 6H), 1.39–1.23 (m, 22H), 0.87 (s, 9H), 0.88 (t,  $J = 7.2$  Hz, 3H), 0.04 (s, 6H);  $^{13}\text{C}$  NMR (100 MHz,  $\text{CDCl}_3$ )  $\delta$  164.5, 137.8, 134.1, 79.3, 63.5, 33.5, 33.0, 32.1, 29.6, 29.6, 29.5, 29.5, 29.5, 29.4, 29.0, 28.6, 26.2, 26.0, 24.9, 22.9, 18.6, 14.3,  $-5.1$ ; HRMS (ESI) calcd for  $\text{C}_{27}\text{H}_{53}\text{O}_3\text{Si}$  ( $\text{M} + \text{H}$ ) $^+$   $m/z$  453.3764, found 453.3750.

## 2.4.4 Diastereoselective Reductions

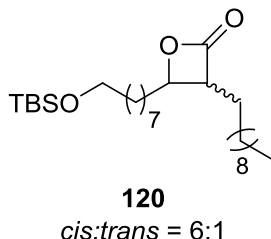
### 2.4.4.1 1,4-Reduction under cobalt catalysis



*cis/trans*-4-(8-*tert*-Butyldimethylsilyloxy)octanyl-3-decyloxetan-2-one (**120**). *Z/E*-4-(8-*tert*-Butyldimethylsilyloxy)octanyl-3-decanylideneoxetan-2-one (**116**) (0.34 g, 0.77 mmol) was dissolved in a mixture of THF:MeOH (10.3 mL, 8.5:1.8). This solution was cooled to  $-10$  °C, followed by the addition of  $\text{CoCl}_2(\text{PPh}_3)_2$  (0.10 g, 0.15 mmol) and then portion-wise addition of  $\text{NaBH}_4$  (0.17 g, 4.5 mmol) within 10 min. The mixture was vigorously stirred for 2 h between  $-7$  and  $-5$  °C. The reaction mixture was filtered through a pad of celite, and the celite was washed with  $\text{CHCl}_3$  (10 mL). The filtrate was washed with 2M HCl (10 mL), dried ( $\text{MgSO}_4$ ) and concentrated. The  $^1\text{H}$  NMR *trans:cis* ratio of the crude reaction mixture was 2:1. Purification by flash column chromatography on silica gel (petroleum ether/EtOAc 49:1) provided **120** as a colorless oil (0.24 g, 71%). The *trans*-isomer was separable by careful column chromatography using the same solvent system. *trans*-**120** colorless oil (0.16 g, 47%): IR (neat) 2925, 2854, 1822, 1463, 1254, 1097  $\text{cm}^{-1}$ ;  $^1\text{H}$  NMR (400 MHz,  $\text{CDCl}_3$ )  $\delta$  4.21 (ddd,  $J = 7.2, 6.0, 4.0$  Hz, 1H), 3.60 (t,  $J = 6.6$  Hz, 2H), 3.17 (ddd,  $J = 8.8, 6.6, 4.0$  Hz, 1H), 1.91–1.77 (m, 2H), 1.76–1.64 (m, 2H), 1.55–1.46 (m, 2H), 1.45–1.22 (m, 26H), 0.89 (s, 9H), 0.90–0.86 (m, 3H), 0.05 (s, 6H);  $^{13}\text{C}$  NMR (100 MHz,

CDCl<sub>3</sub>)  $\delta$  171.9, 78.4, 63.5, 56.4, 34.7, 33.0, 32.1, 29.8, 29.7, 29.6, 29.5, 29.4, 28.1, 27.2, 26.0, 25.2, 22.9, 18.6, 14.3, -5.1; HRMS (ESI) calcd for C<sub>27</sub>H<sub>55</sub>O<sub>3</sub>Si (M + H)<sup>+</sup>  $m/z$  455.3909, found 455.3926.

#### 2.4.4.2 Hydrogenation under palladium catalysis



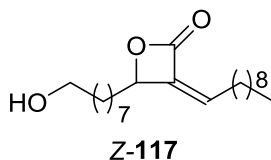
***cis/trans*-4-(8-*tert*-Butyldimethylsilyloxy)octanyl-3-decyloxetan-2-one (120).** A solution of *Z/E*-4-(8-*tert*-butyldimethylsilyloxy)octanyl-3-decanylideneoxetan-2-one (**116**) (0.23 g, 0.51 mmol) in THF (6 mL) was hydrogenated by stirring at rt in an atmosphere of hydrogen in the presence 10% palladium on carbon (0.016 g, 0.015 mmol). After 5 h of stirring, the catalyst was filtered through a pad of celite, and the celite was washed with CHCl<sub>3</sub> (15 mL). The mixture was then concentrated. The <sup>1</sup>H NMR *trans:cis* ratio of the crude reaction mixture was 1:6. Purification by flash column chromatography on silica gel (petroleum ether/EtOAc 49:1) provided **120** as a colorless oil (0.17 g, 72%). The *cis*-isomer was separable by careful column chromatography using the same solvent system. *cis*-**120** colorless oil (99 mg, 43%): IR (neat) 2925, 2854, 1821, 1463, 1253, 1096 cm<sup>-1</sup>; <sup>1</sup>H NMR (400 MHz, CDCl<sub>3</sub>)  $\delta$  4.52 (ddd,  $J$  = 9.9, 6.3, 4.2 Hz, 1H), 3.60 (t,  $J$  = 6.6 Hz, 2H), 3.62–3.55 (m, 1H), 1.82–1.58 (m, 4H), 1.56–1.46 (m, 2H), 1.39–1.25 (m, 26H), 0.89 (s, 9H), 0.88 (t,  $J$  = 7.0 Hz, 3H), 0.05 (s, 6H); <sup>13</sup>C NMR (100 MHz, CDCl<sub>3</sub>)  $\delta$  172.5, 75.9, 63.4, 52.9, 33.0, 32.1, 30.4, 29.8, 29.7, 29.6, 29.5, 29.5, 27.8, 26.2, 25.9, 25.7, 24.1, 22.9, 18.6, 14.3, -5.1; HRMS (ESI) calcd for C<sub>27</sub>H<sub>55</sub>O<sub>3</sub>Si (M + H)<sup>+</sup>  $m/z$  455.3920, found 455.3939.

#### 2.4.5 Cleavage of silyl protecting group

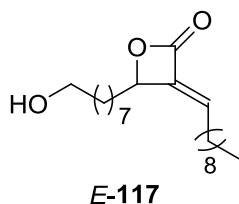
##### General procedure

Pyridinium *p*-toluenesulfonate (PPTS) (0.3 equiv) was added to a solution of silyl ether (1.0 equiv, 0.07 M in EtOH/DCM, 1:1). The resulting mixture was then placed in a pre-heated oil bath (55 °C) for 3 h

under reflux. The reaction was allowed to cool to rt. Et<sub>3</sub>N (10 volumes) was added and the reaction mixture was concentrated. The crude product was purified by flash column chromatography on silica gel.

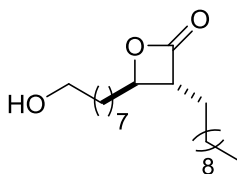


**Z-3-Decylidene-4-(8-hydroxy)octanyloxetan-2-one (Z-117).** The general procedure was followed using Z-4-(8-*tert*-butyldimethylsilyloxy)octanyl-3-decanylideneoxetan-2-one (Z-116) (0.27 g, 0.59 mmol). Purification by flash column chromatography on silica gel (hexanes/EtOAc 5:1) provided Z-117 as a colorless oil (0.197 g, 98%): IR (neat) 3378 (br), 2923, 2854, 1802, 1464, 1146, 1112 cm<sup>-1</sup>; <sup>1</sup>H NMR (400 MHz, CDCl<sub>3</sub>) δ 5.84 (ddd, *J* = 7.9, 7.9, 1.2 Hz, 1H), 4.88–4.82 (m, 1H), 3.64 (t, *J* = 6.6 Hz, 2H), 2.56–2.41 (m, 2H), 1.80 (app q, *J* = 6.7 Hz, 2H), 1.61–1.52 (m, 2H), 1.50–1.41 (m, 2H), 1.40–1.17 (m, 22H), 0.88 (t, *J* = 6.6 Hz, 3H); <sup>13</sup>C NMR (100 MHz, CDCl<sub>3</sub>) δ 164.4, 137.6, 136.5, 78.8, 63.2, 33.9, 32.9, 32.1, 29.7, 29.5, 29.5, 29.4, 29.4, 29.2, 29.1, 29.0, 25.9, 24.8, 22.9, 14.3; HRMS (ESI) calcd for C<sub>21</sub>H<sub>39</sub>O<sub>3</sub> (M + H)<sup>+</sup> *m/z* 339.2899, found 339.2895.



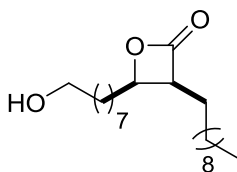
**E-3-Decylidene-4-(8-hydroxy)octanyloxetan-2-one (E-117).** The general procedure was followed using E-4-(8-*tert*-butyldimethylsilyloxy)octanyl-3-decanylideneoxetan-2-one (E-116) (0.11 g, 0.25 mmol). Purification by flash column chromatography on silica gel (hexanes/EtOAc 5:1) provided E-117 as a colorless oil (54 mg, 64%): IR (neat) 3345 (br), 2923, 2853, 1808, 1462, 1116, 1033 cm<sup>-1</sup>; <sup>1</sup>H NMR (400 MHz, CDCl<sub>3</sub>) δ 6.32 (ddd, *J* = 7.9, 7.9, 1.6 Hz, 1H), 5.00–4.94 (m, 1H), 3.62 (t, *J* = 6.6 Hz, 2H), 2.09 (app q, *J* = 7.5 Hz, 2H), 1.96–1.85 (m, 1H), 1.82–1.69 (m, 1H), 1.60–1.40 (m, 4H), 1.39–1.17 (m, 22H), 0.87 (t, *J* = 6.6 Hz, 3H); <sup>13</sup>C NMR (100 MHz, CDCl<sub>3</sub>) δ 164.5, 137.7, 134.2, 79.3, 63.1, 33.4, 32.9, 32.0,

29.6, 29.6, 29.5, 29.5, 29.4, 29.4, 29.0, 28.6, 25.9, 24.8, 22.8, 14.3; HRMS (ESI) calcd for  $C_{21}H_{39}O_3$  ( $M + H$ )<sup>+</sup>  $m/z$  339.2899, found 339.2904.



*trans*-**118**

***trans*-3-Decyl-4-(8-hydroxy)octanyloxetan-2-one (*trans*-118).** The general procedure was followed using *trans*-4-(8-*tert*-butyldimethylsilyloxy)octanyl-3-decyloxetan-2-one (*trans*-**120**) (0.13 g, 0.28 mmol). Purification by flash column chromatography on silica gel (hexanes/EtOAc 5:1) provided *trans*-**118** as a colorless oil (47 mg, 50%): IR (neat) 3332 (br), 2919, 2851, 1794, 1467, 1146  $cm^{-1}$ ;  $^1H$  NMR (400 MHz,  $CDCl_3$ )  $\delta$  4.24–4.17 (m, 1H), 3.63 (t,  $J$  = 6.4 Hz, 2H), 3.19–3.11 (m, 1H), 1.90–1.76 (m, 2H), 1.76–1.61 (m, 2H), 1.60–1.50 (m, 2H), 1.48–1.20 (m, 26H), 0.87 (t,  $J$  = 5.8 Hz, 3H);  $^{13}C$  NMR (100 MHz,  $CDCl_3$ )  $\delta$  171.9, 78.4, 63.2, 56.4, 34.6, 32.9, 32.1, 29.8, 29.7, 29.6, 29.5, 29.5, 29.4, 28.1, 27.2, 25.9, 25.2, 22.9, 14.3; HRMS (ESI) calcd for  $C_{21}H_{41}O_3$  ( $M + H$ )<sup>+</sup>  $m/z$  341.3056, found 341.3079.



*cis*-**118**

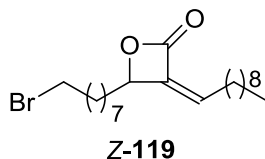
***cis*-3-Decyl-4-(8-hydroxy)octanyloxetan-2-one (*cis*-118).** The general procedure was followed using *cis*-4-(8-*tert*-butyldimethylsilyloxy)octanyl-3-decyloxetan-2-one (*cis*-**120**) (0.058 g, 0.13 mmol). Purification by flash column chromatography on silica gel (hexanes/EtOAc 5:1) provided *cis*-**118** as a colorless oil (32 mg, 75%): IR (neat) 3296 (br), 2918, 2849, 1795, 1468, 1155, 1060  $cm^{-1}$ ;  $^1H$  NMR (400 MHz,  $CDCl_3$ )  $\delta$  4.52 (ddd,  $J$  = 10.0, 6.4, 4.0 Hz, 1H), 3.63 (t,  $J$  = 6.6 Hz, 2H), 3.62–3.55 (m, 1H), 1.81–1.46 (m, 6H), 1.45–1.18 (m, 26H), 0.87 (t,  $J$  = 6.6 Hz, 3H);  $^{13}C$  NMR (100 MHz,  $CDCl_3$ )  $\delta$  172.5, 75.9, 63.2, 52.9, 32.9, 32.1, 30.4, 29.8, 29.7, 29.6, 29.6, 29.5, 29.5, 29.4, 27.8, 25.9, 25.7, 24.1, 22.9, 14.3; HRMS (ESI) calcd for  $C_{21}H_{41}O_3$  ( $M + H$ )<sup>+</sup>  $m/z$  341.3056, found 341.3083.



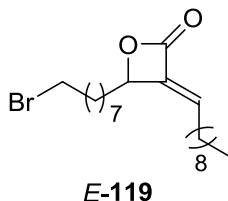
## 2.4.6 Appel bromination

### General procedure

Tetrabromomethane (CBr<sub>4</sub>) (1.5 equiv) and triphenylphosphine (PPh<sub>3</sub>) (3 equiv) were added to the alcohol solution (1 equiv, 0.03 M in DCM) at 0 °C. After 1 h, the reaction mixture was diluted with petroleum ether (5 volumes) and then concentrated. The crude product was adsorbed onto silica gel (dry loaded) and then purified by flash column chromatography on silica gel to give the bromide.

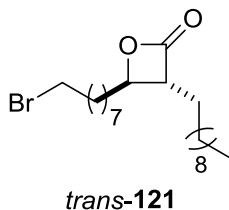


**Z-4-(8-Bromo)octanyl-3-decanylideneoxetan-2-one (Z-119).** The general procedure was followed using Z-3-decylidene-4-(8-hydroxy)octanyloxetan-2-one (Z-117) (0.20 g, 0.58 mmol). Purification by flash column chromatography on silica gel (hexanes/EtOAc 49:1) provided Z-119 as a colorless oil (96 mg, 41%): IR (neat) 2923, 2854, 1804, 1463, 1115, 1066 cm<sup>-1</sup>; <sup>1</sup>H NMR (400 MHz, CDCl<sub>3</sub>) δ 5.84 (ddd, *J* = 7.9, 7.9, 1.0 Hz, 1H), 4.87–4.80 (m, 1H), 3.39 (t, *J* = 6.8 Hz, 2H), 2.55–2.40 (m, 2H), 1.88–1.74 (m, 4H), 1.50–1.37 (m, 4H), 1.36–1.18 (m, 20H), 0.87 (t, *J* = 6.6 Hz, 3H); <sup>13</sup>C NMR (100 MHz, CDCl<sub>3</sub>) δ 164.3, 137.6, 136.5, 78.7, 34.1, 33.9, 32.9, 32.0, 29.7, 29.5, 29.4, 29.3, 29.2, 29.1, 29.0, 28.8, 28.3, 24.7, 22.8, 14.3; HRMS (ESI) calcd for C<sub>21</sub>H<sub>38</sub>BrO<sub>2</sub> (M + H)<sup>+</sup> *m/z* 401.2055, found 401.2033.

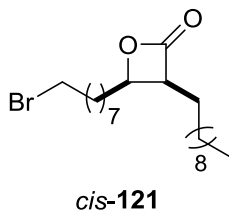


**E-4-(8-Bromo)octanyl-3-decanylideneoxetan-2-one (E-119).** The general procedure was followed using E-3-decylidene-4-(8-hydroxy)octanyloxetan-2-one (E-117) (0.054 g, 0.16 mmol). Purification by flash column chromatography on silica gel (hexanes/EtOAc 98:1) provided E-119 as a colorless oil (40 mg, 63

IR (neat) 2924, 2854, 1811, 1462, 1118, 1049  $\text{cm}^{-1}$ ;  $^1\text{H}$  NMR (400 MHz,  $\text{CDCl}_3$ )  $\delta$  6.33 (ddd,  $J = 7.8$ , 7.8, 1.6 Hz, 1H), 5.02–4.94 (m, 1H), 3.40 (t,  $J = 6.8$  Hz, 2H), 2.10 (app q,  $J = 7.5$  Hz, 2H), 1.98–1.70 (m, 4H), 1.57–1.39 (m, 4H), 1.38–1.18 (m, 20H), 0.88 (t,  $J = 6.6$  Hz, 3H);  $^{13}\text{C}$  NMR (100 MHz,  $\text{CDCl}_3$ )  $\delta$  164.5, 137.8, 134.2, 79.3, 34.1, 33.4, 33.0, 32.0, 29.6, 29.5, 29.5, 29.4, 29.4, 29.0, 28.8, 28.6, 28.3, 24.8, 22.9, 14.3; HRMS (ESI) calcd for  $\text{C}_{21}\text{H}_{38}\text{BrO}_2$  ( $\text{M} + \text{H}$ ) $^+$   $m/z$  401.2055, found 401.2064.



***trans*-4-(8-Bromo)ocatanyl-3-decyloxetan-2-one (*trans*-121).** The general procedure was followed using *trans*-3-decyl-4-(8-hydroxy)octanyloxetan-2-one (*trans*-**118**) (0.10 g, 0.31 mmol). Purification by flash column chromatography on silica gel (hexanes/EtOAc 49:1) provided *trans*-**121** as a colorless oil (0.12 g, 95%): IR (neat) 2924, 2854, 1822, 1464, 1121  $\text{cm}^{-1}$ ;  $^1\text{H}$  NMR (400 MHz,  $\text{CDCl}_3$ )  $\delta$  4.19 (ddd,  $J = 7.2$ , 6.0, 4.1 Hz, 1H), 3.39 (t,  $J = 6.8$  Hz, 2H), 3.15 (ddd,  $J = 8.8$ , 6.6, 4.0 Hz, 1H), 1.89–1.77 (m, 4H), 1.76–1.18 (m, 28H), 0.86 (t,  $J = 6.6$  Hz, 3H);  $^{13}\text{C}$  NMR (100 MHz,  $\text{CDCl}_3$ )  $\delta$  171.7, 78.2, 56.3, 34.6, 34.1, 32.9, 32.0, 29.7, 29.7, 29.4, 29.4, 29.3, 28.7, 28.2, 28.0, 27.1, 25.2, 22.8, 14.3; HRMS (ESI) calcd for  $\text{C}_{21}\text{H}_{40}\text{BrO}_2$  ( $\text{M} + \text{Na}$ ) $^+$   $m/z$  425.2020, found 425.2011.



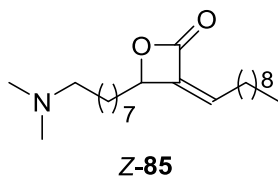
***cis*-4-(8-Bromo)ocatanyl-3-decyloxetan-2-one (*cis*-121).** The general procedure was followed using *cis*-3-decyl-4-(8-hydroxy)octanyloxetan-2-one (*cis*-**118**) (14 mg, 0.042 mmol). Purification by flash column chromatography on silica gel (hexanes/EtOAc 49:1) provided *cis*-**121** as a colorless oil (13 mg, 78%): IR (neat) 2922, 2853, 1821, 1732, 1463, 1122  $\text{cm}^{-1}$ ;  $^1\text{H}$  NMR (400 MHz,  $\text{CDCl}_3$ )  $\delta$  4.56–4.48 (m, 1H), 3.63–3.55 (m, 1H), 3.45–3.35 (m, 2H), 1.90–1.80 (m, 2H), 1.79–1.18 (m, 30H), 0.92–0.80 (m, 3H);  $^{13}\text{C}$  NMR

(100 MHz, CDCl<sub>3</sub>)  $\delta$  172.5, 75.9, 52.9, 34.2, 33.0, 32.1, 30.4, 29.9, 29.8, 29.7, 29.6, 29.5, 29.4, 29.4, 28.8, 28.3, 27.8, 25.8, 24.2, 22.9, 14.3; HRMS (ESI) calcd for C<sub>21</sub>H<sub>40</sub>BrO<sub>2</sub> (M + H)<sup>+</sup>  $m/z$  found.

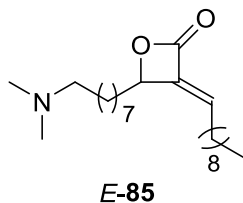
#### 2.4.7 Nucleophilic substitution of the bromide with dimethylamine

##### General procedure

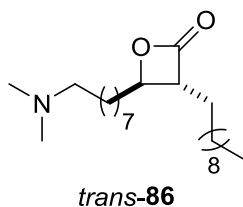
Dimethylamine in H<sub>2</sub>O (40%, 1.0 equiv) and NaHCO<sub>3</sub> (1.0 equiv) were added to a solution of the bromide (1.0 equiv, 0.05 M in DMF) and the mixture was heated at reflux while stirring for 24 h. The mixture was then allowed to cool to rt, concentrated, dissolved in DCM (20 volumes relative to bromide) and then washed with water (20 volumes x 2). The organic layer was dried (NaSO<sub>4</sub>) and concentrated.



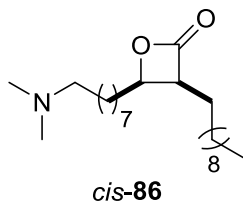
**Z-3-Decanylidene-4-(8-dimethylamino)octanyloxetan-2-one (Z-85).** The general procedure was followed using Z-4-(8-bromo)octanyl-3-decanylideneoxetan-2-one (**Z-119**) (0.16 g, 0.41 mmol). Purification by flash column chromatography on silica gel (NH<sub>4</sub>OH/MeOH/CHCl<sub>3</sub> 2:4.5:175) provided **Z-85** as a brown oil (55 mg, 37%): IR (neat) 2926, 2855, 1806, 1713, 1215 cm<sup>-1</sup>; <sup>1</sup>H NMR (400 MHz, CDCl<sub>3</sub>)  $\delta$  5.84 (ddd,  $J$  = 7.9, 7.9, 1.1 Hz, 1H), 4.86–4.80 (m, 1H), 2.56–2.41 (m, 2H), 2.44 (s, 6H), 1.78 (app q,  $J$  = 7.4 Hz, 2H), 1.66–1.55 (m, 2H), 1.49–1.37 (m, 4H), 1.36–1.18 (m, 22H), 0.86 (t,  $J$  = 6.6 Hz, 3H); <sup>13</sup>C NMR (100 MHz, CDCl<sub>3</sub>)  $\delta$  164.4, 137.5, 136.6, 78.8, 59.3, 44.6, 33.9, 32.0, 29.6, 29.5, 29.4, 29.4, 29.2, 29.1, 29.0, 27.2, 26.5, 24.7, 22.8, 14.3; HRMS (ESI) calcd for C<sub>23</sub>H<sub>44</sub>NO<sub>2</sub> (M + H)<sup>+</sup>  $m/z$  366.3361, found 366.3441.



***E*-3-Decanylidene-4-(8-dimethylamino)octanyloxetan-2-one (*E*-85).** The general procedure was followed using *E*-4-(8-bromo)octanyl-3-decanylideneoxetan-2-one (*E*-119) (0.038 g, 0.095 mmol). Purification by flash column chromatography on silica gel (NH<sub>4</sub>OH/MeOH/CHCl<sub>3</sub> 2:4.5:175) provided *E*-85 as a brown oil (7.6 mg, 22%): <sup>1</sup>H NMR (400 MHz, CDCl<sub>3</sub>) δ 6.34 (ddd, *J* = 7.8, 7.8, 1.6 Hz, 1H), 5.01–4.96 (m, 1H), 2.26–2.20 (m, 2H), 2.21 (s, 6H), 2.11 (app q, *J* = 7.4 Hz, 2H), 1.98–1.85 (m, 1H), 1.83–1.70 (m, 1H) 1.68–1.18 (m, 26H), 0.88 (t, *J* = 6.3 Hz, 3H).

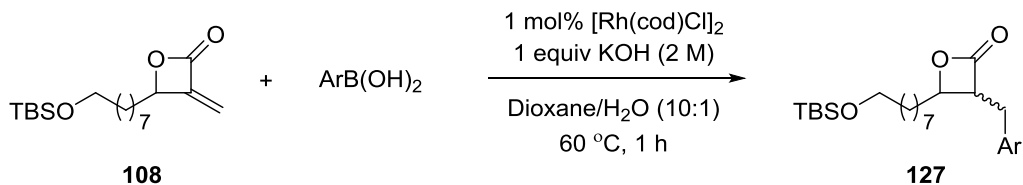


***trans*-3-Decyl-4-(8-dimethylamino)octanyloxetan-2-one (*trans*-86).** The general procedure was followed using *trans*-4-(8-bromo)ocatanyl-3-decyloxetan-2-one (*trans*-121) (0.04 g, 0.099 mmol). Purification by flash column chromatography on silica gel (NH<sub>4</sub>OH/MeOH/CHCl<sub>3</sub> 2:4.5:175) provided *trans*-86 as a brown oil (12 mg, 33%): IR (neat) 2923, 2853, 1823, 1624, 1464, 1118 cm<sup>-1</sup>; <sup>1</sup>H NMR (400 MHz, CDCl<sub>3</sub>) δ 4.21 (ddd, *J* = 7.2, 5.9, 4.0 Hz, 1H), 3.16 (t, *J* = 6.8 Hz, 2H), 3.15 (ddd, *J* = 8.8, 6.6, 4.0 Hz, 1H), 2.35–2.25 (m, 2H), 2.28 (s, 6H), 1.89–1.77 (m, 2H), 1.76–1.65 (m, 2H), 1.53–1.20 (m, 26H), 0.88 (t, *J* = 6.6 Hz, 3H); <sup>13</sup>C NMR (100 MHz, CDCl<sub>3</sub>) δ 171.8, 78.4, 59.9, 56.4, 45.4, 34.7, 32.1, 29.9, 29.8, 29.7, 29.6, 29.5, 29.4, 28.1, 27.5, 27.2, 25.3, 22.9, 14.3; HRMS (ESI) calcd for C<sub>23</sub>H<sub>46</sub>NO<sub>2</sub> (M + H)<sup>+</sup> *m/z* 368.3518, found 368.3609.



***cis*-3-Decyl-4-(8-dimethylamino)octanyloxetan-2-one (*cis*-86).** The general procedure was followed using *cis*-4-(8-bromo)ocatanyl-3-decyloxetan-2-one (*cis*-121) (0.034 g, 0.084 mmol). Purification by flash column chromatography on silica gel (NH<sub>4</sub>OH/MeOH/CHCl<sub>3</sub> 2:4.5:175) provided *cis*-86 as a brown oil (7.6 mg, 24%): IR (neat) 2923, 2854, 1822, 1464, 1119 cm<sup>-1</sup>; <sup>1</sup>H NMR (400 MHz, CDCl<sub>3</sub>) δ 4.52 (ddd, *J* = 10.2, 6.4, 4.1 Hz, 1H), 3.59 (ddd, *J* = 8.6, 6.8, 6.8 Hz, 1H), 2.26–2.20 (m, 2H), 2.22 (s, 6H), 1.82–1.18 (m, 32H), 0.88 (t, *J* = 6.6 Hz, 3H); <sup>13</sup>C NMR (100 MHz, CDCl<sub>3</sub>) δ 172.6, 76.0, 60.2, 52.9, 45.8, 32.1, 30.4, 29.8, 29.8, 29.7, 29.6, 29.6, 29.5, 29.5, 28.0, 27.8, 27.7, 25.8, 24.2, 22.9, 14.3; HRMS (ESI) calcd for C<sub>23</sub>H<sub>46</sub>NO<sub>2</sub> (M + H)<sup>+</sup> *m/z* 368.3529, found 368.3510.

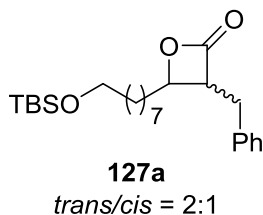
#### 2.4.8 Rh-catalyzed conjugate additions of aryl boronic acids to α-methylene-β-lactones 108



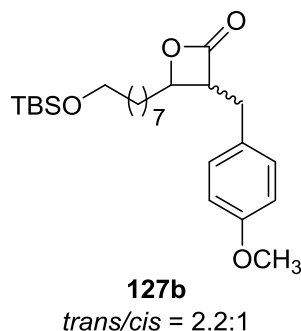
##### General procedure

Aryl boronic acid (1.5 equiv, 0.75 mmol unless otherwise noted) and 1 mol % [Rh(cod)Cl]<sub>2</sub> (0.0050 mmol, 2.5 mg) were placed in a reaction tube equipped with a stir bar. The reaction tube was capped with a rubber septum then filled and back-filled with N<sub>2</sub> three times. Aqueous 2 M KOH (1 equiv, 0.25 mL) was added, followed by the α-methylene-β-lactone **108** (0.50 mmol unless otherwise noted) dissolved in dioxane (2.5 mL). The resulting yellow solution was stirred in an oil bath at 60 °C for 1 h. The reaction was quenched with saturated aqueous NH<sub>4</sub>Cl (5 mL) and extracted with Et<sub>2</sub>O (3 x 10 mL). The combined organic extracts were dried (Na<sub>2</sub>SO<sub>4</sub>) and concentrated *in vacuo*. An aliquout of the reaction mixture was

analyzed by  $^1\text{H}$  NMR to determine the diastereoselectivity. The crude mixture was purified by flash column chromatography. In all cases, the *trans* isomers were obtained as the major products.

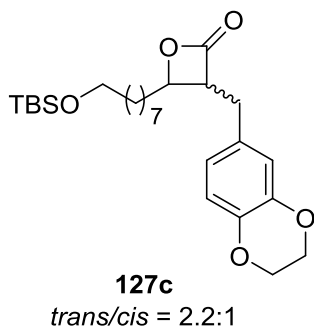


***trans/cis*-3-Benzyl-4-(8-*tert*-butyldimethylsilyloxy)octanyloxetan-2-one (127a).** The general procedure was followed using 4-(8-*tert*-butyldimethylsilyloxy)octanyl-3-methylenioxetan-2-one (**108**) (0.40 g, 1.3 mmol) and phenylboronic acid (0.24 g, 2.0 mmol). The  $^1\text{H}$  NMR *trans:cis* ratio of the crude reaction mixture was 2:1. Purification by flash column chromatography on silica gel (hexanes/EtOAc 98:2) provided **127a** as a colorless oil (0.39 g, 79%). The *trans*-isomer was separable by careful column chromatography using the same solvent system. *trans*-**127a** (colorless oil): IR (neat) 2927, 2854, 1821, 1455, 1249, 1093  $\text{cm}^{-1}$ ;  $^1\text{H}$  NMR (400 MHz,  $\text{CDCl}_3$ )  $\delta$  7.34–7.18 (m, 5 H), 4.27 (ddd,  $J$  = 6.7, 6.7, 4.1 Hz, 1H), 3.59 (t,  $J$  = 6.6 Hz, 2H), 3.45 (ddd,  $J$  = 9.5, 5.6, 4.1 Hz, 1H), 3.16 (dd,  $J$  = 14.3, 5.7 Hz, 1H), 3.00 (dd,  $J$  = 14.2, 9.3 Hz, 1H), 1.83–1.75 (m, 1H), 1.63–1.55 (m, 1H), 1.52–1.45 (m, 2H), 1.32–1.04 (m, 10H), 0.90 (s, 9H), 0.05 (s, 6H);  $^{13}\text{C}$  NMR (100 MHz,  $\text{CDCl}_3$ )  $\delta$  170.9, 137.4, 129.0, 128.8, 127.2, 77.7, 63.4, 57.5, 34.4, 34.0, 33.0, 29.5, 29.3, 29.2, 26.2, 25.9, 24.8, 18.5, –5.1; HRMS (ESI) calcd for  $\text{C}_{24}\text{H}_{41}\text{O}_3\text{Si}$  ( $\text{M} + \text{H}^+$ )  $m/z$  405.2825, found 405.2827.



***trans/cis*-4-(8-*tert*-Butyldimethylsilyloxyoctanyl)-3-(4-methoxyphenylmethyl)oxetan-2-one (127b).**

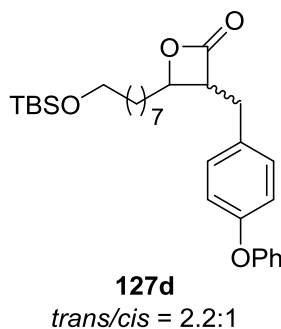
The general procedure was followed using 4-(8-*tert*-butyldimethylsilyloxy)octanyl-3-methyleneoxetan-2-one (**108**) and 4-methoxyphenylboronic acid. The  $^1\text{H}$  NMR *trans*:*cis* ratio of the crude reaction mixture was 2.2:1. Purification by flash column chromatography on silica gel (hexanes/EtOAc 40:1) provided **127b** as a colorless oil (0.17 g, 85%). The isomers were separated by careful column chromatography using the same solvent system. *trans*-**127b** (colorless oil): IR (neat) 2928, 2855, 1820, 1513, 1247, 1095  $\text{cm}^{-1}$ ;  $^1\text{H}$  NMR (400 MHz,  $\text{CDCl}_3$ )  $\delta$  7.13–7.07 (m, 2H), 6.87–6.82 (m, 2H), 4.25 (ddd,  $J$  = 6.8, 6.8, 4.2 Hz, 1H), 3.79 (s, 3 H), 3.57 (t,  $J$  = 6.6 Hz, 2H), 3.41 (ddd,  $J$  = 9.5, 5.7, 4.2 Hz, 1H), 3.09 (dd,  $J$  = 14.4, 5.8 Hz, 1H), 2.95 (dd,  $J$  = 14.4, 9.0 Hz, 1H), 1.82–1.75 (m, 1 H), 1.63–1.58 (m, 1H), 1.52–1.45 (m, 2H) 1.34–1.08 (m, 10H), 0.89 (s, 9H), 0.04 (s, 6H);  $^{13}\text{C}$  NMR (100 MHz,  $\text{CDCl}_3$ )  $\delta$  171.1, 158.9, 129.9, 129.3, 114.5, 77.6, 63.5, 57.8, 55.5, 34.4, 33.1, 33.0, 29.6, 29.4, 29.3, 26.2, 26.0, 24.9, 18.6, –5.1; HRMS (ESI) calcd for  $\text{C}_{25}\text{H}_{43}\text{O}_4\text{Si}$  ( $\text{M} + \text{H}$ ) $^+$   $m/z$  435.2931, found 435.2929. *cis*-**127b** (colorless oil): IR (neat) 2927, 2854, 1821, 1247, 1094  $\text{cm}^{-1}$ ;  $^1\text{H}$  NMR (400 MHz,  $\text{CDCl}_3$ )  $\delta$  7.16–7.11 (m, 2H), 6.88–6.83 (m, 2H), 4.58 (ddd,  $J$  = 6.4, 6.4, 3.6 Hz, 1H), 3.95 (ddd,  $J$  = 8.8, 7.2, 7.2 Hz, 1H), 3.79 (s, 3H) 3.60 (t,  $J$  = 6.6 Hz, 2H), 3.12 (dd,  $J$  = 15.0, 7.4 Hz, 1H), 2.92 (dd,  $J$  = 15.0, 8.8 Hz, 1H), 1.82–1.75 (m, 1H), 1.71–1.62 (m, 1H), 1.53–1.49 (m, 2H) 1.39–1.24 (m, 10H), 0.89 (s, 9H), 0.05 (s, 6H);  $^{13}\text{C}$  NMR (100 MHz,  $\text{CDCl}_3$ )  $\delta$  171.8, 158.7, 129.8, 129.6, 114.4, 76.2, 63.5, 55.5, 53.8, 33.1, 30.6, 29.6, 29.5, 29.4, 29.1, 26.2, 26.0, 25.8, 18.6, –5.0; HRMS (ESI) calcd for  $\text{C}_{25}\text{H}_{43}\text{O}_4\text{Si}$  ( $\text{M} + \text{H}$ ) $^+$   $m/z$  435.2931, found 435.2930.



***trans/cis*-3-(1,4-benzodioxane-6-methyl)-4-(8-*tert*-Butyldimethylsilyloxy)octanyloxetan-2-one (127c).**

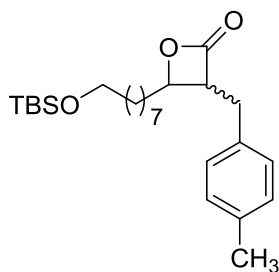
The general procedure was followed using 4-(8-*tert*-butyldimethylsilyloxy)octanyl-3-methylenioxetan-2-one (**108**) and 1,4-benzodioxane-6-boronic acid. The  $^1\text{H}$  NMR *trans:cis* ratio of the crude reaction mixture was 2.2:1. Purification by flash column chromatography on silica gel (hexanes/EtOAc 40:1) provided **127c** as a colorless oil (0.19 g, 89%). The *trans*-isomer was separable by careful column chromatography using the same solvent system. *trans*-**127c** (colorless oil): IR (neat) 2927, 2855, 1821, 1287, 1096, 1068  $\text{cm}^{-1}$ ;  $^1\text{H}$  NMR (400 MHz,  $\text{CDCl}_3$ )  $\delta$  6.80 (d,  $J$  = 8.2 Hz, 1H), 6.71–6.67 (m, 1H), 6.64 (dd,  $J$  = 8.2, 1.5 Hz, 1H), 4.28–4.23 (m, 1H), 4.23 (s, 4H), 3.59 (t,  $J$  = 6.5 Hz, 2H), 3.40 (ddd,  $J$  = 9.4, 5.3, 5.3 Hz, 1H), 3.04 (dd,  $J$  = 14.4, 5.6 Hz, 1H) 2.88 (dd,  $J$  = 14.3, 9.3 Hz, 1H), 1.83–1.77 (m, 1H), 1.64–1.59 (m, 1H), 1.51–1.46 (m, 2H) 1.33–1.08 (m, 10H), 0.89 (s, 9H), 0.04 (s, 6H);  $^{13}\text{C}$  NMR (100 MHz,  $\text{CDCl}_3$ )  $\delta$  171.1, 143.8, 142.8, 130.5, 121.8, 117.8, 117.6, 77.7, 64.6, 64.5, 63.5, 57.6, 34.4, 33.3, 33.0, 29.6, 29.4, 29.3, 26.2, 26.0, 24.9, 18.6,  $-5.0$ ; HRMS (ESI) calcd for  $\text{C}_{26}\text{H}_{43}\text{O}_5\text{Si}$  ( $\text{M} + \text{H}$ ) $^+$   $m/z$  463.2880, found 463.2872.





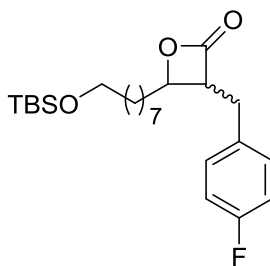
***trans/cis*-4-(8-*tert*-Butyldimethylsilyloxy)octanyl-3-(3-phenoxyphenylmethyl)oxetan-2-one (127d).**

The general procedure was followed using 4-(8-*tert*-butyldimethylsilyloxy)octanyl-3-methyleneoxetan-2-one (**108**) and 3-phenoxyphenylboronic acid. The  $^1\text{H}$  NMR *trans*:*cis* ratio of the crude reaction mixture was 2.2:1. Purification by flash column chromatography on silica gel (hexanes/EtOAc 39:1) provided **127d** as a colorless oil (0.17 g, 72%). The *trans*-isomer was separable by careful column chromatography using the same solvent system. *Trans*-**127d** (colorless oil): IR (neat) 2927, 2854, 1822, 1488, 1237, 1095  $\text{cm}^{-1}$ ;  $^1\text{H}$  NMR (400 MHz,  $\text{CDCl}_3$ )  $\delta$  7.36–7.30 (m, 2H), 7.18–7.13 (m, 2H), 7.13–7.08 (m, 1H), 7.01–6.94 (m, 4H), 4.28 (ddd,  $J = 6.7, 6.7, 4.0$  Hz, 1H), 3.59 (t,  $J = 6.6$  Hz, 2H), 3.44 (ddd,  $J = 9.2, 5.8, 4.1$  Hz, 1H), 3.14 (dd,  $J = 14.4, 5.9$  Hz, 1H), 2.99 (dd,  $J = 14.4, 9.0$  Hz, 1H), 1.86–1.78 (m, 1 H), 1.66–1.59 (m, 1 H), 1.53–1.46 (m, 2H) 1.35–1.10 (m, 10H), 0.89 (s, 9H), 0.04 (s, 6H);  $^{13}\text{C}$  NMR (100 MHz,  $\text{CDCl}_3$ )  $\delta$  170.9, 157.3, 156.6, 132.1, 130.2, 130.0, 123.6, 119.4, 119.1, 77.6, 63.5, 57.6, 34.4, 33.3, 33.0, 29.6, 29.5, 29.3, 26.2, 26.0, 24.9, 18.6, –5.1; HRMS (ESI) calcd for  $\text{C}_{30}\text{H}_{45}\text{O}_4\text{Si}$  ( $\text{M} + \text{H}$ ) $^+$   $m/z$ : 476.3196, found 476.3208.



**127e**  
*trans/cis* = 2.5:1

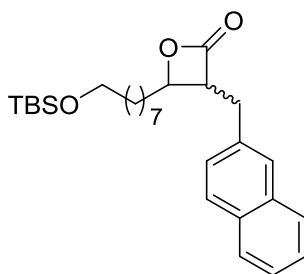
***trans/cis*-4-(8-*tert*-Butyldimethylsilyloxy)octanyl-3-(4-methylphenylmethyl)oxetan-2-one (127e).** The general procedure was followed using 4-(8-*tert*-butyldimethylsilyloxy)octanyl-3-methyleneoxetan-2-one (**108**) and *p*-tolylboronic acid. The  $^1\text{H}$  NMR *trans:cis* ratio of the crude reaction mixture was 2.5:1. Purification by flash chromatography on silica gel (hexanes/EtOAc 40:1) provided **127e** as a colorless oil (0.15 g, 78%). The *trans*-isomer was separated by careful column chromatography using the same solvent system. *trans*-**127e** (colorless oil): IR (neat) 2927, 2854, 1821, 1249, 1093  $\text{cm}^{-1}$ ;  $^1\text{H}$  NMR (400 MHz,  $\text{CDCl}_3$ )  $\delta$  7.14–7.10 (m, 2H), 7.09–7.05 (m, 2H), 4.26 (ddd,  $J$  = 6.8, 4.0, 4.0 Hz, 1H), 3.59 (t,  $J$  = 6.6 Hz, 2H), 3.43 (ddd,  $J$  = 9.4, 5.6, 4.0 Hz, 1H), 3.12 (dd,  $J$  = 14.3, 5.7 Hz, 1H) 2.96 (dd,  $J$  = 14.3, 9.2 Hz, 1H), 2.32 (s, 3H), 1.82–1.74 (m, 1H), 1.63–1.58 (m, 1H), 1.52–1.45 (m, 2H) 1.33–1.05 (m, 10H), 0.89 (s, 9H), 0.05 (s, 6H);  $^{13}\text{C}$  NMR (100 MHz,  $\text{CDCl}_3$ )  $\delta$  171.1, 136.9, 134.3, 129.8, 128.8, 77.7, 63.5, 57.7, 34.4, 33.6, 33.1, 29.6, 29.4, 29.3, 26.0, 24.9, 21.2, 18.6, –5.0; HRMS (ESI) calcd for  $\text{C}_{25}\text{H}_{43}\text{O}_3\text{Si}$  ( $\text{M} + \text{H}$ ) $^+$   $m/z$  419.2981, found 419.2958.



**127f**  
*trans/cis* = 1.7:1

***trans/cis*-4-(8-*tert*-Butyldimethylsilyloxy)octanyl-3-(4-fluorophenylmethyl)oxetan-2-one (127f).** The general procedure was followed using 4-(8-*tert*-butyldimethylsilyloxy)octanyl-3-methyleneoxetan-2-one

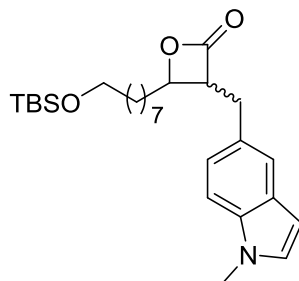
(**108**) and 4-fluorophenylboronic acid. The  $^1\text{H}$  NMR *trans*:*cis* ratio of the crude reaction mixture was 1.7:1. Purification by flash column chromatography on silica gel (hexanes/EtOAc 98:2) provided **127f** as a colorless oil (0.16 g, 84%). The *trans*-isomer was separable by careful column chromatography using the same solvent system. *trans*-**127f** (colorless oil): IR (neat) 2926, 2854, 1820, 1510, 1222, 1092  $\text{cm}^{-1}$ ;  $^1\text{H}$  NMR (400 MHz,  $\text{CDCl}_3$ )  $\delta$  7.20–7.13 (m, 2 H), 7.05–6.97 (m, 2 H), 4.25 (ddd,  $J = 6.8, 6.8, 4.1$  Hz, 1 H), 3.59 (t,  $J = 6.6$  Hz, 2 H), 3.42 (ddd,  $J = 8.9, 6.0, 4.1$  Hz, 1 H), 3.13 (dd,  $J = 14.4, 6.0$  Hz, 1 H), 2.99 (dd,  $J = 14.4, 8.9$  Hz, 1H), 1.84–1.77 (m, 1 H), 1.64–1.57 (m, 1 H), 1.52–1.45 (m, 2 H) 1.35–1.10 (m, 10 H), 0.90 (s, 9 H), 0.05 (s, 6 H);  $^{13}\text{C}$  NMR (100 MHz,  $\text{CDCl}_3$ )  $\delta$  170.8, 162.2 (d,  $J_{\text{C-F}} = 244.2$  Hz), 133.0 (d,  $J_{\text{C-F}} = 3.1$  Hz), 130.5 (d,  $J_{\text{C-F}} = 8.1$  Hz), 116.0 (d,  $J_{\text{C-F}} = 21.4$  Hz), 77.5, 63.5, 57.6, 34.4, 33.2, 33.0, 29.5, 29.4, 29.3, 26.2, 25.9, 24.9, 18.6,  $-5.1$ ; HRMS (ESI) calcd for  $\text{C}_{24}\text{H}_{40}\text{FO}_3\text{Si}$  ( $\text{M} + \text{H}^+$ )  $m/z$  423.2731, found 423.2732.



**127g**  
*trans*/*cis* = 2.4:1

*trans*/*cis*-4-(8-*tert*-Butyldimethylsilyloxy)octanyl-3-(2-naphthylmethyl)oxetan-2-one (**127g**). The general procedure was followed using 4-(8-*tert*-butyldimethylsilyloxy)octanyl-3-methyleneoxetan-2-one (**108**) (0.40 g, 1.2 mmol) and 2-naphthylboronic acid (0.31 g, 1.8 mmol). The  $^1\text{H}$  NMR *trans*:*cis* ratio of the crude reaction mixture was 2.4:1. Purification by flash column chromatography on silica gel (hexanes/EtOAc 98:2) provided **127g** as a colorless oil (0.49 g, 88%). The *trans*-isomer was separable by careful column chromatography using the same solvent system. *trans*-**127g** (colorless oil): IR (neat) 2927, 2854, 1819, 1249, 1093  $\text{cm}^{-1}$ ;  $^1\text{H}$  NMR (400 MHz,  $\text{CDCl}_3$ )  $\delta$  7.85–7.77 (m, 3H), 7.65 (s, 1H), 7.52–7.44 (m, 2H), 7.32 (dd,  $J = 8.4, 1.4$  Hz, 1H), 4.43 (ddd,  $J = 6.7, 6.7, 4.1$  Hz, 1H), 3.58 (t,  $J = 6.6$  Hz, 2H),

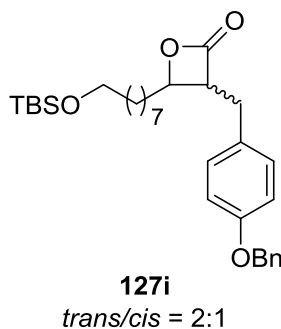
3.61–3.52 (m, 1H), 3.34 (dd,  $J = 14.3, 5.6$  Hz, 1H), 3.16 (dd,  $J = 14.3, 9.4$  Hz, 1H), 1.82–1.75 (m, 1H), 1.63–1.55 (m, 1H), 1.49–1.41 (m, 2H) 1.25–1.00 (m, 10H), 0.91 (s, 9H), 0.06 (s, 6H);  $^{13}\text{C}$  NMR (100 MHz,  $\text{CDCl}_3$ )  $\delta$  170.9, 134.8, 133.7, 132.6, 128.9, 127.9, 127.7, 127.4, 126.9, 126.5, 126.0, 77.7, 63.4, 57.4, 34.4, 34.2, 33.0, 29.5, 29.3, 29.2, 26.2, 25.9, 24.8, 18.6,  $-5.1$ ; HRMS (ESI) calcd for  $\text{C}_{28}\text{H}_{43}\text{O}_3\text{Si}$  ( $\text{M} + \text{H}$ ) $^+$   $m/z$  455.2981, found 455.2953.



**127h**  
*trans/cis* = 1.6:1

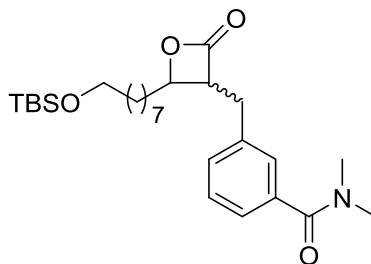
***trans/cis*-4-(8-*tert*-Butyldimethylsilyloxy)octanyl-3-(1-methyl-5-indolylmethyl)oxetan-2-one (127h).**

The general procedure was followed using 4-(8-*tert*-butyldimethylsilyloxy)octanyl-3-methyleneoxetan-2-one (**108**) and 1-methyl-5-indolylboronic acid. The  $^1\text{H}$  NMR *trans:cis* ratio of the crude reaction mixture was 1.6:1. Purification by flash column chromatography on silica gel (hexanes/EtOAc 97:3) provided **127h** as a colorless oil (0.15 g, 71%). The *trans*-isomer was separable by careful column chromatography using the same solvent system. *trans*-**127h** (colorless oil): IR (neat) 2926, 2854, 1817, 1246, 1095  $\text{cm}^{-1}$ ;  $^1\text{H}$  NMR (400 MHz,  $\text{CDCl}_3$ )  $\delta$  7.42 (s, 1H), 7.28–7.26 (m, 1H), 7.05–7.03 (m, 2H), 6.43 (d,  $J = 3.0$  Hz, 1H), 4.31 (ddd,  $J = 6.7, 6.7, 4.1$  Hz, 1H), 3.78 (s, 3H), 3.58 (t,  $J = 6.6$ , Hz, 2H), 3.50 (ddd,  $J = 9.4, 5.4, 4.1$  Hz, 1H), 3.26 (dd,  $J = 14.3, 5.5$ , Hz, 1H), 3.10 (dd,  $J = 14.3, 9.3$  Hz, 1H), 1.78–1.72 (m, 1H), 1.60–1.54 (m, 1H), 1.50–1.43 (m, 2H) 1.35–1.05 (m, 10H), 0.90 (s, 9H), 0.05 (s, 6H);  $^{13}\text{C}$  NMR (100 MHz,  $\text{CDCl}_3$ )  $\delta$  171.5, 136.1, 129.6, 129.1, 128.1, 122.5, 120.9, 109.8, 100.9, 77.8, 63.5, 58.2, 34.5, 34.1, 33.1, 33.0, 29.5, 29.4, 29.3, 26.2, 26.0, 24.9, 18.6,  $-5.0$ ; HRMS (ESI) calcd for  $\text{C}_{27}\text{H}_{44}\text{NO}_3\text{Si}$  ( $\text{M} + \text{H}$ ) $^+$   $m/z$  458.3090, found 458.3059.



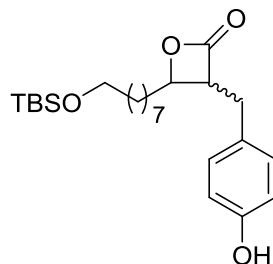
***trans/cis*-4-(8-*tert*-Butyldimethylsilyloxy)octanyl-3-(3-benzyloxyphenylmethyl)oxetan-2-one (127i).**

The general procedure was followed using 4-(8-*tert*-butyldimethylsilyloxy)octanyl-3-methyleneoxetan-2-one (**108**) (0.20 g, 0.61 mmol) and 3-(benzyloxy)phenylboronic acid (0.21 g, 0.92 mmol). The  $^1\text{H}$  NMR *trans:cis* ratio of the crude reaction mixture was 2:1. Purification by flash column chromatography on silica gel (hexanes/EtOAc 40:1) provided **127i** as a colorless oil (0.22 g, 71%). The *trans*-isomer was separable by careful column chromatography using the same solvent system. *trans*-**127i** (colorless oil): IR (neat) 2928, 2855, 1821, 1255, 1095, 1027  $\text{cm}^{-1}$ ;  $^1\text{H}$  NMR (400 MHz,  $\text{CDCl}_3$ )  $\delta$  7.45–7.36 (m, 4H), 7.35–7.30 (m, 1H), 7.23 (t,  $J = 7.9$  Hz, 1H), 6.87 (dd,  $J = 8.1, 2.1$  Hz, 1H), 6.82–6.77 (m, 2H), 5.06 (s, 2H), 4.24 (ddd,  $J = 6.7, 6.7, 4.1$  Hz, 1H) 3.58 (t,  $J = 6.6$  Hz, 2H), 3.43 (ddd,  $J = 9.5, 5.6, 4.1$  Hz, 1H), 3.13 (dd,  $J = 14.3, 5.7$  Hz, 1H) 2.96 (dd,  $J = 14.3, 9.3$  Hz, 1H), 1.81–1.70 (m, 1H), 1.62–1.44 (m, 3H), 1.35–1.15 (m, 10H), 0.89 (s, 9H), 0.04 (s, 6H);  $^{13}\text{C}$  NMR (100 MHz,  $\text{CDCl}_3$ )  $\delta$  171.0, 159.4, 139.0, 137.1, 130.2, 128.8, 128.2, 127.7, 121.4, 115.6, 113.6, 70.2, 63.5, 57.4, 34.4, 34.0, 33.1, 29.6, 29.4, 29.3, 26.2, 26.0, 24.9, 18.6, –5.0; HRMS (ESI) calcd for  $\text{C}_{31}\text{H}_{47}\text{O}_4\text{Si}$  ( $\text{M} + \text{H}$ ) $^+$   $m/z$  511.3244, found 511.3223.



**127j**  
*trans/cis* = 1.6:1

***trans*-4-[8-(*tert*-Butyldimethylsilyloxy)octanyl]-3-(3-(*N,N* dimethylcarbamoyl)benzyl)oxetan-2-one (127j).** The general procedure was followed using 4-(8-*tert*-butyldimethylsilyloxy)octanyl-3-methyleneoxetan-2-one (**108**) and 3-(dimethylcarbamoyl)phenylboronic acid. The  $^1\text{H}$  NMR *trans*:*cis* ratio of the crude reaction mixture was 1.6:1. Purification by flash column chromatography on silica gel (hexanes/EtOAc 97:3) provided **127j** as a colorless oil (0.16 g, 67%). The *cis*-isomer was separable by careful column chromatography using the same solvent system. *cis*-**127j** (colorless oil): IR (neat) 2926, 2854, 1817, 1737, 1634, 1461, 1389, 1253, 1092  $\text{cm}^{-1}$ ;  $^1\text{H}$  NMR (400 MHz,  $\text{CDCl}_3$ )  $\delta$  7.39–7.32 (m, 1 H), 7.27 (d,  $J$  = 7.3, 3 H), 4.59 (ddd,  $J$  = 9.9, 6.3, 3.5 Hz, 1 H), 3.97 (dd,  $J$  = 14.6, 8 Hz, 1 H), 3.58 (t,  $J$  = 6.6 Hz, 1 H), 3.17 (dd,  $J$  = 15.0, 7.9 Hz, 1 H), 3.10 (br s, 3H), 2.98 (dd,  $J$  = 15.1, 8.4 Hz, 1 H), 2.97 (br s, 3H) 1.82–1.74 (m, 1 H), 1.68–1.61 (m, 1 H), 1.51–1.47 (m, 2 H) 1.28 (br s, 10 H), 0.88 (s, 9 H), 0.03 (s, 6 H);  $^{13}\text{C}$  NMR (100 MHz,  $\text{CDCl}_3$ )  $\delta$  171.4, 138.1, 137.1, 129.8, 129.0, 127.2, 125.7, 76.0, 63.4, 53.3, 33.0, 30.6, 29.9, 29.8, 29.6, 29.4, 29.4, 26.2, 25.9, 25.7, 18.6, –5.0; HRMS (ESI) calcd for  $\text{C}_{27}\text{H}_{46}\text{NO}_4\text{Si}$  ( $\text{M} + \text{H}$ ) $^+$   $m/z$  476.3196, found 476.3208.



**127k**  
*trans/cis* = 2:1

***trans/cis*-4-(8-*tert*-Butyldimethylsilyloxyoctanyl)-3-(4-hydroxyphenylmethyl)oxetan-2-one (127k).**

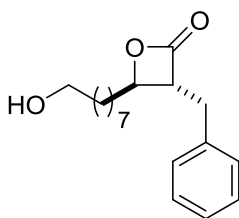
The general procedure was followed using 4-(8-*tert*-butyldimethylsilyloxy)octanyl-3-methyleneoxetan-2-one (**108**) and 4-hydroxyphenylboronic acid. The  $^1\text{H}$  NMR *trans*:*cis* ratio of the crude reaction mixture was 2:1. Purification by flash column chromatography on silica gel (hexanes/EtOAc 70:30) provided **127k** as a colorless oil (0.13 g, 68%). The isomers were separated by careful column chromatography using the same solvent system. *trans*-**127k** (colorless oil): IR (neat) 3402 (br), 2928, 2855, 1819, 1801, 1516, 1252, 1096  $\text{cm}^{-1}$ ;  $^1\text{H}$  NMR (400 MHz,  $\text{CDCl}_3$ )  $\delta$  7.07–7.01 (m, 2H), 6.81–6.75 (m, 2H), 5.85 (br s, 1H), 4.25 (ddd,  $J$  = 6.9, 6.9, 4.0 Hz, 1H), 3.64 (t,  $J$  = 6.8 Hz, 2H), 3.39 (ddd,  $J$  = 9.7, 5.3, 4.2 Hz, 1H), 3.12 (dd,  $J$  = 14.3, 5.4 Hz, 1H), 2.89 (dd,  $J$  = 14.3, 10.0 Hz, 1H), 1.83–1.75 (m, 1H), 1.57–1.48 (m, 1H), 1.29–1.24 (m, 2H) 1.35–0.95 (m, 10H), 0.89 (s, 9H), 0.09 (s, 6H);  $^{13}\text{C}$  NMR (100 MHz,  $\text{CDCl}_3$ )  $\delta$  171.3, 155.2, 130.0, 129.2, 116.0, 77.8, 63.7, 58.1, 34.3, 33.2, 32.6, 29.4, 29.1, 29.1, 26.2, 25.6, 24.6, 18.7, –5.0; HRMS (ESI) calcd for  $\text{C}_{24}\text{H}_{41}\text{O}_4\text{Si}$  ( $\text{M} + \text{H}$ ) $^+$   $m/z$  421.2774, found 421.2746. *cis*-**127k** (colorless oil): IR (neat) 3379 (br), 2927, 2855, 1797, 1516, 1252, 1095  $\text{cm}^{-1}$ ;  $^1\text{H}$  NMR (400 MHz,  $\text{CDCl}_3$ )  $\delta$  7.10–7.05 (m, 2H), 6.80–6.75 (m, 2H), 5.35 (br s, 1H), 4.57 (ddd,  $J$  = 10.0, 6.3, 4.0 Hz, 1H), 3.96 (ddd,  $J$  = 9.0, 7.0, 7.0 Hz, 1H), 3.61 (t,  $J$  = 6.7 Hz, 2H), 3.11 (dd,  $J$  = 15.0, 7.2 Hz, 1H), 2.91 (dd,  $J$  = 15.0, 9.1 Hz, 1H), 1.82–1.72 (m, 1H), 1.69–1.62 (m, 1H), 1.54–1.47 (m, 2H) 1.37–1.20 (m, 10H), 0.90 (s, 9H), 0.07 (s, 6H);  $^{13}\text{C}$  NMR (100 MHz,  $\text{CDCl}_3$ )  $\delta$  172.0, 154.8, 129.7, 129.7, 115.9, 76.4, 63.7, 53.6, 32.9, 30.4, 29.4, 29.3, 29.3, 29.1, 26.2, 25.8, 25.7, 18.6, –5.0; HRMS (ESI) calcd for  $\text{C}_{24}\text{H}_{41}\text{O}_4\text{Si}$  ( $\text{M} + \text{H}$ ) $^+$   $m/z$  421.2774, found 421.2743.

## 2.4.9 Elaboration of $\beta$ -lactones 127

### 2.4.9.1 Cleavage of silyl protecting group

#### General procedure

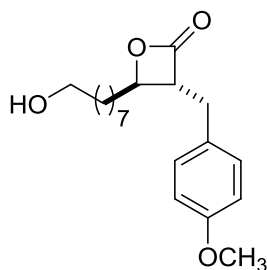
Pyridinium *p*-toluenesulfonate (PPTS) (0.3 equiv) was added to a solution of silyl ether (1.0 equiv, 0.07 M in EtOH/DCM, 1:1). The resulting mixture was then placed in a pre-heated oil bath (55 °C) for 3 h under reflux. The reaction was allowed to cool to rt. Et<sub>3</sub>N (10 volumes) was added and the reaction mixture was concentrated. The crude product was purified by flash column chromatography on silica gel.



*trans*-**128a**

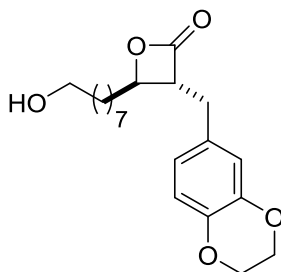
***trans*-3-Benzyl-4-(8-hydroxy)octanyloxetan-2-one (*trans*-128a).** The general procedure was followed using *trans*-3-benzyl-4-(8-*tert*-butyldimethylsilyloxy)octanyloxetan-2-one (**127a**) (0.11 g, 0.27 mmol). Purification by flash column chromatography on silica gel (hexanes/EtOAc 3:2) provided *trans*-**128a** as a colorless oil (70 mg, 89%): IR (neat) 3390 (br), 2926, 2855, 1815, 1455, 1123, 1068 cm<sup>-1</sup>; <sup>1</sup>H NMR (400 MHz, CDCl<sub>3</sub>)  $\delta$  7.35–7.14 (m, 5H), 4.30–4.23 (m, 1H), 3.62 (t, *J* = 6.3 Hz, 2H), 3.48–3.41 (m, 1H), 3.16 (dd, *J* = 14.2, 5.3 Hz, 1H), 2.99 (dd, *J* = 13.8, 9.5 Hz, 1H), 1.82–1.71 (m, 1H), 1.63–1.48 (m, 3H), 1.43–1.00 (m, 10H); <sup>13</sup>C NMR (100 MHz, CDCl<sub>3</sub>)  $\delta$  171.0, 137.4, 129.1, 128.8, 127.3, 77.7, 63.1, 57.5, 34.4, 34.0, 32.9, 29.4, 29.3, 29.2, 25.8, 24.8; HRMS (ESI) calcd for C<sub>18</sub>H<sub>27</sub>O<sub>3</sub> (*M* + *H*)<sup>+</sup> *m/z* 291.1960, found 291.1982.





***trans*-128b**

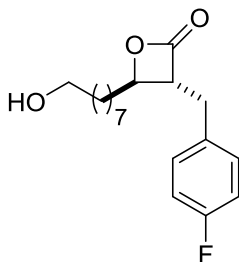
***trans*-4-(8-Hydroxy)octanyl-3-(4-methoxyphenylmethyl)oxetan-2-one (*trans*-128b).** The general procedure was followed using *trans*-4-(8-*tert*-butyldimethylsilyloxy)octanyl-3-(4-methoxyphenylmethyl)oxetan-2-one (**127b**) (0.059 g, 0.13 mmol). Purification by flash column chromatography on silica gel (hexanes/EtOAc 3:2) provided *trans*-**128b** as a colorless oil (35 mg, 81%): IR (neat) 3395 (br), 2926, 2854, 1814, 1512, 1245, 1118, 1031  $\text{cm}^{-1}$ ;  $^1\text{H}$  NMR (400 MHz,  $\text{CDCl}_3$ )  $\delta$  7.13–7.08 (m, 2H), 6.88–6.83 (m, 2H), 4.25 (ddd,  $J$  = 6.8, 6.8, 4.1 Hz, 1H), 3.79 (s, 3 H), 3.67–3.59 (m, 2H), 3.41 (ddd,  $J$  = 9.4, 5.8, 4.1 Hz, 1H), 3.09 (dd,  $J$  = 14.4, 5.8 Hz, 1H), 2.95 (dd,  $J$  = 14.4, 9.1 Hz, 1H), 1.83–1.72 (m, 1 H), 1.64–1.49 (m, 3H), 1.36–1.14 (m, 10H);  $^{13}\text{C}$  NMR (100 MHz,  $\text{CDCl}_3$ )  $\delta$ : 171.1, 158.9, 129.9, 129.3, 114.5, 77.6, 63.2, 57.8, 55.5, 34.4, 33.1, 32.9, 29.5, 29.3, 29.2, 25.9, 24.9; HRMS (ESI) calcd for  $\text{C}_{19}\text{H}_{29}\text{O}_4$  ( $\text{M} + \text{H}$ ) $^+$   $m/z$  321.2066, found 321.2046.



***trans*-128c**

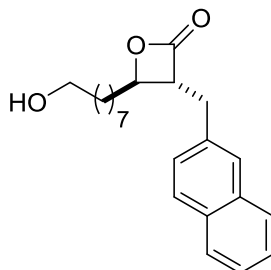
***trans*-3-(1,4-Benzodioxane-6-methyl)-4-(8-hydroxy)octanyloxetan-2-one (*trans*-128c).** The general procedure was followed using *trans*-4-(8-*tert*-butyldimethylsilyloxy)octanyl-3-(1,4-benzodioxane-6-methyl)oxetan-2-one (**127c**) (0.027 g, 0.058 mmol). Purification by flash column chromatography on silica gel (hexanes/EtOAc 3:2) provided *trans*-**128c** as a colorless oil (9 mg, 43%): IR (neat) 3420 (br), 2928, 2855, 1818, 1508, 1352, 1067  $\text{cm}^{-1}$ ;  $^1\text{H}$  NMR (400 MHz,  $\text{CDCl}_3$ )  $\delta$  6.80 (d,  $J$  = 8.2 Hz, 1H), 6.71–

6.67 (m, 1H), 6.65 (dd,  $J = 8.2, 1.8$  Hz, 1H), 4.29–4.23 (m, 1H), 4.24 (s, 4H), 3.67–3.59 (m, 2H), 3.40 (ddd,  $J = 9.4, 5.2, 5.2$  Hz, 1H), 3.05 (dd,  $J = 14.4, 5.6$  Hz, 1H), 2.89 (dd,  $J = 14.4, 9.3$  Hz, 1H), 1.83–1.73 (m, 1H), 1.65–1.50 (m, 4H), 1.39–1.15 (m, 10H);  $^{13}\text{C}$  NMR (100 MHz,  $\text{CDCl}_3$ )  $\delta$  171.0, 143.8, 142.8, 130.6, 121.8, 117.8, 117.6, 77.7, 64.6, 64.5, 63.2, 57.6, 34.4, 33.3, 32.9, 29.6, 29.4, 29.3, 25.9, 24.9; HRMS (ESI) calcd for  $\text{C}_{20}\text{H}_{29}\text{O}_5$  ( $\text{M} + \text{H}$ ) $^+$   $m/z$  349.2015, found 349.1999.



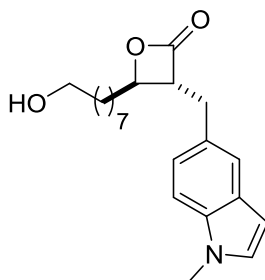
*trans*-**128f**

*trans*-3-(4-Fluorophenylmethyl)-4-(8-hydroxy)octanyloxetan-2-one (*trans*-**128f**). The general procedure was followed using *trans*-4-(8-*tert*-butyldimethylsilyloxy)octanyl-3-(4-fluorophenylmethyl)-oxetan-2-one (**127f**) (0.023 g, 0.054 mmol). Purification by flash column chromatography on silica gel (hexanes/EtOAc 3:2) provided *trans*-**128f** as a colorless oil (12 mg, 71%): IR (neat) 3362 (br), 2923, 2854, 1820, 1739, 1510, 1222  $\text{cm}^{-1}$ ;  $^1\text{H}$  NMR (400 MHz,  $\text{CDCl}_3$ )  $\delta$  7.19–7.14 (m, 2H), 7.05–6.98 (m, 2H), 4.25 (ddd,  $J = 6.7, 6.7, 4.0$  Hz, 1H), 3.78 (s, 3H), 3.64 (m, 2H), 3.43 (ddd,  $J = 9.1, 6.0, 4.1$  Hz, 1H), 3.13 (dd,  $J = 14.4, 6.0$  Hz, 1H), 2.99 (dd,  $J = 14.4, 9.0$  Hz, 1H), 1.85–1.74 (m, 1H), 1.65–1.50 (m, 4H), 1.38–1.15 (m, 10H);  $^{13}\text{C}$  NMR (100 MHz,  $\text{CDCl}_3$ )  $\delta$  170.7, 162.2 (d,  $J_{\text{C-F}} = 244.0$  Hz), 133.1 (d,  $J_{\text{C-F}} = 3.0$  Hz), 130.5 (d,  $J_{\text{C-F}} = 8.0$  Hz), 116.0 (d,  $J_{\text{C-F}} = 21.0$  Hz), 77.4, 63.2, 57.6, 34.4, 33.2, 32.9, 29.5, 29.4, 29.3, 25.9, 24.9; HRMS (ESI) calcd for  $\text{C}_{18}\text{H}_{26}\text{FO}_3$  ( $\text{M} + \text{H}$ ) $^+$   $m/z$  309.1866, found 309.1868.



*trans*-**128g**

*trans*-4-(8-Hydroxy)octanyl-3-(2-naphthylmethyl)oxetan-2-one (*trans*-**128g**). The general procedure was followed using *trans*-4-(8-*tert*-butyldimethylsilyloxy)octanyl-3-(2-naphthylmethyl)oxetan-2-one (**127g**) (0.10 g, 0.23 mmol). Purification by flash column chromatography on silica gel (hexanes/EtOAc 3:2) provided *trans*-**128g** as a colorless oil (53 mg, 68%): IR (neat) 3382 (br), 2928, 2855, 1817, 1125  $\text{cm}^{-1}$ ;  $^1\text{H}$  NMR (400 MHz,  $\text{CDCl}_3$ )  $\delta$  7.81–7.77 (m, 3H), 7.64 (s, 1H), 7.48 (dddd,  $J = 13.5, 6.9, 1.6, 1.6$  Hz, 2H), 7.32 (dd,  $J = 8.4, 1.6$  Hz, 1H), 4.33 (ddd,  $J = 6.7, 6.7, 4.1$  Hz, 1H), 3.60 (t,  $J = 6.6$  Hz, 2H), 3.56 (ddd,  $J = 9.8, 5.6, 4.1$  Hz, 1H), 3.34 (dd,  $J = 14.3, 5.6$  Hz, 1H), 3.16 (dd,  $J = 14.3, 9.5$  Hz, 1H), 1.82–1.71 (m, 1H), 1.63–1.53 (m, 1H), 1.52–1.43 (m, 2H), 1.37–1.00 (m, 10H);  $^{13}\text{C}$  NMR (100 MHz,  $\text{CDCl}_3$ )  $\delta$  171.0, 134.9, 133.7, 132.6, 128.9, 127.9, 127.7, 127.5, 126.9, 126.6, 126.1, 77.8, 63.2, 57.5, 34.4, 34.2, 32.9, 29.3, 29.2, 25.8, 24.9; HRMS (ESI) calcd for  $\text{C}_{22}\text{H}_{29}\text{O}_3$  ( $\text{M} + \text{H}$ ) $^+$   $m/z$  341.2117, found 341.2135.



*trans*-**128h**

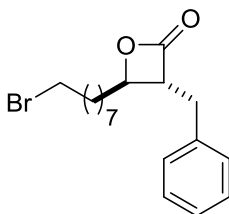
*trans*-4-(8-Hydroxy)octanyl-3-(1-methyl-5-indolylmethyl)oxetan-2-one (*trans*-**128h**). The general procedure was followed using *trans*-4-(8-*tert*-butyldimethylsilyloxy)octanyl-3-(1-methyl-5-indolylmethyl)oxetan-2-one (**127h**) (0.098 g, 0.2 mmol) and PPTS (0.02 g, 0.06 mmol). Purification by flash column chromatography on silica gel (hexanes/EtOAc 3:2) provided *trans*-**128h** as a colorless oil (68 mg, 52%). IR (neat) 3355 (br), 2926, 2854, 1813, 1122, 1077  $\text{cm}^{-1}$ ;  $^1\text{H}$  NMR (400 MHz,  $\text{CDCl}_3$ )  $\delta$  7.43–7.40

(m, 1H), 7.29–7.26 (m, 1H), 7.06–7.02 (m, 2H), 6.44–6.42 (m, 1H), 4.31 (ddd,  $J = 6.4, 6.4, 4.0$  Hz, 1H), 3.79 (s, 3H), 3.61 (t,  $J = 6.6$  Hz, 2H), 3.50 (ddd,  $J = 9.4, 5.4, 4.1$  Hz, 1H), 3.26 (dd,  $J = 14.3, 5.5$  Hz, 1H), 3.10 (dd,  $J = 14.3, 9.3$  Hz, 1H), 1.80–1.69 (m, 1H), 1.62–1.47 (m, 3H), 1.35–1.05 (m, 10H); HRMS (ESI) calcd for  $C_{21}H_{30}NO_3$  ( $M + H$ )<sup>+</sup>  $m/z$  344.2226, found 344.2206.

### 2.4.9.2 Appel Bromination

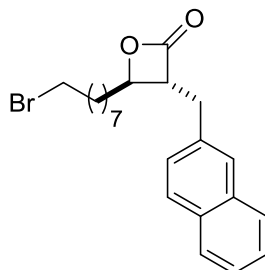
#### General procedure

Tetrabromomethane ( $CBr_4$ ) (1.5 equiv) and triphenylphosphine ( $PPh_3$ ) (3 equiv) were added to the alcohol solution (1 equiv, 0.03 M in DCM) at 0 °C. After 1 h, the reaction mixture was diluted with petroleum ether (5 volumes) and then concentrated. The crude product was adsorbed onto silica gel (dry loaded) and then purified by flash column chromatography on silica gel to give the bromide.



*trans*-**129a**

*trans*-3-Benzyl-4-(8-bromo)octanyloxetan-2-one (*trans*-**129a**). The general procedure was followed using *trans*-3-benzyl-4-(8-hydroxy)octanyloxetan-2-one (*trans*-**128a**) (0.07 g, 0.24 mmol). Purification by flash column chromatography on silica gel (hexanes/EtOAc 47:3) provided *trans*-**129a** as a colorless oil (54 mg, 63%): IR (neat) 2926, 2854, 1817, 1454, 1115, 1064  $cm^{-1}$ ;  $^1H$  NMR (400 MHz,  $CDCl_3$ )  $\delta$  7.37–7.14 (m, 5H), 4.27 (ddd,  $J = 6.7, 6.7, 4.2$  Hz, 1H), 3.46 (ddd,  $J = 9.6, 5.5, 4.2$  Hz, 1H), 3.39 (t,  $J = 6.8$  Hz, 2H), 3.17 (dd,  $J = 14.3, 5.6$  Hz, 1H), 3.00 (dd,  $J = 14.3, 9.4$  Hz, 1H), 1.88–1.72 (m, 3H), 1.64–1.52 (m, 1H), 1.43–1.33 (m, 2H), 1.31–1.13 (m, 8 H);  $^{13}C$  NMR (100 MHz,  $CDCl_3$ )  $\delta$  170.9, 137.4, 129.0, 128.8, 127.2, 77.7, 57.5, 34.3, 34.1, 33.9, 32.9, 29.3, 29.1, 28.6, 28.2, 24.8; HRMS (ESI) calcd for  $C_{18}H_{26}BrO_2$  ( $M + H$ )<sup>+</sup>  $m/z$  353.116, found 353.1090.



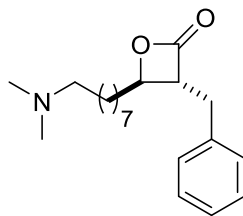
*trans*-**129g**

*trans*-4-(8-Bromo)octanyl-3-(2-naphthylmethyl)oxetan-2-one (*trans*-**129g**). The general procedure was followed using *trans*-4-(8-hydroxy)octanyl-3-(2-naphthylmethyl)oxetan-2-one (*trans*-**128g**) (0.053 g, 0.15 mmol). Purification by flash column chromatography on silica gel (hexanes/EtOAc 47:3) provided *trans*-**129g** as a colorless oil (47 mg, 75%): IR (neat) 2925, 2854, 1817, 1601, 1463, 1376, 1340, 1269, 1119, 1067  $\text{cm}^{-1}$ ;  $^1\text{H}$  NMR (400 MHz,  $\text{CDCl}_3$ )  $\delta$  7.87–7.75 (m, 3H), 7.65 (s, 1H), 7.54–7.43 (m, 2H), 7.32 (d,  $J$  = 8.3 Hz, 1H), 4.37–4.29 (m, 1H), 3.56 (ddd,  $J$  = 9.4, 4.7, 4.7 Hz, 1H), 3.36 (t,  $J$  = 6.7 Hz, 2H), 3.37–3.31 (m, 1H), 3.16 (dd,  $J$  = 14.2, 9.6 Hz, 1H), 1.83–1.70 (m, 3H), 1.64–1.51 (m, 1H), 1.37–1.21 (m, 2H) 1.20–0.97(m, 8H);  $^{13}\text{C}$  NMR (100 MHz,  $\text{CDCl}_3$ )  $\delta$  170.9, 134.9, 133.7, 132.6, 128.9, 127.9, 127.7, 127.4, 126.9, 126.6, 126.1, 77.8, 57.5, 34.4, 34.2, 34.1, 32.9, 29.2, 29.1, 28.6, 28.2, 24.8; HRMS (ESI) calcd for  $\text{C}_{22}\text{H}_{28}\text{BrO}_2$  ( $\text{M} + \text{H}$ ) $^+$   $m/z$  403.1273, found 403.1285.

#### 2.4.9.3 Nucleophilic substitution of the bromide with dimethylamine

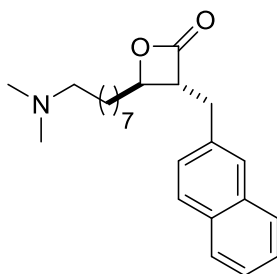
##### General procedure

Dimethylamine in  $\text{H}_2\text{O}$  (40%, 1.0 equiv) and  $\text{NaHCO}_3$  (1.0 equiv) were added to a solution of the bromide (1.0 equiv, 0.05 M in DMF) and the mixture was heated at reflux while stirring for 24 h. The mixture was then allowed to cool to rt, concentrated, dissolved in DCM (20 volumes relative to bromide) and then washed with water (20 volumes x 2). The organic layer was dried ( $\text{NaSO}_4$ ) and concentrated.



***trans*-130a**

***trans*-3-Benzyl-4-(8-dimethylamino)octanyloxetan-2-one (*trans*-130a).** The general procedure was followed using *trans*-3-benzyl-4-(8-bromo)octanyloxetan-2-one (*trans*-129a) (0.054 g, 0.15 mmol). Purification by flash column chromatography on silica gel (NH<sub>4</sub>OH/MeOH/CHCl<sub>3</sub> 2:2.5:175) provided *trans*-130a as a brown oil (15 mg, 31%): IR (neat) 2927, 2855, 1697, 1253, 1097 cm<sup>-1</sup>; <sup>1</sup>H NMR (400 MHz, CDCl<sub>3</sub>) δ 7.35–7.19 (m, 5H), 4.27 (ddd, *J* = 6.7, 6.7, 4.0 Hz, 1H), 3.45 (ddd, *J* = 9.5, 5.7, 4.1 Hz, 1H), 3.17 (dd, *J* = 14.3, 5.7 Hz, 1H), 3.00 (dd, *J* = 14.3, 9.4 Hz, 1H), 2.25–2.21 (m, 2H), 2.21 (s, 6H), 1.83–1.72 (m, 1H), 1.63–1.52 (m, 1H), 1.48–1.38 (m, 2H), 1.32–1.13 (m, 8 H); <sup>13</sup>C NMR (100 MHz, CDCl<sub>3</sub>) δ; HRMS (ESI) calcd for C<sub>20</sub>H<sub>32</sub>NO<sub>2</sub> (M + H)<sup>+</sup> *m/z* 318.2437, found 318.2426.



***trans*-130g**

***trans*-4-(8-Dimethylamino)octanyl-3-(2-naphthylmethyl)oxetan-2-one (*trans*-130g).** The general procedure was followed using *trans*-4-(8-bromo)octanyl-3-(2-naphthylmethyl)oxetan-2-one (*trans*-129g) (0.047 g, 0.1 mmol). Purification by flash column chromatography on silica gel (NH<sub>4</sub>OH/MeOH/CHCl<sub>3</sub> 2:2.5:175) provided *trans*-130g as a brown oil (12 mg, 28%): IR (neat) 2925, 2853, 1819, 1115 cm<sup>-1</sup>; <sup>1</sup>H NMR (400 MHz, CDCl<sub>3</sub>) δ 7.85–7.76 (m, 3H), 7.64 (s, 1H), 7.47 (m, 2H), 7.31 (dd, *J* = 8.4, 1.6 Hz, 1H), 4.33 (ddd, *J* = 6.7, 6.7, 4.0 Hz, 1H), 3.56 (ddd, *J* = 9.5, 5.5, 4.1 Hz, 1H), 3.34 (dd, *J* = 14.3, 5.6 Hz, 1H), 3.17 (dd, *J* = 14.3, 9.4 Hz, 1H), 2.26–2.19 (m, 2H), 2.22 (s, 6H), 1.83–1.71 (m, 1H), 1.63–1.51 (m, 1H),

1.43–1.34 (m, 4H) 1.22–1.00 (m, 8H);  $^{13}\text{C}$  NMR (100 MHz,  $\text{CDCl}_3$ )  $\delta$  171.0, 134.9, 133.8, 132.7, 128.9, 127.9, 127.8, 127.5, 126.9, 126.6, 126.1, 77.8, 60.1, 57.5, 45.7, 34.4, 34.2, 29.9, 29.5, 29.5, 29.2, 27.9, 27.6, 24.9; HRMS (ESI) calcd for  $\text{C}_{24}\text{H}_{34}\text{NO}_2$  ( $\text{M} + \text{H}$ ) $^+$   $m/z$  368.2590, found 368.2589.

## 2.5 References

1. For representative syntheses of  $\beta$ -lactones containing natural products: (a) Pommier, A.; Pons, J. M. *Synthesis* **1995**, 729; (b) Yang, H. W.; Romo, D. *J. Org. Chem.* **1997**, 62, 4.; (c) Dymock, B. W.; Kocienski, P. *J. Synthesis* **1998**, 11, 1655; (d) Reddy, L. R.; Saravanan, P.; Corey, E. J. *J. Am. Chem. Soc.* **2004**, 126, 6230.
2. Representative reviews on  $\beta$ -lactone synthesis: (a) Yang, H. W.; Romo, D. *Tetrahedron* **1999**, 55, 6403; (b) Orr, R. K.; Calter, M. A. *Tetrahedron* **2003**, 59, 3545; (c) Schneider, C. *Angew. Chem. Int. Ed.* **2002**, 41, 744; (d) Paull, D. H.; Weatherwax, A.; Lectka, T. *Tetrahedron* **2009**, 65, 6771; (e) Purohit, V. C.; Matla, A. S.; Romo, D. *Heterocycles* **2008**, 76, 949.
3. For recent publications: (f) Chidara, S.; Lin, Y. *Synlett* **2009**, 1675; (g) Wang, X.; Shao, P.; Lv, H.; Ye, S. *Org. Lett.* **2009**, 5, 687; (i) Ganji, P.; Doyle, D. J.; Ibrahim, H. *Org. Lett.* **2011**, 13, 3142; (j) Mondal, M.; Ibrahim, A. A.; Wheeler, K. A.; Kerrigan, N. J., *Org. Lett.* **2010**, 12, 1664; (k) Kull, T.; Cabrera, J.; Peters, R. *Chem. Eur. J.* **2010**, 16, 9132; (l) Ibrahim, A. A.; Wei, P.; Harzmann, G. D.; Kerrigan, N. J. *J. Org. Chem.* **2010**, 75, 7901; (m) Aronica, L. A.; Mazzoni, C.; Caporusso, A. M. *Tetrahedron* **2010**, 66, 265.
4. Weibel, E. K.; Hadvary, P.; Hochuli, E.; Kupfer, E.; Lengsfeld, H. *J. Antibiot.* **1987**, 40, 1081.
5. Hochuli, E.; Kupfer, E.; Maurer, R.; Meister, W.; Mercadal, Y.; Schmidt, K. *J. Antibiot.* **1987**, 40, 1086.
6. Fernandez, E.; Borgstrom, B. *Lipids* **1990**, 25, 549.
7. Hermier, D.; Hales, P.; Brindley, D. N. *FEBS Letters* **1991**, 286, 186.
8. Hogan, S.; Fleury, A.; Hadvary, P.; Lengsfeld, H.; Meier, M. K.; Triscari, J.; Sullivan, A. C. *Int. J. Obesity* **1987**, 11, 35.
9. Umezawa, H.; Aoyagi, T.; Hazato, T.; Uotani, K.; Kojima, F.; Hamada, M.; Takeuchi, T. *J. Antibiot.* **1978**, 31, 797.



10. Kondo, S.; Uotani, K.; Miyamoto, M.; Hazato, T.; Naganawa, H.; Aoyagi, T.; Umezawa, H. *J. Antibiot.* **1978**, *31*, 797.
11. Umezawa, H.; Aoyagi, T.; Uotani, K.; Hamada, M.; Takeuchi, T.; Takahashi, S. *J. Antibiot.* **1980**, *33*, 1594.
12. Tomoda, H.; Kumagai, H.; Takahashi, Y.; Tanaka, Y.; Iwai, Y.; Omura, S. *J. Antibiot.* **1988**, *41*, 247.
13. Tomada, H.; Kumaga, H.; Tanaka, H.; Omura, S. *Biochim. Biophys. Acta* **1987**, 922, 351.
14. Kumagai, H.; Tomoda, H.; Omura, S. *J. Antibiot.* **1990**, *43*, 397.
15. Tymiak, A. A.; Culver, C. A.; Malley, M. F.; Gougoutas, J. Z. *J. Org. Chem.* **1985**, *50*, 5491.
16. Hadvary, P.; Lengsfeld, M.; Wolfer, H. *Biochem. J.* **1988**, *256*, 357.
17. Hadvary, P.; Sidler, W.; Meister, W.; Vetter, W.; Wolfer, H. *J. Biol. Chem.* **1991**, 266, 2021.
18. Mulzer, J.; Hoyer, K.; Muller-Fahrnow, A. *Angew. Chem. Int. Ed.* **1997**, *36*, 1476.
19. Pommier, A.; Pons, J.-M. *Synthesis* **1993**, 441.
20. Zemribo, R.; Champ, M. S.; Romo, D. *Synlett* **1996**, 278.
21. Fournier, L.; Gaudel-Siri, A.; Kocienski, P. J.; Pons, J. M. *Synlett* **2003**, 107.
22. Black, T. H.; Zhang, Y.; Huang, J.; Smith, D. C.; Yates, B. E. *Synth. Commun.* **1995**, *25*, 15.
23. (a) Mulzer, J.; Kerkmann, K. *J. Am. Chem. Soc.* **1980**, *102*, 3620; (b) Parsons, P. J.; Cowell, J. K. *Synlett* **2000**, 107.
24. Mulzer, J.; Chucholowski, A. *Angew. Chem. Int. Ed.* **1982**, *21*, 777.
25. Parsons, P. J.; Cowell, J. K. *Synlett* **2000**, 107.
26. Harrowven, D. C.; Dainty, R. F. *Tetrahedron Lett.* **1995**, *36*, 6739.
27. Tom, C. T.; Martin, B. R. *ACS Chem. Biol.* **2013**, *8*, 46.
28. (a) Martin, B. R.; Cravatt, B. F. *Nat. Methods* **2009**, *6*, 135; (b) Ivaldi, C.; Martin, B. R.; Kieffer-Jaquinod, S.; Chapel, A.; Levade, T.; Garin, J.; Journet, A. *PLoS One* **2012**, *7*, e37187; (c) Li, Y.; Martin, B. R.; Cravatt, B. F.; Hofmann, S. L. *J. Biol. Chem.* **2012**, *287*, 523; (d) Martin, B. R.; Wang, C.; Adibekian, A.; Tully, S. E.; Cravatt, B. F. *Nat. Methods* **2012**, *9*, 84; (e) Kang, R.;

- Wan, J.; Arstikaitis, P.; Takahashi, H.; Huang, K.; Bailey, A. O.; Thompson, J. X.; Roth, A. F.; Drisdel, R. C.; Mastro, R.; Green, W. N.; Yates, J. R.; Davis, N. G.; El-Husseini, A. *Nature* **2008**, *456*, 904; (f) Yang, W.; Di Vizio, D.; Kirchner, M.; Steen, H.; Freeman, M. R. *Mol. Cell Proteomics* **2010**, *9*, 54 (g) Jones, M. L.; Collins, M. O.; Goulding, D.; Choudhary, J. S.; Rayner, J. C. *Cell Host & Microbe* **2012**, *12*, 246.
29. Duncan, J. A.; Gilman, A. G. *J. Biol. Chem.* **1998**, *273*, 15830.
30. Rocks, O.; Peyker, A.; Kahms, M.; Verveer, P. J.; Koerner, C.; Lumbierres, M.; Kuhlmann, J.; Waldmann, H.; Wittinghofer, A.; Bastiaens, P. I. H. *Science* **2005**, *307*, 1746.
31. Long, J. Z.; Cravatt, B. F. *Chem. Rev.* **2011**, *111*, 6022.
32. Kong, E.; Peng, S.; Chandra, G.; Sarkar, C.; Zhang, Z.; Bagh, M. B.; Mukherjee, A. B. *J. Biol. Chem.* **2013**, *288*, 9112.
33. (a) Dekker, F. J.; Rocks, O.; Vartak, N.; Menninger, S.; Hedberg, C.; Balamurugan, R.; Wetzel, S.; Renner, S.; Gerauer, M.; Scholermann, B.; Rusch, M.; Kramer, J. W.; Rauh, D.; Coates, G. W.; Brunsveld, L.; Bastiaens, P. I.; Waldmann, H. *Nat. Chem. Biol.* **2010**, *6*, 449; (b) Xu, J.; Hedberg, C.; Dekker, F. J.; Li, Q.; Haigis, K. M.; Hwang, E.; Waldmann, H.; Shannon, K. *Blood* **2012**, *119*, 1032.
34. Hedberg, C.; Dekker, F. J.; Rusch, M.; Renner, S.; Wetzel, S.; Vartak, N.; Gerding-Reimers, C.; Bon, R. S.; Bastiaens, P. I. H.; Waldmann, H. *Angew. Chem. Int. Ed.* **2011**, *50*, 9832.
35. Rusch, M.; Zimmermann, T. J.; Burger, M.; Dekker, F. J.; Gormer, K.; Triola, G.; Brockmeyer, A.; Janning, P.; Bottcher, T.; Sieber, S. A.; Vetter, I. R.; Hedberg, C.; Waldmann, H. *Angew. Chem. Int. Ed.* **2011**, *50*, 9838.
36. Rocks, O.; Gerauer, M.; Vartak, N.; Koch, S.; Huang, Z. P.; Pechlivanis, M.; Kuhlmann, J.; Brunsveld, L.; Chandra, A.; Ellinger, B.; Waldmann, H.; Bastiaens, P. I. *Cell* **2010**, *141*, 458.
37. Takeichi, M. *Curr. Opin. Cell Biol.* **1993**, *5*, 806.
38. Downward, J. *Nat. Rev. Cancer* **2003**, *3*, 11.
39. Purohit, C. V.; Richardson, D. R.; Smith, W. J.; Romo, D. *J. Org. Chem.* **2006**, *71*, 4549.

40. (a) Calter, M. A. *J. Org. Chem.* **1996**, *61*, 8006; (b) Calter, M. A.; Orr, R. K.; Song, W. *Org. Lett.* **2003**, *5*, 4745.
41. Richardson, D. R.; Ma, G.; Oyola, Y.; Zancanella, M.; Knowles, M. L.; Cieplak, P.; Romo, D.; Smith, W. J. *J. Med. Chem.* **2008**, *51*, 5285.
42. (a) Raju, R.; Howell, A. R. *Org. Lett.* **2006**, *8*, 2139; (b) Camara, K.; Lasota, C. C.; Kamat, S. S.; Cravatt, B. F.; Howell, A. R. *Bioorg. Med. Chem. Lett.* **2015**, *25*, 317.
43. Chatterjee, A. K.; Morgan, J. P.; Scholl, M.; Grubbs, R. H. *J. Am. Chem. Soc.* **2000**, *122*, 3783.
44. Kamat, S. S.; Camara, K.; Parsons, W. H.; Chen, D.-H.; Dix, M. M.; Bird, T. D.; Howell, A. R.; Cravatt, B. F. *Nat. Chem. Biol.* **2015**, *11*, 164.
45. Martinez, I.; Andrews, A. E.; Emch, J. D.; Ndakala, A. J.; Wang, J.; Howell, A. R. *Org. Lett.* **2003**, *5*, 399.
46. (a) Adam, W.; Albert, R.; Dachs Grau, N.; Hasemann, L.; Nestler, B.; Peters, E.-M.; Peters, K.; Prechtel, F.; von Schnering, H. G. *J. Org. Chem.* **1991**, *56*, 5778; (b) Campi, E. M.; Dyall, K.; Fallon, G.; Jackson, W. R.; Perlmutter, P.; Smallridge, A. J. *Synthesis* **1990**, 855.
47. Weber, F.; Schmidt, A.; Röse, P.; Fischer, M.; Burghaus, O.; Hilt, G. *Org. Lett.* **2015**, *17*, 2952.
48. Baughman, T. W.; Sworen, J. C.; Wagener, K. B. *Tetrahedron* **2004**, *60*, 10943.
49. For selected early examples, see: (a) Sakai, M.; Hayashi, H.; Miyaura, N. *Organometallics* **1997**, *16*, 4229; (b) Takaya, Y.; Ogasawara, M. Hayashi, T.; Sakai, M.; Miyaura, N. *J. Am. Chem. Soc.* **1998**, *120*, 5579.
50. For a review, see: Fagnou, K.; Lautens, M. *Chem. Rev.* **2003**, *103*, 169.
51. (a) Itooka, R.; Iguchi, Y.; Miyaura, N. *J. Org. Chem.* **2003**, *68*, 6000; (b) Hayashi, T.; Takahashi, M.; Takaya, Y.; Ogasawara, M. *J. Am. Chem. Soc.* **2002**, *124*, 5052.
52. Chen, G.; Tokunaga, N.; Hayashi, T. *Org. Lett.* **2005**, *7*, 2285.

53. a) Shintani, R.; Ueyama, K.; Yamada, I.; Hayashi, T. *Org. Lett.* **2004**, *6*, 3425; (b) Shintani, R.; Duan, W. L.; Hayashi, T. *J. Am. Chem. Soc.* **2006**, *128*, 5628.
54. De Risi, C.; Fanton, G.; Pollini, G. P.; Trapella, C.; Valente, F.; Zanirato, V. *Tetrahedron: Asymm.* **2008**, *19*, 131.
55. (a) Yu, M. S.; Lantos, I.; Peng, Z.-Q.; Yu, J.; Cacchio, T. *Tetrahedron Lett.* **2000**, *41*, 5647; (b) Johnson, T. A.; Curtis, M. D.; Beak, P. *J. Am. Chem. Soc.* **2001**, *123*, 1004; (c) Amat, M.; Bosch, J.; Hidalgo, J.; Canto', M.; Pe'rez, M.; Llor, N.; Molins, E.; Miravittles, C.; Orozco, M.; Luque, J. *J. Org. Chem.* **2000**, *65*, 3074; (d) Amat, M.; Hidalgo, J.; Bosch, J. *Tetrahedron Asymm.* **1996**, *7*, 1591.
56. Hargrave, J. D.; Bish, G.; Frost, C. G. *Chem. Commun.* **2006**, 4389.
57. Croix, C.; Prié, G.; Chaulet, C.; Viaud-Massuard, M.-C. *J. Org. Chem.* **2015**, *80*, 3264.
58. Allen, J. C.; Kociok-Köhn, G.; Frost, C. G. *Org. Biomol. Chem.* **2012**, *10*, 32.
59. (a) Sato, M.; Ogasawara, H.; Sekiguchi, K.; Kaneko, C. *Heterocycles* **1984**, *22*, 2563; (b) Sato, M.; Ban H.; Kaneko, C. *Tetrahedron Lett.* **1997**, *38*, 6689.
60. Nelson, S. G.; Dura, R. D.; Peelen, T. *J. Org. React.* **2013**, *82*, 471.
61. (a) Zou, G.; Wang, Z.; Zhu, J.; Tang, J. *Chem. Commun.* **2003**, 2438. (b) Zou, G.; Guo, J.; Wang, Z.; Huang, W.; Tang, J. *Dalton Trans.* **2007**, 3055.
62. Malapit, C. A.; Luvaga, I. K.; Caldwell, D. R.; Schipper, N. K. Howell, A. R. *Org. Lett.* **2017**, *19*, 4460.

63. Ponzano, S.; Bertozzi, F.; Mengatto, L.; Dionisi, M.; Armirotti, A.; Romeo, E.; Berteotti, A.; Fiorelli, C.; Tarozzo, G.; Reggiani, A.; Duranti, A.; Tarzia, G.; Mor, M.; Cavalli, A.; Piomelli, D.; Bandiera, T. *J. Med. Chem.* **2013**, *56*, 6917.